ÉCOLE DE TECHNOLOGIE SUPÉRIEURE
UNIVERSITÉ DU QUÉBEC

THÈSE PAR ARTICLES PRÉSENTÉE À
L'ÉCOLE DE TECHNOLOGIE SUPÉRIEURE

COMME EXIGENCE PARTIELLE
À L'OBTENTION DU
DOCTORAT EN GÉNIE
Ph.D.

PAR
BARIL, Yannick-Vincent

DÉVELOPPEMENT D'UN SYSTÈME DE FIXATION OSSEUSE PAR TRESSE EN ALLIAGE À MÉMOIRE DE FORME

MONTRÉAL, LE 22 MAI 2009

© Baril, Yannick, 2009

PRÉSENTATION DU JURY

CETTE THÈSE A ÉTÉ ÉVALUÉE

PAR UN JURY COMPOSÉ DE :

M. Vladimir Brailovski, directeur de la thèse
Département de génie mécanique à l'École de technologie supérieure

Mme Nicola Hagemeister, présidente du jury
Département de génie de la production automatisé à l'École de technologie supérieure

M. Patrick Terriault, membre du jury
Département de génie mécanique à l'École de technologie supérieure

M. Yvan Petit, membre du jury
Département de génie mécanique à l'École de technologie supérieure

M. Michel Assad, examinateur externe
Orthopédie et biomatériaux, AccelLAB Inc.

ELLE A FAIT L'OBJET D'UNE SOUTENANCE DEVANT JURY ET PUBLIC

9 AVRIL 2009

À L'ÉCOLE DE TECHNOLOGIE SUPÉRIEURE

AVANT-PROPOS

Cette thèse est la continuation des travaux débutés lors de ma maîtrise, achevée en octobre 2004, ce qui implique que les contributions apparentes de l'un et l'autre se trouvent entremêlées. Il est donc important ici de faire la part des choses et de présenter la contribution effective du travail doctoral.

Deux demandes de brevet d'invention ont été déposées.

En collaboration avec les professeurs V. Brailovski, P. Terriault et le Dr R. Cartier, les travaux concernant l'écriture de la demande de brevet « Système de fermeture du sternum » PCT/CA2005/001859 ont été parachevés le 6 décembre 2005. Le système de fermeture a été dimensionné et un guide de sélection de sa géométrie a été proposé. La rédaction du brevet est l'œuvre de *Tessier et associés*. Malgré l'ordre officiel des auteurs apparaissant sur le brevet, il est entendu que je suis l'inventeur principal de cette solution technique.

Toujours en collaboration avec les professeurs V. Brailovski, P. Terriault et le Dr R. Cartier, les travaux concernant la demande de brevet « Méthodologie et dispositif d'installation du système de fermeture du sternum » PCT/CA2007/002361 ont été complétés le 24 décembre 2007. Cette invention, qui a aussi demandé la participation de M. Chartrand, étudiant à la maîtrise, de F. Wallman et d'E. Plamondon, étudiants stagiaires, inclut la réalisation de 3 concepts dont deux ont été fabriqués sous forme de prototypes. La rédaction du brevet est l'œuvre de *Tessier et associés*. Malgré l'ordre officiel des auteurs apparaissant sur le brevet, il est entendu que je suis l'inventeur principal de cette solution technique.

Deux publications originales ont été écrites.

Un premier article qui présente l'ensemble des résultats d'essais fonctionnels du système de fermeture du sternum intitulé « Median sternotomy: comparative testing of braided superelastic and monofilament stainless steel sternal sutures » a été publié en mars 2009 dans le journal *Proceedings of the Institution of Mechanical Engineers Part H: Journal of Engineering in Medicine*, vol. 223, no 3, p. 363-374.

Un second article, « Fatigue properties of superelastic Ti-Ni filaments and braided cables for bone fixation », a été soumis au *Journal of Biomedical Materials Research: Part B: Applied Biomaterials* en décembre 2008.

Une publication en collaboration

M. Chartrand, étudiant à la maîtrise, a mis en œuvre et testé le banc d'essai « simulateur du sternum » que j'ai conceptualisé, avec l'aide du professeur V. Brailovski et d'E. Plamondon, étudiant stagiaire. Ce banc d'essai a fait l'objet d'un article accepté par la revue *Journal of Experimental Techniques* (Chartrand, Brailovski et Baril, déc. 2008) et qui est présenté en annexe I de ce document. Ce banc d'essai innovateur permet de simuler le comportement du sternum lors de l'installation du système de fermeture et permet d'appliquer des chargements latéraux, monotoniques, cycliques ou impulsifs, de façon symétrique ou asymétrique le long du sternum. Il permet aussi de recueillir des données absentes dans la littérature, soit les forces appliquées à l'interface entre les deux parties du sternum fermé et ce, tout au long de l'essai.

Quatre comptes-rendus de conférence ont également été publiés

- Baril, Y., V. Brailovski, P. Terriault et R. Cartier (2005). « Feasibility study of a new sternal closure device using tubular braided superelastic Nitinol structures ». *Materials & Processes for Medical Devices Conference* (nov. 2005), Boston, É.-U.
- Baril, Y., V. Brailovski, P. Terriault et R. Cartier (2008). « Modeling and testing of a new sternal closure device using tubular mesh-like superelastic structure ». *SMST-2006* : *International Conference on Shape Memory and Superelastic Technology* (mai 2006), Pacific Grove, É.-U.
- Baril, Y., V. Brailovski, M. Chartrand, P. Terriault et R. Cartier (2008). « In-vitro testing of a new superelastic sternum closure component ». *SMST-2007* (déc. 2007), Tsukuba, Japon
- Baril, Y., V. Brailovski et P. Terriault (2008). « Fatigue properties of superelastic Ti-Ni filaments used in braided cables for bone fixation ». *3rd International Conference on Smart Materials* (Juin, 2008), Acireale, Sicile, Italie.

REMERCIEMENTS

Je voudrais d'abord remercier mon directeur Vladimir Brailovski qui m'a fait confiance et m'a encouragé pendant ces dix dernières années. Merci pour votre soutien constant tout au long de ce projet.

Merci à mon amour, Mélanie, pour son support et son aide continuelle. Je voudrais aussi remercier mes deux rayons de soleil, Jaëlle et Maïté pour leurs éclats de rire qui éclairent mes journées.

Merci aussi à Raymond Cartier et à Patrick Terriault pour leurs conseils éclairants ainsi qu'au personnel technique de l'ÉTS, Patrick Sheridan, Michel Drouin, Serge Plamondon, Alain Grimard et Hugo Landry pour leur soutien.

Merci à tous mes collègues du LAMSI, Alexandre, Charles, Daniel, Dominique, Émeric, Jean-Sébastien, Kajsa, Karina, Pierre-Luc, Sébastien, Thomas, Vincent et Yan. Merci pour votre aide, vos encouragements, mais aussi pour tous ces agréables moments perdus à discuter. Un merci tout particulier aux stagiaires ayant participé à ce projet, Frédéric, Étienne et Karine. Merci aussi à Maxime, dont la collaboration à ce projet fut inestimable.

Merci enfin à ma famille sans qui je ne serais pas rendu là où je suis et à qui je dois une grande partie de cette deuxième brique de papier.

DÉVELOPPEMENT D'UN SYSTÈME DE FIXATION OSSEUSE PAR TRESSE EN ALLIAGE À MÉMOIRE DE FORME

BARIL, Yannick-Vincent

RÉSUMÉ

Ce projet a pour objectif de développer un système de fixation osseuse par tresse en alliage à mémoire de forme. Le développement de la tresse, débuté lors de précédents travaux, est complété. Ainsi, ce nouveau système de fixation osseuse augmente la stabilité de la fermeture et limite la contrainte de contact entre le système de fermeture et l'os. L'alliage à mémoire de forme superélastique permet de conserver une force de fermeture même si l'os s'est affaissé, alors que la géométrie du système, qui prend une forme méplate lors du contact avec l'os, augmente l'aire de contact.

Tandis que le fil en acier inoxydable standard est généralement torsadé pour être installé sur le sternum, une autre procédure doit être utilisée pour installer la tresse en alliage à mémoire de forme. Un nouveau système d'installation est donc conçu. Celui-ci a la particularité de charger la tresse et de limiter cette charge à une valeur maximale, ce qui optimise les caractéristiques de la tresse. L'outil peut aussi sertir le manchon utilisé pour fixer la tresse.

Les caractéristiques fonctionnelles des systèmes de fermeture par tresse et par fil en acier inoxydable sont ensuite comparées sur un banc d'essai maison simulant le comportement de la cage thoracique. Ce nouveau banc d'essai simule l'installation du système de fermeture, génère un chargement quasi statique et simule l'application de quintes de toux. Il permet aussi d'acquérir une donnée absente dans la littérature, la force de compression résiduelle, qui est un excellent indicateur de la stabilité du sternum. À l'aide de ce banc, la tresse en alliage à mémoire de forme se révèle plus performante que son équivalent en acier inoxydable lors de l'application répétée de charges importantes comme la quinte de toux tandis que leurs performances sont similaires lors de l'application de charges quasi statiques.

Pour finir, la vie en fatigue de la tresse est évaluée. Un chargement à déformation contrôlée est appliqué et fait varier la déformation moyenne et la déformation alternée. Les résultats suggèrent que la tresse pourrait supporter les perturbations externes anticipées, telles que des quintes de toux. Par ailleurs, bien que la déformation alternée soit le facteur le plus influent, la déformation moyenne a aussi un impact. Le chargement de la tresse devrait idéalement se situer à une déformation moyenne au centre du plateau de transformation afin de pouvoir bénéficier à la fois du comportement superélastique et d'une maximisation de sa vie en fatigue.

DESIGN OF A BRAIDED SHAPE MEMORY ALLOY BINDING COMPONENT

BARIL, Yannick-Vincent

ABSTRACT

This project aims to develop a shape memory alloy braided bone fixation system. The development of the braid, started in previous work is completed. Thus, this new bone fixation system increases the closure stability while limiting the contact pressure between the closure system and the bone. The superelastic material sustains the bone parts together even if bone collapse occurred whereas the tubular braided shape, which flattens at the contact of the bone surface, increases the closure contact area.

While standard monofilament stainless steel sutures are simply crossed, pulled and twisted to retain both sternum halves, the shape memory alloy braid must be installed with a particular procedure. To do so, a new installation device is designed. This system has the particularity of applying a specific tension to the braid and to limit this load to a maximum value, which optimizes its retention characteristics. The tool can also crimp the sleeve used to secure the braid.

The new braided sutures and the monofilament stainless steel suture are then compared on a new custom test bed modeling the rib cage behavior. This new test bed simulates the installation of the closure system on the sternum, generates a quasi static lateral loading and a dynamic simulation of coughing fits. The residual compressive force, which is an excellent indicator of the stability of the sternum and is absent in the literature, can also be measured. Using this bench, the braided suture is better than the competitive stainless steel suture to keep the closure closed following the repeated application of important loads similar to coughing fits. Yet, performances are similar to the standard stainless steel suture for quasi static loading.

Finally, the fatigue life of the cable is evaluated. The results of strain-controlled fatigue testing under variable mean and alternating strain conditions demonstrate that the braid could withstand anticipated external disturbances such as coughing fits. Moreover, even though alternating strain is the most influent parameter, mean strain also has a significant impact on the fatigue life of both the filament and the braid. An improvement in the braided cable's fatigue life is observed under mean strains corresponding to the middle of the superelastic loop plateau.

TABLE DES MATIÈRES

Page

LISTE DES TABLEAUX

Page

LISTE DES FIGURES

LISTE DES ABRÉVIATIONS, SIGLES ET ACRONYMES

SDF	Système de fermeture
AMF	Alliage à mémoire de forme
LAMSI	Laboratoire sur les alliages à mémoire de forme et les systèmes intelligents
STENT	Endoprothèse vasculaire

LISTE DES SYMBOLES ET UNITÉS DE MESURE

$F(A_f^{\sigma})$	Force atteinte à la fin de la transformation austénitique sous contrainte, N
$F(M_f^{\sigma})$	Force atteinte à la fin de la transformation martensitique sous contrainte, N
F_{COMP}	Force de compression, N
$F_{COMP,RES}$	Force de compression résiduelle, N
F_i	Force d'installation du système de fermeture, N
F_r	Force menant à la rupture de la tresse en alliage superélastique, N
F_s	Force à laquelle le sternum se fait altérer, N
F_{TENS}	Force de tension, N
$F_{TENS,MAX}$	Force de tension maximale, N
$F_{TENS,O}$	Force de tension menant à l'ouverture de la liaison du sternum, N
L	Longueur du sternum, m
r	Rayon du sternum, m
T	Force d'ouverture latérale sur le sternum, N
δ	Ouverture du sternum, mm
δ_{PERM}	Ouverture permanente du sternum, mm

INTRODUCTION

Le système classique de fermeture du sternum par fil en acier inoxydable est le plus couramment utilisé lors des chirurgies cardiaques à cœur ouvert. Toutefois, le nombre de complications associées à son utilisation demeure passablement élevé. Plusieurs systèmes de fermeture du sternum ont donc été développés pour tenter de pallier les problèmes occasionnés par le système de fermeture par fil.

Un système de fermeture prometteur composé d'une tresse tubulaire faite de filaments en alliage superélastique titane-nickel a récemment été développé par le Laboratoire sur les alliages à mémoire de forme et les systèmes intelligents (LAMSI) de l'École de technologie supérieure. Des travaux supplémentaires de conception et de validation sont cependant nécessaires avant que celui-ci puisse être utilisé dans des essais cliniques. Ce projet de doctorat a pour objectifs de dimensionner le système par tresse en alliage superélastique en établissant les paramètres de design, de concevoir un système d'installation permettant d'imposer une tension précise à la tresse lors de l'installation, d'effectuer la validation fonctionnelle du système et de réaliser une étude en fatigue du système développé.

Ce document présente l'ensemble des travaux reliés à la conception et à la validation du système de fermeture du sternum par tresse tubulaire faite de filaments en alliage superélastique. L'introduction générale traite de la problématique particulière du système de fermeture du sternum et des solutions existantes au problème. Les méthodes préconisées pour la modélisation in vitro des systèmes de fermeture y sont également présentées, de même que l'état de l'art sur les essais en fatigue appliqués aux systèmes de fermeture du sternum en général et aux alliages superélastiques en particulier. Le chapitre 2 décrit les solutions proposées (brevets 1 et 2), soit le système de fermeture du sternum par tresse tubulaire superélastique et la pince permettant son installation. Le chapitre 3 présente la méthodologie utilisée pour la validation du système de fermeture. Les chapitres 4 et 5 traitent respectivement de la validation fonctionnelle (article 1) et en fatigue (article 2) de la tresse superélastique. Cet ouvrage se termine par une conclusion rappelant les résultats importants de la thèse.

CHAPITRE 1

INTRODUCTION GÉNÉRALE

La tresse tubulaire faite de filaments en alliage superélastique est probablement adaptable à de nombreuses applications en orthopédie où la stabilité d'une liaison osseuse est un objectif important. Par exemple, des travaux récents de notre équipe ont démontré que ces câbles pourraient potentiellement être utilisés pour maintenir la position du grand trochanter à la suite de son ostéotomie pratiquée lors du remplacement d'une prothèse fémorale. Cependant, puisque la présente thèse porte exclusivement sur la fermeture du sternum, seule cette application est traitée dans ce chapitre. La problématique de la fermeture du sternum est d'abord présentée. Ensuite, deux sections traitent respectivement des systèmes de fermeture existants et des outils proposés pour mener à bien ces fermetures. Les aspects associés à la modélisation du sternum in vitro et à la méthodologie d'essais en fatigue des câbles orthopédiques terminent ce chapitre.

1.1 Problématique et description des particularités du système de fermeture du sternum

L'opération à cœur ouvert constitue encore l'opération la plus courante lors des pontages coronariens, des transplantations cardiaques et de plusieurs autres opérations touchant les organes se trouvant à l'intérieur de la cage thoracique (709 000 opérations aux États-Unis en 2002 (Rosamond et al., 2007)). Cette opération permet d'obtenir une voie d'accès aisée aux organes internes de la cage thoracique et elle est bien supportée par une grande majorité de patients. Malgré cela, la fermeture de la cage thoracique suite à l'opération est sujette à une mauvaise guérison dans environ 2 % des cas (Casha et al., 2001b). Les problèmes associés sont très variables, allant de l'infection de la plaie à la rupture du sternum. Ces problèmes apparaissent généralement dans les 30 jours suivant l'opération (Shroyer et al., 2003) et peuvent causer la mort du patient (Stahle et al., 1997).

Toute opération à cœur ouvert débute par l'ouverture du thorax. Une fois les couches superficielles retirées, le sternum est découpé à l'aide d'une scie oscillante électrique le long

de sa ligne médiane (figure 1.1a). Le sternum est un os long et plat qui fait la jonction entre les côtes de la cage thoracique. Il mesure environ 17 cm de long par 1 cm d'épaisseur et 2,5 cm de largeur. L'os est constitué de trois parties (figure 1.1b): le manubrium, le corps et l'appendice xiphoïde. Enfin, l'extérieur du sternum est composé d'une mince couche d'os compacte et rigide (os cortical), tandis que l'intérieur est composé d'un tissu spongieux moins rigide et fortement vascularisé (Gray et Lewis, 1918). Le comportement mécanique général du sternum est défini comme étant celui des os spongieux (Casha et al., 2001b).

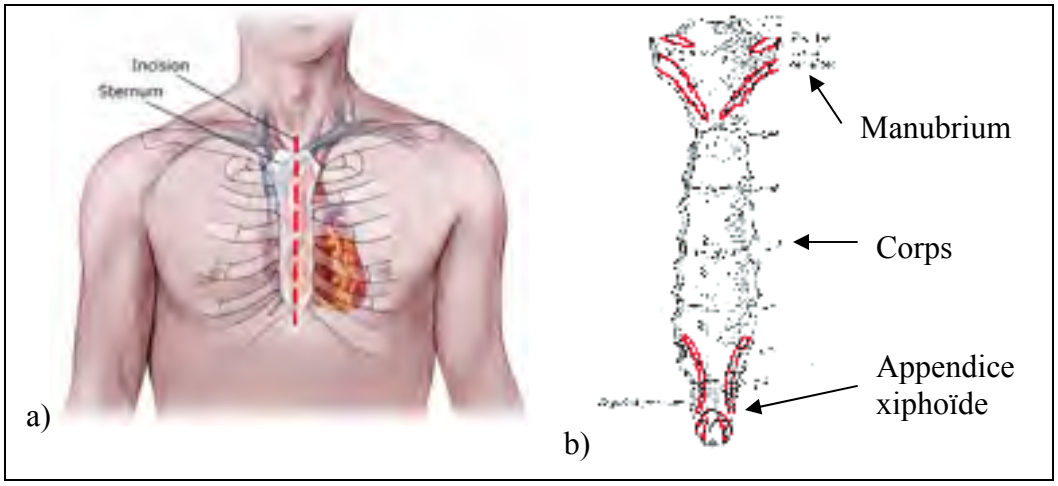

Figure 1.1 a) Schéma d'une sternotomie; b) Composition du sternum.
Tirée de a)©medmovie.com 2002[1] (Inconue, 2002) et b) adapté de Gray et Lewis (1918)[2].

Une fois l'opération complétée, la cage thoracique est refermée par le chirurgien. La fermeture du thorax consiste à mettre les deux parties du sternum en contact et à y appliquer une pression, pour mettre la fracture en compression. Cela limite le mouvement relatif des deux parties en contact et favorise l'ostéogenèse, c'est-à-dire la formation du tissu osseux (Eggers, Shindler et Pomerat, 1949). Ainsi, les techniques de fermeture du sternum

[1] Avec la permission de : ©medmovie.com Tout droits réservés

[2] Avec la permission de : ©Bartleby.com, Inc.Tout droits réservés

employées font généralement appel à l'ajout de liens, tel qu'illustré à la figure 1.2. Une tension est appliquée sur les liens pour que la fracture soit effectivement mise en compression. Selon le type de système de fermeture, de 1 à 10 liens peuvent être ainsi mis en place. Dans le cadre de cette thèse, chacun des liens de la fermeture du sternum est défini comme étant un « système de fermeture du sternum » (SDF).

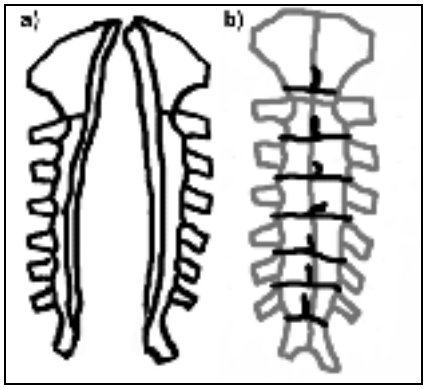

Figure 1.2 Illustration d'une fermeture du sternum par fil : a) sternum découpé; b) sternum refermé à l'aide de sept fils de fermeture.

1.2 Systèmes de fermeture existants

La fermeture par fils est la première technique qui a été proposée (Milton, 1987). Elle demeure également la technique la plus populaire, car elle est simple d'utilisation. Quatre à huit fils (Losanoff et al., 2004) forment une boucle qui passe autour du sternum (péristernalement) ou à l'intérieur (transsternalement). Dans ce dernier cas, le sternum est alors percé à l'aide de l'aiguille du fil de suture. Initialement, des fils d'argent étaient utilisés, mais ils ont ensuite été remplacés par des fils d'acier inoxydable. La technique de suture par fils la plus populaire consiste à utiliser six fils simples, soit un fil sur le manubrium (partie supérieure du sternum) et cinq, sur le corps du sternum.

Bien qu'il soit populaire, le SDF par fils inoxydable n'est pas exempt de problèmes. Les fils exercent une très forte contrainte au point de contact entre le sternum et le système de fermeture. Cette forte contrainte est la cause d'une grave complication associée à la

fermeture du sternum (figure 1.3), soit la rupture du sternum à la suite de son sectionnement par les fils (Robicsek, Daugherty et Cook, 1977).

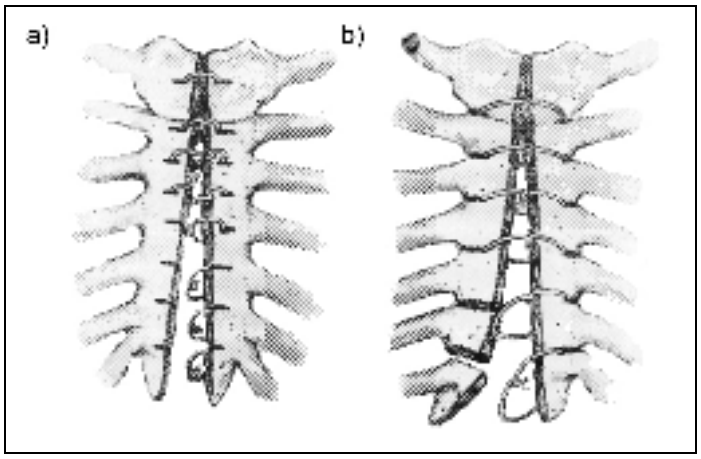

Figure 1.3 Rupture d'un sternum relié avec un SDF à fils : a) SDF transsternal; b) SDF péristernal.
Tirée de Robicsek, Daugherty et Cook (1977).

Ainsi, de nombreuses autres façons d'installer les fils ont été développées afin de diminuer les contraintes sur le sternum ou d'augmenter la rigidité du système (Casha et al., 2001a). Par exemple, Robicsek, Daugherty et Cook (1977) proposent d'ajouter aux fils péristernaux simples deux autres fils longitudinaux passant autour des côtes sur lesquels les premiers fils viennent s'appuyer. Cela permet de diminuer la pression de contact entre les fils et le sternum. Une autre méthode populaire, décrite dans plusieurs ouvrages, est la méthode « figure en 8 » qui consiste à croiser les fils derrière le sternum (Di Marco et al., 1989). Cette technique a pour but d'augmenter la rigidité dans la direction rostro-caudalde. Une multitude d'autres systèmes par fils existent (Losanoff, Jones et Richman, 2002).

D'autres systèmes que les fils ont également été développés dans le but d'augmenter la rigidité et de diminuer la pression appliquée sur le sternum. La figure 1.4 présente quelques exemples décrits en détail plus bas.

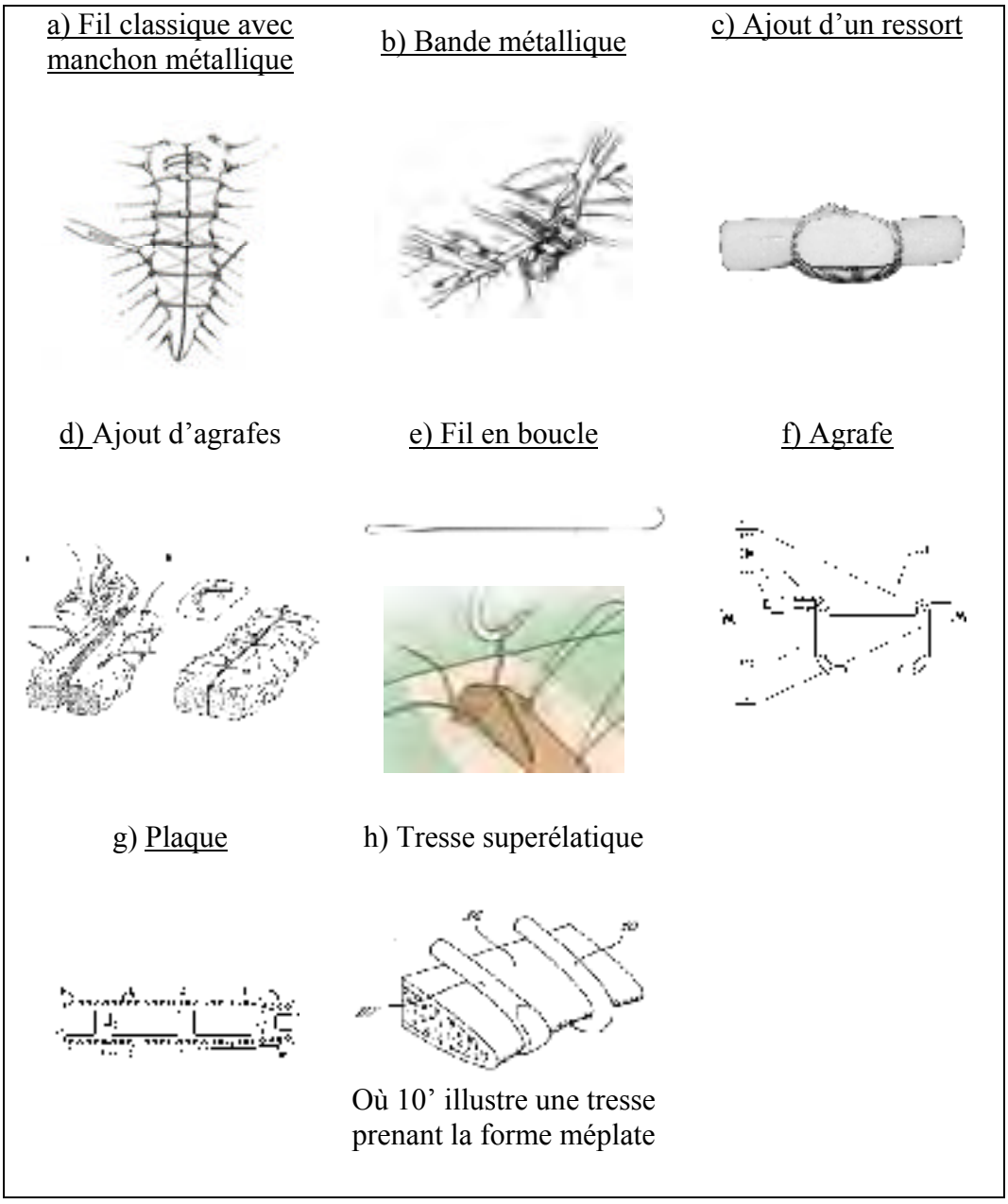

Figure 1.4 Techniques modernes de fermeture du sternum.
a) fil de suture standard fixé par des manchons métalliques (Di Marco et al., 1989); b) bande métallique (Soroff et al., 1996); c) diminution de la pression par pression par l'ajout de ressort augmentant le diamètre (McGregor et al., 2003); d) plaque rigide (Astudillo, 1992); e) agrafe (Lemer, 2002); f) fil en forme de boucle pouvant être serré à l'aide d'un crochet (Kiessling et al., 2005); g) ajout d'agrafes (Okutan, Tenekeci et Kutsal, 2005); h) tresse superélastique (Brailovski et al., 2006).

L'utilisation de rubans comme SDF diminue le risque de rupture en augmentant la surface de contact entre l'os et le SDF (figure 1.4b). Les rubans, tels que les *Sterna-band* (Stony Brook Surgical Innovations, Inc., Stony Brook, NY, ÉU), sont faciles à retirer, car ils peuvent être sectionnés par une simple paire de ciseaux (Soroff et al., 1996). Un mécanisme à cliquet permet une fixation aisée de la fracture. Par contre, les rubans manquent de souplesse et n'épousent pas bien la géométrie du sternum (Cheng et al., 1993; Losanoff, Richman et Jones, 2002). Leur géométrie fait en sorte qu'ils ne peuvent traverser l'os facilement et qu'ils doivent obligatoirement être passés péristernalement. Leur forte largeur est incommodante, car ils déplacent les muscles en place pour épouser la forme du sternum. Leurs bords tranchants coupent parfois les muscles et causent ainsi une hémorragie interne. De plus, il semble que l'utilisation de rubans ne présente pas d'avantage marqué au niveau de la rigidité du système : la rigidité de la fermeture des rubans est en effet moins grande ou comparable à celle des fils puisque généralement quatre rubans sont utilisés au lieu de 6 à 10 pour les fils (Cheng et al., 1993).

D'autres systèmes misent sur l'augmentation de la surface de contact avec le sternum pour réduire les risques de rupture. À titre d'exemple, McGregor et al. (2003) proposent de faire passer le fil d'acier inoxydable péristernalement et à l'intérieur d'un ressort en acier inoxydable (figure 1.4c). Cela réduit significativement la contrainte de contact entre le SDF et le sternum et permet de doubler la charge latérale supportable par le système, mais cela ne modifie pas la rigidité de la fermeture. D'autre part, la masse du SDF se trouve considérablement augmentée par la présence du ressort et le fil doit être passé péristernalement, ce qui limite la versatilité du système proposé. Okutan, Tenekeci et Kutsal (2005) proposent d'insérer des agrafes, similaires aux agrafes utilisées en construction ou en papeterie, entre le fil qui pénètre dans l'os lors d'un passage péristernal et l'os du sternum, ce qui a pour effet de réduire la contrainte en ce point (figure 1.4d).

Dans la même veine, Kiessling et al. (2005) présentent un système de fermeture fait d'un fil faisant une boucle (figure 1.4e). Au point où les deux extrémités du fil se rejoignent pour former la boucle, une aiguille est placée pour l'installation sur le sternum. La boucle est passée autour du sternum et ses deux extrémités sont torsadées à l'aide d'un outil en forme de

crochet, ce qui permet d'appliquer la force de fermeture de la même façon que sur un fil. Cette configuration permet de passer deux fils simultanément au lieu d'un seul, ce qui fait doubler l'aire de contact avec le sternum, et ainsi, la rigidité du SDF. Selon les résultats présentés, l'utilisation de cette technique réduit significativement les cas d'instabilité du sternum (1 cas versus 6 pour une fermeture par fil simple ($p < 0,05$)). Un système similaire a été testé avec succès par Losanoff et al. (2007). La limitation majeure est la même que pour la précédente technique, soit que le passage simultané de deux fils empêche le passage transsternal. Par conséquent, l'auteur ne suggère son utilisation que pour des cas à haut facteur de risque.

Les agrafes constituent le SDF le plus rigide et le plus fiable de tous (figure 1.4f). Par exemple, Negri et al. (2002) font l'évaluation d'agrafes en alliage à mémoire de forme qui maintiennent la liaison osseuse grâce à l'élasticité du matériau qui la compose. Par contre, les agrafes sont des pièces massives et peuvent entraîner des douleurs ou des désagréments importants au patient. Ce système de fermeture n'est donc utilisé que sur les patients chez qui le risque de rupture du sternum ou d'infection est important. Ce même constat peut être fait pour les SDF par plaque (figure 1.4g) qui sont très rigides, mais sont très massifs en plus d'être généralement longs à installer.

Comme solution au problème de stabilité du sternum, nous proposons un système de fermeture en alliage superélastique sous forme d'une tresse tubulaire (Baril, 2004), illustré à la figure 1.4h. Ce système est une modification du système classique par fil en acier inoxydable et peut donc être installé selon les mêmes arrangements. Il permet d'augmenter l'aire de contact entre le SDF et le sternum et il bénéficie de la superélasticité pour améliorer la stabilité de la liaison. La description détaillée de ce système est faite au chapitre 2 (p. 26).

Outre les systèmes décrits ici, plusieurs autres viennent s'ajouter à la liste comme les rubans de Mersilene (Puc et al., 2000), et plus récemment, un système complexe incorporant des fils et des ancrages (Rousseau, Weadock et Chatlynne, 2008).

1.3 Outils d'installation des systèmes de fermeture existants

Plusieurs outils ont été proposés à ce jour pour faciliter la pose du SDF et réduire les manipulations du chirurgien (Abboudi, 2001; Johnson et al., 2002; Lemer, 2002; Magovern, 2000; Miller et S., 2003; Scott, 2001; Songer et Korhonen, 1998). Néanmoins, les chirurgiens préfèrent encore la méthode manuelle classique. Un fil en acier inoxydable combiné à une aiguille courbé est passé à travers ou autour des parties du sternum afin de les joindre. Une fois les fils adéquatement positionnés, le chirurgien torsade les fils à l'aide de pinces pour qu'une tension soit effectivement appliquée.

Cette méthode présente toutefois quelques inconvénients. Le plus important est sans doute que lorsque le sternum est fermé manuellement, il est difficile, voire impossible, d'évaluer de façon précise la force appliquée au système de fermeture et de reproduire cette force d'un système de fermeture à l'autre. Or, l'application d'une tension prédéterminée au système de fermeture permet de limiter la pression de contact entre le SDF et l'os et ainsi diminuer le risque de défaillance au niveau de la surface de contact (découpage du sternum sous l'effet d'une toux sévère ou d'une respiration profonde). De plus, le fonctionnement du système de fermeture du sternum par tresse tubulaire superélastique dépend de l'application précise de cette charge au risque d'en diminuer l'efficacité en appliquant une charge trop faible, ou de l'altérer, en appliquant une charge trop importante.

Mentionnons que tous les appareils qui ont été proposés à ce jour pour améliorer la pose du SDF peuvent être catégorisés selon le type de système de fermeture : les agrafes, les fils et plaques, ou les fils seulement.

La première catégorie d'appareils, dont un exemple est illustré à la figure 1.5, effectue la totalité du travail d'installation. L'outil illustré facilite : le perçage du sternum (4) à l'aide des deux forets (65,66), la pose de l'agrafe (131) par l'action du poussoir (142) et le contrôle de la position finale de l'agrafe après son installation par la pince de positionnement (13,22) (Lemer, 2002).

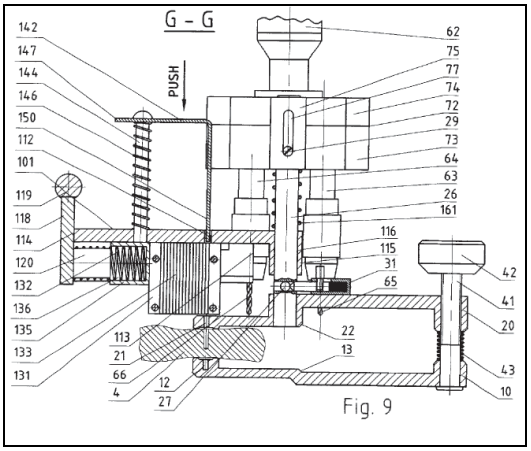

Figure 1.5 Exemple d'outil d'installation pour un SDF à broches.
Tiré de Lemer (2002).

Le second type d'outil, dont un exemple est illustré à la figure 1.6, facilite la pose d'une plaque ou d'un fil sur le sternum (Abboudi, 1996; Brown, 1998; Crossett, Willard et Albuquerque, 1980; Gabbay, Randall et Hills, 1989; Magovern, 2000; Miller et S., 2003). La mise sous tension du fil est encore une fois effectuée manuellement par le chirurgien.

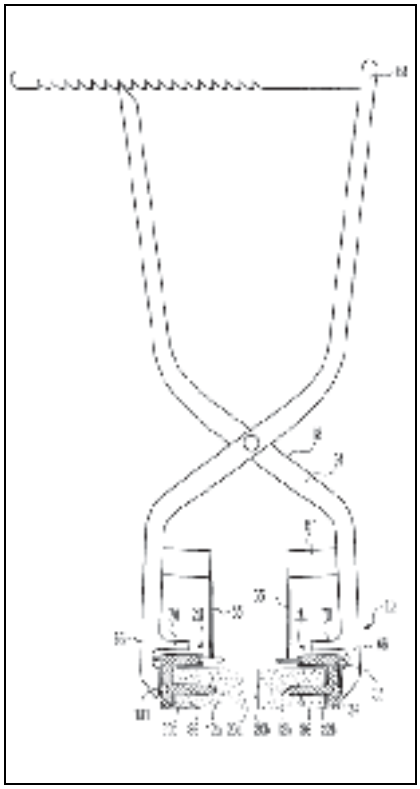

Figure 1.6 Exemple d'outil d'installation pour un SDF à plaques et fils.
Tiré d'Abboudi (2001).

Enfin, la troisième catégorie d'appareils facilite l'installation de SDF de type « fils ». Certains de ces appareils sont également conçus pour permettre le contrôle de la force appliquée (Johnson et al., 2002; Songer et Korhonen, 1998; Sutherland et Vascocellos, 1988). Cependant, la force appliquée n'étant pas limitée mécaniquement, il est encore possible de dépasser la tension visée et d'endommager les tissus osseux. De plus, la procédure de mise sous tension s'effectue à l'aide d'un mouvement de rotation qui nécessite l'utilisation simultanée des deux mains.

En analysant les systèmes existants, les exigences fonctionnelles suivantes doivent être considérées. Pour être en mesure d'appliquer une charge précise sur le SDF sans risquer de la dépasser, un système d'installation des SDF doit pouvoir soustraire le SDF de tout chargement excédentaire. Son utilisation doit être aisée et, de préférence, la mise sous tension

doit être faite d'une seule main et sans mouvement de rotation. Ainsi, le chirurgien peut utiliser son autre main pour stabiliser l'appareil, ce qui réduit le risque de blesser le patient. Ces exigences seront considérées comme objectifs de design lors du développement de notre outil d'installation.

1.4 Validation *in vitro* des systèmes de fermeture du sternum

Plusieurs méthodes d'évaluation des systèmes de fermeture du sternum sont utilisées dans la littérature et sont tour à tour décrites dans cette section. Des modèles de chargement sont développés pour déterminer les charges à appliquer sur les systèmes de fermeture et établir les bases de comparaison entre les SDF. Certains auteurs utilisent des moyens de comparaison des systèmes par calculs théoriques. D'autres utilisent les essais expérimentaux pour évaluer les systèmes en laboratoire.

1.4.1 Modèles de chargement

Tel que décrit plus haut, les liens unissant les deux parties du sternum doivent supporter les charges normales imposées par la respiration sans que le sternum se sépare. Ils doivent également supporter des charges plus sévères, comme des quintes de toux, sans se rompre ou couper le sternum. Le modèle de Casha et al. (1999) est universellement reconnu lorsqu'il s'agit de déterminer les charges maximales appliquées sur les SDF lors d'une importante quinte de toux.

Modèle de Casha et al.

Casha et al. (1999) proposent un modèle mathématique de cylindre sous pression pour évaluer la force de sollicitation qu'une quinte de toux applique sur le sternum. L'équation suivante établit cette relation :

$$T = rLP, \tag{1.1}$$

où T est la force requise pour maintenir le sternum fermé, r est le rayon transverse de la cage thoracique, L est la longueur du sternum et P est la pression relative générée à l'intérieur de

la cage thoracique lors d'une quinte de toux. En substituant, dans l'équation 1.1, les dimensions du thorax (environ 15 cm de rayon, 25 cm de long) et la pression maximale pouvant être atteinte lors d'une importante quinte de toux (40 kPa pendant une période de 200 millisecondes), on obtient la force de sollicitation :

$$T = rLP = (0{,}15m \times 0{,}25m) \times 40kPa = 1500\ N\,. \qquad (1.2)$$

Pour connaître la charge appliquée par la cage thoracique sur le SDF par fil, on divise la charge totale par le nombre minimum de fils, soit un minimum de 6 fils. On obtient alors une charge de 250 N par SDF. Cette dernière force est reconnue par la majorité des auteurs comme étant la force maximale qu'un SDF doit être en mesure de supporter.

Validation du modèle de Casha et al.

Selon Casha, Yang et Cooper (1999), leur modèle a été validé par l'étude de McGregor, Trumble et Magovern (1999) qui ont testé quatre sujets cadavériques ayant subi une sternotomie refermée à l'aide de 7 fils péristernaux. Dans cette étude, deux types de chargements sont appliqués : a) une charge latérale sur le sternum entier de 220±40 N qui cause une ouverture de 1,85 ± 0,14 mm et b) une pression intrathoracique de 63 ±21 mmHg (8,4 ± 2,8 kPa) à l'aide de deux ballons salins installés de chaque côté du thorax dans les cavités pleurales causant une ouverture de 2,14 ± 0,11 mm.

En considérant que les deux chargements, le chargement latéral et l'augmentation de la pression interne, génèrent approximativement la même ouverture, Casha, Yang et Cooper (1999) suggèrent donc que 260 N de force latérale est équivalente à une pression de 5,6 kPa (42 mmHg) (Eq 1.3). En substituant la pression de 5,6 kPa dans l'équation (1.1) et en utilisant un rayon un peu plus important que dans leur modèle initial (17 cm) et une longueur de 25 cm, ils obtiennent une charge latérale de 240 N, proche de la valeur de 260 N (Eq. 1.4) extrapolée des résultats de McGregor, Trumble et Magovern (1999), ce qui confirmerait la validité de leur modèle de chargement.

$$\left.\begin{array}{c} 260\ N \Rightarrow\approx 2\ mm \\ 5,6\ kPa \Rightarrow\approx 2\ mm \end{array}\right\} \Rightarrow 260\ N \Leftrightarrow 5,6\ kPa \qquad (1.3)$$

$$\left.\begin{array}{c} 5.6kPa \Leftrightarrow 260N \\ T = rLP = (0,17m \times 0,25m) \times 5.6kPa \approx 240N \end{array}\right\} 260N_{\text{exp.}} \approx 240N_{\text{model}} \qquad (1.4)$$

À l'aide de cette même étude sur des sujets cadavériques, McGregor, Trumble et Magovern (1999) montrent aussi que les efforts latéraux, comme ceux appliqués lors d'une quinte de toux, sont plus dommageables pour l'intégrité du sternum que ceux appliqués dans les directions orthogonales. Ils proposent donc de se baser uniquement sur les forces appliquées latéralement au sternum pour effectuer la comparaison des systèmes de fermeture. D'autant plus que les forces appliquées dans cette direction sont estimables à l'aide d'un modèle mathématique simple (Éq. 1.1), alors qu'elles sont inconnues dans les autres directions.

Critique du modèle de Casha et al.

Étant donné qu'une pression de 5,6 kPa cause déjà une ouverture de 2 mm au processus xiphoïde, les sujets de l'étude de McGregor, Trumble et Magovern (1999) se disloqueraient si on leur appliquait les 40 kPa proposés par (Casha, Yang et Cooper, 1999).

En effet, lors d'expérimentations en laboratoire sur des fils simples, Casha et al. (1999) démontrent que les fils de suture standards se « détorsadent » à une charge d'environ 225 N et que les fils pénètrent dans l'os du sternum en permettant la séparation des deux moitiés de l'os pour une charge de 10 kg (98 N) répétée 25 fois (Casha et al., 2001b). Même pour une pression de toux qualifiée de « normale » par Casha, Yang et Cooper (1999), trois fois plus faible que la pression maximale, une force de 560 N serait développée sur un sternum complet, ce qui détruirait la majorité des sternums fermés. En fait, la plus grande charge qui a été appliquée sur des sternums complets, et non sans endommager les sternum, est de 100 N par SDF (Losanoff et al., 2007). Cette charge a été appliquée 160 fois sur des sternums de sujets cadavériques reliés par 8 fils péristernaux (800N pour le sternum complet).

En somme, nous croyons que le modèle de Casha et al. surestime les charges d'ouverture de façon significative. Par conséquent, la charge de 1500 N peut être utilisée comme valeur de référence, mais non comme seuil de performance en deçà de laquelle un SDF ne serait pas fiable.

Finalement, les études comparatives de différents SDF deviennent donc un outil essentiel. Ainsi, dans le cadre de cette thèse, nous prévoyons appliquer, pour les essais de charge cyclique, 80 % des 1500 N proposés par Casha et al. pour un sternum complet. Cette charge sera supportée par l'ensemble des systèmes que nous allons tester (voir au chapitre 4).

1.4.2 Modèles mathématiques

Les modèles mathématiques permettent de tester virtuellement un grand nombre de systèmes biomécaniques à un coût relativement faible. Dans le cas des SDF, leur utilisation permettrait de mieux connaître les phénomènes d'interaction mécanique entre le sternum et le système de fermeture. La recension des écrits suggère toutefois que, jusqu'à maintenant, l'utilisation des modèles mathématiques a été relativement rare.

Certains auteurs modélisent uniquement la contrainte de contact. La loi de Hertz est directement appliquée par Jutley et al. (2001) bien qu'elle ne soit valable que pour de faibles déformations de matériaux élastiques. D'autres auteurs utilisent la méthode des éléments finis pour faire la même démonstration (Casha et al., 2001a).

John (2008) présente un modèle statique du système de fermeture du sternum afin d'évaluer la charge dans le câble pour d'autres fermetures que la fermeture péristernale simple. Il compare deux sutures en huit combinées avec quatre sutures simples et une suture plus complexe appelée « suture longitudinale croisée antérieure ».

Un modèle numérique 3D de cage thoracique construit à partir de coupes tomodensitométriques (*CT scan*) est utilisé pour modéliser des systèmes de fermeture du sternum par fil d'acier simple (péristernal) et par fil en figure de 8 (Bruhin et al., 2005). Toutefois, le système proposé est trop complexe tandis que les chargements imposés sont

trop simplistes. La dynamique des efforts appliqués sur la cage thoracique devrait être mieux connue avant de s'encombrer d'un tel modèle.

Pour pallier aux lacunes des modèles 2D sans avoir les problèmes de définition des chargements et des conditions frontière reliées au modèle 3D, nous avons développé une méthode de calcul utilisant la méthode des éléments finis 1D (Baril, 2004). Ce modèle représente le système mécanique de la fermeture du sternum en trois ressorts au comportement mécanique non-linéaire, soit deux ressorts en compression et un ressort en tension (Figure 1.7), et il permet la comparaison de systèmes de fermeture dont la géométrie est similaire.

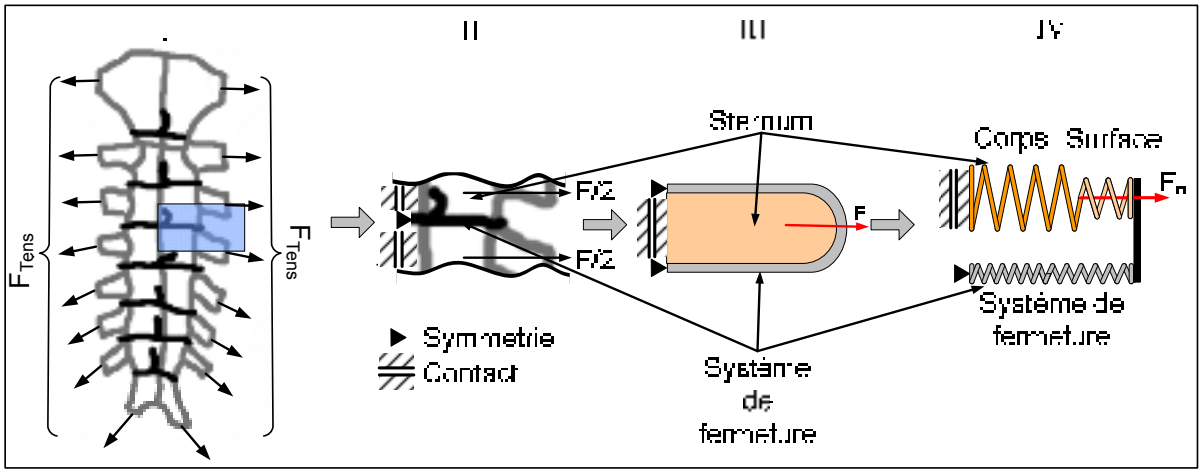

Figure 1.7 Simplification du système de fermeture.
Réduction du sternum complet (I) à un seul fil et une seule moitié (II); un état à deux dimensions (III); puis, à une seule dimension (IV); la force extérieure est appliquée entre les deux ressorts. F_{TENS} est la force totale appliquée sur le sternum; F est la force appliquée sur un SDF.

Ce modèle numérique utilise le modèle de chargement de Casha et al. (1999) pour appliquer les efforts externes et ainsi simuler des quintes de toux. En utilisant des propriétés de matériaux simulant la plasticité, il est possible de simuler l'effet d'une surcharge sur les forces refermant la liaison. Une application de ce modèle est illustrée à l'annexe IV.

1.4.3 Modèles physiques de laboratoire

La majorité des travaux visant à comparer divers systèmes de fermeture du sternum utilisent les essais en laboratoire. Les modèles utilisés pour simuler le sternum sont biologiques ou synthétiques.

Modèles biologiques

Les modèles biologiques visent à se rapprocher le plus possible de l'application réelle. Dans certaines études, des sternums retirés d'animaux sont montés sur un banc d'essai (Hale, Anderson et Johnson, 1999), Dans d'autres, des spécimens cadavériques humains sont utilisés (Casha et Gauci, 2003; Losanoff et al., 2007; Losanoff et al., 2004).

Modèles en matériaux synthétiques

Les modèles synthétiques se divisent en deux catégories. On retrouve d'abord des sternums rigides qui ne simulent pas le comportement du sternum, mais seulement sa géométrie. Ce type de modèle sert à comparer la rigidité du système de fermeture sans égard au comportement du sternum (Jutley et al., 2001).

L'autre type de modèles utilise les mousses polymériques qui ont pour fonction de simuler le comportement d'un os. Ces systèmes permettent une comparaison plus fine du comportement global des systèmes de fermeture. Les modèles en polyuréthane représentent le sternum en totalité (Casha et al., 2001a; Cohen et Griffin, 2002; Pai et al., 2007; Pai et al., 2005) ou en partie (Bruhin et al., 2005). De plus, des mousses de polyuréthane de densités différentes sont utilisées afin de simuler des sternums de rigidités différentes.

Deux études font le pont entre les modèles biologiques et synthétiques du sternum. L'étude de Trumble, McGregor et Magovern (2002) reproduit les essais des McGregor, Trumble et Magovern (1999) avec un modèle du sternum complet en polyuréthane d'une densité 0,32 g/cm^3. Les résultats obtenus montrent que lors d'essais statiques, les modèles de sternum en polyuréthane représentent bien le comportement du sternum d'un sujet cadavérique humain. La seconde étude (Hale, Anderson et Johnson, 1999) est

particulièrement intéressante parce qu'elle compare directement des sternums de porc et des sternums synthétiques. Deux densités de polyuréthane sont utilisées, soit 0,24 g/cm^3 et 0,48 g/cm^3, afin de simuler respectivement des sternums de porc rigide et moins rigide. Les courbes de force-déplacement mesurées suggèrent que le comportement des modèles de polyuréthane est similaire à celui des modèles biologiques (voir la figure 1.8).

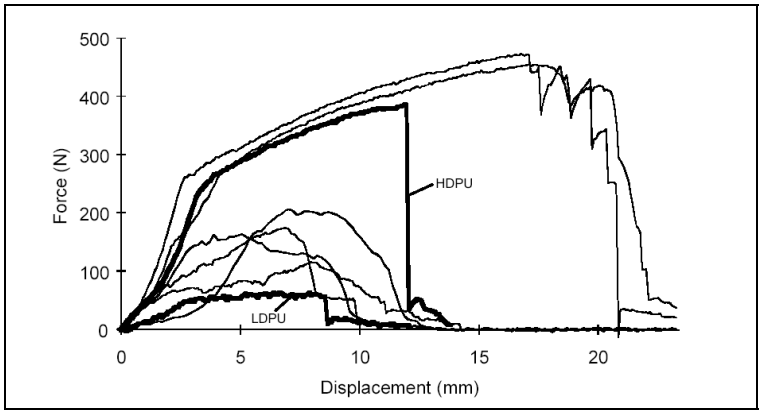

Figure 1.8 Courbes force-déplacement pour des modèles de polyuréthane (lignes grasses) (0,24 g/cm^3 (LDPU) et 0,48 g/cm^3 (HDPU)), se faisant découper par un fil d'acier, et pour un modèle biologique de porc (lignes fines).
Tirée de Hale, Anderson et Johnson (1999)

Malgré les résultats de ces études comparatives et malgré le fait que la majorité des études a pour objectif de comparer des systèmes de fermeture plutôt que d'obtenir des valeurs absolues, certains auteurs n'apprécient toujours pas les modèles synthétiques. Ils prétendent que l'utilisation d'un matériau ne représentant pas parfaitement le comportement viscoplastique du sternum discrédite les résultats obtenus (Casha et Gauci, 2003).

1.4.4 Conclusion

Lors d'une étude préliminaire (Baril, 2004), un modèle mathématique et un modèle en laboratoire d'os de sternum simplifié ont été utilisés pour comparer les SDF. Dans la présente thèse doctorale, nous préconisons l'utilisation d'un modèle synthétique en polyuréthane d'une densité de 0.32 g/cm^3 pour représenter le comportement d'un sternum de rigidité moyenne. Les caractéristiques de ce type de matériau sont plus homogènes que celles d'un

modèle biologique, ce qui en fait un meilleur outil pour discriminer les performances d'un SDF par rapport à un autre. De plus, le nombre de répétition peut aisément être augmenté. La géométrie du sternum, de même que le mode de distribution des SDF le long du sternum, pouvant avoir leur importance, il est préférable d'utiliser des modèles de sternum complet. De plus, la mousse de polyuréthane est également un matériau viscoplastique, ce qui permet de comparer le comportement des SDF lors de charges répétées dans le temps.

1.5 Résistance en fatigue des câbles de suture biomédicaux

Un des aspects importants à vérifier lors du développement d'un nouvel implant permanent est la résistance en fatigue de ce dernier. La section suivante traite donc des aspects reliés aux essais en fatigue sur des systèmes de fermeture du sternum et sur la fatigue des alliages titane-nickel superélastique.

1.5.1 Vie en fatigue des fils de suture du sternum

La majorité des études portant sur un système complet de SDF imposent un nombre de cycles de chargement inférieur à 200 cycles. Losanoff et al. (2007) présentent l'étude comportant le plus grand nombre de cycles sur des systèmes complets, soit 160 cycles à 800 N. De plus, dans ces études, bien que certaines ruptures de fils soient rapportées, la détérioration apparait plutôt comme une accumulation de dommages au niveau du sternum. Pour un système de fermeture par fil en acier inoxydable classique, Losanoff et al. (2007) observent que cette détérioration induit un déplacement des fragments de 4,84 mm en moyenne. L'ampleur des détériorations mesurées dans cette étude est similaire à ce qui est répertorié dans la littérature.

Jutley, Shepherd et Hukins (2003) ont testé des boucles de SDF contenant des vis sternales annulées au travers desquelles on a fait passer le fil en acier inoxydable n^{o} 5 pour réduire les contraintes de contact sur le sternum. Ces essais démontrent que pour une charge dite « standard » soit de 41 à 83 N (environ de 50 à 100 MPa dans le fil), ce système supporte entre 25 000 et 30 000 cycles. Le ratio R utilisé (dans ce cas, la force maximum sur la force minimum) est de 10, tel que recommandé par la norme ASTM F1717 sur les implants dédiés

à la colonne vertébrale. Cette étude n'étant pas comparative, nous ne connaissons pas le nombre de cycles supporté par un système classique soumis à des sollicitations équivalentes.

Compte tenu de ces informations, notre système doit donc démontrer des avantages mécaniques lors de l'imposition d'une charge mécanique relativement élevée, à savoir 800 N durant un nombre de cycles relativement faible (≈ 200) sur un modèle de sternum complet. Il doit aussi être en mesure de supporter un nombre de cycles beaucoup plus important, soit environ 25 000 cycles, pour une charge maximale de 83 N pour une seule boucle.

Par ailleurs, Chun-Ming et al. (2005) ont étudié les causes de rupture des fils de SDF en acier inoxydable retirés des patients après une période variant entre 5 et 729 jours postopératoires (moyenne : 149). Ces ruptures peuvent être causées par des raisons différentes qui sont répertoriées dans l'article sans discrimination : a) application d'une charge excessive par le chirurgien lors de la torsade des bouts du fil, b) corrosion par piqûration, c) propagation de fissures sous contrainte par corrosion en bout de fissure et d) fatigue par corrosion. Ces résultats montrent que le milieu corrosif présent dans le corps est un enjeu important et que des essais en fatigue dans une solution simulant les fluides organiques devraient ultimement être faits. Ce type d'essais n'est cependant pas prévu dans le cadre de cette thèse doctorale.

1.5.2 Vie en fatigue de composantes biomédicales superélastiques

Dans le domaine biomédical, deux modes de sollicitation peuvent être employés lors des études en fatigue. Le premier mode, le contrôle en déformation, est le plus couramment utilisé parce qu'il est facile à implémenter. C'est d'ailleurs le mode choisi par l'ensemble des articles cités dans cette section. Le deuxième mode, le contrôle en contrainte, est probablement plus proche du cas réel en orthopédie. Par contre, pour les alliages superélastiques, ce mode de sollicitation est difficile à mettre en œuvre lorsque l'on désire caractériser le comportement global de l'implant. Il serait en effet difficile de générer une contrainte précise à l'intérieur d'une boucle d'hystérésis. Il a donc été choisi de faire les essais de résistance en fatigue en mode de déformation contrôlée.

Tous les auteurs s'accordent sur le fait que la déformation alternée a plus d'effet sur la vie en fatigue des alliages titane-nickel superélastiques que la déformation moyenne et que plus la contrainte alternée est élevée, moins grande est la vie en fatigue. Cela a été vérifié pour la flexion rotative d'outils odontologiques pour le traitement de canal (Bahia, Gonzalez et Buono, 2006; Bahia, Fonseca Dias et Buono, 2006; Cheung et Darvell, 2007; Robertson et al., 2007; Tobushi et al., 2000; Young et Vliet, 2005) et lors d'essais sur des branches d'endoprothèses vasculaires (STENTS) (Gong et al., 2004; Harrison et Lin, 2000; Pelton, Gong et Duerig, 2003).

Par contre, l'influence de la déformation moyenne sur la vie en fatigue ne fait pas consensus (Eiselstein, Sire et James, 2005). Les résultats semblent varier en fonction de la méthodologie utilisée, du type de chargement et du type d'échantillon.

Les auteurs qui ont étudié les chargements en flexion affirment qu'il y a augmentation de la résistance en fatigue avec l'augmentation de la déformation moyenne. Lors d'essais sur des branches de stents, Pelton, Gong et Duerig (2003) montrent que la résistance en fatigue diminue lorsque la déformation moyenne passe de -4 à 1 %, et qu'au contraire, elle augmente lorsque la déformation alternée passe de 1 à 4 %. Dans une étude similaire, Harrison et Lin (2000) évaluent qu'une déformation moyenne variant entre 0 et 4 % a pour effet d'augmenter la limite de vie en fatigue, et ce, pour des déformations alternées allant jusqu'à 3,5 %.

Dans le cas des études effectuées avec des chargements en tension, il n'y a pas consensus. Certains obtiennent un effet bénéfique de l'augmentation de la déformation moyenne comme Gong et al. (2004) qui obtiennent un nombre de cycle à la rupture stable pour les déformations moyennes variant entre 0 et 2 % et qui augmente pour des déformations moyennes variant entre 2 et 4 %. Ces résultats proviennent d'essais uniaxiaux en tension sur des tubes, dont ils font varier à la fois la déformation moyenne (entre 0 et 4 %) et la déformation alternée (entre 0,2 et 1 %). De façon similaire, lors d'une étude sur des fils, Morgan, Painter et Moffat (2003) obtiennent une augmentation de la résistance en fatigue avec l'augmentation de la déformation moyenne. Toutefois, lors d'essais sur des tubes, Tabanli, Simha et Berg (2001) obtiennent des vies en fatigue réduites lorsque la sollicitation

est à l'intérieur du plateau de transformation (2 et 6 %) plutôt qu'à l'extérieur (0,3 et 9,3 %), pour une déformation alternée constante de 0,21 %.

Stankiewicz, Robertson et Ritchie (2007) ont abordé la question différemment en étudiant plutôt l'initiation et la propagation de fissures sur des échantillons provenant de tubes. Leurs résultats suggèrent que l'augmentation de la contrainte moyenne accélère l'initiation de la fissure, tandis que la contrainte alternée accélère sa propagation. Ce résultat implique une dégradation des propriétés en fatigues avec l'augmentation de la déformation moyenne.

En résumé, quelques auteurs notent une amélioration de l'endurance des alliages titane-nickel lorsque le chargement moyen se situe entre 0 et 6 % en flexion (Gong et al., 2004; Harrison et Lin, 2000; Morgan, Painter et Moffat, 2003; Pelton, Gong et Duerig, 2003). D'autres notent une diminution des propriétés à l'intérieur du plateau de transformation en tension (Tabanli, Simha et Berg, 2001), ou une influence néfaste de l'augmentation de la contrainte moyenne puisqu'elle contribue à l'initiation de fissure (Stankiewicz, Robertson et Ritchie, 2007).

Il est donc important, vu l'absence de consensus, de vérifier l'impact de la déformation moyenne sur la résistance en fatigue des SDF superélastique. Cela est d'autant plus vrai que cette déformation moyenne peut être influencée à la hausse ou à la baisse en fonction de la force d'installation des SDF.

1.6 Problématique

Le système de fermeture du sternum en alliage superélastique tubulaire tressé, initialement présenté dans mon travail de mémoire (Baril, 2004), n'était qu'un démonstrateur de concept et n'était pas applicable cliniquement sans que d'autres travaux de recherche soient accomplis. Ce concept ne possédait pas de système de fixation ni de système d'installation. Autrement dit, il ne pouvait faire le travail pour lequel il a été conçu, à savoir maintenir deux parties d'os en contact durant la période d'ostéogenèse. Pour combler ce besoin, l'objet de liaison permettant de fixer les deux extrémités de la tresse ensemble et le système

d’installation doivent donc être créés. Ce système d’installation doit être en mesure d’appliquer une charge maximale fixe correspondante à la charge idéale d’installation pour la tresse tubulaire en alliage superélastique sélectionnée. Il doit aussi assurer le maintien de la boucle du système de fermeture en place par l’entremise d’un objet de liaison.

Deuxièmement, bien que le système ait été comparé à un système par fil classique, la comparaison a été faite sur un modèle simplifié où les systèmes comparés étaient installés à des charges initiales identiques. D’autres travaux sont requis pour déterminer comment se comporte la tresse dans un environnement plus complexe comme celui d’un modèle du sternum complet. Dans cette optique, il est nécessaire de définir de quelle façon et selon quelles variables le système classique en acier inoxydable n^{o} 5 et le système en alliage superélastique seront comparés.

Précisons qu’il est généralement admis qu’un système de fermeture rigide réduit le mouvement des deux parties du sternum et donc réduit le risque de complication postopératoire en favorisant leur union. Plus la rigidité du système de fermeture est grande, plus l'ouverture du sternum lors d’une perturbation externe est petite et plus la force de tension de séparation requise pour générer une ouverture du sternum est grande. Cependant, une rigidité élevée seule n'est pas synonyme de système de fermeture réussi. Plusieurs études ont déterminé que l’ouverture du sternum se produit bien avant l'application de la force maximum pouvant être soutenue par le système de fermeture, et ce indépendamment du type de système employé. La raison de ce phénomène est qu’un dommage permanent de l‘os ou du système de fermeture aura comme conséquence une perte de forces de compression à l'interface entre les moitiés du sternum, et par conséquent, une diminution de la stabilité de la liaison. Ceci dit, la capacité d’un système de fermeture de réappliquer la compression sur le sternum après le retrait de la perturbation est complètement négligée dans la littérature courante. Cette donnée est pourtant importante parce qu’une diminution significative de la pression d’interface a pour effet de limiter l’ossification de l’os en réduisant la stabilité. C’est donc principalement sur cette donnée, nommée « la force de fermeture résiduelle », que nous comparerons les différents SDF.

Enfin, les propriétés en fatigue de la tresse demeurent une inconnue de taille. Il est important de vérifier l'impact de la déformation moyenne car celle-ci pourrait être influencée à la hausse ou à la baisse en fonction de la force d'installation des SDF et ces résultats pourraient influer sur les forces d'installation recommandées. Par ailleurs, en connaissant les facteurs qui influencent la vie en fatigue de ces tresses, la technologie leur production pourrait être améliorée.

1.7 Objectif de la recherche

L'objectif général de ce projet est de développer un système de fermeture du sternum par tresse superélastique. Ce système doit donc être pouvoir être installé manuellement, se maintenir en place de façon autonome et soutenir les charges auxquelles il peut être confronté aussi bien ou mieux qu'un système de fermeture classique.

Le premier objectif est d'assurer la conception d'un outil d'installation permettant l'utilisation de la fermeture du sternum par tresse de façon autonome avec l'aide d'un système de fixation pouvant être utilisé dans une salle d'opération. Cette conception doit inclure un objet de liaison ainsi qu'un outil permettant d'induire la tension appropriée dans la tresse.

Le deuxième objectif est de comparer les systèmes de fermeture du sternum dans leurs conditions d'exploitation. La tresse superélastique fixée à l'aide de l'objet de liaison et installée à l'aide de l'outil d'installation, sera donc comparée aux fils de fermeture en acier inoxydable installés de façon classique. Pour ce faire, un nouveau banc d'essai qui simule le comportement de la cage thoracique lors de l'installation des systèmes de fermetures doit être conçu. Divers types de sollicitation y seront testés, notamment l'application d'une charge statique et la simulation de quintes de toux. Ce nouveau banc permettra aussi la mesure de nouvelles variables de réponse comme la charge de compression à l'interface entre les deux moitiés de sternum et la force générant l'ouverture de la liaison.

Le troisième objectif est de comprendre le comportement en fatigue de la tresse en alliage à mémoire de forme. Dans le cadre de ce projet, seul le comportement en tension simple de la tresse sera testé. Les essais en fatigue effectués sont des essais axiaux sur une vaste plage de sollicitation. Pour bien comprendre les facteurs qui influencent la vie en fatigue de la tresse, les filaments qui constituent la tresse seront aussi testés et une étude comparative sera menée.

CHAPITRE 2

SOLUTION TECHNIQUE (SYNTHÈSE DES BREVETS)

Au plan médical, il serait avantageux de diminuer la fréquence des complications postopératoires (infection grave, rupture du sternum, etc.) lors de chirurgies thoraciques. L'utilisation d'un nouveau système de fermeture du sternum, qui ne présente pas les inconvénients des systèmes actuels tout en présentant certaines caractéristiques avantageuses, pourrait constituer une partie de la solution. Plus précisément, un système de fermeture par tresse tubulaire en alliage superélastique est proposé. Cette nouvelle technologie a été développée au laboratoire sur les matériaux et les systèmes intelligents (LAMSI) de l'école de technologie supérieure au cours des dernières années (Brailovski et al., 2006). Elle a fait l'objet de deux brevets qui sont résumés dans les pages suivantes et qu'il est possible de consulter en entier aux annexes II et III. La tresse en alliage superélastique, qui est un implant fermant le sternum, a fait l'objet du premier brevet (Brailovski et al., 2006). Le second brevet décrit l'outil d'installation du système de fermeture (Brailovski et al., 2007). Celui-ci a été conceptualisé pour la tresse en alliage superélastique, mais il pourrait également servir pour d'autres systèmes de fixation osseuse par fil ou câble.

2.1 Tresse en alliage superélastique

Le système de fermeture du sternum proposé combine les avantages des fils et des rubans, sans en présenter les inconvénients principaux. Ainsi, le nouveau système permet :

1. la diminution de la contrainte de surface avec le sternum, en comparaison avec les SDF par fils, ce qui permet de maintenir une fermeture stable (figure 2.1);
2. l'augmentation de la stabilité de la fermeture par l'application d'une force de compression constante;
3. une aisance de manipulation;
4. l'absence de bords tranchants, ce qui diminue les risques d'hémorragies.

Ce système novateur est obtenu par la combinaison de deux caractéristiques principales : une géométrie originale, soit une structure tubulaire tressée et l'utilisation d'un matériau aux propriétés remarquables, soit un alliage à mémoire de forme superélastique. Ces deux aspects sont traités en détail dans les sections suivantes.

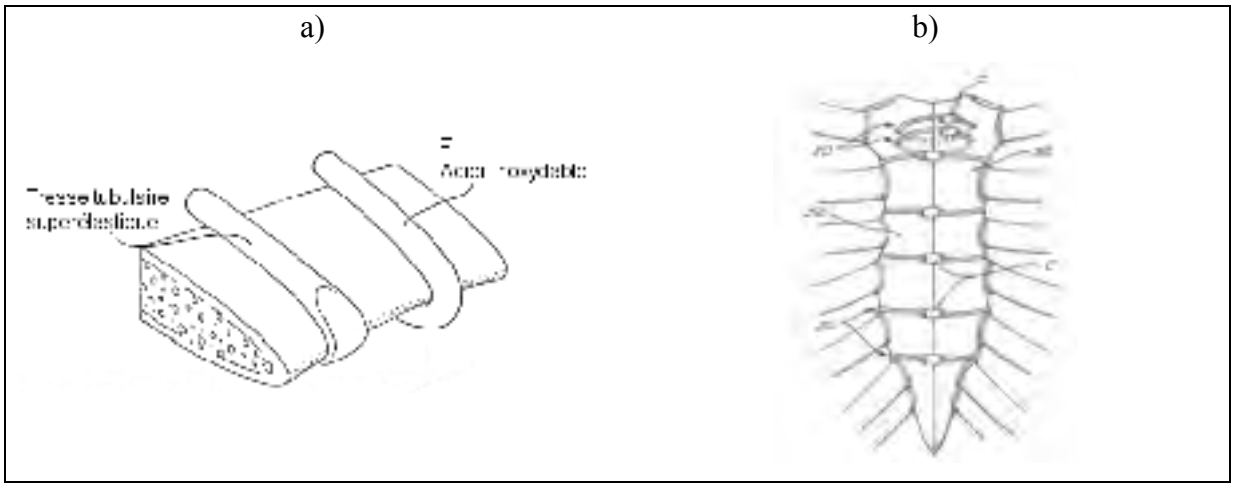

Figure 2.1 Concept de fermeture du sternum par tresse : (a) génération d'une forme méplate lorsque le système est en contact avec le sternum, (b) vue générale d'une installation suggérée.
Tirée de Brailovski et al (2006)

Géométrie

Le système développé possède une géométrie particulière qui est celle d'une tresse tubulaire formée d'un certain nombre de filaments (entre 16 et 72) pouvant avoir entre 0,05 et 0,2 mm de diamètre. La géométrie de la tresse offre une structure axisymétrique, présentée à la figure 2.2, d'une grande souplesse ayant un diamètre de passage comparable aux SDF conventionnels par fils d'acier inoxydable avec laquelle elle partage sa forme allongée. Ces caractéristiques permettent une installation aisée préservant les tissus environnants et utilisant les mêmes techniques de passage que pour les fils d'acier. La forme tubulaire diminue la contrainte de surface en prenant une forme méplate au contact avec le sternum. Cette forme s'approche de la forme aplatie qu'ont les rubans.

D'autres versions de la même solution technique pourraient être recouvertes d'un composant quelconque. La structure pourrait par exemple être recouverte d'un tissu polymérique pour le rendre plus lisse, ou encore, des agents favorisants la guérison de la plaie ou d'autres médicaments pourraient enduire la structure ou y être introduits. Enfin, la structure pourrait contenir une âme en son centre afin de générer différentes formes facilitant le passage ou diminuant encore plus la contrainte sur le sternum.

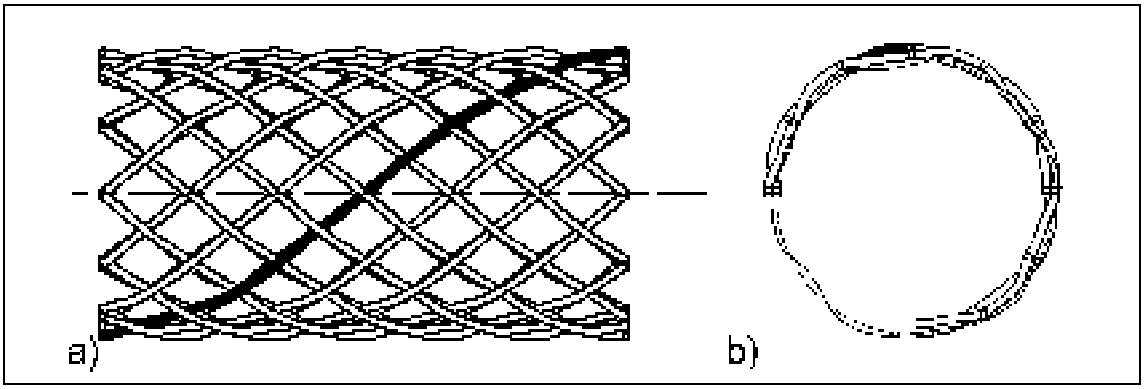

Figure 2.2 Schéma de la tresse tubulaire : (a) vue de plan, (b) vue de dessus.

Matériau

La tresse est constituée, au moins en partie, d'un alliage à mémoire de forme (AMF) de titane-nickel qui a la propriété d'être superélastique à la température du corps. Ce comportement superélastique qui est illustré à la figure 2.3 présente les avantages suivants :

1. Il permet au SDF de maintenir la force sur le sternum non nulle (force résiduelle) même si le sternum s'est affaissé partiellement. Ceci est illustré aux points A-B-C de la figure 2.3.

2. Le matériau bénéficie du principe d'interférence dynamique (Duerig, Pelton et Stockel, 1997). Il a donc la propriété de se rigidifier lors d'une impulsion (par exemple lors d'une quinte de toux) (C-D) et de fournir une charge quasi constante (D-E) qui est définie par la hauteur du plateau supérieur. Une fois la perturbation passée, la force appliquée par le

système de fermeture sur le sternum revient à la charge initiale sur le plateau inférieur (E-F-C).

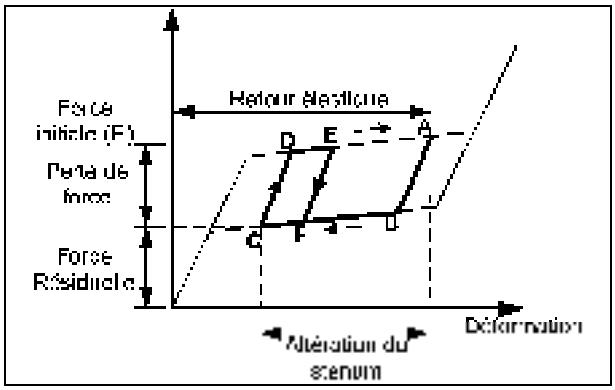

Figure 2.3 Principe de banque de déformation (A-B-C) et de l'interférence dynamique (C-D-E-F-C).

Le maintien par le système de fermeture d'une charge de compression constante malgré un léger affaissement du sternum fait en sorte d'augmenter la stabilité de la liaison puisque c'est cette charge qui maintient les deux parties de sternum en place.

Outre que l'AMF à base de titane-nickel a des propriétés mécaniques remarquables, il est aussi un matériau privilégié dans le domaine biomédical. Ainsi, depuis 1996, la Food and Drug Administration (FDA) a autorisé l'utilisation de plusieurs implants permanents en Nitinol, ce qui démontre que cet alliage est viable et peut être considéré pour un système permanent de fermeture du sternum. Les AMF utilisés comme implants ont également une faible interférence avec les champs magnétiques (Shabalovskaya, Ryhanen et Yahia, 2001), ce qui n'est pas le cas de l'acier inoxydable (Chinzei, Kikinis et Jolesz, 1999). Cette propriété est importante parce qu'elle permet aux patients ayant subi une opération thoracique d'avoir accès à un appareil d'imagerie par résonance magnétique.

En somme, la solution proposée combine les avantages d'une forme tubulaire tressée et d'un alliage à mémoire de forme superélastique. Jusqu'à maintenant, les avantages du nouveau

dispositif ont seulement été présentés de manière théorique. Dans la section suivante, nous décrivons succinctement les étapes ayant mené à la validation de la solution proposée.

2.1.1 Validation préliminaire de la solution proposée

Dans le cadre des travaux ayant menés au dépôt d'un brevet, la validation du concept a été effectuée. Cette validation comprenait un modèle numérique par éléments finis, un modèle empirique permettant d'évaluer le comportement de la tresse en fonction de ces paramètres de fabrication, une étude expérimentale et un exemple d'application qui incluait le développement d'une méthodologie de sélection de la tresse. Les trois premières étapes seront très brièvement abordées puisqu'elles ont été en très grande partie décrites dans les travaux de maîtrise de Baril (2004). La méthodologie de sélection de la tresse, qui est incluse dans l'exemple d'application, a toutefois été développée dans le cadre de cette thèse doctorale et sera décrite avec plus de détails. Outre le brevet lui-même (Brailovski et al., 2006), ces travaux de validation ont également fait l'objet d'une autre publication (Baril et al., 2006) qu'il est possible de consulter à l'annexe IV.

Modèle numérique par éléments finis

Un modèle par éléments finis 1D simule la fermeture du sternum par analogie avec un système de joint boulonné. Ce modèle montre que le matériau superélastique permet le maintien d'une plus grande force résiduelle que les matériaux conventionnels sans égard à la géométrie du SDF. Ils sont capables de refermer le sternum pour des charges 60 % plus importantes parce que les AMF sont en mesure d'absorber un certain affaissement de la surface du sternum sans perdre la totalité de la force de compression initiale. Cet effet est d'autant plus avantageux qu'il n'agit pas au détriment de la force de perturbation extérieure menant à l'ouverture du sternum. En effet, les systèmes de fermeture en AMF laissent la liaison du sternum s'ouvrir à une charge très semblable (moins de 8 % d'écart) à celle des fils en acier, soit environ 70 N.

Modèle empirique prédisant le comportement de la tresse

Un modèle empirique a été généré afin de prédire le comportement de la tresse tubulaire en AMF à partir des paramètres qui la définissent soit : le comportement d'un filament, le nombre de filaments et l'avance par tours de la tresse. Ce modèle permet de déterminer les paramètres de la tresse qui répondront le mieux aux exigences du sternum dont les propriétés sont connues. Les résultats suggèrent que le comportement de la tresse est généralement proportionnel au comportement des filaments qui la composent, tel que montré à la figure 2.4. La force à la rupture (Fr), à la fin du plateau de transformation direct ($F(M_f^{\sigma})$) et indirecte ($F(A_f^{\sigma})$) sont proportionnelles à ceux d'un filament unique.

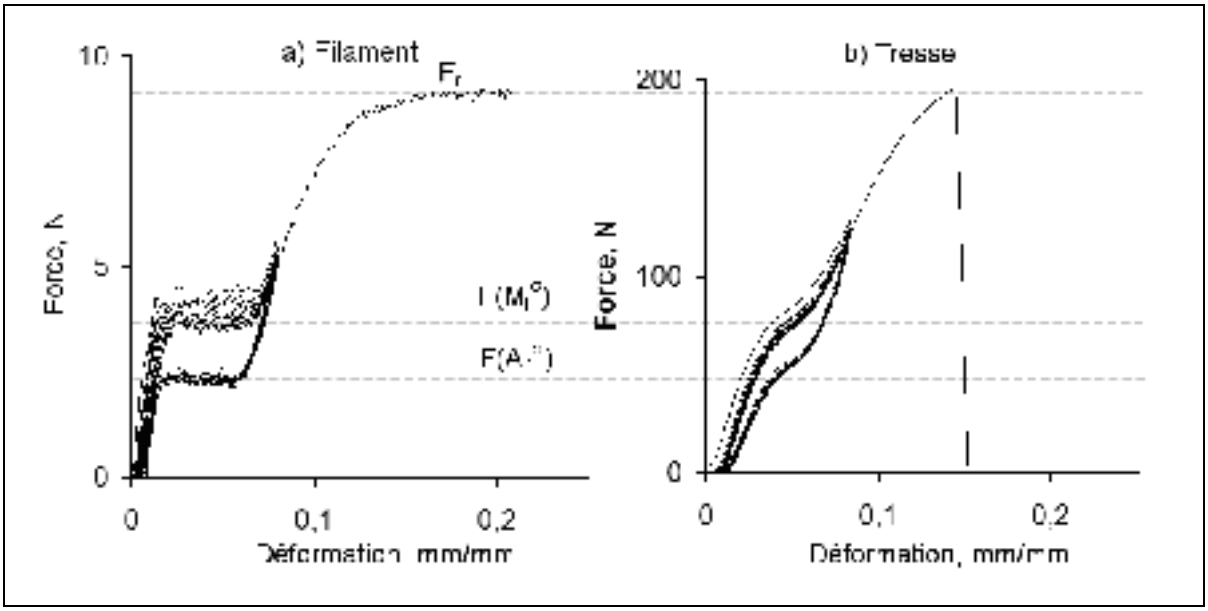

Figure 2.4 Illustration du comportement mécanique du filament (a) et de la tresse (b).

Étude expérimentale

Des essais en laboratoire ont permis de comparer le SDF par tresse en AMF et le fil d'acier inoxydable standard. Ces résultats montrent qu'en moyenne, pour le SDF par tresse en AMF, la charge de compression entre les deux parties du sternum est de 30 % supérieure à celle mesurée pour un système de fermeture par fil d'acier. Ces résultats sont constants peu importe le type de passage, la densité de l'os ou le type de chargement. Il est important de

noter ici que la tresse et le fil étaient fixés à l'aide des mors du banc d'essai. Ils ne comprenaient pas de système d'objet de liaison comme tel.

Méthodologie de sélection de la tresse

Afin de profiter au maximum des caractéristiques avantageuses de la tresse, il faut être en mesure de sélectionner la tresse qui sera appropriée à l'environnement où elle sera installée, en tenant compte des caractéristiques du sternum et des efforts maximaux devant être supportés par le système de fermeture. Par exemple, la tresse sélectionnée sera différente selon s'il s'agit d'un sternum fragile (celui d'une patiente souffrant d'ostéoporose, par exemple) ou d'un sternum de rigidité normale.

Deux catégories de paramètres doivent être prises en compte : les paramètres qui définissent les charges d'installation et ceux qui définissent le fonctionnement de la tresse en AMF en service. La figure 2.5 illustre ce que devrait être une tresse idéale permettant une charge d'installation faible protège le sternum et une force minimale à la rupture suffisante pour éviter le bris en service.

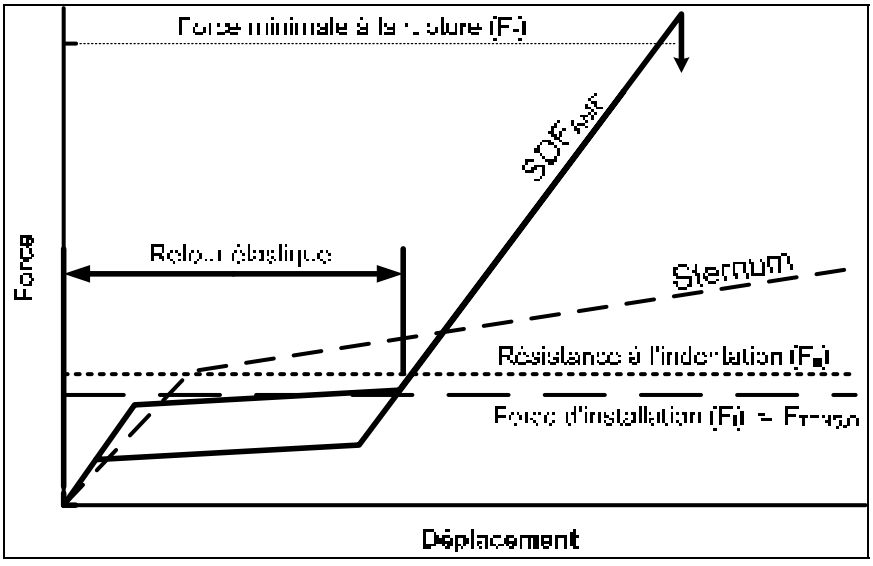

Figure 2.5 Schéma illustrant le comportement d'une tresse idéale.

Paramètres fonctionnels d'installation

Pour bénéficier au maximum des avantages du SDF superélastique, la force appliquée sur le SDF lors de l'installation (F_i) doit se situer aussi près que possible de la fin du plateau supérieur de la boucle superélastique. La fin du plateau supérieur doit être un peu sous la résistance à l'indentation du sternum (force à laquelle le SDF pénètre dans l'os (F_s)). Si la fin du plateau supérieur est bien en deçà de la force d'indentation, le sternum va s'ouvrir à des charges de perturbation inférieures. Si la force à la fin du plateau est plus grande que la force d'indentation, le chirurgien peut endommager le sternum durant l'installation du SDF et il doit donc limiter la charge d'installation, ce qui va réduire le retour élastique disponible.

Paramètres fonctionnels de service

Pour prévenir la rupture du SDF lors du service (par ex. à la suite d'une quinte de toux), celle-ci doit avoir une limite de force à la rupture (F_r) suffisante pour résister aux perturbations postopératoires.

Pour pouvoir bénéficier du comportement superélastique de la tresse, l'hystérésis en contrainte doit être minimale et la force à la fin du plateau inférieure de transformation doit être plus grande que zéro.

2.1.2 Conclusion

Pour diminuer la fréquence des complications postopératoires lors de chirurgies thoraciques, un nouveau système de fermeture par tresse est proposé. Ce système implique une nouvelle géométrie, la tresse tubulaire qui s'affaisse lors du contact avec l'os, ce qui permet d'augmenter la surface de contact tout en conservant les avantages des fils lors de leur manipulation. Il implique aussi, en synergie avec la géométrie, un matériau spécial, l'alliage à mémoire de forme superélastique, qui permet de conserver la charge de fermeture malgré un affaissement de l'os du sternum.

Des travaux de validation expérimentale et numérique démontrent que ce nouveau système de fermeture est viable lorsqu'il est comparé avec le système fermeture du sternum courant

en acier inoxydable et peut réduire la détérioration du sternum par la diminution de la contrainte de contact avec le SDF. De plus, il augmente la stabilité du SDF tout en conservant une charge statique et non nulle sur le sternum.

Une méthodologie de sélection de la tresse est aussi proposée. La sélection est faite à partir des caractéristiques du sternum et des efforts maximaux devant être supportés par le système de fermeture. La charge d'installation recommandée se situe à la fin du plateau de transformation et varie en fonction de la tresse sélectionnée.

Bien que prometteur, le système de fermeture du sternum par tresse tubulaire superélastique est incomplet. En effet, il manque un outil d'installation pour rendre possible l'utilisation clinique de ce système. Cet outil est décrit dans la section suivante.

2.2 Outil d'installation d'un système de fermeture du sternum

Tel que mentionné précédemment, lorsque le sternum est fermé à l'aide de la méthode manuelle classique, il est difficile d'évaluer de façon précise la force appliquée au SDF et de reproduire cette force d'un SDF à l'autre. Or, l'application d'une tension prédéterminée au SDF permet de limiter la pression de contact entre le SDF et l'os et ainsi diminuer le risque de défaillance au niveau de la surface de contact (découpage du sternum sous l'effet d'une toux sévère ou d'une respiration profonde).

D'autre part, le SDF en forme de tresse tubulaire superélastique, décrit dans les sections précédentes, ne peut être installé à l'aide de la méthode classique ni à l'aide des autres outils qui ont été développés à ce jour.

En effet, pour bénéficier de la force de retour élastique, la boucle doit être installée à une tension précise (figure 2.5). Ensuite, pour fixer la boucle en place, il n'est pas possible de tordre la tresse tubulaire superélastique de manière permanente, comme il est possible de le faire avec le fil en acier inoxydable. Une autre méthode doit être utilisée.

Un nouvel outil a donc été conçu pour permettre l'installation de ce nouveau SDF tout en réduisant les inconvénients associés à l'installation des autres types de systèmes de fermeture par fils.

Nous avons établi que le prototype développé devait absolument présenter les caractéristiques suivantes :

1. Contrôler automatiquement la mise sous tension, ce qui ne peut pas être réalisé par aucun des mécanismes existants. Cette automatisation permet d'appliquer une tension prédéterminée sur chacun des fils du SDF, s'assurant ainsi d'une répétitivité des caractéristiques mécanique du SDF;
2. Éliminer tout mouvement en rotation de la part du chirurgien, pour assurer une plus grande stabilité lors de la manipulation de l'appareil, et par conséquent, une plus grande facilité d'utilisation.

Pour être concrètement utilisable lors de chirurgies, l'outil idéal devrait également présenter les caractéristiques suivantes :

1. Les mécanismes doivent être réduits au minimum et être facilement démontables afin de faciliter le processus de stérilisation qui doit être complété individuellement pour toutes les pièces du prototype.
2. La mise sous tension, le sertissage et la coupe de l'excédent de tresse doivent être complétés avec un minimum de manipulations de la part de l'usager. Par exemple, la coupe de l'excédent de tresse devrait idéalement être complétée pendant la manipulation nécessaire au sertissage.
3. L'outil d'installation doit être le plus léger possible pour faciliter les manipulations.
4. La boucle doit pouvoir être posée par une personne seule.

Plusieurs concepts et prototypes ont ainsi été développés afin d'atteindre les objectifs visés. Bien que les mécanismes de fonctionnement diffèrent quelque peu, les 4 étapes maîtresses de l'installation du SDF (figure 2.6) restent les mêmes, soient :

a) Pose préliminaire du SDF;
b) Application d'une tension prédéterminée sur le SDF;
c) Sertissage d'un manchon sur le SDF tout en maintenant la tension pour compléter l'installation;
d) Retrait de l'appareil, couper la tresse en surplus et réarmement.

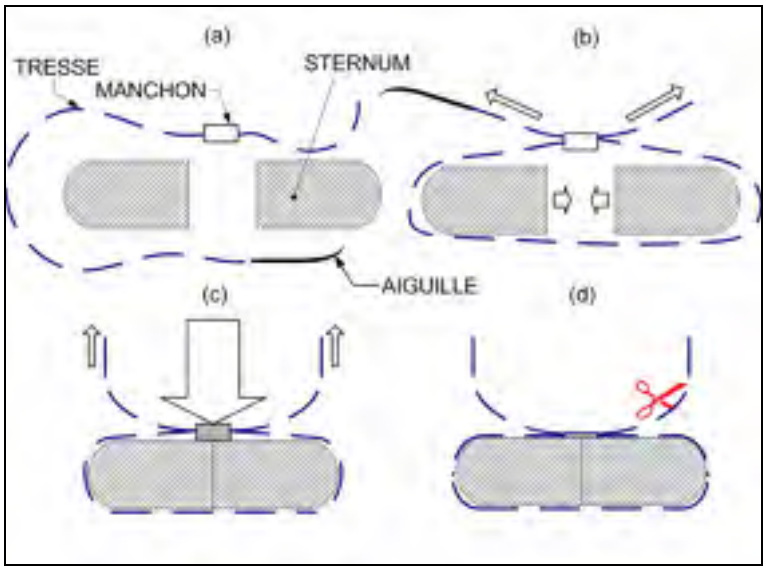

Figure 2.6 Installation du SDF superélastique en quatre étapes en vue de coupe transverse : (a) passage de la tresse autour du sternum; (b) application d'une consigne en tension et rapprochement des moitiés de sternum; (c) sertissage du manchon; (d) coupe de l'excédent de la tresse.
Tirée de : Chartrand, Brailovski et Baril (2009).

Dans cette section, seul le prototype B sera illustré (figure 2.7) et décrit en détail. Nous vous référons au brevet (Brailovski et al., 2007) présenté en annexe III pour les prototypes A et C.

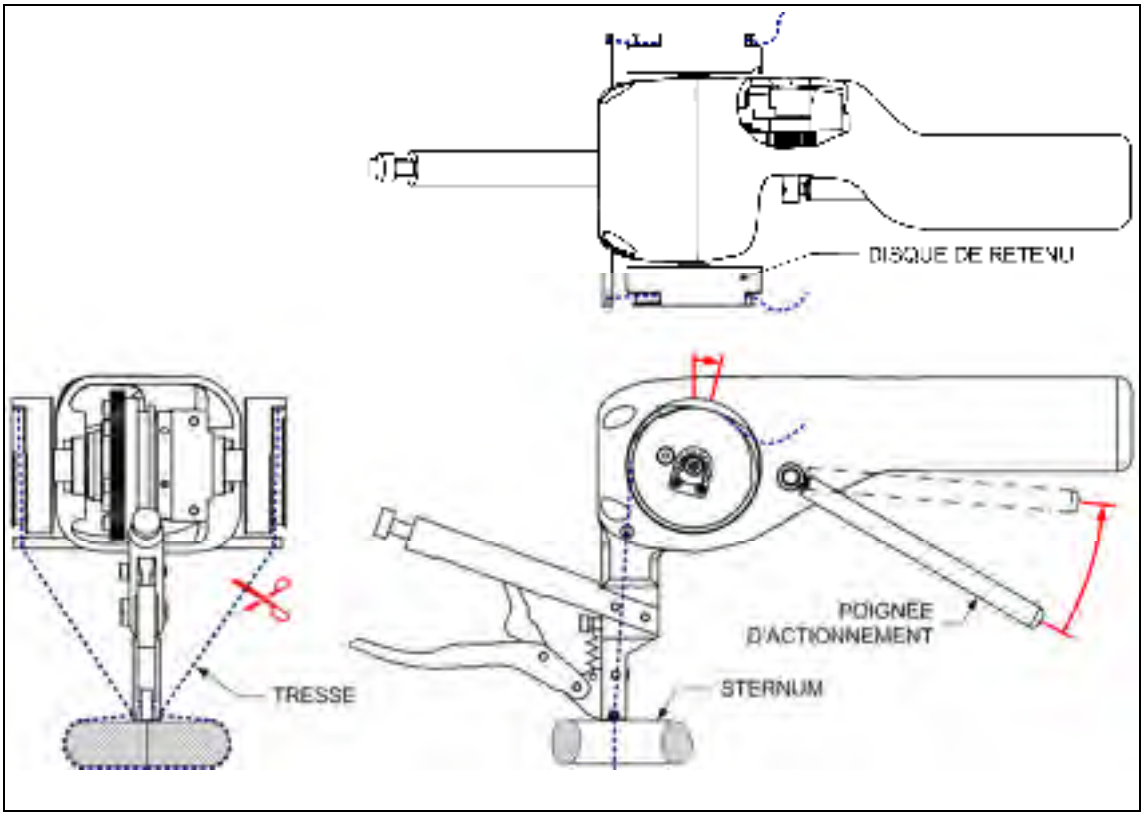

Figure 2.7 Vue globale de l'appareil d'installation (prototype B).
Tirée de Chartrand (2008).

2.2.1 Pose préliminaire du SDF

Le SDF est installé autour du sternum de la même façon que pour un fil en acier inoxydable. Les configurations de pose utilisées pour le fil en acier sont facilement reproduites par la tresse tubulaire superélastique. La tresse est assemblée avec aiguille et manchon (figure 2.8). En effet, il a rapidement été déterminé que seule l'utilisation d'un manchon pouvait faire le lien entre les deux parties du système de fermeture et faire un travail de maintien adéquat dans l'espace limité situé entre la partie antérieure du sternum et la peau.

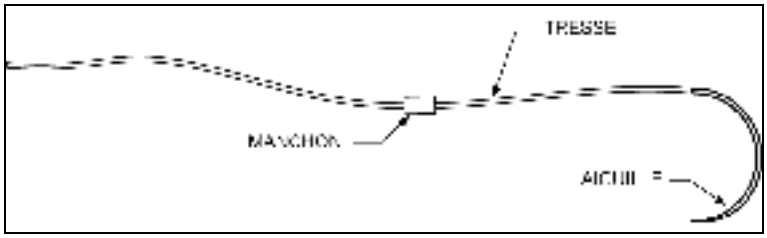

Figure 2.8 Tresse assemblée avec aiguille et manchon.
Tirée de Chartrand (2008).

2.2.2 Application d'une tension prédéterminée sur le SDF

Une fois le passage de la tresse autour du sternum complété, l'appareil est positionné au-dessus du sternum et les extrémités du SDF sont fixées à l'aide de disques de retenue. En entraînant la poignée d'actionnement vers le haut, une rotation est imposée aux disques de retenue et une tension est créée sur la boucle. Les flèches illustrées à la figure 2.7 indiquent le sens du mouvement pour la poignée et le disque. Lorsque la tension, et donc le couple sur l'arbre d'entrainement, prédéterminée est atteinte, un mécanisme automatique limitant le couple, illustré à la figure 2.10 arrête toute rotation additionnelle des disques de retenue et leur position est maintenue.

La figure 2.9 illustre le fonctionnement de l'un de ces disques. Tout d'abord, l'usager doit faire pivoter la came pour permettre l'insertion de la tresse entre celle-ci et le mur de retenu figure 2.9a). Une fois la came relâchée, un ressort, au centre de la came, ramène la came vers le mur de retenue (figure 2.9b). Une fois le fil en place, toute tension supplémentaire dans la tresse a pour effet d'augmenter la pression générée par la came sur cette dernière parce qu'elle génère un couple positif sur la came (dans le sens de la flèche de la figure 2.9b).

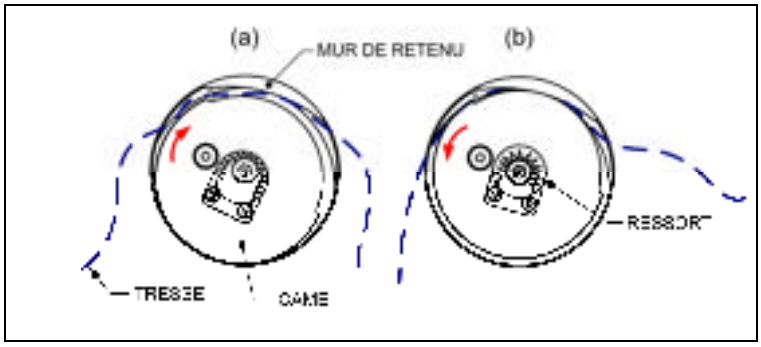

Figure 2.9 Principe de fonctionnement d'un disque de retenue lors de (a) l'installation de la tresse et du (b) relâchement de la came.
Tirée de Chartrand (2008).

Lors de l'atteinte de la consigne en tension, le limiteur de couple de la figure 2.10 libère les disques de retenue de tout chargement excédentaire appliqué par l'usager. Des roues libres à rouleaux viennent empêcher toute rotation en sens contraire de la mise sous tension, ainsi empêchant le relâchement des tresses. Le système de transmission de mouvement est présenté sur la vue de couple de la figure 2.10.

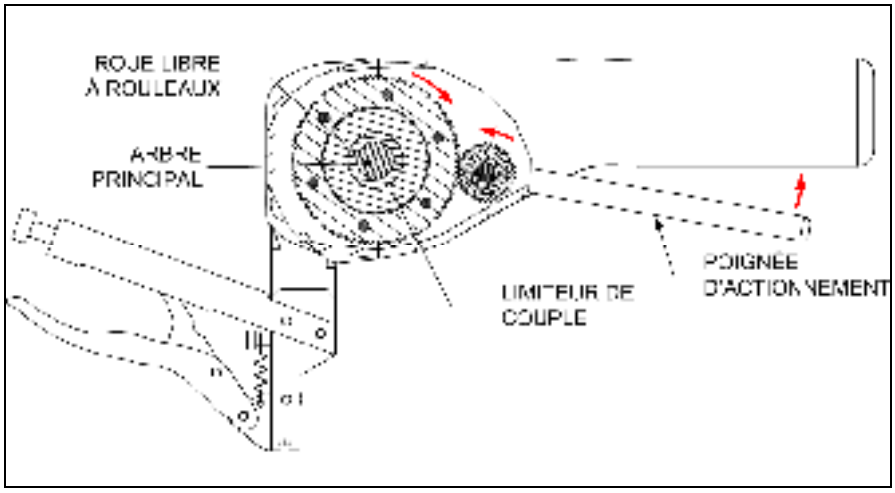

Figure 2.10 Vue générale du mécanisme d'entraînement.
Tirée de Chartrand (2008).

2.2.3 Sertissage du manchon

Lorsque la tension désirée est appliquée à la boucle du SDF, le manchon, qui a préalablement été positionné au pied de l'appareil lors de l'étape précédente, est déformé plastiquement. En actionnant la poignée de sertissage vers le haut (figure 2.11a), le manchon est serti (figure 2.11b) pour retenir la boucle en place de façon permanente.

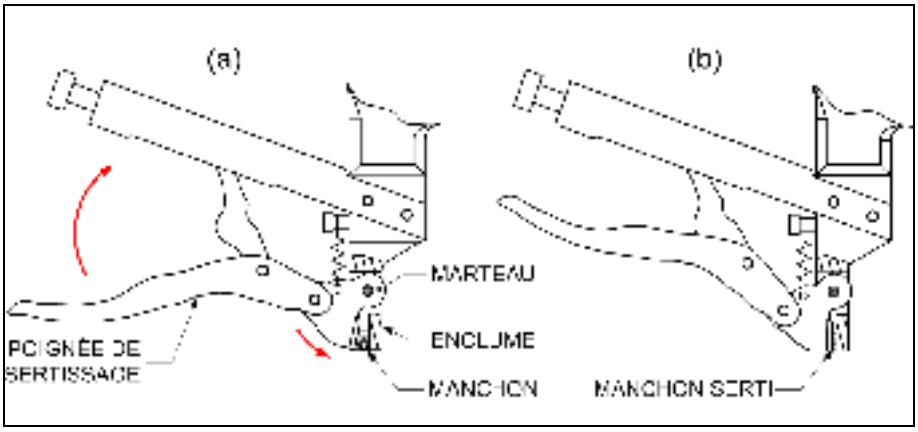

Figure 2.11 Principe de fonctionnement du pied de l'appareil lors de (a) la pose du manchon et du (b) sertissage du manchon.
Tirée de Chartrand (2008).

La charge d'écrasement du manchon peut être réglée en ajustant la vis d'ajustement (figure 2.12). Plus la vis est engagée dans le manche, plus l'espace initial entre le marteau et l'enclume est important. La figure 2.12 montre la différence pour un engagement d_2 (b) supérieur à d_1 (a); la poignée de sertissage a une position de départ beaucoup plus basse pour (b) que pour (a), permettant ainsi l'application d'une plus grande force d'écrasement.

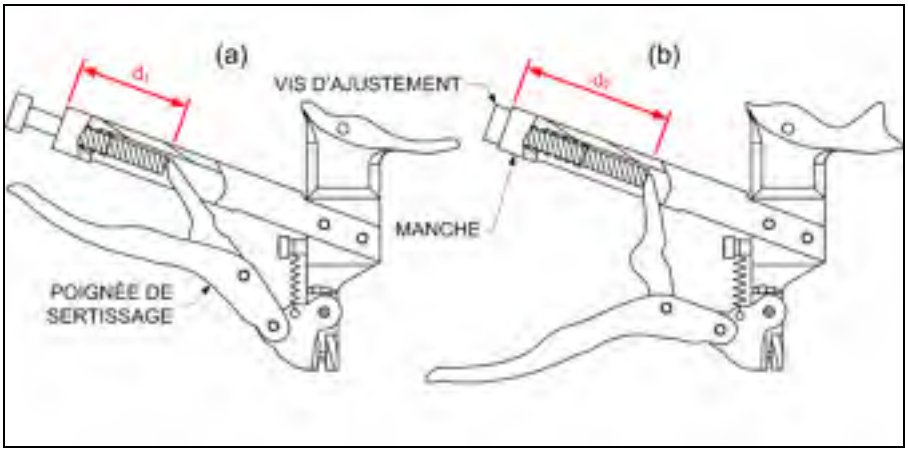

Figure 2.12 Positionnement de la vis d'ajustement pour le sertissage pour une position de la poignée de sertissage (a) haute et (b) basse.
Tirée de Chartrand (2008).

2.2.4 Retrait de l'appareil

Pour compléter l'installation et libérer l'appareil, la tresse est coupée à la section comprise entre le pied de l'appareil (où a lieu le sertissage) et les disques de retenue. Une coupe supplémentaire près du manchon serti est ensuite nécessaire pour bien enlever l'excédent. On réarme ensuite l'appareil en enlevant la tresse coincée dans la came. L'outil est à nouveau prêt à réinstaller une autre boucle.

2.2.5 Conclusion

Le prototype d'outil a été testé sur des sternums en matériau synthétique par le Dr. Cartier, chirurgien cardiaque à l'Institut de cardiologie de Montréal. Ces tests préliminaires ont montré que l'outil est fonctionnel et permet l'installation de la tresse tubulaire tressée, selon les étapes décrites précédemment.

Ce nouvel outil d'installation présente la majorité des caractéristiques attendues. Il permet le contrôle automatique de la mise sous tension, ce qui assure la répétitivité des caractéristiques mécaniques du SDF lors de l'installation. Les mouvements en rotation sont aussi éliminés; l'appareil est donc stable lors de la manipulation. Enfin, le développement d'un tel outil est

essentiel pour que la tresse tubulaire puisse éventuellement être utilisée lors de chirurgies car aucun des outils existants ne peut l'installer. D'autre part, le prototype n'est pas plus lourd qu'une scie sternale, il est facilement démontable pour permettre sa stérilisation et il peut être utilisé par une personne seule.

Bien que cet outil soit prometteur, son ergonomie et son automatisation devront être améliorées pour qu'il soit aussi rapide et intuitif à utiliser que les outils classiques. Par exemple :

- l'ajustement de la tension s'avère laborieux, car l'outil doit être démonté à chaque fois;
- les étapes d'installation (mise sous tension, sertissage et coupe de l'excédent) sont complétées à l'aide de manipulations distinctes, ce qui allonge le temps d'opération (entre 12 et 15 minutes pour 7 tresses) et la complexité de la procédure d'installation.

Ces défis devront donc être résolus avant que la tresse tubulaire tressée et l'outil d'installation soient utilisés de manière courante lors de chirurgies thoraciques. Ce type de travail relève toutefois plus d'une équipe de design industriel que du travail d'une équipe de recherche universitaire.

CHAPITRE 3

MÉTHODOLOGIE

Les deux études présentées dans le cadre de cette thèse ont chacune leur méthodologie propre. Ce chapitre comporte donc deux parties distinctes : a) validation de la fonctionnalité du système de fermeture sur un banc d'essai simulant un sternum et b) évaluation du comportement en fatigue de la tresse sur un banc d'essai axial.

3.1 Étude fonctionnelle

Cette étude comparative entre les SDF par tresse superélastique et les SDF classiques en acier inoxydable fait l'objet de l'article 1 (Baril et al., 2009) présenté au chapitre 4. Dans les prochaines sections, les aspects principaux de la méthodologie sont décrits : variables de réponses pour l'analyse, matériel, équipement utilisé et procédure expérimentale.

3.1.1 Variables de réponse

Tel que mentionné précédemment, les bancs d'essai présentés dans la littérature courante s'attardent essentiellement à mesurer l'ouverture de la liaison osseuse à la suite d'un chargement. Les travaux présentés ici prennent une seconde variable en compte, soit la capacité d'un système de fermeture de réappliquer la compression sur le sternum après le retrait de la charge.

Nous utilisons donc ici deux paramètres fonctionnels : la force menant à l'ouverture de la liaison osseuse et la force résiduelle de compression à l'interface à cette liaison. Ces paramètres reflètent la capacité d'un système de fermeture de maintenir la compression entre les deux moitiés de sternum lors d'un chargement simple ou répété (figure 3.1).

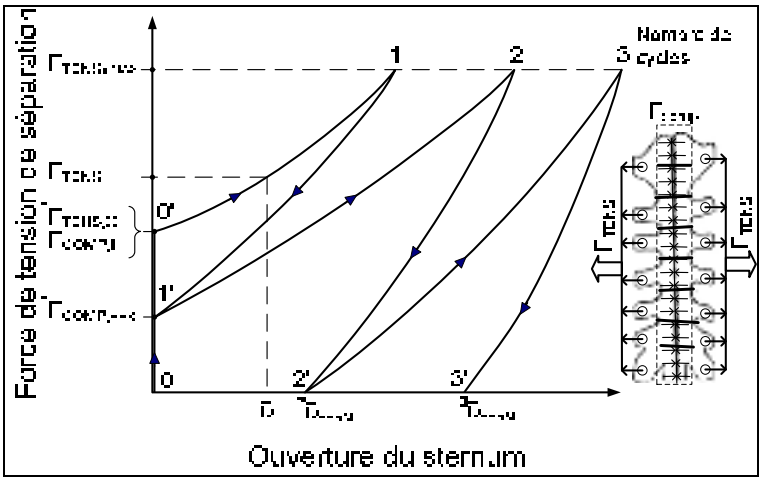

Figure 3.1 Illustration du comportement mécanique d'un système de fermeture du sternum et des variables d'entrée et de sortie

F_{TENS}, $F_{TENS,MAX}$, $F_{TENS,O}$, sont respectivement les forces de tension appliquées, maximales et provoquant l'ouverture. $F_{COMP,I}$ et $F_{COMP,RES}$ sont les forces de compression à l'interface des deux moitiés de sternum à l'installation et une fois F_{TENS} retirée.
Tirée de Baril et al. (2009).

Lors de l'application de la force de perturbation externe ($F_{TENS} \leq F_{TENS,MAX}$), les mesures suivantes sont prises :

1. L'ouverture (δ) du sternum associé (0-0'-1 (figure 3.1)) à l'application de la force de perturbation, ce qui permet de mesurer la rigidité du système de fermeture complet. Une rigidité plus importante implique une ouverture du sternum plus faible et vice-versa.
2. La force de séparation du sternum ($F_{TENS,O}$) qui est nécessaire pour ouvrir le sternum. Cette caractéristique est complémentaire à la rigidité du sternum.

Une fois que la force de perturbation est retirée (1-1'), les variables suivantes sont mesurées :

1. la force de compression résiduelle à l'interface ($F_{COMP,RES}$);
2. l'ouverture permanente du sternum (δ_{PERM}), le cas échéant, qui constitue une mesure complémentaire.

Toutes ces valeurs peuvent être mesurées pendant et à la suite de chacun des cycles d'un chargement répété (1'-2-2', 2'-3-3', etc.). Ce sont donc ces paramètres qui seront utilisés dans l'étude fonctionnelle pour la comparaison des systèmes de fermeture.

3.1.2 Matériel et équipement

Système de fermeture tubulaire tressé en alliage superélastique

Le SDF tubulaire tressé en alliage superélastique est fabriquée à partir d'un filament de 0,1 mm de diamètre fait dans un alliage BTR-BB (Ti-50.8 at % Ni) ayant subi 36 % de travail à froid (MEMRY CORP, Bethel, CT, USA). Le SDF de 24 filaments est tressé sur une machine à tresser WARDWELL (Central Falls, RI, USA) à raison de 1 croisement/mm sur un mandrin en aluminium de 3,2 mm de diamètre. La tresse est ensuite traitée à une température de 350 °C (15 min) pour fixer la forme tubulaire et obtenir les caractéristiques optimales soit : le plateau de transformation supérieur en deçà de la force d'indentation du sternum, et la force à la rupture au dessus de 250 N pour une boucle de fermeture (Baril et al., 2006, annexe III).

Puisque la tresse tubulaire en AMF présente un comportement superélastique, elle ne peut être tordue. Elle doit être sertie avec un outil d'installation, tel que celui décrit dans la section 2.2. Le manchon en acier inoxydable fait donc intégralement partie du système de fermeture du sternum par tresse tubulaire en AMF.

Monofilament en acier inoxydable

Des monofilaments en acier inoxydable No.5 ETHICON (Ethicon Inc, Somerville, NJ, USA) sont utilisés dans le cadre de l'étude comparative. Ce système de fermeture du sternum est couramment utilisé lors de chirurgies thoraciques. Il a été simplement torsadé selon la même technique que lors d'une chirurgie, et ce, sous la supervision directe d'un chirurgien cardiaque.

Modèles de sternum

Des modèles de sternum en mousse de polyuréthane d'une densité de 0.32g/cm^3 sont utilisés (Sawbones Corporation, Vashon Island, WA, USA). Ces modèles permettent de répliquer en partie les propriétés des sternums cadavériques. De plus, la mousse de polyuréthane présente un comportement viscoplastique, qui, bien que non totalement identique à celui de l'os humain, permet d'effectuer des essais comparatifs en fatigue. La densité choisie est la plus fréquemment rencontrée dans la littérature et elle représente le comportement mécanique du sternum moyen (Hale, Anderson et Johnson, 1999).

Banc d'essai

Le banc d'essai utilisé pour cette étude (figure 3.2) est décrit en détail à l'annexe I. C'est un banc de traction planaire actionné par deux pistons asservis permettant d'imposer une large plage de sollicitation tant statique que dynamique. Il peut appliquer des charges symétriques ou asymétriques et il est en mesure de simuler le comportement du sternum lors de la pose du système de fermeture, ce qui permet de s'approcher des conditions d'installation réelle. Il permet aussi de tester l'outil de fermeture dans des conditions proches de celles rencontrées en clinique en simulant le comportement de la cage thoracique lors de la phase de fermeture.

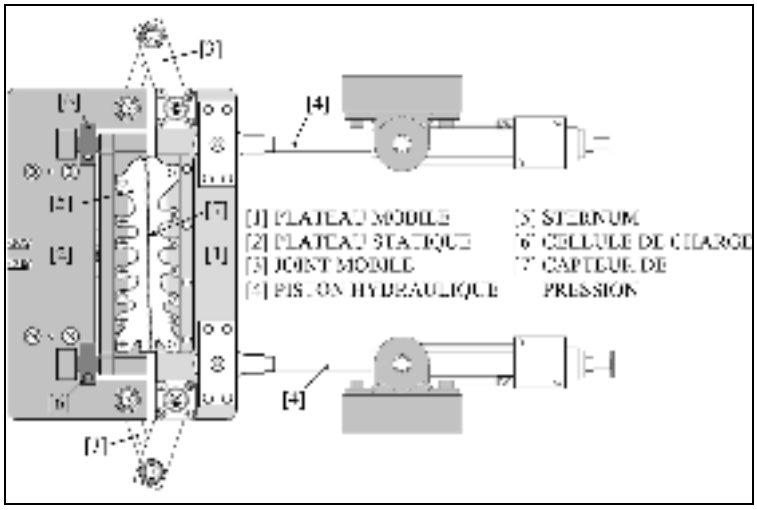

Figure 3.2 Vue schématique du banc d'essai.
Tirée de Chartrand (2008).

Pour permettre l'acquisition des variables de mesure, le banc est équipé de huit capteurs de pression FLEXIFORCE A201-100 (Tekscan Inc, Boston, MA, USA) qui mesurent la force de compression présente entre les deux moitiés du sternum ainsi que d'un extensomètre vidéo qui mesure l'ouverture de la liaison sternale.

3.1.3 Procédure expérimentale

Des tests statiques et dynamiques sont effectués pour comparer la performance du SDF par fil en acier inoxydable no 5. ETHICON et le SDF tubulaire tressé superélastique à 24 filaments. Chaque sternum artificiel est coupé longitudinalement avec une scie sauteuse et fermé à l'aide de l'un des deux systèmes de fermeture par l'installation de 7 liens, tel que décrit par Dasika, Trumble et Magovern (2003). Cette configuration combine 5 SDF péristernaux placés à égale distance le long du corps du sternum avec deux SDF transsternaux respectivement placés au niveau du manubrium et du xiphoïde.

Tests statiques : ils permettent d'évaluer la rigidité et la résistance statique du SDF. Ils consistent en l'application incrémentielle d'une force de séparation transverse à chacune des deux parties du sternum. Un exemple de séquence de chargement est illustré à la figure 3.3a.

Après stabilisation de la réponse du système à l'application d'une charge donnée, la force de compression est calculée au milieu du sternum. F_{COMP} correspond à la somme des réponses de chacun des huit capteurs de pression et de l'ouverture du sternum à chacun des points de contrôle. Après chaque incrément, la force de séparation est ramenée à zéro afin de mesurer la force résiduelle ($F_{COMP,RES}$) et le déplacement permanent du milieu du sternum (δ_{PERM}).

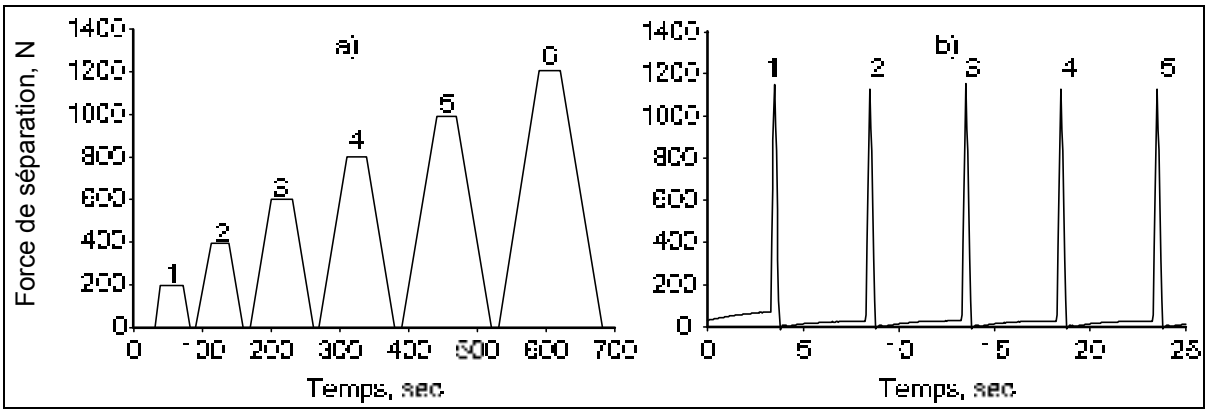

Figure 3.3 Séquences de chargement statique (a) et dynamique (b).

Tests dynamiques : ils permettent d'évaluer la résistance du SDF à la toux ou à un mouvement soudain et impliquent l'application de la force de séparation maximum sur une courte période. Un exemple de séquence de chargement est illustré à la figure 3.3b. Dans des études antérieures, la toux a été caractérisée comme une montée en pression de 200 ms suivie par deux phases expiratoires consécutives d'une durée de 30 à 50 ms et de 200 à 500 ms respectivement (McCool, 2006). Dans notre étude, une approximation triangulaire des patrons de toux a été utilisée. La toux a été caractérisée comme une montée en pression de 200 ms suivie d'une phase expiratoire, combinant les deux phases identifiées par McCool (2006), d'une durée de 230 ms. Après chaque quinte de toux, $F_{COMP,RES}$ est mesuré afin de vérifier la stabilité du sternum à travers le processus.

3.2 Étude de vie en fatigue

Le but de cette étude est double. Premièrement, nous désirons estimer la vie en fatigue d'un SDF par tresse en alliage superélastique. Deuxièmement, nous désirons comprendre les

facteurs qui influencent la vie en fatigue de ces tresses de façon à pouvoir améliorer leur performance. Pour répondre à ces objectifs, les filaments qui constituent la tresse sont testés selon un large éventail de déformations moyenne et alternée de façon à obtenir un bon aperçu du comportement de la résistance en fatigue. Les filaments sont considérés comme étant les éléments témoins permettant de définir la résistance en fatigue maximale atteignable par la tresse. Les tresses sont aussi testées selon des modalités comparables. La comparaison des résultats obtenus pour les filaments et pour les tresses mène à une analyse de l'écart entre les résultats. Cette étude est présentée en détail dans l'article 2 au chapitre 5. Le matériel, l'équipement, ainsi que l'étendue du plan d'expérience, sont donnés dans la présente section.

3.2.1 Matériel

Deux types d'échantillons sont testés. Le premier est une tresse en alliage à mémoire de forme tubulaire telle que décrite dans la section matériel de l'étude fonctionnelle (section 3.1.2, page 46). Le second est le filament qui constitue la tresse. Le filament est présenté sous deux formes dans l'étude : le premier est le filament tel que reçu de la compagnie SAES MEMRY (Bethel, CT, É.U.) et traité en fil droit selon les mêmes spécifications que la tresse, il est utilisé pour l'étude comparative principale; le second est un filament retiré d'une tresse qui a subi l'ensemble du traitement thermomécanique de mise en forme, ce filament est utilisé pour expliquer une partie de la différence de la résistance en fatigue entre la tresse et le filament.

3.2.2 Équipement

Les tests de fatigue mécanique sont effectués sur une machine de traction ENDURATEC ELF 3200 (BOSE Corp., MI, USA) équipée d'un bain d'eau et d'un chauffe-eau électronique.

L'analyse des surfaces de rupture est faite à l'aide d'un microscope électronique HITACHI S-3600N (Japan), utilisé à 15KV.

La température de transformation est mesurée à l'aide d'un diffractomètre rayon X X`PERT PRO (PANALYTICAL, Pays-Bas) utilisant des radiations CuKα à 45 KV et un taux de chauffage de 35 K/min.

3.2.3 Procédure expérimentale

Pour s'assurer que les essais débutent dans le même état de phase, les échantillons sont préalablement étirés à 8 % de déformation avant d'être relâchés au niveau de déformation minimale de l'essai. Cet étirement initial important, produit de la martensite alignée dans le sens de la déformation, ce qui devient l'état initial de l'essai, tout en simulant une surcharge importante lors de l'installation. Les essais sont effectués à une fréquence de 2 Hz dans un bain d'eau maintenant la température à 37°C. Cette fréquence a été vérifiée comme produisant le taux de chargement maximal pouvant être imposé de façon à limiter l'échauffement induit par la transformation de phase de l'échantillon pour toutes les modalités de l'essai. La limite de nombre de cycles de l'essai est fixée à 100 000 cycles.

La plage de déformation moyenne imposée est de 2 à 7,1 % pour les filaments et les tresses. La plage de déformation alternée est de 0,6 à 3.8 % pour les filaments et de 0,3 à 3.8 %, pour les tresses. En effet, la résistance en fatigue plus faible des tresses fait en sorte que la plage d'essais est étendue vers les faibles niveaux de déformations alternées. Les modes de déformation moyenne et alternée sont combinés pour assurer que l'échantillon est constamment tendu et que la déformation maximale ne dépasse pas le seuil de rupture de l'échantillon dès le premier cycle. Chaque modalité testée est répétée au moins une fois.

À partir de ces essais, le nombre de cycles à la rupture est comptabilisé ainsi que les contraintes moyennes et alternées, une fois que l'échantillon est stabilisé (200^{e} cycle). Les contraintes mesurées permettent de faire un parallèle entre un chargement à déformation contrôlé et un chargement à contrainte contrôlé.

CHAPITRE 4

ARTICLE #1 « MEDIAN STERNOTOMY: COMPARATIVE TESTING OF BRAIDED SUPERELASTIC AND MONOFILAMENT STAINLESS STEEL STERNAL SUTURES »

Y. Baril[1], V. Brailovski[1],, M. Chartrand[1], P. Terriault[1], R. Cartier[2]

[1]École de technologie supérieure, 1100 rue Notre-Dame Ouest,

Montreal (PQ), Canada, H3C 1K3l

[2]Montreal Heart Institute, 5000 rue Bélanger, Montréal (PQ), Canada, H1T 1C8

Ce chapitre est publié comme un article dans « Proceedings of the Institution of Mechanical Engineers Part H: Journal of Engineering in Medicine », vol. 223, no 3, p. 363-374.

Résumé

Cet article, publié dans « *Proceedings of the Institution of Mechanical Engineers Part H: Journal of Engineering in Medicine »* (DOI: 10.1243/09544119JEIM481), est consacré à la validation et à la comparaison des caractéristiques fonctionnelles de la tresse en alliage superélastique et d'un système de fermeture standard. Les tresses sont installées sur des sternums en polyuréthane à l'aide d'un outil de mise sous tension standard permettant de déterminer précisément la charge appliquée. Les tresses sont maintenues en place grâce à un manchon en acier inoxydable. Pour leur part, les systèmes en acier inoxydable *Ethicon no 5* sont installés en utilisant la technique classique, c'est-à-dire en torsadant les bouts à l'aide d'une pince chirurgicale. Les deux systèmes sont installés selon la même configuration.

Les systèmes sont testés sur le banc d'essai simulateur de sternum décrit dans l'article présenté en annexe I (Chartrand, Brailovski et Baril, 2009). Ils sont soumis à des essais en mode statique et en mode dynamique. Le premier essai permet de caractériser le système en fonction de la force latérale appliquée, alors que le second vise à modéliser des quintes de toux et à suivre l'impact de celles-ci sur la capacité du système à maintenir la liaison osseuse.

Les mesures comparatives sont faites sur la base de deux variables : l'ouverture de la liaison osseuse et la force de compression à l'interface à cette liaison.

Les résultats montrent que le système de fermeture par tresse superélastique permet l'ouverture du sternum à des charges similaires à celles du système classique. Toutefois, le système par tresse applique une charge relative plus importante à la suite d'une perturbation que ne le fait le système classique. Il a donc la même capacité de maintien de la fermeture, mais permet de réappliquer une charge plus importante une fois la perturbation passée.

Abstract

A new device to reduce the risk of postoperative complications following median sternotomy is proposed, made of a superelastic shape memory alloy and called Braided Tubular Superelastic (BTS) suture. This study compares the viability of the BTS suture to that of the standard Monofilament Stainless Steel (MSS) suture. A custom test bench was developed to perform comparative testing of the two sternal closure systems. Sternal models made of polyurethane were closed using common wiring configurations. Static and dynamic tensile separation forces, up to a maximum of 1200 N, were then applied to the closed sternums. The MSS and BTS sutures are compared in terms of the force required to completely open the sternum, the compression force at the sternum midline, and the permanent sternum opening. With a smaller sternum opening and a higher tensile separation force, the MSS suture showed greater rigidity than the BTS suture. The BTS suture, however, displayed a better capacity to reapply compression forces at the sternum midline following the repetitive application and release of tensile separation forces. These results confirm the potential of the BTS suture technology, but further studies using cadaveric sterna are needed to definitely attest to the benefits of using the BTS suture to improve bone healing.

4.1 Notation

BTS	Braided Tubular Superelastic suture
CI	Confidence Interval

MSS	Monofilament Stainless Steel suture
F_{COMP}	Compressive force, N
$F_{COMP,RES}$	Compressive force after disturbance, N
F_{TENS}	Tensile separation force, N
$F_{TENS,MAX}$	Maximum separation force, N
$F_{TENS,O}$	Separation force needed to initiate the sternum midline separation, N
F_u	Force needed to reach the end of the upper superelastic plateau, N
F_l	Force at the end of the lower superelastic plateau, N
F_s	Force leading to the degradation of the sternal bone, N
F_r	Force leading to the rupture of the Braided Tubular Superelastic suture, N
F_d	Post-operation disturbance on a Braided Tubular Superelastic suture, N
M	Control point situated at the manubrium of the sternum model
MS1	Control point situated at cranial midsternum
MS2	Control point situated at caudal midsternum
SD	Standard Deviation
X	Control point situated at the xiphoid
δ	Sternum opening, mm
δ_{PERM}	Permanent sternum opening, mm

4.2 Introduction

Surgeons routinely use between six to ten stainless steel wires to close a severed sternum following a median sternotomy, which is a surgical procedure that provides access to the thoracic cavity. For most patients, this technique allows healing of the cut sternum, however, in some cases, post-operative stresses on the closure loops may cause the thin wires to cut into and through the bone of the sternum [1,2]. To address this issue a novel Braided Tubular

Superelastic (BTS) closure device is designed to decrease the contact pressure with the sternum and subsequently, the risk of dehiscence (PCT/CA05/01859).

This paper presents a comparative study between the new device, the crimped BTS suture, and the standard twisted Monofilament Stainless Steel (MSS) suture. Static and dynamic tests were performed, using a custom test bench to measure their performance characteristics, specifically, the compression force applied at the sternum midline following the closure of the severed sternum.

4.3 Performance Characteristics of a Sternal Closure System

It is believed that a rigid closure system that reduces motion at the sternum midline under loading reduces the risk of post-operative complications by promoting an earlier union of the sternum halves [3]. The higher the rigidity of the closure system, the smaller the sternum opening and the higher the tensile separation force required to initiate an opening at the sternum midline. However, high rigidity alone is not synonymous with a successful closure system. It has been determined in several studies [1,4,5] that opening of the sternum occurs well before the application of the maximum force that can be supported by the closure system, irrespective of the type of system used. This is because when substantial stresses are transferred to the sternum, either by implant installation procedures or by post-operative events (e.g. coughing), localized bone tissue damage may occur in the implant-tissue contact zone. Furthermore, with polymer suture material, the suture itself can manifest stress relaxation under normal service conditions, thus resulting in a loss of compression at the sternum midline.

Once the tensile separation forces are removed, any permanent bone or suture damage will result in a loss of compression forces at the interface between the sternum halves, and consequently, in a decrease of the bond stability. This capacity of the closure system to reapply compression on the sternum after the load has been removed is completely neglected in the current literature. This is significant, because a non-union then results from the lack of pressure at the sternum midline interface, preventing ossification [6].

This study establishes two main performance characteristics that reflect the capacity of a closure system to maintain positive pressure between sternum halves, under single-cycle and multiple-cycle loading (figure 4.1).

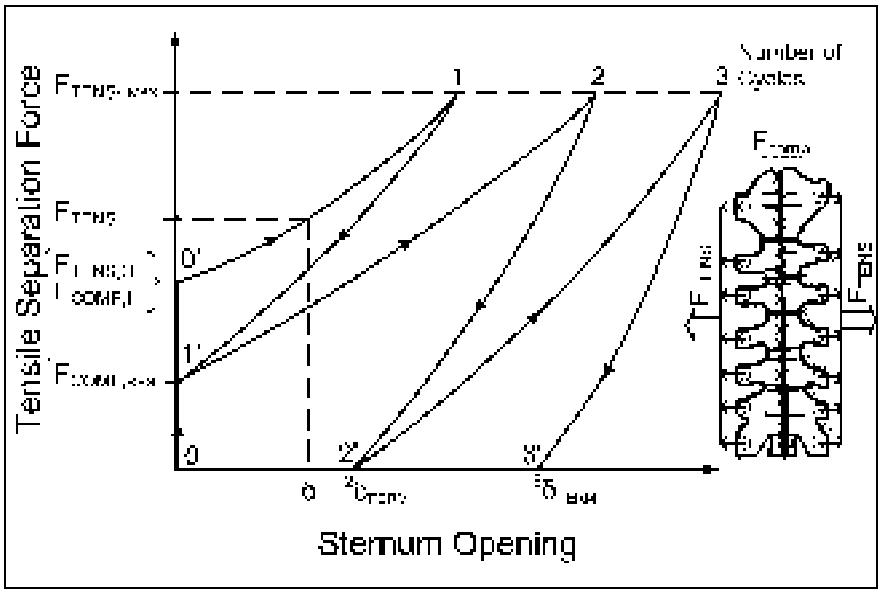

Figure 4.1 Performance characteristics of a sternal closure system.

1. Following a tensile separation force application ($F_{TENS} \leq F_{TENS,MAX}$), the corresponding sternum opening (δ) can be measured at the sternum midline (0-0'-1 (figure 4.1)), from which the rigidity of the whole closure system can be evaluated. A higher rigidity will imply smaller sternum openings and vice-versa. A complementary characteristic to the rigidity can also be assessed, namely, the tensile separation force ($F_{TENS,O}$) needed to initiate the sternum midline separation (0-0').

2. Following tensile separation force application and release, the residual compression force ($F_{COMP,RES}$) applied at the sternum midline (0'-1-1') can be measured. Again, a complementary performance characteristic to the residual compression force can also be

evaluated, namely, the permanent sternum opening (δ_{PERM}), following repetitive tensile separation force applications and releases (1'-2-2', 2'-3-3', etc.).

In this study, the proposed performance characteristics will be assessed for the two closure systems: Braided Tubular Superelastic (BTS) suture and Monofilament Stainless Steel (MSS) suture, under identical experimental conditions.

4.4 Description and Functional Requirements of the BTS and MSS Sutures

4.4.1 BTS Suture

The system presented here, the Braided Tubular Superelastic (BTS) suture, is a tubular mesh-like device shaped like a braided tube, and made of superelastic Nitinol (Titanium-Nickel shape memory alloy). Its tubular geometry offers a highly flexible axisymmetric structure, which reduces contact stresses through a planar contact with the sternum when it is wrapped around the latter. This form resembles the flattened form of a sternal band [4]. The superelastic behavior of Nitinol (see figure 4.2) allows a non-zero force to be applied to the sternum even though the width of the sternum tends to decrease due to the nature of the healing process (A-B-C (figure 4.2)). In addition, Nitinol benefits from the so-called dynamic interference phenomenon [7], manifesting significant hardening under external impulses, such as coughing, for example (C-D). If the external forces continue to increase, Nitinol provides a quasi-constant pressure (D-E) defined by the height of the upper plateau of the superelastic loop. Once the disruption is over, the force applied by the closure system to the sternum returns to its former level on the lower plateau (E-F-C).

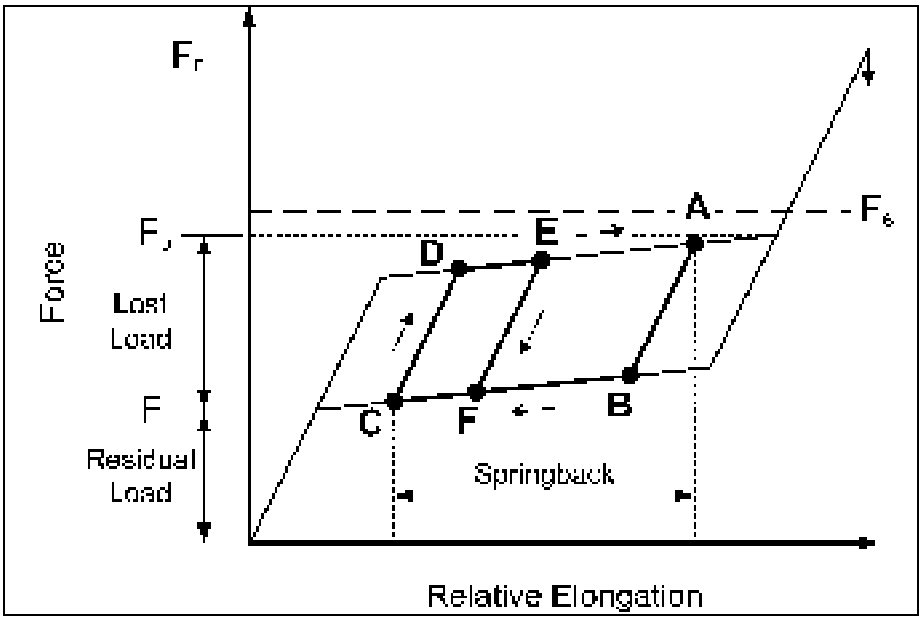

Figure 4.2 Schematization of the superelastic behavior and functional requirements for the BTS suture force-displacement characteristics.

To prevent failure of the sternum suture during post-operative disturbances such as coughing, while maximizing residual compressive forces between sternum halves when a disturbance is over, the force-displacement characteristics of the BTS suture must meet the following requirements:

Installation requirements:

- To fully exploit the superelastic advantage of the BTS suture, the force applied to the suture during installation should be as close as possible to the end of the upper superelastic plateau (F_u), F_u should be slightly lower than the cut-in resistance of the sternum bones (F_s). If F_u is significantly less than F_s, the sternum will open at lower disturbance forces. If F_u exceeds F_s, the surgeon could damage sternum bones during installation or limit the installation force under F_s to preserve the bones' integrity, which results in less available superelastic springback.

Service requirements:

- To prevent suture failure, the suture should present a force-to-rupture (F_r) sufficient to sustain forces generated by post-operation disturbances (F_d).
- To benefit from the superelastic behavior of the suture, the force at the end of the lower transformation plateau (F_l) must be greater than zero.

To summarize the requirements, the superelastic suture must comply with the following three conditions:

- $F_u \leq F_{inst} < F_s$; the suture installation force should lie between the cut-in resistance of the sternum bones (F_s) and the end of the upper superelastic plateau (F_u) in order to benefit from superelastic behavior.
- $F_r > F_d$; the force-to-rupture of the suture (F_r) should exceed the post-operation disturbance force (F_d) to prevent failure of the suture.
- $F_l > 0$; the force at the end of the lower transformation plateau should be above zero to preserve superelasticity.

4.4.2 MSS suture

The dimensions and functional requirements for stainless steel surgical fixation wire are in accordance with the ASTM specification [8].

4.5 Materials and Equipment

4.5.1 BTS suture

The superelastic suture is manufactured from a Ø0.1 mm filament of BTR-BB (Ti-50.8 at %Ni) alloy with 36% of cold-work supplied by MEMRY CORP (Bethel, CT, USA). The 24-filament suture is braided with a 12.7 mm pitch on a 3.2 mm aluminum core using a

WARDWELL (Central Falls, RI, USA) braiding machine. With the core in place, the braided structure is then heat-treated at 350°C (15 min) to preserve its tubular shape. The general behaviors of the single filament and braided suture are shown in figure 4.3a and figure 4.3b. The ultimate force-to-rupture (F_r), the end of the direct transformation plateau (F_u), and the end of the reverse transformation plateau (F_l) of the braid are proportional to those of the single filament, with a scale factor of around 20. See Table 1 for BTS suture force characteristics.

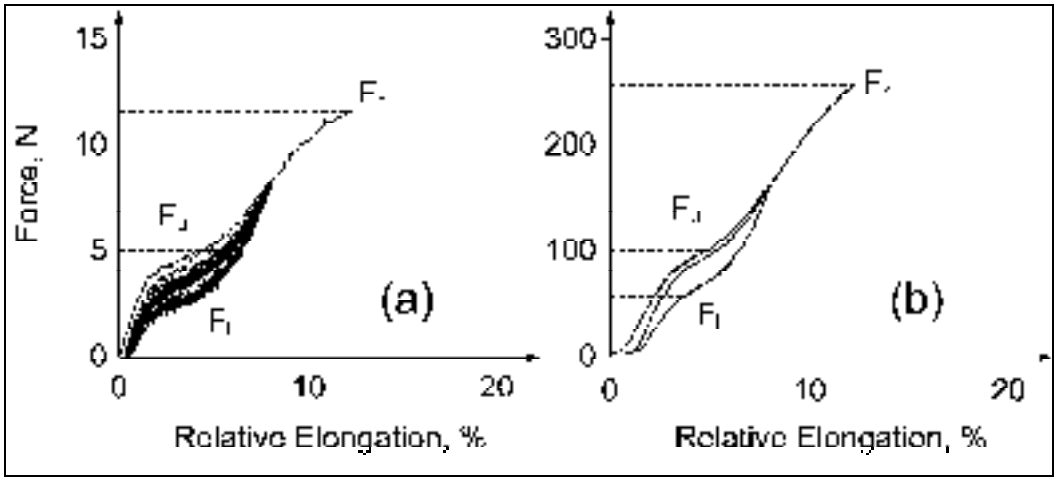

Figure 4.3 (a) Single superelastic filament and (b) 24-filament BTS suture.

Given the superelastic nature of the BTS suture, the braid is impossible to twist and so it must be crimped with a special apparatus described later in the methodology. Stainless steel crimps become thereof part of the BTS suture closure system.

4.5.2 MSS suture

For the comparative study, No. 5 ETHICON monofilament stainless steel (Ethicon Inc, Somerville, NJ, USA) sternal suture is used. This standard closure is twisted under the direct supervision of a cardiac surgeon as commonly performed in the operation room. See table 4.1 for MSS suture force characteristics.

Table 4.1

Mechanical properties of closure wire and braid used

Mechanical propriety	MSS	BTS
F_l (N)		57 ± 4
F_u (N)		121 ± 4
F_{yield} (N)	201 ± 5	210 ± 6
F_r (N)	355 ±5	248 ± 10
Data are mean values ± SD (MSS n=4; BTS n=5)		

4.5.3 Sternum model

The sternum models used in this study are made of a solid polyurethane foam with a density of 0.32 g/cm^3 (Sawbones Corporation, Vashon Island, WA, USA), which partially replicates the properties of cadaveric sterna [9]. This foam also manifests a viscoelastic behavior, which, while not similar to human bone, allows for fatigue testing comparison.

4.5.4 Testing bench

To perform the comparative testing of the MSS and BTS sternal sutures, a custom test bench was developed [10]. The existing test benches are not designed to use a common platform for the installation and mechanical testing of sternal closure systems. Most test benches use tensile testing machines with vertical sternum positioning, which does not correspond to sternum closures in a position replicating in-vivo conditions [11-17]. The testing bench developed here provides the same set-up for installation and post-installation testing, which allows data acquisition of the compression forces applied at the sternum midline during installation and service-stimulated conditions (coughing, breathing).

Figure 4.4a shows a schematic overview of the test bench. Two hydraulic cylinders (1) (1-1/8-MH-TF-4-D, Scheffer Corporation, Cincinnati, OH, USA) provide the lateral motion for the mobile frame (2), linked to the static frame (3) by a pair of mobile arms (4) which confine movement to a horizontal plane. The displacement of each cylinder is controlled by a high-precision servo valve (not shown in figure 4.4a) (27A50F-1E02-999 Servo valve, HR Textron Operation, Santa Clarica, CA, USA), and their strokes are individually measured by displacement laser sensors (5). Each half of the severed sternum (6) is held in place with shoulder screws (7) measuring 5 mm in diameter, passed through the rib struts.

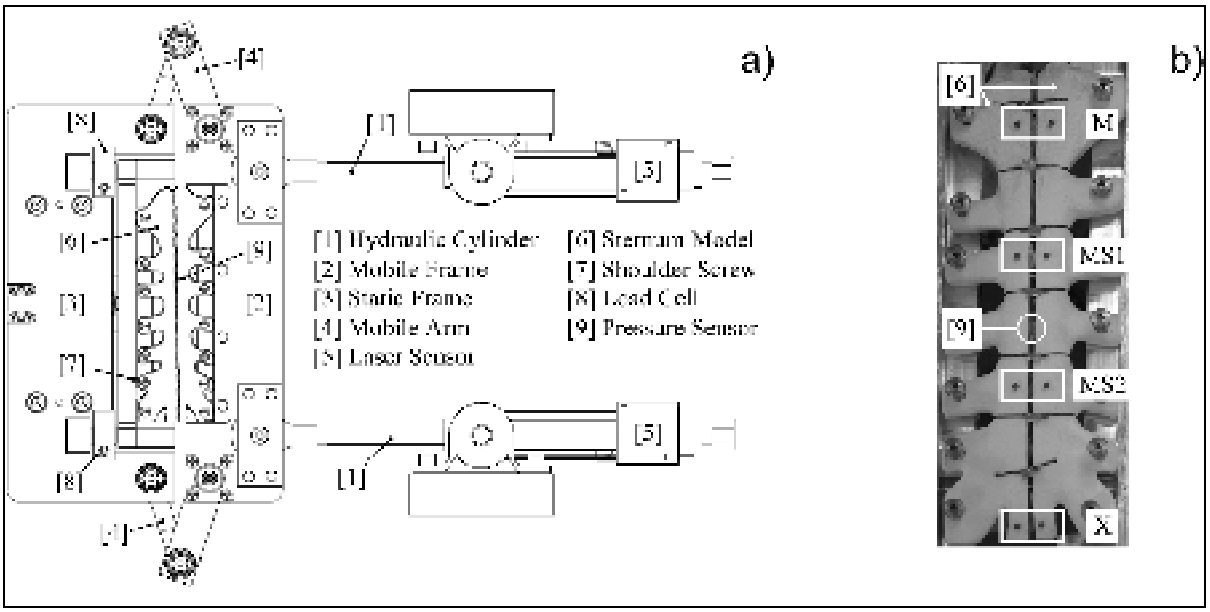

Figure 4.4 Schematic overview of the test bench (a) and closed sternum model with BTS suture using the 7S configuration with the locations used to evaluate sternum opening and typical pressure sensor at the sternum midline (b).

The tensile separation force applied by the cylinders to the closed sternum is recorded by a set of three load cells (8) (LC703-200, Omega Engineering Inc, Stamford, CT) with a capacity of 200 lb (889 N) (one of which is hidden under the static frame and so is not visible in Fig. 4a). An algorithm computes the summarized force applied on the sternum from the input of the three load cells. It is worth noting that in this study, all of the external forces applied to the sternum are symmetrical. The force at the interface between the sternum halves is measured by a series of eight pressure sensors (9) (Flexiforce A201-100, Tekscan Inc, Boston, MA, USA), each with a capacity of 100 lb (445 N), equally distributed along the sternum midline. The displacement between both sternum halves is recorded in parallel with a videoextensometer and Dot Measurement Software (model ME-46, Messphysik Material Testing, Austria) at four different control points (figure 4.4b). Adapting a nomenclature previously used by Pai et al [16,17] to locate the points, point M is situated at the manubrium, points MS1 and MS2 at the midsternum, and point X at the xiphoid.

To apply a precise installation force to the BTS suture loop, the following procedure is employed (figure 4.5a). To maximize the safe springback of the BTS suture (step II-III, Fig. 5a), a tensioner (figure 4.5b) (Pilling, Philadelphia, PA, USA), instrumented with strain gauges and linked to a strain gauge transducer (P3, Vishay Intertechnology, Inc, Malvern, PA, USA), is used to apply an initial compression force (F_i) just above the end of the direct transformation plateau (F_u, figure 4.3b, between 100 and 120 N). The tensioner follows the threading of the suture around or through the sternum (step I, figure 4.5a). Next, a pair of crimping pliers is used to plastically deform a stainless steel (316L annealed) cylindrical sleeve (external diameter of 3.2 mm, 0.4 mm thick and 5 mm long) that is used to retain the suture extremities (step III, figure 4.5a). To complete the installation, the loose ends are cut near the crimped joint (step IV, figure 4.5a). An installation device that will facilitate the realization of these four installation steps is currently under development [see Appendix].

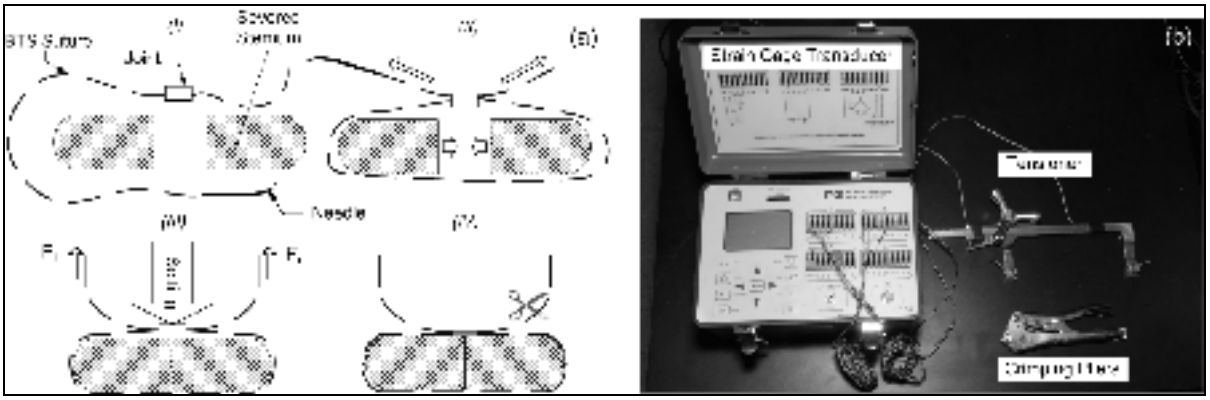

Figure 4.5 (a) Suture installation procedure: I) suture treading; II) first closure of sternum halves; III) suture installation force application and joint setting; IV) suture cutting; (b) installation tools used.

The LabView software (LabView 8.2, National Instrument Corp., Austin, TX, USA) performs a real-time recording of the forces measured by the three load cells and eight pressure sensors with an NI PCI-6229 acquisition card (National Instrument Corp). Data exchange between LabView and the videoextensometer is coordinated during post-processing with Excel (Microsoft Corp., Redmond, WA, USA).

4.6 Testing Methodology

Static and dynamic testing completed within this study compare the performances of the standard No. 5 ETHICON MSS and 24-filament BTS sternal sutures. Each artificial sternum was severed longitudinally with a band saw and closed with either a No. 5 ETHICON MSS or a BTS suture. Figure 4.4b shows the 7S wiring configuration used for both closure systems. This wiring configuration, the same as Dasika's [18], combines five peristernal closures equally distanced along the sternum corpus, with two transsternal closures, one at the manubrium, and the other at the xiphoid.

Both systems were installed following the same sequence, even though the stainless steel suture was installed using a conventional twisting procedure and the BTS suture required the use of the special tensioning device and clamps. Once the midline gap is manually decreased by pulling on all the sutures simultaneously with the help of an assistant, the closures are sequentially fixed, progressing from the xiphoïd to the manibrium. To reproduce the realistic situation of sternal closure, all of the tests start at cycle 1 with no precycling.

Static testing, employed to evaluate the rigidity and static resistance of the sternal closure, consists of incremental application of the tensile separation force to both halves of the sternum (200 N by step), up to a maximum force of 1200 N. Figure 4.6a, b, and c shows the loading sequence, the eight pressure sensors' responses and the displacement at the sternum midline at four control points, respectively, as a function of time. Values given by pressure sensor 4 and control point MS1 at the 4^{th} increment of force are used as examples of data extraction in figure 4.6a, b, and c.

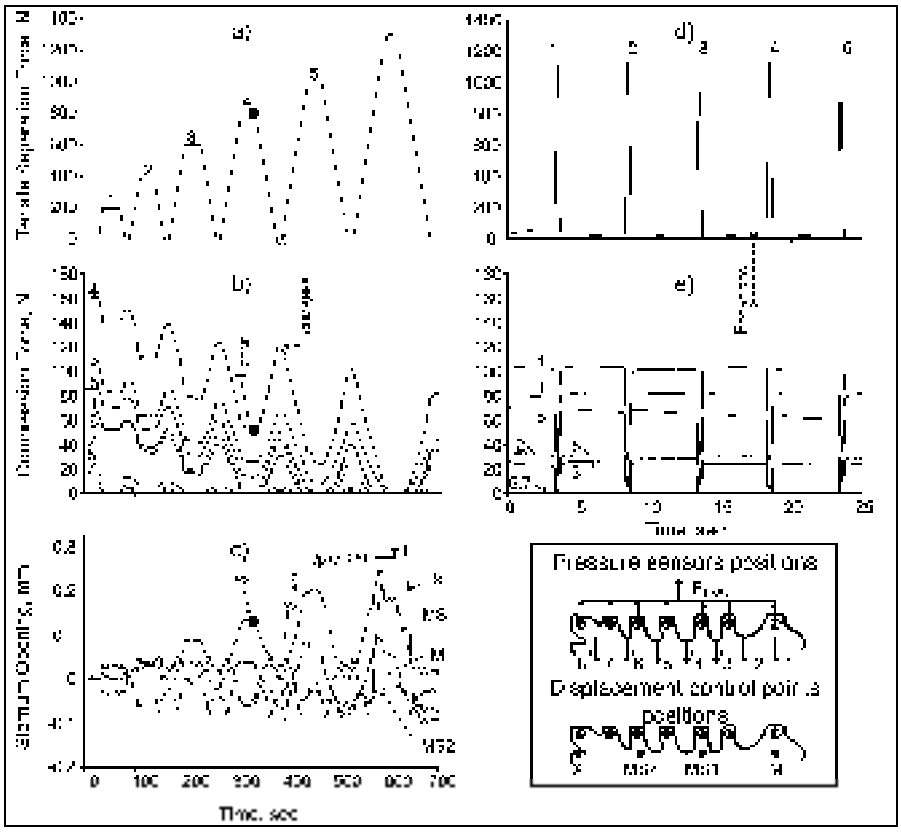

Figure 4.6 Examples of loading patterns as a function of time executed on MSS closure systems (a) static loading sequence (b) the 8 pressure sensors response for static loading (c) displacement at the sternum midline at 4 control points for static loading (d) five simulated coughing fit of the dynamic loading sequence (e) pressure sensor responses for dynamic loading.

The 30-second dwell time for each step provides system stabilization and allows calculation of the compression force at the sternum midline (F_{COMP}) as the sum of eight pressure sensor responses and the sternum opening (δ) at each of four control points. After each increment, the tensile separation force is brought back to zero in order to measure the residual force ($F_{COMP,RES}$) and the permanent displacement at the sternum midline (δ_{PERM}).

Dynamic testing, which evaluates the resistance of the sternal closure to coughing or sudden movement, involves application of the maximum tensile separation force of 1200 N over a short period. Previous studies have characterized coughing with pressure building up for 200 ms followed by two expiratory phases, lasting approximately 30 to 50 ms and 200 to 500 ms

respectively [6]. In our study, a triangular approximation of the coughing pattern was used, with the pressure building up for 200 ms and the combined expiratory phases lasting 230 ms. Five simulated coughing fits and the corresponding pressure sensor responses are shown in Fig. 6d and e. The residual compression force at the sternum midline ($F_{COMP,RES}$) is recorded after each coughing fit as illustrated in Fig 6e for the third cycle. This loading pattern was applied until failure occurred.

For static testing, statistical differences ($p<0.05$) between the closure systems are examined with an unpaired Student's t test. The same procedure is used to compare a) the compression force at the sternum midline (F_{COMP}) and the sternum opening (δ) during application of the tensile separation force, and b) the residual compression force ($F_{COMP,RES}$) and the permanent sternum opening (δ_{PERM}) after the tensile separation force is removed. Dynamic testing uses an unpaired Student's t test to compare the residual compression force at the sternum midline ($F_{COMP,RES}$) after each coughing fit is applied. Static and dynamic tests are performed with five samples for each closure system ($n_{TOT} = 20$).

4.7 Results

4.7.1 Static testing

Figure 4.7 presents the displacement at the sternum midline for each of four control points as a function of the tensile separation force and the compression force at the sternum midline (F_{COMP}) as a result of the tensile separation force applied to the MSS (figure 4.7a) and BTS (figure 4.7b) sutures. Both systems behave in a similar fashion, with a larger opening in the lower region of the sternum (MS2 and X locations) and a smaller opening in the upper region (M and MS1 locations). For each of the control points, no significant differences between the two closure systems were observed for tensile separation forces less than 1000 N. However, when tensile separation force exceeds 1000 N, significant differences ($p<0.05$) are observed for the MS1 and MS2 control points, with the MSS suture allowing a smaller sternum opening than the BTS suture. Table 4.2 shows the sternum opening measured at the sternum midline under 1200 N of tensile separation force and includes the midline compression force upon installation of both devices. Zero compression force at the sternum midline gives

significantly different tensile separation forces (F_{TENS}) of 1034±57 and 1221±73 N, respectively, which are the minimum required to completely open the sternum midline ($p<0.05$).

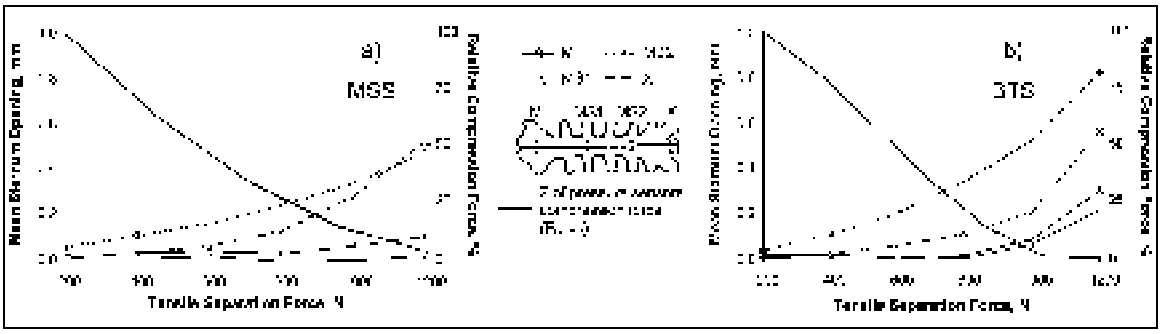

Figure 4.7 Sternum opening force for and relative compression force (F_{COMP}) as a function of tensile separation force (a) No. 5 ETHICON MSS and (b) 24-filament BTS suture. Both systems use the 7S configuration. Compression forces are in percentage of the installation force because both systems do not apply the same initial force; Data are mean values (n=5).

It should be mentioned that even though two hydraulic cylinders impose equal forces to the common -- for all rib struts -- rigid link, the rigidity of the ribs, sternum core and sutures are not equally distributed along the sternum midline, which results in a non-uniform midline opening. In our particular case, the inversion of MS2 and X displacements is due to a pivot effect created by the xiphoïd closure. The measurements at the X point are made outside the zone of closure, contrarily to the measurement at the MS2 point. This non-uniform distortion of artificial sterna has been observed in other studies [17].

Table 4.2

Sternum opening as a function of location for 1200 N of tensile separation force and installation forces for each system

Sternum Opening (mm)*			
Location	MSS	BTS	*p* Value
M	0.09 ± 0.10	0.21 ± 0.13	0.167
MS1	0.01 ± 0.06	0.29 ± 0.14	0.003
MS2	0.47 ± 0.13	0.82 ± 0.20	0.010
X	0.52 ± 0.33	0.55 ± 0.42	0.869
Sternum installation forces (N)**			
	462 ± 51	556 ± 30	0.007
Data are mean values ± SD (* n=5; ** n=10)			

Figure 4.8 shows the residual compression force ($F_{COMP,RES}$) and permanent sternum opening at the MX2 control point (δ_{PERM}) after release of the tensile separation force. After a complete loading cycle, 40±4 and 46±6% of the initial compression force is reapplied, and permanent openings of 0.13±0.08 and 0.11±0.12 mm are obtained for the MSS and BTS sutures, respectively, showing no significant differences ($p>0.05$).

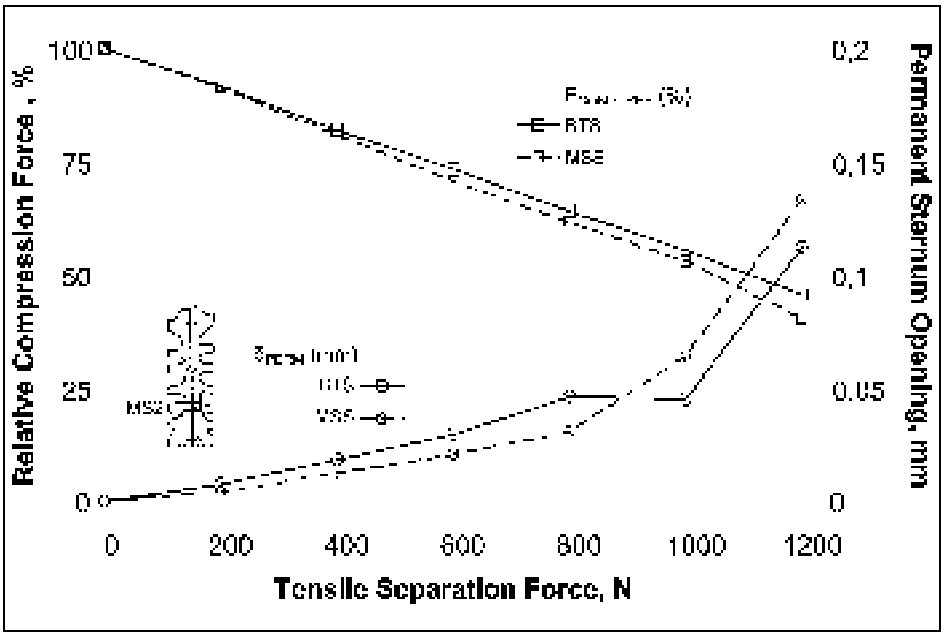

Figure 4.8 Relative residual compression force ($F_{COMP,RES}$) and permanent sternum opening (δ_{PERM}) as a function of released tensile separation. Compression forces are in percentage of the installation force because both systems do not apply the same initial force; data are mean values (n=5).

4.7.2 Dynamic testing

With dynamic testing, significant differences ($p < 0.05$) are observed at every cycle, with the BTS suture reapplying a greater percentage of its midline installation compression force. Figure 4.9 compares the mean sternum midline residual compression forces ($F_{COMP,RES}$) and their confidence interval as a function of the number of simulated coughing fits. See also table 4.3 for $F_{COMP,RES}$ in terms of mean and standard deviation.

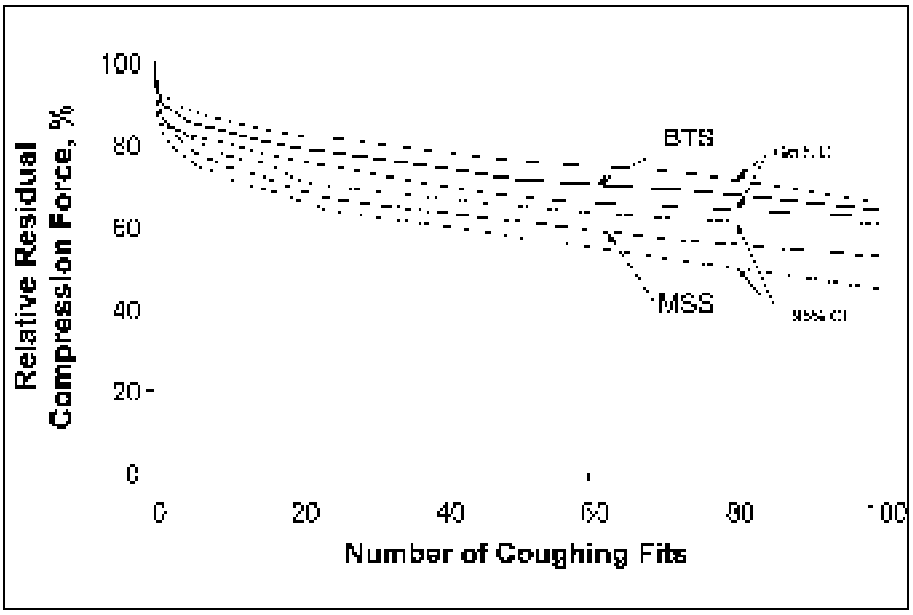

Figure 4.9 Relative residual compression force in respect of the number of coughing fit simulations; data are mean values, with a 95% CI (n=5 [0-50[; n=4 [50-100])

Table 4.3

Relative residual compression force as a function of the number of coughing fits and installation forces for each sternum closure

Relative Residual Compression Force (%)			
Coughing fits	MSS	BTS	*p* Value
1	85 ± 2	90 ± 3	0.023
5	78 ± 3	85 ± 3	0.014
10	74 ± 3	83 ± 3	0.002
25	66 ± 3	77 ± 4	0.001
50	61 ± 4[a]	71 ± 4[a]	0.012
100	53 ± 8[a]	64 ± 4[a]	0.033
	installation forces (N)		
	588 ± 54	394 ± 59	0.000

Data are mean values ± SD (n=5)

[a] n=4 caused by earlier ribs failure

4.8 Discussion

Static testing on the full-scale model shows that the standard ETHICON no. 5 MSS suture is stiffer than the novel 24-filament BTS suture, and allows less sternum opening at the most solicited locations (MS1 and MS2). The tensile separation force (F_{TENS}) required to completely separate the sternum midline is 15% higher for the MSS than for the BTS suture. However, no significant differences in the tensile separation force and permanent sternum

opening for both systems are found below F_{TENS} = 1200 N. These results suggest that once the sternum is open, the stainless steel suture allows a smaller sternum opening than the superelastic suture. However, when there is no opening, both systems have a similar behavior.

Dynamic testing shows that a higher residual compression force (F_{COMP_RES}) is applied by the BTS suture following the repetitive application and release of a tensile separation force. At the 100th cycle, the BTS suture applies 11% more compression than the MSS suture (64 versus 53% of the initial compression force or a gain of 20%).

4.8.1 Previous studies

A comparative study published by the authors on the BTS versus standard Monofilament Stainless Steel (MSS) suture confirms that the BTS system assures higher sternum closure stability. Numerical results showed that the relative residual force measured after an external load application and release should be 60% higher for the superelastic than for the stainless steel closure [19]. Experimental results – on the Sawbones polyurethane blocs – exhibited an average gain of 30% for the relative residual force provided by the BTS suture compared to the MSS suture ($p \leq 0.05$) [20]. The present study confirms the gain of the superelastic suture over the stainless steel suture under repetitive application and release of tensile separation forces, here in the case of simulated coughing tests.

4.8.2 Ribs struts failure

Another point to stress is that in most cases, the rib struts failed before the closure system fails, and thus, the maximum tensile separation force that could be supported by a closure system itself before failure was never reached. With dynamic testing, one sample for each closure system had to be discarded because of an early rib failure, bringing the total number of samples to six for each closure system. An improved fixation method for the sternum must be developed, and to that end, better placements of the holes to minimize the stress concentration or embedding of the ribs are possible solutions.

4.8.3 Pressure sensors

An intrusive presence of the pressure sensors at the interface was initially suspected to be modifying the behavior of the sternum under tension. However, preliminary tests completed with stainless steel sutures showed no significant difference for the sternum with or without pressure sensors.

4.9 Conclusion

This study suggests that the Braided Tubular Superelastic (BTS) suture reapplies higher compression forces at the sternum midline during repetitive loading, while being less rigid than the classic Monofilament Stainless Steel (MSS) suture. The authors conclude that for a given tensile separation force, a sternum closure system that applies a higher compression force after the disruption is over is better than a sternum closure system that limits opening with a risk of sternal dehiscence. Furthermore, higher sternum midline compression forces reduce the risk of subsequent opening as they increase the force needed to open the sternum again. The test bench developed for sternum testing proves the viability of the BTS installation and testing technology. Subsequent research should continue in order to definitely confirm the potential of BTS suture technology to improve bone healing.

4.10 Acknowledgement

This work was performed in the framework of a research program supported by the Natural Sciences and Engineering Research Council of Canada (NSERC) and Valeo Management L.P.

4.11 References

1. Casha AR, Gauci M, Yang L, Saleh M, Kay PH, Cooper GJ. Fatigue testing median sternotomy closures. Eur J Cardio-Thorac. 2001;19(3):249-53.

2. Robicsek F, Daugherty HK, Cook JW. The prevention and treatment of sternum separation following open-heart surgery. J Thorac Cardiovasc Surg. 1977;73(2):267-8.

3. Sargent LA, Seyfer AE, Hollinger J, Hinson RM, Graeber GM. The healing sternum: a comparison of osseous healing with wire versus rigid fixation. Ann Thorac Surg. 1991;52(3):490-4.

4. Casha AR, Yang L, Kay PH, Saleh M, Cooper GJ. A biomechanical study of median sternotomy closure techniques. Eur J Cardio-Thorac. 1999;15(3):365-9.

5. McGregor WE, Trumble DR, Magovern JA. Mechanical analysis of midline sternotomy wound closure. J Thorac Cardiovasc Surg. 1999;117(6):1144-5.

6. McCool FD. Global Physiology and Pathophysiology of Cough: ACCP Evidence-Based Clinical Practice Guidelines. Chest. 2006;129(1_suppl):48S-53.

7. Duerig T, Pelton A, Stockel D. Superelastic Nitinol for Medical Devices. Med Plast Buimat Mag MPV Arch. 1997:1-14.

8. F 1350. Standard Specification for Wrought 18 Chromium-14 Nickel- 2.5 Molybdenum Stainless Steel Surgical Fixation Wire (UNS S31673). in Annual book of ASTM standards. Philadelphia: American Society for Testing and Materials; 2001. p. 684-5.

9. Trumble DR, McGregor WE, Magovern JA. Validation of a bone analog model for studies of sternal closure. Ann Thorac Surg. 2002;74(3):739-44.

10. Chartrand M, Brailovski V, Baril Y. Test Bench and Methodology for Sternal Closure System Testing Exp Techniques. 2008:Submited.

11. Cohen DJ, Griffin LV. A biomechanical comparison of three sternotomy closure techniques. Ann Thorac Surg. 2002;73(2):563-8.

12. Dasika UK, Trumble DR, Magovern JA. Lower sternal reinforcement improves the stability of sternal closure. Ann Thorac Surg. 2003;75(5):1618-21.

13. Losanoff JE, Collier AD, Wagner-Mann CC, Richman BW, Huff H, Hsieh F-h, et al. Biomechanical comparison of median sternotomy closures. Ann Thorac Surg. 2004;77(1):203-9.

14. Losanoff JE, Foerst JR, Huff H, Richman BW, Collier AD, Hsieh FH, et al. Biomechanical porcine model of median sternotomy closure. J Surg Res. 2002;107(1):108-12.

15. Ozaki W, Buchman SR, Iannettoni MD, Frankenburg EP. Biomechanical study of sternal closure using rigid fixation techniques in human cadaver. Ann Thorac Surg. 1998;65(6):1660-5.

16. Pai S, Gunja N, Dupak E, McMahon N, Coburn J, Lalikos J, et al. A Mechanical Study of Rigid Plate Configurations for Sternal Fixation. Ann Biomed Eng. 2007;35(5):808-16.

17. Pai S, Gunja NJ, Dupak EL, McMahon NL, Roth TP, Lalikos JF, et al. In Vitro Comparison of Wire and Plate Fixation for Midline Sternotomies. Ann Thorac Surg. 2005;80(3):962-8.

18. Dasika UK, Magovern JA. Lower sternal reinforcement to improve median sternotomy closure: Reply. Ann Thorac Surg. 2004;77(6):2261-2.

19. Baril Y, Brailovski V, Terriault P, Cartier R. Feasibility study of a new sternal closure device using tubular braided superelastic Nitinol structures. Materials & Processes for Medical Devices Conference 14-16 Nov.; Boston, MA, USA. ASM International; 2005. p. 243-8.

20. Baril Y, Brailovski V, Chartrand M, Terriault P, Cartier R. In-vitro testing of a new superelastic sternum closure component. SMST-2007, International Conference on Shape Memory and Superelastic Technologies; Tsukuba, Japan. "In press".

4.12 Appendix : Installation Device for the Braided Tubular Superelastic (BTS) Suture

While standard monofilament stainless steel sutures are simply crossed, pulled and twisted following state-of-the-art manipulations to retain both sternum halves, the superelastic suture requires a specific installation procedure for two reasons. First, to benefit from the spring-back force following a disruption, the loop must be installed at a precise tension (figure 4.2). Secondly, to retain a loop, the superelastic nature of the BTS suture makes any permanent twisting impossible. Therefore, an installation tool that could apply a precise tension to a loop of the BTS suture and plastically deform the joint that would retain the loop is developed.

A global view of the installation tool is presented in Fig. 10. A front, side and top view are presented in Figures. 4.10a, 4.10b and 4.10c, respectively. For each of the steps previously described in Fig. 5, a brief description of the mechanism that accomplishes the above mentioned step will be provided.

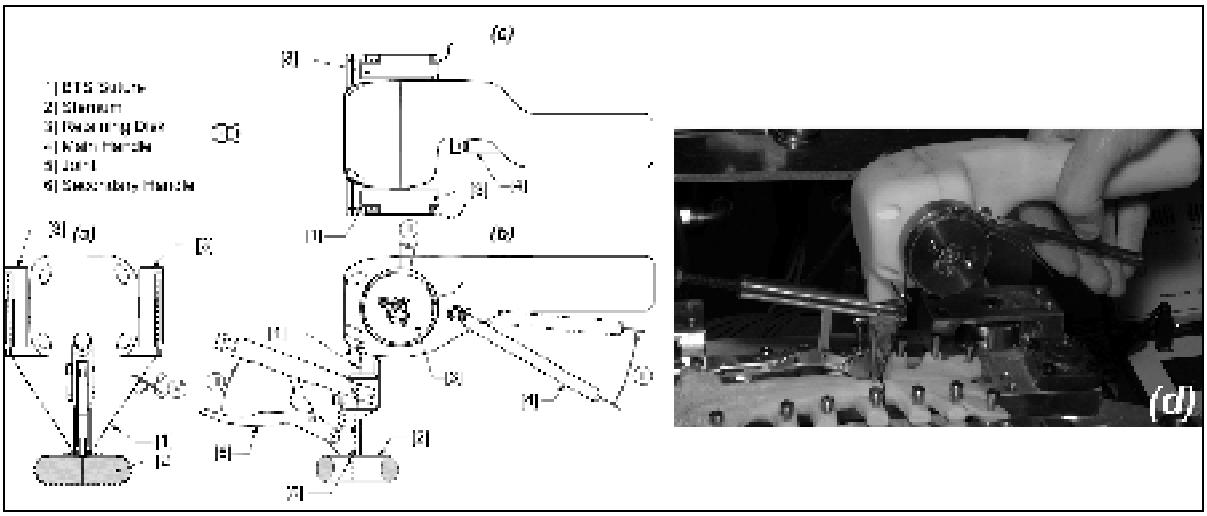

Figure 4.10 Front (a), side (b) and top (c) view of the developed installation tool; picture of the installation tool during the installation process (d).

Step I, Threading of the suture (Step I): the threading of the Superelastic suture (1) around the sternum (2) is completed without the support of the installation tool, the same way it would be accomplished for a stainless steel wire.

Step II, Application of a Tension (Step II): once the threading is completed, the installation tool is positioned over the sternum (2) and each extremity of the suture (1) is fixed through retaining disks (3). By activating the main handle (4) upward, the user applies a tension to the suture loop by rotating the retaining disks (3). The arrows associated with the Step II marker indicate the direction of the movement for the handle (4) and retaining disks (3). When the desired tension is reached, an automatic mechanism stops any supplementary rotation to the retaining disks (3), and their positions are maintained.

Step III, Crimping of the Joint (Step III): once the tension applied to the BTS suture (1) reaches the desired value, the joint (5) is plastically deformed to permanently retain the loop (1), with the joint (5) previously positioned at the base of the installation tool. By activating the secondary handle (6) upward, the user crimps the joint (5) permanently. The arrow associated with the Step III marker indicates the direction of the movement for the handle (6).

Step IV, Completion of the Installation (Step IV): The installation is completed with the cut of the suture between the base of the installation tool and the retaining disks (3), as shown by the Step IV marker. Doing so will allow a clearance of the apparel, and a final cut, near the crimped joint (5), is completed to finalize the installation.

CHAPITRE 5

ARTICLE #2 « FATIGUE PROPERTIES OF SUPERELASTIC TI-NI FILAMENTS AND BRAIDED CABLES FOR BONE FIXATION »

Y.Baril[1], V. Brailovski[1]

[1]École de technologie supérieure, 1100 rue Notre-Dame Street Ouest,

Montreal (PQ), Canada, H3C 1K3l

Ce chapitre est soumis comme un article à « Journal of Biomedical Materials Research: Part B: Applied Biomaterials ». Numéro de confirmation : JBMR-B-08-0659.

Résumé

L'article soumis à « *Journal of Biomedical Materials Research: Part B: Applied Biomaterials* » (déc. 2008) a trois objectifs principaux. Le premier est d'établir les performances en fatigue de la tresse superélastique. Le second est de déterminer dans quelle zone de la courbe contrainte-déformation la tresse devrait être initialement chargée. Cet objectif inclut la caractérisation de l'impact de la déformation moyenne sur la vie en fatigue des alliages Ni-Ti superélastiques, sujet qui demeure controversé dans la communauté scientifique. Le troisième est d'identifier les causes d'une diminution marquée de la vie en fatigue lors du passage du filament à la tresse. Pour ce faire, deux plans d'essais ont été construits. Un premier visait l'évaluation des caractéristiques de vie en fatigue du filament. Ce plan est constitué d'une série d'essais discrétisant une large zone d'essais dans le domaine de « déformation moyenne – déformation alternée » se situant sur le plateau de transformation et ses abords. Le second, testant la tresse, met plus l'accent sur les bas niveaux de déformation alternée de façon à atteindre la limite des essais (10^5 cycles).

Les résultats démontrent que, la déformation alternée est le facteur le plus influent, mais la contrainte moyenne a aussi un impact et le chargement de la tresse devrait idéalement se situer à une déformation moyenne correspondant au centre du plateau de transformation. La limite de l'essai (10^5 cycles) est atteinte pour le filament soumis à une déformation alternée

de l'ordre de 1 %, alors qu'elle est atteinte à une déformation alternée de 0,3 %, pour la tresse. Il est aussi démontré que la détérioration de la vie en fatigue de la tresse est due entre autres : a) à la flexion qui se produit dans les filaments croisés dans la tresse ce qui augmente significativement la déformation moyenne locale, b) à un défaut de production générant des égratignures en surface du filament etc) à la friction entre les filaments lors de la sollicitation de la tresse.

Abstract

A new cable for bone fixation, a braided hollow tubular structure made of superelastic Ti-Ni filaments, was developed. To evaluate the fatigue life of the cable and the impact of braiding on fatigue life, a comparative fatigue study was conducted on both the braided cable and the single filament. The results of strain-controlled fatigue testing under variable mean and alternating strain conditions demonstrated that: a) even though alternating strain is the most influent parameter, mean strain also has a significant impact on the fatigue life of both the filament and the braid; an improvement in the braided cable's fatigue life is observed under mean strains corresponding to the middle of the superelastic loop plateau; and b) run-out (10^5 cycles) is reached at 1% of alternating strain for the filament, and at 0.3% for the braided cable. It was proved that the negative impact of braiding on fatigue life is most likely caused: a) by friction-induced damage of the braided filaments during cable manufacturing and b) by locally occurring bending in the vicinity of the filaments' crossing, combined with the interfilament fretting during repetitive stretching of the braided cable.

5.1 Introduction

A new bonding device for bone fixation involving superelastic shape memory alloys has been developed by our laboratory [1]. This device is a tubular-shaped braided cable used to tightly wrap two or more bone parts together and thus limit their relative movement. The superelastic cable used as a binding element provides two novel features for bone fixation. Firstly, it keeps the compression forces constant, even though the cerclage geometry varies as a result of the bone remodeling, thus preventing cable loosening. Secondly, it flattens out,

providing a better force distribution at the bone-cable interface and reducing the risk of cutting through the bone. To achieve these goals, the device must be tightened up to an initial force that assures the stability of the joint. When used as a sternal closure cable, the device will sustain alternative loading due to post-operative perturbations such as coughing and deep respiration, and, when used in orthopedics, it will moderate the stresses of walking and stair climbing.

Many studies have been conducted to evaluate the impact of alternating (oscillating) strain on the fatigue life of Ti-Ni superelastic alloys [2-6], but only a few have focused on the impact of the mean strain [7-10]. All of these studies agree that alternating strain has a greater effect on fatigue life than mean strain, and that the higher the alternating strain, the shorter the fatigue life. As for the mean strain influence on the superelastic fatigue life of Ti-Ni alloys, there is no consensus [11]. It is worth noting that several authors even reported an improvement in the endurance limit when mean strain increases from 2 to 4% in bending [7-9] and from 0 to 4% in tension [8,10].

The main goal of this study was to evaluate the fatigue life of the Ti-Ni superelastic braided cable as compared to that of the single filament used in its manufacturing. The fatigue life characteristics of both the filament and the braid were obtained for a large range of mean and alternating strains. For a specific application of the developed braided cable, the results obtained here can be used to determine the prestrain to be applied to the cable during its installation and the maximum alternating strains it can sustain under service conditions.

5.2 Material and equipment

A 0.1 mm diameter filament of BTR-BB (Ti-50.8at%Ni) alloy with 36% of cold-work (Memry Corp., Bethel, CT, USA) was heat treated at 350°C (15 min) in large loops and then water quenched to ambient temperature. The 24-filament suture was braided from the as-drawn material with 1 pick/mm on a ∅3.2 mm aluminum core using a WARDWELL (RI, USA) braiding machine. With the core in place, the braided structure was then heat treated at 350°C (15 min). Samples were produced in two batches and processing variation was

verified as not having a significant impact on the material properties. From these two batches, individual filaments were kept aside to evaluate the impact the braiding procedure might have on their properties.

The characteristic austenite finish temperature (A_f =10^{o}C) was measured using an X`PERT PRO Diffractometer (PANALYTICAL, Netherlands) with CuKα radiation and a heating rate of 35 K/min. The mechanical fatigue testing was performed using an ENDURATECH ELF 3200 (BOSE Corp., MI, USA) equipped with a water bath and an electric heater to keep the testing temperature at 37^{o}C and to reduce thermal variations caused by the phase transformation-induced self-heating of the tested specimens. Free and fracture surfaces of the tested filaments and braids were observed using a scanning electron microscope, an HITACHI S-3600N (Japan), at 15KV.

5.3 Experimental methodology

5.3.1 Normalization of the experimental domain

Preliminary uniaxial testing was performed to delimit an experimental domain in terms of the applied mean and alternating strains. Six specimens of both the filament and the braid were tested, from 0 to 8% of strain for 10 loading-unloading cycles followed by their stretching up to failure as shown in figure 5.1.

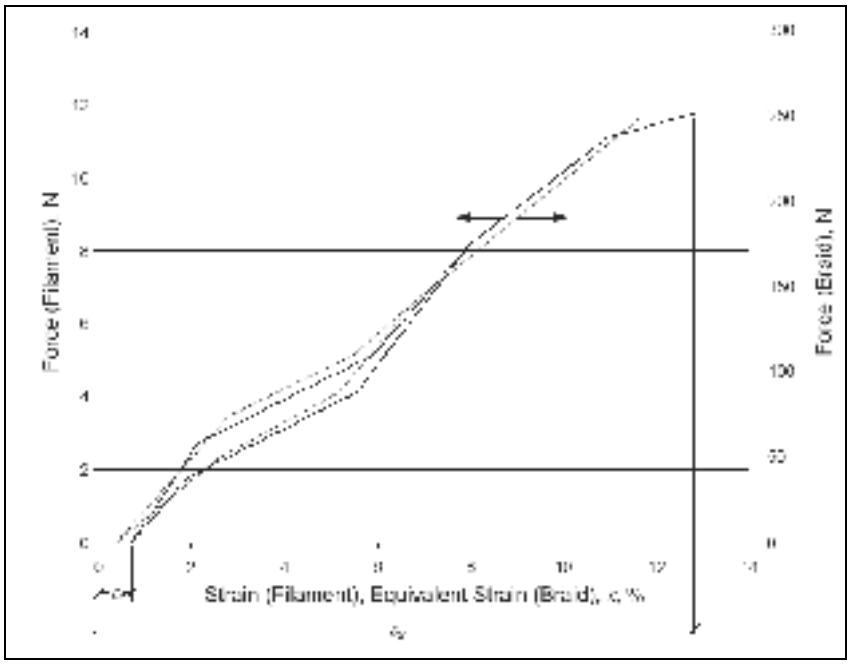

Figure 5.1 Schematized force-elongation diagram for the filament and the braid

Obtained from this preliminary testing, the residual (ε_r) and the failure (ε_u) strains are presented in table 5.1 in terms of their mean (SD), minimum and maximum values. Based on these results, the strain range for the subsequent fatigue testing is then normalized between ε_r =0 and ε_u=1 so that $[0\ 1] \in \bar{\varepsilon} \leftrightarrow [\varepsilon_r, \varepsilon_u] \in \varepsilon$. To allow a common-base comparison, the force-elongation curves of the single filament and the braid are normalized in respect to the single filament's results. (Note that for the braided cable, stress and strain are taken as equivalent parameters using the summarized cross-sectional area of 24 filaments and the length of the braided cable specimen).

Table 5.1

Values of ε_r at the 10^{th} cycle and ε_u (failure)

	Strain (%)			
	Filament (number of samples=6)		Braid (number of samples=6)	
	ε_r	ε_u	ε_r	ε_u
Mean (SD)	0.712 (0.374)	12.814 (1.733)	0.393 (0.179)	11.64 (0.809)
Min	0.115	10.980	0.179	10.902
Max	1.276	15.840	0.546	12.828

5.3.2 Experimental plan

Once the experimental domain is normalized, the following points are considered in order to build a plan for fatigue experiments.

a) The minimum strain imposed to the sample must never result in a null stress (no loosening) during testing.

b) The maximum imposed strain must not cause a rupture of the sample during the first cycle.

c) The mean strain is varied as widely as possible within the superelastic plateau, while being limited to respect conditions a) and b).

Following from these statements, to avoid an early failure or null stress in the sample, the experimental plan does not impose $\bar{\varepsilon}>0.95$ or $\bar{\varepsilon}<0.05$. Also, the mean strain is limited to 0.5 so that our efforts are concentrated on the phase transformation zone (superelastic plateau).

We can translate the previously introduced limits into equations, thus obtaining the following three conditions in the normalized deformation domain:

$$\begin{cases} (\bar{\varepsilon}_m - \bar{\varepsilon}_a) > 0.05 \\ (\bar{\varepsilon}_m + \bar{\varepsilon}_a) < 0.95 \\ \bar{\varepsilon}_m < 0.5 \end{cases}, \qquad 5.1$$

where $\bar{\varepsilon}_m$ and $\bar{\varepsilon}_a$ are the normalized mean and alternating strains. More attention is given to lower values of alternating strain using a progressive discretization of the experimental plan. Figure 2a illustrates the 28-modality experimental plan used for the single filament, and figure 5.2b shows the 25-modality experimental plan for the braid. The braid testing is focused on lower levels of alternating strains with the addition of an experimental line at $\bar{\varepsilon}_a$ = 0.025, because preliminary testing has shown that braiding results in a significant decrease in fatigue life as compared to a single filament. figure 5.2c,d show schematized stress-strain diagrams.

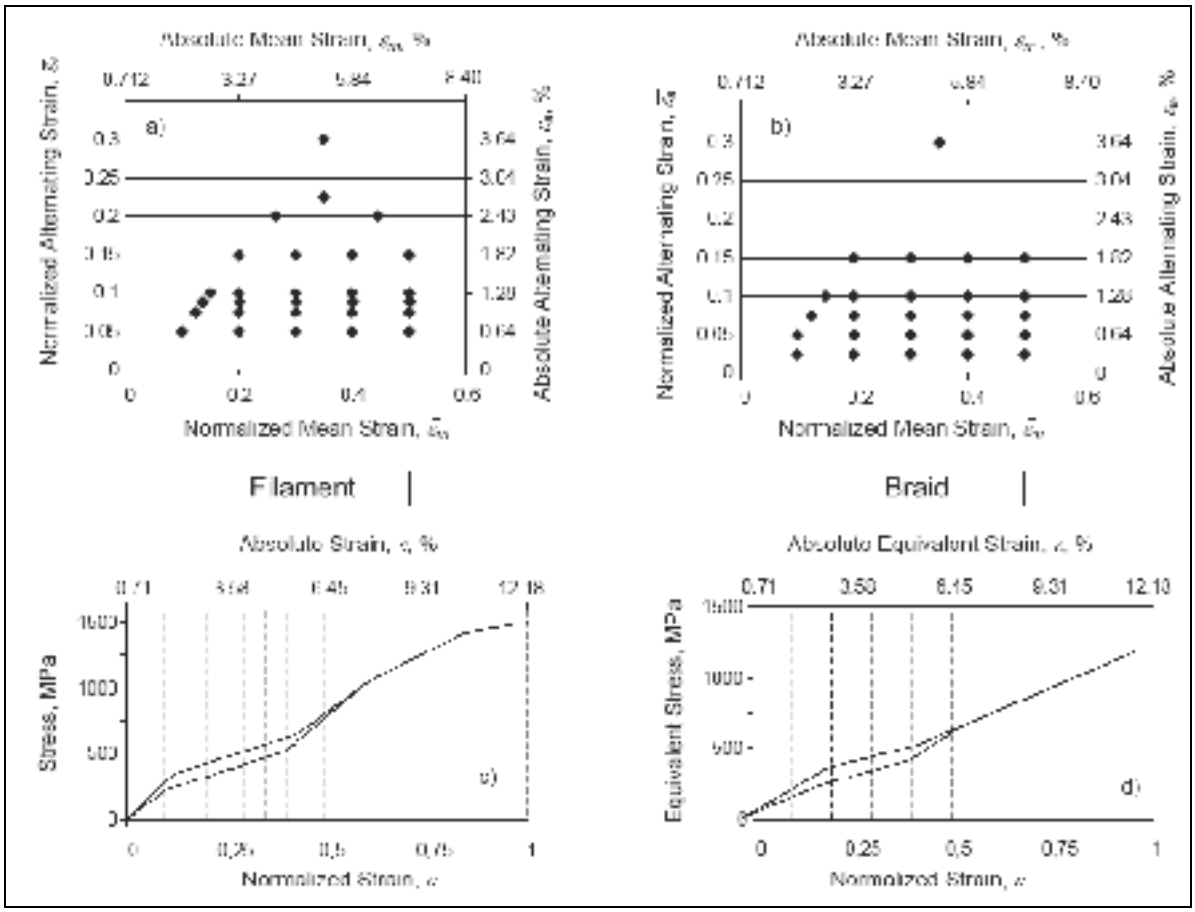

Figure 5.2 Experimental plan: $\bar{\varepsilon}_m$ (ε_m) and $\bar{\varepsilon}_a$ (ε_a) are normalized (absolute) mean and alternating strains for filament (a) and braid (b); schematized stress-strain diagram presenting superelastic loop with different levels of mean strain (dotted lines) for filament (c) and braid (d).

5.3.3 Experimental procedure

To start testing from the same phase state and simulate a real-life case when a superelastic device must be installed at a higher strain before starting its operational lifetime, each sample was first loaded up to an initial 8% strain (prestrain), unloaded to a selected minimum strain and then cycled at a given alternating strain, in conformity with the experimental plans of figure 5.2. To limit the edge effects from the specimen clamped in the tensile machine jaws, each filament specimen was fixed through a cardboard frame. While the sample was being assembled in the frame, it was gently stretched to avoid any loosening. Once installed in the clamping jaws, the sides of the frame were cut to allow free movement of the jaws. Braids

were affixed simply in the jaws because preliminary testing demonstrated that this method was the least invasive.

Tests were completed at a frequency of 2 Hz in the strain-controlled mode. Induced elongations were directly measured by the testing machine's LVDT. All tests were performed in a water bath at 37°C until specimen failure or till 100,000 cycles (the "run-out" conditions) were reached.

A result was kept for further analysis if it fulfilled two conditions: a) the rupture occurred neither in the grips nor close to them and b) the stress-strain diagrams of two samples tested under the same modality were similar.

5.4 Results

5.4.1 Filament

The results of the fatigue testing of the single filament are reported in figure 5.3. It can be observed that, for a given mean strain, the higher the alternating strain and the shorter the fatigue life. This result is straightforward because the higher the alternating strain, the larger the volume of the material subjected to the stress-induced phase transformation and the higher the probability of crack initiation through the defect-accumulation mechanisms that accompany interface movement. The situation becomes more complicated when considering mean strain variations. Two main regions, in respect to the mean strain, can be delimited in Figure 3a,b: the first corresponding to alternating strains less than $\bar{\varepsilon}_a = 0.075$ ($\varepsilon_a = 0.9\%$), and the second, to the alternating strains greater than $\bar{\varepsilon}_a = 0.075$. In the first region, an increase in the mean strain from 0.1 (1.6%) to 0.4 (5.3%) seems to have no influence on fatigue life within the imposed run-out at 105 cycles. In the second region, for a given alternating strain, the higher the mean strain, the shorter the fatigue life.

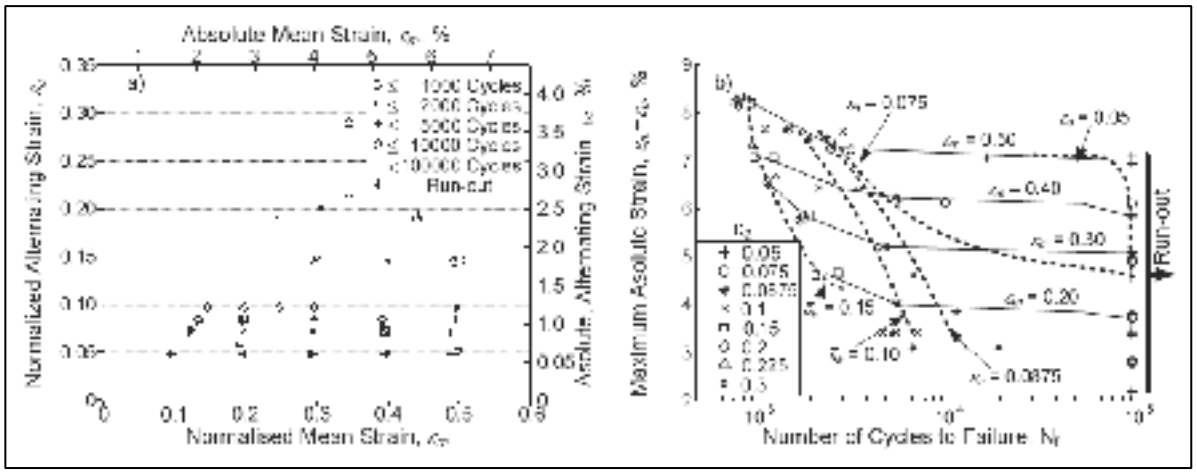

Figure 5.3 Test data points for filaments in terms of: a) mean and alternating strains and b) maximum strain as a function of the number of cycles to rupture.

A significant improvement in fatigue life for mean strains under 0.4 (5.3%) and alternating strains under 0.075 (0.9%) is due to the deformation mechanisms that, in this case, do not involve stress-induced phase transformation, but rather elastic deformation of either single-phase austenite or stress-induced martensite, or of the mixed austenite/martensite compound. Elastic deformation is reputed as being less fatigue-life threatening than deformation due to phase transformation [12] and does yield the longest fatigue lives observed in this study. (When the mean strain exceeds 0.4 (5.3%) however, a large scatter in fatigue life data is observed because of the higher overall level of stress in the sample and therefore the higher probability of crack initiation.)

For alternating strains exceeding $\bar{\varepsilon}_a = 0.075$, there is a significant dependence of the fatigue life on the mean strain variations because, even for a constant alternating strain, higher mean strains correspond to higher stress variations, as seen from figure 5.4a. The same is true for the case of increasing alternating strains (figure 5.4b). Given that fatigue cracks nucleate and grow when stresses vary, the larger the stress variations, the shorter the fatigue life from crack initiation to material rupture.

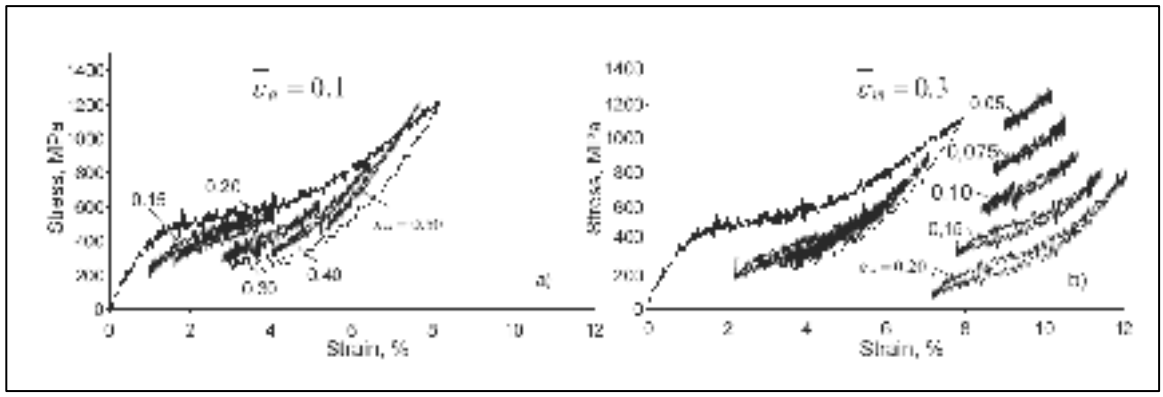

Figure 5.4 Stress-strain diagrams for the filament: a) constant alternating strain of $\bar{\varepsilon}_a = 0.1$, b) constant mean strain of $\bar{\varepsilon}_m = 0.3$; both graphs include the 1st and the 200th cycles.

To sum up these observations, figure 5.5 presents the same data points as figure 5.4, but plotted as functions of alternating and mean stresses and regrouped by alternating (Figure 5a) and mean (Figure 5b) strains. It can be seen, for example, that for the same alternating strain of $\bar{\varepsilon}_a = 0.1$, an increase in mean strain from $\bar{\varepsilon}_m = 0.15$ to 0.4 corresponds to an increase in alternating stress from 210 to 300 MPa (figure 5.5a) and to a fatigue life decrease from 6000 to 3000 cycles (figure 5.5a).

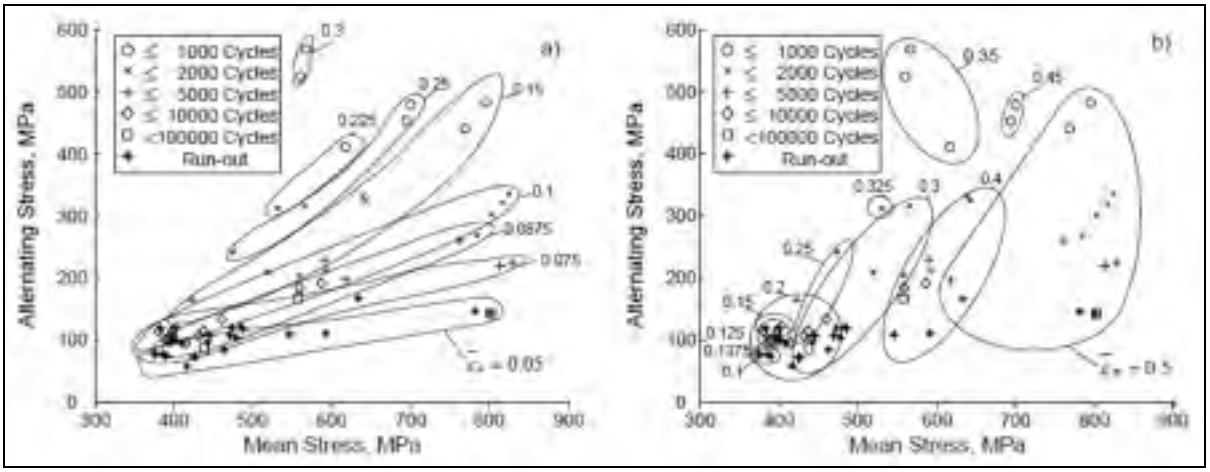

Figure 5.5 Test data points for the filament in terms of mean stress and alternating stress: a) regrouped by alternating strains; b) regrouped by mean strains.

5.4.2 Braided cable

Figure 5.6 shows the test data points obtained for the braided cable. The number of cycles to failure indicated in figure 5.6a,c corresponds to the failure of the first filament. This failure is easily detectable during fatigue testing -- it corresponds to the beginning of the redistribution of the total load supported by the braided cable on the remaining filaments. From this first failure, since the strain-controlled testing mode was used, the braid starts to lose its load-bearing capacity. figure 5.6b,d corresponds to the braided cable maintaining 50% of its initial stiffness. It can be observed that the braided cable can maintain more than 50% of its initial stiffness beyond 10^5 cycles (run-out condition) if the alternating strains are smaller than $\bar{\varepsilon}_a$ = 0.025.

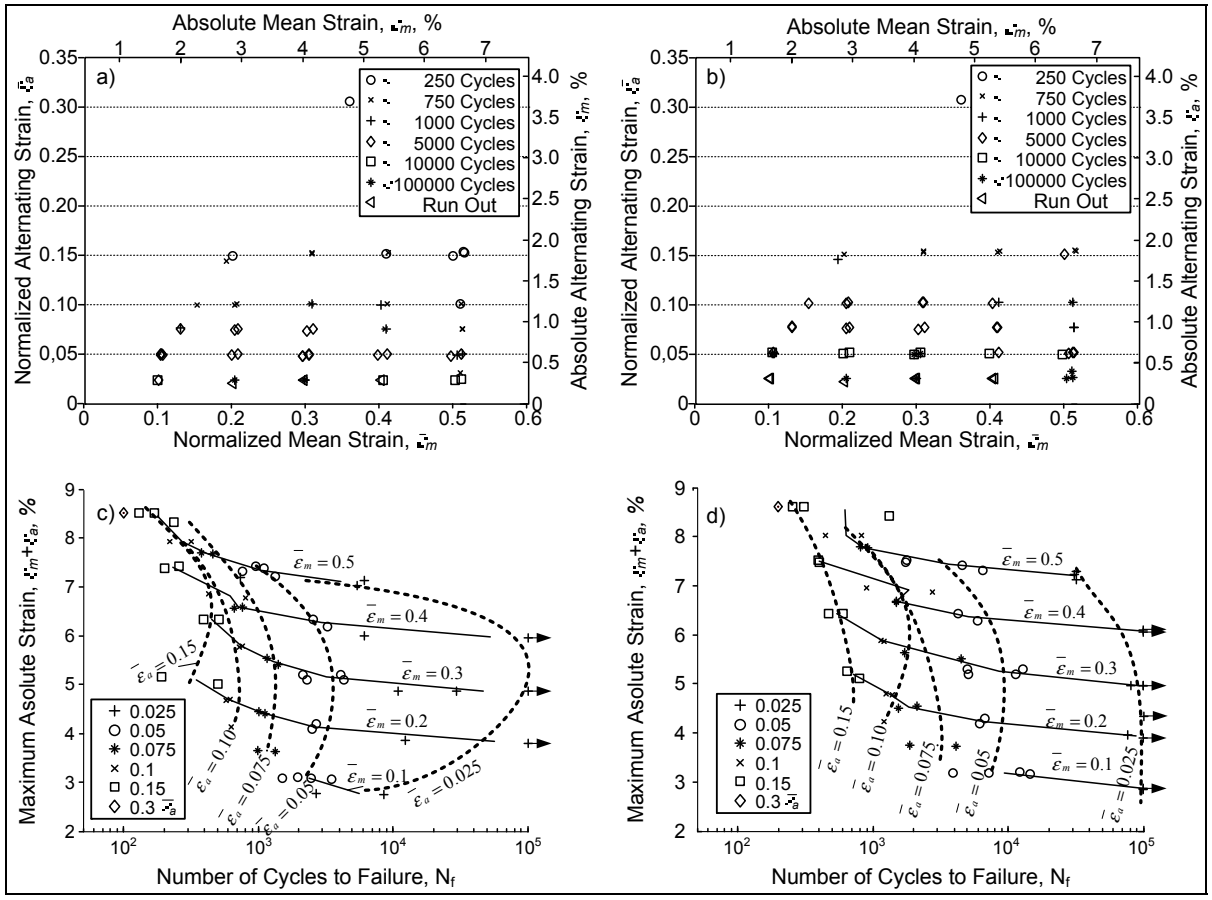

Figure 5.6 Test data points for the braid in terms of mean and alternating strains: a) 1st filament failure, b) 50% of the initial stiffness. Maximum strain as a function of the number of cycles to failure: c) 1st filament failure, d) 50% of the initial stiffness.

In figure 5.6a,b, a certain increase in fatigue life can be observed for mean strains of $\bar{\varepsilon}_m = 0.3$, which corresponds to a decrease in alternating stresses when cycling is performed in the middle of the superelastic loop (figure 5.7a,b).

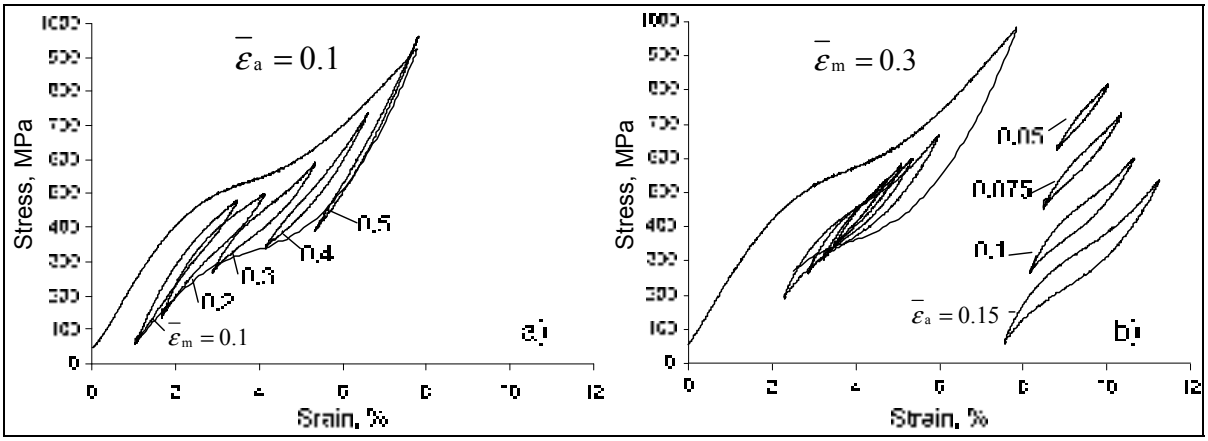

Figure 5.7 Stress-strain diagrams of the braid; a) constant alternating strain of $\bar{\varepsilon}_a = 0.1$, b) constant mean strain of $\bar{\varepsilon}_m = 0.3$; both graphs include the 1st and the 200th cycles.

In figure 5.8a,b, mean and alternating stresses and the number of cycles to failure of the first filament are regrouped for different alternating and mean strains.

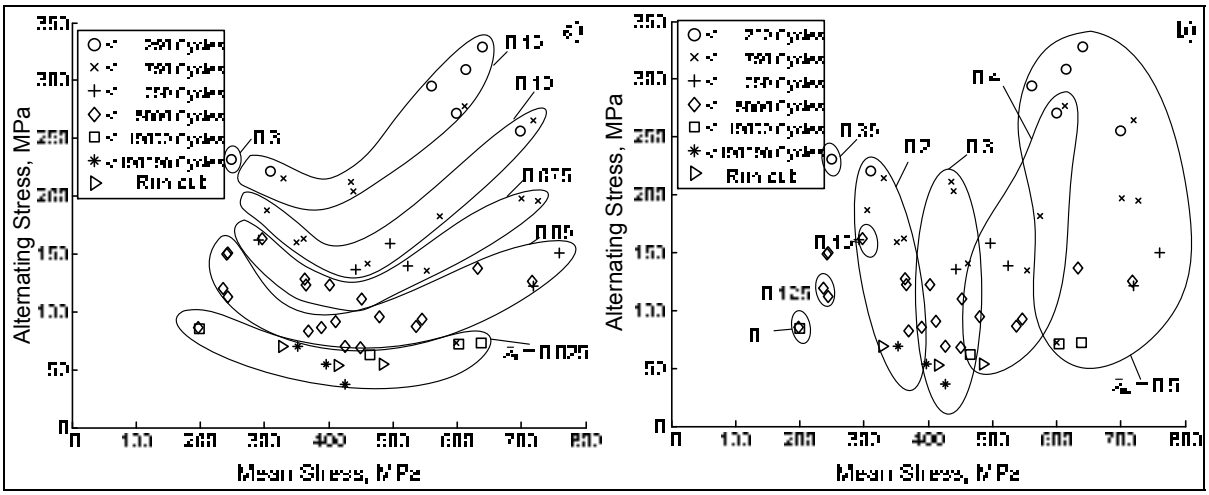

Figure 5.8 Test data points for the braid in terms of mean and alternating stresses at the 200th cycle for the failure of the first filament: data regrouped by alternating (a) and mean (b) strains.

5.5 Discussion

Fatigue testing demonstrated that mean and alternating strains have an impact on the fatigue life of both the filament and the braided cable. In general, the higher the mean and the alternating strains, the higher the alternating stresses, which results in a decrease in fatigue life. However, for the braid, the application of mean strains corresponding to the middle of the upper plateau of the superelastic loop results in a reduction of the alternating stresses, and thus in an increase in the fatigue life. It is therefore recommended to install the braided closure system at a strain slightly over the middle of the transformation plateau ($0.2 \le \bar{\varepsilon}_m \le 0.4$), to benefit from the superelastic behavior[1] and from the increased fatigue life. Let us consider the use of the superelastic braided cable for sternal closure. It is known that during important coughing (coughing pressure of 240 mmHg[13]), the maximum force applied to a sternal suture loop is about 200 N, which corresponds to 100 N on a single strand. It is also known that when a sternal separation force of 200 N is applied through a monofilament stainless steel suture to a sheep sternum, the suture cuts the sternum [14] rather than failing mechanically. In our case, static tensile testing of the superelastic braided cable averaged an ultimate breaking force of 268±58 N, which is higher than what is generated during coughing [15]. Moreover, when a variable force of 100 N is applied to the braided cable,

equivalent stresses of 530 MPa will be generated, which corresponds to a minimum fatigue life of 2000 cycles (figure 5.8). This means that a patient must cough continuously for approximately 3h at a rate of 10 coughs per minute[15] to provoke fatigue failure of the sternal suture -- a quite improbable situation.

5.6 Comparative analysis of the filament and braided cable fatigue properties

By comparing the results of the fatigue testing of the single filament and of the braid, it appears that the fatigue life of the braid is much shorter, under identical testing conditions. For example, under alternating strains $\bar{\varepsilon}_a \leq 0.1$, the fatigue life of the braided cable is four times shorter than that of the single filament. Given that both the single filament and the filament in the braided cable are made from the same material with identical thermomechanical history, the following hypotheses may explain the observed phenomenon:

1. Braiding technology induces fatigue-life threatening damages to the filament (tearing, surface scratches, etc.)
2. Friction between filaments during repetitive braid stretching (fretting) removes material from the contact zones and facilitates fatigue crack nucleation.
3. Filament waving in the braided cable results in local bending and therefore in higher strains as compared to equivalent strains determined for the whole cable.

To verify the first hypothesis, on the negative impact of braiding technology, the fatigue resistance of a single filament prior to braiding and that of a single filament taken out from the braid were compared under the same testing conditions ($\bar{\varepsilon}_m$ = 0.1 – 0.5, $\bar{\varepsilon}_a$ = 0.05 – 0.1) and a significant degradation of the fatigue resistance caused by braiding was observed as illustrated in figure 5.9 for a selected mean strain of $\bar{\varepsilon}_m$ = 0.3.

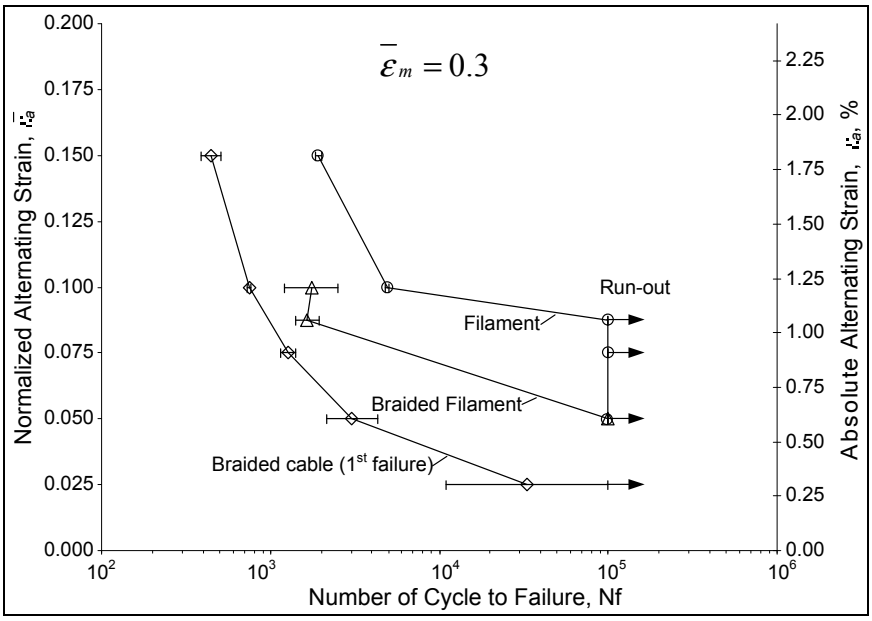

Figure 5.9 Comparison of three manufacturing stage for a mean strain of $\bar{\varepsilon}_m = 0.3$, alternating strain vs number of cycle to failure for the filament, the braided filament and the braided cable; values are logarithmic mean and deviation (two repetitions).

By combining two observations: a certain quantity of Ti-Ni powder (identified by XRD analysis) found inside the braiding machine and abrasive wear traces (scratches) observed on some filaments (see SEM images of figure 5.10a), it is possible to suppose that excessive friction between the filaments and the guiding parts of the braiding equipment could be a reason for such a degradation.

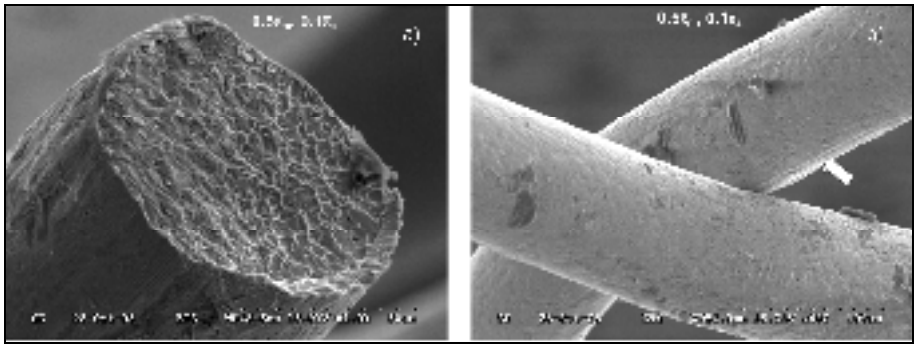

Figure 5.10 Braided filament with $0.5\bar{\varepsilon}_m$ and $0.1\bar{\varepsilon}_a$: a) fractographic and b) macroscopic images.

To verify the second hypothesis, based on fretting, fracture surface SEM observations were made on a single and a braided filament that failed during fatigue testing. In both cases, the fracture mechanism can be interpreted as ductile because it is characterized by significant local plastic deformation in the rupture zone (figure 5.10a). Moreover, even though there is no clear evidence of surface deterioration, an arrow in figure 5.10b shows a defect zone, most probably resulted from fretting, which could ultimately contribute to the filament failure.

To verify the third hypothesis, locally-induced bending, a simplified parametric geometrical model was developed to calculate strain amplification when the braid passes from its free (figure 5.11a) to its stretched (figure 5.11b) state.

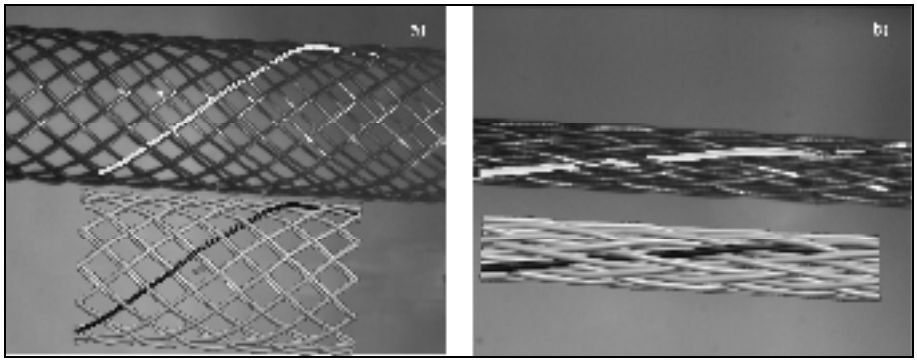

Figure 5.11 Parametric model versus macroscopic pictures of the free (a) and stretched (b) braid. The black-colored filament from the model is superposed as a white-colored one on the braid picture.

5.6.1 Model description

The geometric parameters of the proposed model are shown in figure 5.12. The whole braid is described here by a unitary set of four filaments, identified by numbers 1 to 4 in figure 5.12a,b, repeated $n/4$ times around the braid axis. The angle between two consecutive filaments going in the same direction is $4\pi/n$ (figure 5.12b).

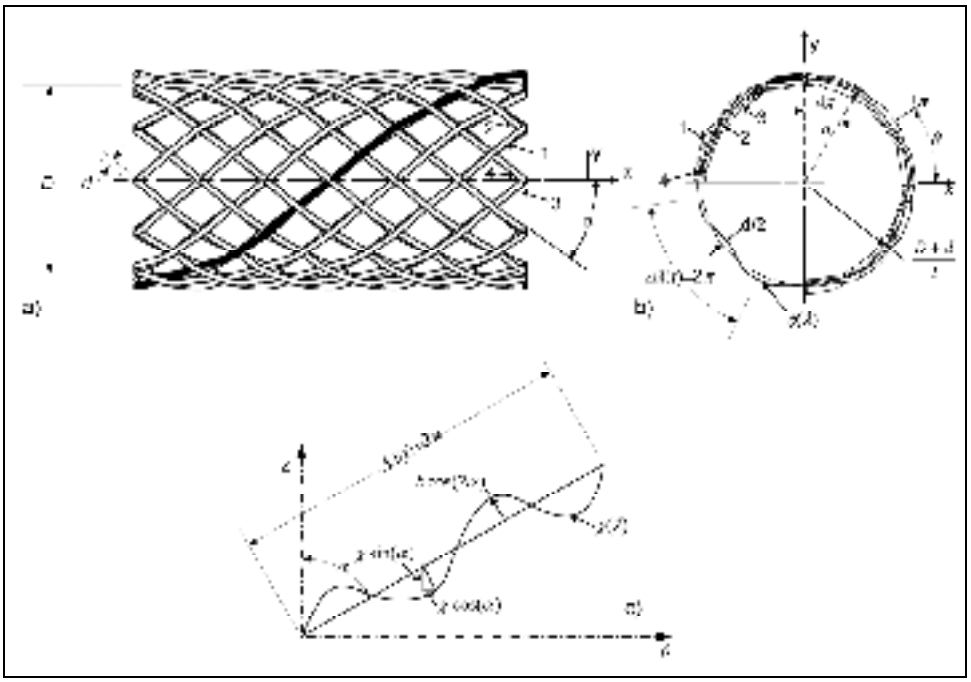

Figure 5.12 Parametric model of the braided cable in the cylindrical coordinate system: (a) lateral view; (b) plan $r\theta$; (c) plan $z\theta$, schematic representation of the χ function.

The spatial position of the filament's axis is described using the following parametric representation within the cylindrical coordinate system:

$$f(t) = \left[r(t), \theta(t)), z(t))\right] = \begin{bmatrix} \dfrac{\left(\pm d\phi(\lambda(t)) + D\right)}{2}, \\ \pm t + \kappa(\alpha, \chi(\lambda(t), \alpha, \phi(\lambda(t))), \\ \dfrac{L \bullet t}{2\pi} - \chi(\lambda(t), \alpha, \phi(\lambda(t)))\sin(\alpha) \end{bmatrix} \qquad 5.2$$

where *d, D* and *L* are the design parameters of the braided structure representing the diameter of the single filament, the inside diameter of the braid and the projected length of a single filament on the braid axis over one revolution ($t = 0 \rightarrow 2\pi$), respectively. Parameter α represents the helix angle and is given by the following equation:

$$\alpha = \arctan\left(\frac{\pi(d+D)}{L}\right), \qquad 5.3$$

and λ is the parameter defining the waving period as a function of the number of filaments in the braid n:

$$\lambda = \frac{n*t \pm \pi}{4}. \qquad 5.4$$

The ± sign in equations 5.1 and 5.3 is determined in respect to the filament position and given in table 5.2.

Table 5.2

Signs to be used in equations 2 and 4.

	Equation number		
Filament	2(r)	2(θ)	4
1	+	+	-
2	-	-	+
3	-	+	-
4	+	-	+

Functions ϕ and χ describe the filament axis trajectory in plans $r\theta$ (figure 5.12b) and $z\theta$ (figure 5.12c), respectively. The function χ maximizes when the helix angle α approaches zero. Parameter b is a constant, introduced to determine the amplitude of χ. Function κ is the projection of function χ on the angular dimension θ.

$$\phi = -\frac{315}{128}\int \sin(\lambda(t))^9 d\lambda; \qquad 5.5$$

$$\chi = 3.1417 b\phi \sin(\lambda(t))\cos(2\alpha); \qquad 5.6$$

$$\kappa = \arctan\left(\frac{\chi(\lambda(t),\alpha,\phi(\lambda(t)))\cos(\alpha)}{r}\right). \qquad 5.7$$

During the deformation of the braided cable, three successive states should be distinguished: a free state, an elongated state, and a stretched state. The combined local strain in the braided filament can therefore be calculated as a superposition of three strains: the equivalent strain (ε) and two strain components resulting from the variation of the curvature radius of the braided filament when the cable is elongated ($\varepsilon_{curv}^{elong}$) and then stretched ($\varepsilon_{curv}^{str}$). The equivalent strain in the filament corresponds to the equivalent strain in the braid because the angle between the axis of the filament and the cable is smaller than 0.174rad when the cable is in its stretched position.

$$\varepsilon_{local,total} = \varepsilon + \varepsilon_{curv}^{elong} + \varepsilon_{curv}^{str} \qquad 5.8$$

Maximum strains related to the variation of the curvature radius for both elongated and stretched braids can be calculated with equation (5.7), where the local radii of curvature are determined using the sensitivity analysis function implemented in the PROENGINEER commercial software.

$$\varepsilon_{curv} = \frac{d}{2}\left(\frac{1}{\rho_{final}} - \frac{1}{\rho_{init}}\right). \qquad 5.9$$

All the data necessary for the calculations are gathered in Table 3.

5.6.2 Free braid

For the free braid, parameters d, n, L, D and b are directly measured on the physical model (table 5.3).

Table 5.3

Braided cable model parameters and resulting local strain

Parameters	Braided cable states		
	Free braid	Elongated braid	Stretched braid
	Measured values		
d, mm	0.1		
n, mm	24		
L, mm	12.5	16.11	16.11 - 17.4; $\varepsilon \in [0,8\%]$
D, mm	3.2	0.53	
b, mm	0.0125	0.0125	
	Calculated values		
ρ, mm	0.698	0.745	0.745…0.862
ε, %	0	0	0…8
ε_{curv}, %	0	0.445	0…0.91
$\varepsilon_{local,total}$, %	0	0.445	0.445…9.355

5.6.3 Elongated braid

Parameter L for the elongated position is calculated using the assumption that during elongation, the length of the filament remains constant and can be estimated to be equal to the linear helix located at a distance d from the braid's inner diameter. During elongation, the braid diameter D is reduced until one wire comes in contact with two surrounding wires --

this position is assumed to be the initial position of the braid for further stretching. It is calculated using equations (1-7), and Table 3 shows that from the free braid to the elongated braid, the radius of curvature of the braided filament passes from 0.698 mm to 0.745 mm, thus generating a maximum strain of $\varepsilon_{curv,ellongation}$=0.445%.

5.6.4 Stretched braid

The braided cable is stretched by increasing the length parameter *L*, while keeping the diameter *D* constant because the filaments are assumed to be already in contact. To simulate application of the equivalent strain (ε) varying from 0 to 8% (8% corresponds to the maximum absolute strain generated in the braided cable during fatigue testing $\varepsilon_m + \varepsilon_a$, see figure 5.2), the variation factor for parameter *L* will be [1.00, 1.08] and the minimum curvature radius will subsequently vary in a quasi linear way as follows:

$$\rho = 1.46 * \varepsilon + 0.745, \varepsilon \in [0, 8\%], \qquad 5.10$$

where 1.46 and 0.745 are experimentally determined parameters. Total local strain can now be calculated for each of the tested modalities using equation (5.7), see table 5.3.

To illustrate this point, sign x in figure 5.13 indicates the maximum equivalent strain and the corresponding fatigue life (more than 10^5) of the single filament subjected to $\bar{\varepsilon}_m = 0.3; \bar{\varepsilon}_a = 0.05$ testing. If the same filament is now part of the braided cable and the same testing conditions were applied, the real strains in the filament would be higher ($\bar{\varepsilon}_m = 0.34; \bar{\varepsilon}_a = 0.055$, sign +) and the fatigue life shorter ($6 \cdot 10^4$ cycles).

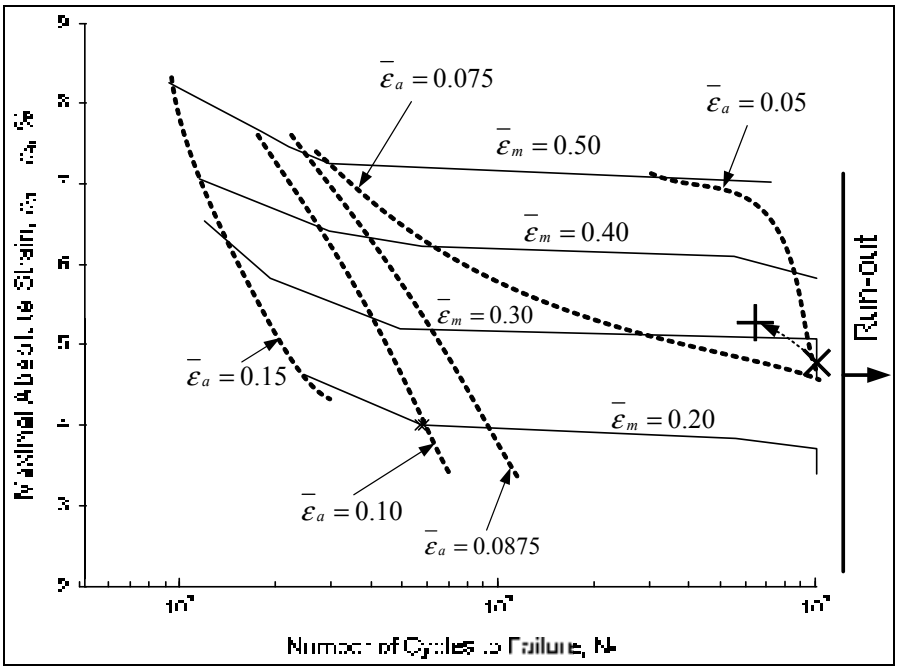

Figure 5.13 Impact of the variation of radius of curvature.

5.7 Conclusion

The hypothesis that the local filament bending has a negative impact on the fatigue life of the braided cable only partially justifies the significant discrepancy in the fatigue life of the braided cable and the single filament. However, this factor, combined with the friction-induced damage of the braided filaments during cable manufacturing and the inter-filament friction during repetitive stretching (fretting), appear to be three major explanations for the lower fatigue performances of the braided cable compared to the single filament. Surface finish treatments of the filaments intended to improve its wear resistance, adjustment of the braiding technology and optimization of the braid pattern are therefore three main avenues to improve the fatigue life of superelastic braided cables for bone fixation.

5.8 Acknowledgments

This work has been performed in the framework of a research program supported by the Natural Sciences and Engineering Research Council of Canada (NSERC) and Valeo

Management L.P. The authors would like to thank Mr. E. Plamondon and Ms. K. Boutin for their assistance in fatigue testing and Dr K. Inaekyan, for XRD analyses.

5.9 References

1. Baril Y, Brailovski V, Chartrand M, Cartier R. Median sternotomy: comparative testing of braided superelastic and monofilament stainless steel sternal sutures. Proceedings of the Institution of Mechanical Engineers Part H: Journal of Engineering in Medicine 2008:DOI: 10.1243/09544119JEIM481.

2. Robertson SW, Mehta A, Pelton AR, Ritchie RO. Evolution of crack-tip transformation zones in superelastic Nitinol subjected to in situ fatigue: A fracture mechanics and synchrotron X-ray microdiffraction analysis. Acta Materialia 2007;55(18):6198-6207.

3. Tobushi H, Nakahara T, Shimeno Y, Hashimoto T. Low-Cycle Fatigue of TiNi Shape Memory Alloy and Formulation of Fatigue Life. Journal of Engineering Materials and Technology 2000;122(2):186-191.

4. Bahia MGdA, Fonseca Dias R, Buono VTL. The influence of high amplitude cyclic straining on the behaviour of superelastic NiTi. International Journal of Fatigue 2006;28(9):1087-1091.

5. Young JM, Vliet KJV. Predicting "in vivo" failure of pseudoelastic NiTi devices under low cycle, high amplitude fatigue. Journal of Biomedical Materials Research 2005;72B(1):17-26.

6. Cheung GSP, Darvell BW. Low-cycle fatigue of NiTi rotary instruments of various cross-sectional shapes. International Endodontic Journal 2007;40(8):626-632.

7. Gong X, Pelton AR, Duerig T, A. H. Cyclic properties of superelastic nitinol tubing. Materials & Processes for Medical Devices Conference; 2004 25-27 Aug.; St. Paul, Mn, USA. ASM International. p 26-31.

8. Harrison WJ, Lin ZC. The study of nitinol bending fatigue. In: Russell SM, Pelton AR, editors. SMST-2000, International Conference on Shape Memory and Superelastic Technologies; 2000 30 april to 4 may; Pacific Grove, Ca, U.S.A. SMST Society, Inc. p 391-396.

9. Pelton AR, Gong X-Y, Duerig T. Fatigue testing of diamond-shaped specimens. Materials & Processes for Medical Devices Conference 2003:199-204.

10. Tabanli R, Simha N, Berg B. Mean strain effects on the fatigue properties of superelastic NiTi. Metallurgical and Materials Transactions A 2001;32(7):1866-1869.

11. Eiselstein LE, Sire RA, James BA. Review of fatigue and fracture behavior in NiTi. Materials & Processes for Medical Devices Conference III; 2005 14-16 November; Boston, Ma, U.S.A. p 135-147.

12. Melton KN, Mercier O. Fatigue of NiTi thermoelastic Martensites. Acta Metalurgica 1979;27:137-144.

13. Casha AR, Yang L, Kay PH, Saleh M, Cooper GJ. A biomechanical study of median sternotomy closure techniques. European Journal of Cardio-Thoracic Surgery 1999;15(3):365-369.

14. Casha AR, Gauci M, Yang L, Saleh M, Kay PH, Cooper GJ. Fatigue testing median sternotomy closures. European Journal of Cardio-thoracic Surgery 2001;19(3):249-253.

15. Jutley RS, Shepherd DET, Hukins DWL. Fatigue strength of a wire passing through a cannulated screw: Implications for closure of the sternum following cardiac surgery. Proceedings of the Institution of Mechanical Engineers Part H: Journal of Engineering in Medicine 2003;217(3):221-226.

CHAPITRE 6

DISCUSSION GÉNÉRALE

Ce projet avait pour objectif général de poursuivre le développement d'un système de fermeture du sternum (SDF) par tresse superélastique. Ce système a été initialement présenté dans mon mémoire (Baril, 2004) et n'était alors qu'un démonstrateur de concept. D'autres travaux étaient nécessaires pour démontrer les avantages de la tresse sur la fermeture du sternum conventionnelle par fil en acier inoxydable. Au cours de ces travaux de développement du SDF par tresse, plusieurs contributions scientifiques ont été faites, dont les deux suivantes sont les plus significatives :

1. **Établissement d'un nouveau critère de comparaison entre les systèmes de fermeture du sternum**. En effet, la force de compression résiduelle entre deux moitiés du sternum était complètement absente de la littérature et est pourtant un critère de conception important. En comparant les systèmes de façon conventionnelle, on peut déterminer si un système est plus rigide ou encore s'il résiste à une charge plus importante qu'un autre système, mais la stabilité de la liaison suivant un cycle de chargement/déchargement demeure inconnue (respiration, mouvement, etc.). La force de compression résiduelle permet de connaître l'impact d'un chargement sur la stabilité du SDF lors des prochaines sollicitations. En d'autres mots, ce critère permet de savoir si le SDF peut continuer à faire son travail après avoir subi un déplacement. Cela en fait un excellent indicateur de la capacité d'un SDF à garder la liaison stable et permet d'optimiser le processus d'ostéogenèse.

2. **Conception d'un banc d'essai « simulateur du sternum » permettant de réaliser l'installation du SDF et de le tester sur une même installation.** Le système de fermeture est installé directement sur le banc d'essai qui est monté à l'horizontale, tandis que le comportement de la cage thoracique lors de l'installation est simulé à l'aide d'une commande par retour de force. Une fois le système de fermeture installé, les essais mécaniques sont effectués sans manipulation supplémentaire. Ce banc d'essai permet de

mesurer également la force résiduelle. De plus, le banc d'essai est en mesure d'appliquer des charges non symétriques. Par exemple, les charges appliquées pourraient être plus importantes au xiphoïde qu'au manubrium. Ce banc d'essai a été validé dans le cadre des travaux de maîtrise de Maxime Chartrand (Chartrand, Brailovski et Baril, 2009) avant d'être utilisé pour les tests comparatifs.

Ma thèse doctorale avait également pour objectifs de comparer le SDF par tresse superélastique au fil d'acier inoxydable sur ce nouveau banc d'essai qui simule le comportement de la cage thoracique, de tester la tresse en fatigue pour connaître sa capacité à soutenir des évènements mécaniques répétés et de compléter la solution technique de fermeture par tresse par la conception d'un système d'installation, essentiel pour que le système puisse être utilisé cliniquement. Ces contributions, leurs limites et les recommandations associées sont discutées plus en détail dans les prochaines sections.

6.1 Solution technique : tresse superélastique

À la suite des résultats préliminaires obtenus dans ma maîtrise, des travaux ont été entrepris afin de breveter le concept de tresse superélastique (Baril et al, 2005, 2006). La tresse superélastique a pour principaux avantages de diminuer la contrainte de surface sur l'os du sternum et d'augmenter la stabilité de la fermeture. Ces avantages sont rendus possibles grâce à la combinaison d'une géométrie tubulaire tressée et d'un alliage superélastique de titane-nickel. La géométrie de la tresse lui permet de prendre une forme méplate au contact avec l'os du sternum, ce qui augmente l'aire de contact. L'utilisation d'un alliage superélastique permet de conserver la charge de fermeture même s'il y a détérioration ou remodelage du sternum. Ces travaux ont également permis de développer une méthodologie de fabrication de la tresse en fonction des caractéristiques mécaniques recherchées (Baril et al, 2006).

6.1.1 Tests comparatifs entre les systèmes de fermeture par fils et par tresse superélastique

Dans ma maîtrise, les tests comparatifs ont été réalisés sur un modèle simplifié où les systèmes étaient installés sur des demi-sternums à des charges initiales identiques. D'autres travaux étaient donc requis pour préciser le comportement de la tresse dans un environnement mécanique plus complexe et plus proche de la réalité clinique. Tel que mentionné plus haut, nous souhaitions aussi inclure la force résiduelle dans nos tests comparatifs entre le fil en acier inoxydable et la tresse superélastique.

Les tests mécaniques effectués sur le banc d'essai « simulateur du sternum » ont démontré que le SDF par tresse superélastique est globalement supérieur au système classique par fil inoxydable. Le SDF par tresse superélastique permet en effet l'ouverture du sternum à des charges similaires à celles du système classique. Cependant, lors des tests cycliques modélisant la toux, le SDF par tresse superélastique applique une charge résiduelle plus importante que le système classique, à la suite d'une perturbation externe. L'alliage superélastique de titane-nickel profite d'un important retour élastique qui lui permet de conserver la pression d'interface et ainsi d'assurer la stabilité de la liaison.

Par ailleurs, dans nos travaux, la rupture d'un sternum, qu'il ait été fermé à l'aide de tresses superélastiques ou de fils en acier inoxydable, survient à une charge avoisinant les 1200 N, ce qui est en deçà de la limite de conception de 1500 N proposée par Casha, Yang et Cooper (1999). Il s'agit, malgré tout, d'une des plus importantes charges supportées par un SDF sur des sternums complets soit environ 170 N par fil. Le tableau 6.1 montre des charges maximales imposées lors des essais de traction latérale provenant de différentes études utilisant toutes le même modèle de sternum fixé à l'aide de fils en acier inoxydable. Ce tableau montre également que les résultats sont très variables d'une étude à l'autre, tant pour l'ouverture mesurée, que pour les charges maximales appliquées. Cette variabilité s'explique par les différentes méthodologies expérimentales. Comme la comparaison directe entre différentes études indépendantes est difficile, voire impossible, la comparaison des systèmes à l'intérieur d'un même projet est nécessaire. Cela suggère aussi que la qualité d'un SDF ne peut uniquement être qualifiée par la force atteinte à la rupture.

Tableau 6.1

Résultats d'ouverture maximale du sternum à $F_{TRACmax}$ sur des modèles de sternum complet en polyuréthane avec système de fixation par fil en acier inoxydable

Étude	$F_{TRACmax}$, N	δ_{max}, mm	Technique de mesure	Fermeture du sternum
(Pai et al., 2005)	180	0.53±0.46	CPC	7S
(Dasika, Trumble et Magovern, 2003)	400	1.70±0.47	AM	7S
(Cohen et Griffin, 2002)	630*	1.37	AP	2&8
(Baril et al., 2009)	1200	0.47±0.13	CPC	7S

$F_{TRACmax}$: force de traction maximale appliquée; δ_{max} : ouverture maximale; CPC: cibles près de la coupe; AM: entre les mors attachant le sternum; AP: au piston de la machine; 7S : 7 fils simples; 2&8 : 2 suture en 8. * limite élastique

Limites et recommandations

Il a été observé qu'une fois retirés du banc d'essai, les sternums fixés avec un SDF par tresse superélastique maintiennent la liaison stable, alors que ceux fixés avec un SDF en acier inoxydable sont libres de mouvement. Cette observation qualitative ne pouvait être formellement mesurée par nos équipements, mais il serait intéressant de développer une façon de le quantifier. Cela reflète probablement un manque de sensibilité du système de mesures utilisé lors de cette étude.

D'autre part, quelques observations complémentaires ont été faites lors des tests comparatifs et devraient être prises en compte pour optimiser le comportement de la tresse :

- Le glissement de la tresse dans le manchon a été la défaillance la plus fréquemment observée lors des essais sur le SDF par tresse. Bien qu'il y ait eu autant de glissements de

tresse que de ruptures de fils classiques, il serait souhaitable d'améliorer les manchons de fixation pour réduire la fréquence de ce problème.

- Il serait pertinent de faire un précyclage systématique des câbles avant leur installation sur le sternum. En effet, lorsque les tresses subissent quelques cycles initiaux de sollicitation, la hauteur du plateau de transformation est réduite et la force d'installation nécessaire devient moins grande.

Le banc d'essai présente également une lacune qu'il serait important de corriger s'il est utilisé dans de nouvelles études :

- Les vis de fixation des côtes du sternum sont montées en porte à faux sur le banc ce qui induit une flexion dans le système lors du chargement. Comme le montage réagit de la même façon pour les deux SDF, il les influence donc de la même façon et les résultats obtenus lors de cette étude demeurent valides.

6.1.2 Propriétés en fatigue de la tresse superélastique

La recension des écrits a montré que peu d'études ont effectué un balayage complet de la zone de transformation lors de tests en fatigue sur des alliages superélastiques et que les résultats de ces travaux sont contradictoires. Ainsi, nos travaux visaient d'une part à évaluer la résistance en fatigue de la tresse et d'autre part, à clarifier le comportement en fatigue des fils en alliage superélastiques dans la zone de transformation. Nous souhaitions également préciser quel serait le chargement optimal de la tresse pour maximiser sa vie en fatigue tout en préservant son comportement superélastique, ce qui est essentiel pour la viabilité de l'application.

Les résultats des tests en fatigue effectués sur la tresse superélastique suggèrent que la déformation alternée est le facteur le plus influent, mais que la déformation moyenne a aussi un impact. Par contre, l'impact de la déformation moyenne est différent pour le filament et pour la tresse. Pour le filament, la déformation moyenne a un impact négatif sur la vie en

fatigue alors que pour la tresse, un optimum est atteint pour des déformations se situant au centre du plateau de transformation.

De plus, nos travaux ont montré que la tresse pourrait supporter les perturbations externes anticipées lors de son utilisation clinique, telles que la toux, même si sa vie en fatigue reste inférieure à celle d'un filament. Pour expliquer la détérioration de la vie en fatigue de la tresse, plusieurs hypothèses ont été vérifiées et confirmées : la flexion qui se produit dans les filaments augmente significativement la déformation moyenne locale, des défauts de production génèrent des égratignures en surface du filament et il semble y avoir friction entre les filaments lors de la sollicitation (fretting). Il est donc recommandé d'installer la tresse à une déformation située au centre du plateau de transformation afin de pouvoir profiter de son comportement superélastique tout en maximisant sa vie en fatigue.

Limites et recommandations

Il serait intéressant de prévoir une série d'essais visant à comprendre l'effet de la force d'installation sur la vie en fatigue. En effet, lors d'essais préliminaires, il a été observé que la déformation initiale a un impact important sur la vie en fatigue des échantillons. Cette question mérite d'être vérifiée afin de valider la proposition de précycler les échantillons pour diminuer la hauteur du plateau de transformation.

Par ailleurs, la durée de vie en fatigue de la tresse étant plus limitée que celle du filament, plusieurs pistes peuvent être explorées pour l'améliorer. Par exemple, les filaments pourraient subir un traitement de surface afin d'en améliorer les caractéristiques tribologiques. Le type de tressage pourrait aussi être modifié pour passer d'un tressage 1x1 à un tressage 2x2. C'est-à-dire que 2 fils en croisent 2 plutôt que 1 en croise 1. Cette modification aurait pour effet de réduire la courbure des filaments et donc de diminuer les contraintes locales associées.

6.2 Solution technique : outil d'installation

Enfin, pour que le système puisse être utilisé cliniquement, la solution technique de fermeture par tresse devait être complétée par un système d'installation. Une recension des outils existants nous a permis de constater qu'aucun ne pouvait effectuer cette tâche. Dans le cadre de cette thèse, nous avons donc développé un nouvel outil d'installation. Le système développé sertit le manchon et contrôle automatiquement la charge appliquée, ce qui assure la répétitivité des caractéristiques mécaniques du SDF. De plus, sa manipulation ne requiert aucun mouvement de rotation de la part du chirurgien, ce qui en favorise la stabilité. Enfin, l'installation, le retrait du SDF dans l'appareil et le réarmement sont aisés grâce aux cames rotatives.

Limites et recommandations

Bien que cet outil soit prometteur, certains aspects devront être améliorés avant que la tresse tubulaire et l'outil d'installation puissent être utilisés de manière courante lors de chirurgies thoraciques. L'ajustement de la tension s'avère laborieux, car l'outil doit être démonté à chaque fois. De plus, l'installation (mise sous tension, sertissage et coupe de l'excédent) est actuellement faite à l'aide de manipulations distinctes alors qu'elle devrait idéalement être complétée en une seule étape. Bien que nous préconisions l'utilisation de composantes purement mécaniques, l'incorporation de composantes électroniques de mesure de force et électrique d'actionnement pourrait diminuer le poids et l'encombrement de la pince, ce qui améliorait son ergonomie. Ce type de travail relève toutefois plus d'une équipe de design industriel dédiée à la commercialisation du produit que du travail d'une équipe de recherche universitaire.

CONCLUSION GÉNÉRALE

En somme, dans le cadre de cette thèse doctorale, nous avons développé une solution technique originale au problème de rupture du sternum à la suite d'une sternotomie, soit la tresse superélastique et son système d'installation. Nous avons développé une technologie de fabrication de la tresse et comparé la tresse au fil d'acier inoxydable sur un banc d'essai innovateur qui permet notamment de mesurer la force résiduelle, variable qui n'avait jamais été utilisée auparavant pour comparer les SDF. La vie en fatigue de la tresse et du filament superélastique a également été étudiée.

Les travaux effectués dans le cadre de cette thèse doctorale démontrent que la tresse superélastique maintient la stabilité du sternum plus longtemps que les fils en acier inoxydable. La vie en fatigue de la tresse superélastique est suffisante pour favoriser le contact entre les deux parties du sternum pendant la période de guérison. Ces travaux démontrent que la tresse en alliage superélastique peut constituer une alternative aux fils en acier inoxydable pour la fermeture du sternum, surtout pour les patients à risque de déhiscence sternale.

Cette même tresse pourrait aussi être utilisée comme système de liaison osseuse dans d'autres applications médicales. En orthopédie, cette tresse pourrait être utilisée avantageusement pour remplacer les câbles en cobalt-chrome ou en acier inoxydable qui sont très rigides et possèdent par conséquent un très faible potentiel de retour élastique. L'utilisation de la tresse en alliage à mémoire de forme est d'ailleurs en cours d'étude pour la fixation du grand trochanter à la suite d'une révision de la prothèse fémorale.

Travaux futurs

Certains travaux de recherches supplémentaires devront toutefois être accomplis avant que le processus d'homologation de la tresse puisse être fait.

Tout d'abord, un nouveau manchon de fixation doit être développé avec deux objectifs distincts. Premièrement, il est important de limiter le glissement de la tresse lors des charges maximales. Deuxièmement, le potentiel de corrosion galvanique entre la tresse NiTi et le manchon en acier inoxydable, utilisé dans cette étude, doit être éliminé, car il y a alors un risque que des ions Ni+ soient libérés dans l'organisme. Pour atteindre ces objectifs, l'utilisation d'un manchon en titane devra être envisagée.

Ensuite, une étude de vie en fatigue dans un environnement réactif comme une solution biologique de Rigner devra être réalisée sur une boucle complète incluant son manchon. Cela permettrait d'étudier, en plus de la corrosion galvanique, la corrosion par piqûration, la propagation de fissures sous contrainte par corrosion en bout de fissure et la fatigue par corrosion. Les mêmes variables pourraient aussi être étudiées *in vivo* lors d'une étude sur des animaux.

Finalement, un travail de design doit aussi être accompli sur la pince de fermeture pour en diminuer le poids et en augmenter l'ergonomie.

ANNEXE I

TEST BENCH AND METHODOLOGY FOR STERNAL CLOSURE SYSTEM TESTING

M. Chartrand, V. Brailovski[3], Y. Baril
This chapter is accepted as an article in *Journal of Experimental Techniques.*
Confirmation number EXT-T-0177.R4.

This paper describes a custom test bench developed to perform static and dynamic testing on sternal closure devices used to reunite both halves of a severed sternum following a median sternotomy. The main objective of this test bench is to perform a preclinical comparative analysis of sternal closure devices for two major performance characteristics: sternum opening force (displacement) and compression force at the sternum midline following the application and release of disruption forces caused by simulated deep breathing and coughing. The laterally-applied forces range from 10 to 1800 N (accuracy 2N) with maximum stroke of 120 mm and maximum frequency of 4Hz. Any sternal closure system available on the market can be installed and tested including stainless steel monofilament sutures, cables, plates, metallic or mersilene ribbons, SMA cables, etc.

INTRODUCTION

A sternal closure device is used to join both halves of a severed sternum following a median sternotomy, a procedure in which a longitudinal cut is performed on the breast plate to access the thoracic cavity [1]. Complications such as instability, non-union and infection occur at an incidence of 0.3% to 5%, and are best prevented by maintaining stability of the closure system [2, 3]. To address these issues, new installation methods and alternatives to the commonly used stainless steel wire have been proposed and evaluated [4-9]. However, some crucial performance characteristics are left out during evaluation because existing test benches lack the instruments to measure such parameters. The main objective of this test bench is to perform, in a single setup, preclinical comparative analysis of biomechanical stability sternal closure techniques, evaluating both the compressive pressure and relative displacement at halves interface in simulated deep breathing or coughing.

The main issue with current test benches used to analyse sternal closure systems is that they do not provide a common platform on which a cardiac surgeon could perform sternum openings and closings –as he does in an operating room–, and then test the installed closure device without any additional manipulations of the closed sternum. Most test benches use a computer-controlled tensile testing machine equipped with custom jigs in which the closed

[3] To whom the correspondence should be addressed

sternum is installed [4, 5, 7, 8, 10-13]. This kind of vertical setup makes sternum closure impossible in a position which more closely replicates conditions met *in-vivo*. Having the same setup for installation and testing will allow the acquisition of data on the compression forces applied to the sternum midline during installation of the closure system. The other concern involves the loading distribution of an external disruptive force applied on the sternum midline. With the exact force distribution along the sternum midline unknown, most biomechanical tests are completed with a loading approximation that evenly distributes the disruptive force on a lateral plane. But the need for a versatile bench that could perform symmetrical as well as asymmetrical loading –assuming future research [14] eventually provides additional information on the subject–, was deemed necessary.

MATERIALS AND BENCH DESCRIPTION

Sternum Models. Artificial sternum models made of polyurethane (Sawbones Corporation, Vashon Island, WA, USA) with a foam density of 0.32 g/cm^3 are used in the framework of the present study. Contrarily to the specified data, sternum model density measured using the liquid displacement method was found to be significantly higher: 0.47±0.044 g/cm^3 (mean ± std deviation, n=7). As the material is not homogeneous, the surface being denser than the interior, it is not surprising to measure higher densities than those specified. Trumble *et al*. have shown that these sternum models can be used to approximate the biomechanical properties of cadaveric sterna using common wiring techniques and similar experimental conditions[13]. Therefore, the use of artificial sterna was deemed acceptable for comparative in-vitro testing. In this case, differences observed during comparative testing of two or more sternal closure devices will more clearly represent differences in their mechanical performance rather than variation in bone quality. However, if experiments with cadaveric sterna will be required for further in–depth evaluation, the test bench can easily be adapted for that study through minor modifications of the test rig.

Traction Force. The force vector applied *in-vivo* to the sternum due to coughing fits or deep breathing can be broken down into three orthogonal planes: lateral, anterior-posterior and rostral-caudal. McGregor *et al* [15] have found that for similar traction forces, anterior-posterior and rostral-caudal oriented forces cause less sternal distraction than lateral-oriented forces, which is why the test bench functionalities are limited to the laterally-applied disruptive forces, a simplification used by most authors [4, 5, 8, 10, 12, 16]. These disruptive forces represent a simulation of either deep breathing or coughing fits, which is explained in detail in the Testing Modes and Examples of Application section. The applied force ranges from 10 to 1800 N (accuracy 2N) with maximum stroke of 120 mm and maximum frequency of 4Hz.

Test Bench Apparatus. The apparatus can be divided into three subsystems: the actual test bench, where mechanical testing occurs (Figure 1a); the control and data acquisition computerized system (see Figure 2 for a schematic of the software architecture), and the videoextensometer used to record the opening at the sternum midline.

As shown in Figure 1a, two hydraulic cylinders (1) (1 1/8-MH-TF-4-D, Scheffer Corporation, Cincinnati, OH, USA) provide lateral motion for the mobile frame (2), linked to the static frame (3) by a pair of mobile arms (4) which confine movement in the horizontal plane. The displacement of each hydraulic cylinder is controlled independently by a high

precision servo valve (27A50F-1E02-999 Servo Valve, HR Textron Operation, Santa Clarica, CA, USA), allowing application of symmetrical (or asymmetrical) forces or displacements by the pistons. Each half of the severed sternum (5) is held in place with seven 5 mm shoulder screws (6) passing through the rib struts.

Data Acquisition. The displacement and force feedbacks are ensured by two laser displacement sensors (7) and three load cells (8, 9). The laser sensors (CP24MHT80, Wenglor Sensoric, Germany, resolution - 20 μm; response frequency - 13Hz) measure stroke of each piston individually. The force applied by the cylinders on the closed sternum is recorded by two 200 lb (889 N) capacity load cells (8) (LC703-200, Omega Engineering Inc, Stamford, CT, USA), fixed between the static frame (3) and the load-cell link (9) to measure forces applied by each piston.

To ensure pure lateral loading of the sternum, a third load cell of the same capacity is added to the underside of the frame (not visible in Figure 1a because hidden under the static frame). This load cell is fixed through a ball bearing unit to the frame (3) and link (9) at the mid-span between two load cells (8) and offset from the force application plan. The free body diagram of the load-cell system is shown in Figure 1b, where F1 and F2 are the forces applied by two pistons (1); R1, R2 and R3 are the reaction forces measured by three load cells and M is the flexural moment resulting from the installation misalignment (e). Solving equilibrium equations, the following relations between forces applied by the pistons and load cells readouts are obtained: F1=R1-0.5R3 and F2=R2-0.5R3.

Testing bench force calibration is carried out with a reference load cell replacing sternum model (load cell of an Enduratech 3200 Bose Corporation, Eden Prairie, MN, USA). The calibration process consists of fixing the reference load cell between the mobile frame (2) and load-cell link (9) at an arbitrary distance between load cells (8), activating pistons (1) and measuring R1, R2 and R3 reaction forces. Then, the same procedure is repeated varying the position of the reference load cell between loads cells (8). First, for any position of the reference load cell, the reaction R3 does not exceed 10% of the sum (R1+R2), which satisfies the design objective to minimize bending of the sternum model during testing. Next, the reactions R1, R2 and R3 are used to compute F1 and F2, and the sum (F1+F2) is compared to the force measured by the reference load cell. It was found that for an individual piston, notwithstanding the reference load cell position, the force measurement error is less than 5%, for both pistons, less than 3%, and that the force measurement repeatability error as low as 3%.

The force at the interface between the sternum halves is measured by a series of 100 lb (445 N) capacity pressure sensors (10) (Flexiforce A201-100, Tekscan Inc, Boston, MA, USA). A pair of thin PVC discs is glued on each side of the sensor to evenly distribute the pressure and ensure a more precise reading. Each sensor is held in place on one half of the sternum with a small metal pin pierced through the plastic of the sensor to the sternum polyurethane. A total of 8 pressure sensors are equally distributed along the sternum midline; Figure 1c shows the positioning of the fifth sensor. The sternum opening is recorded with a videoextensometer (ME-46, Dot Measurement software application, Messphysik Material Testing, Austria) at four locations, adapting a nomenclature previously used by Pai *et al*. [8, 12];

point M is situated at the manubrium, points MS1 and MS2 at the midsternum, and point X at the xiphoid (Figure 1c).

A LabView software (LabView 8.2, National Instrument Corp., Austin, TX, USA) controls both pistons either independently or in slave mode and records the instruments' readings in real-time with the NI PCI-6229 acquisition card (National Instrument Corp). Data between LabView and the videoextensometer is coordinated in post-processing with an electric signal of -9.5 to +9.5 volts, corresponding to a period of 20 seconds sent from LabView to the videoextensometer. Post-processing is performed with Excel (Microsoft Corp., Redmond, WA, USA).

Software Control. Several factors influenced the decision to develop a software control for the servo valves rather than a hardware control. First, as previously mentioned, the lateral force applied to the sternum is calculated from the input of three load cells. These calculations should be performed rapidly in order to ensure proper response for the PID controller since the lateral force is used a feedback for several modes of the test bench. Given that three load cells, eight pressure sensors and two displacement laser sensors are sending data to the acquisition card at once, a single desktop computer could not handle the graphic user interface (GUI), data backup, force calculations and PID-related computing rapidly enough. Moreover, two feedbacks are available to the user: displacement feedback (from the laser sensors) and force feedback (from the load cells). Because the different testing modes use either force feedback, displacement feedback or a mixture of the two, the values of the PID controller had to be adjustable quickly and easily, which is not possible with a hardware control. Finally, because users would be installing closure systems on the bench during hydraulic operation, safety issues arose. Built-in safeguards had to be put in place in order to prevent any kind of incident. Software response to an emergency signal had to be fast and perfectly reliable at any given time.

The LabView Real-Time Module accomplishes those objectives in terms of speed and reliability, with a dedicated machine (target) running a Real-Time Operating System (RTOS). The embedded RTOS for the target is a single dedicated kernel that provides maximum reliability for embedded code, which contains the force algorithm and the PID controls. In other words, the processor is entirely dedicated to the execution of the code, with no interference from an external program which could cause a malfunction. This deterministic programming was deemed necessary in order to achieve perfect reliability in the light of the safety concerns mentioned above. Figure 2 shows schematics of the programming architecture for the test bench. The host, with the GUI, is where the user adjusts the settings (testing mode, displacement limits, oil pressure limits, PID values, etc) and sends the desired command to the target. Upon receiving the command from the host, the target computes the servo valves necessary opening based on the feedback from the instruments, thus allowing the cylinders to follow the desired signal. Meanwhile, measurements from the instruments are read by the acquisition card installed on the target, and then sent back to the host to be saved under a readable format. In Figure 3, typical waveforms in terms of force control, readout and error signals are presented to illustrate static (a), deep breathing (b) and coughing fit (c) testing modes.

TESTING METHODOLOGY

It is believed that a rigid closure system that reduces motion at the sternum midline under loading diminishes the risk of post-operative complications by promoting an earlier union of the sternum halves [17]. The higher the rigidity of the closure system, the smaller the sternum opening and the higher the traction force needed to initiate an opening at the sternum midline. However, high rigidity of the closure device is not synonymous with a successful closure system. It has been determined in several studies [15, 18, 19] that the opening of the sternum may occur, irrespectively of the closure system stiffness, well before the application of the maximum force that can be supported by the closure system. This is because when substantial stresses brought on either by implant installation procedures or by post-operative events,–such as coughing–, are transferred to the sternum localized bone tissue damage in the implant-tissue contact zone might occur. Once the disruption is over, any permanent tissue damage will result in a loss of compression forces at the interface between the sternum halves, and consequently, in a decrease of the bond stability. Furthermore, the suture itself can creep under service conditions, thus resulting in a loss of compression at the sternum midline. It should be noted that the capacity of closure systems to reapply compression on the sternum after the load is removed is completely neglected in all the aforementioned studies. This is significant because non-union results from a lack of pressure at the sternum midline interface, preventing ossification [20].

Looking at sternotomy as a process allows us to identify input and output variables from which performance characteristics of a given closure system are obtained.

Input variables:

1. Sternal closure system used to close the severed sternum. Any system available on the market can be installed (stainless steel wires, cables, plates, metallic ribbons, mersilene tape, SMA cables, etc).

2. Compression force applied to the sternum midline during installation of the closure system ($F_{COMP,I}$) following typical installation procedures.

3. Disruptive force applied to the sternum (F_{TRAC}). The amplitude and frequency of the disruption are set by the user respecting the testing modes modalities (see Testing Modes and Examples of Application Section).

Output variables:

1. Traction force needed to completely separate the sternum midline ($F_{TRAC,O}$)

2. Compression force at the sternum midline under a disruptive force (F_{COMP}) or following its application and release ($F_{COMP,RES}$).

3. Sternum opening at four locations along the sternum midline (M, MS1, MS2, X) under a disruptive force (δ) or following its application and release (δ_{PERM}).

In the framework of the present study, the ability of a closure system to maintain compression at the sternum midline is assessed by measuring the permanent displacement (δ_{PERM}) and residual compression force ($F_{COMP,RES}$) over several loading cycles. Figure 4 presents a schematic illustration of the performance characteristics obtained from the aforementioned output variables. For a given traction force ($F_{TRAC} < F_{TRAC,MAX}$), the corresponding sternum opening (δ) is measured and force-displacement curves can be plotted for each closure system. Additionally, the traction force needed to completely separate the sternum midline ($F_{TRAC,O}$) is determined (0-0' for the first cycle). Finally, the permanent sternum opening (δ_{PERM}) and residual compression force ($F_{COMP,RES}$) following a disruptive force application and release (0'-1-1', 1'-2-2' and 2'-3-3') are also obtained. The rate at which the δ_{PERM} increases or remains stable from one cycle to another will determine the system's ability to maintain compression, and a closure system that reapplies a high percentage of the $F_{COMP,I}$ after post-operative distracting events will be less subject to the non-union of the severed sternum.

TESTING MODES AND EXAMPLES OF APPLICATION

In addition to a manual mode, four pre-programmed modes are available for measuring the output variables previously introduced: 1 installation mode and 3 service modes (1 static and 2 dynamic sub-modes representing deep breathing and coughing simulations). In the framework of the present study, seven-wire (7S) sternum closure system is tested (and Dasika *et al*.[5]). This closure configuration comprises two transsternal No. 5 Ethicon stainless steel wires (Somerville, NJ, USA), one at the manubrium, one at the xiphoid and five peristernal wires in-between (see Figure 1b). For each individual testing, a separate sternum model is used.

INSTALLATION MODE

The primary objective of this mode is to replicate the motion of a severed sternum during rewiring under a direct supervision of a cardiac surgeon. Through this replication, compressive force distribution between sternum halves can be measured although the force values may differ from those occurring *in-vivo*. The second objective is to offer a training platform for the surgeon, which will allow him to familiarize himself with closure systems under development[9].

The installation mode offers a neutral position to which the sternum tends to return if no external forces are applied. This mode is force-controlled with an additional displacement feedback to modulate the reaction force of the system. The opening between the sternum halves can be widened or reduced, depending on the direction of the external forces applied by the user. The further the opening is from the neutral point, the higher the resistance of the sternum to the relative motion applied. These parameters can be adjusted to better fit the behaviour experienced *in-vivo* by the surgeon. Compression forces applied to the sternum midline by the closure system during installation ($F_{COMP,I}$) are measured by the pressure sensors located at the sternum midline interface.

Example of Installation Mode Testing

Results for No. 5 stainless steel wires with 7S configuration are shown in Figure 5 for each pressure sensor. Artificial sterna were rewired under a direct supervision of the cardiac surgeon. A mean and standard deviation of 411 ± 70 N for the $F_{COMP,I}$ was obtained from 16 test repetitions.

STATIC SERVICE MODE

The static service mode allows the measurement of the performance characteristics previously introduced: (a) traction force needed to completely separate the sternum midline ($F_{TRAC,O}$); (b) compression force at the sternum midline under a disruptive force (F_{COMP}) or following its application and release ($F_{COMP,RES}$) and (c) sternum opening under a disruptive force (δ) or following its application and release (δ_{PERM}).

Initially, the 1500 N force calculated by Casha [19] (which represents the theoretical chest wall forces during coughing) was to be the maximum traction force applied ($F_{TRAC,MAX}$, Figure 4). However, tests completed in the literature with the same artificial sternum model caused significant displacements at the sternum midline well before 1500 N [4, 5, 8]. An upper limit of 1200 N for the sternum separation force was ruled in order to avoid systematic failures after only one loading cycle. To quantify the level of separation at the sternum midline under loading, the traction force applied to both halves of the sternum is incremented by 200 N (Figure 6a), with the increment value chosen in order to limit the quantity of data to be analysed for each cycle. The dwell time for each step is 30 seconds for stabilizing the system and obtaining a mean of the sternal separation reading from the videoextensometer. After each increment, the traction force is brought back to 0 N to measure the $F_{COMP,RES}$ and δ_{PERM} at the sternum midline. This is repeated with increased increments until the upper value of 1200 N is reached.

Example of Static Service Mode Testing

Results for No. 5 Ethicon wires, with the 7S configuration are presented below (Figure 7) for the first loading cycle (n=5). At 1200 N, the Ethicon allowed an opening of 0.09 ± 0.10 mm at M, 0.01 ± 0.06 mm at MS1, 0.47 ± 0.13 mm at MS2, and finally, 0.52 ± 0.33 mm at X (Figure 7a). Other authors also observe wider sternum openings at the lower region (MS2 and X) than at the upper region (M and MS1). The negative displacement appearing at MS1 location indicates that at this point the sternum model enters in compression as the result of a non-uniform opening.

Figure 7b shows the $F_{TRAC,O}$, $F_{COMP,RES}$ and δ_{PERM} following the application and release of the traction force. An average $F_{TRAC,O}$ of 1221 ± 73 N was needed to completely separate the sternum midline. Only 187 ± 41 N of the 462 ± 51 N initially applied were restored following the release of the 1200 N F_{TRAC}. Finally, a permanent sternum opening of 0.13 ± 0.08 mm was observed at MS2 following the release of the 1200 N F_{TRAC}. Only the permanent displacement at MS2 is plotted because it showed the highest displacement measured. To illustrate in more detail the evolution of the midline compressive forces under different levels of distractive force, a typical response curve is shown in Figure 8.

DEEP BREATHING TESTING MODE

Two measurements are completed with this mode: maximum sternum opening (δ_{PERM}) for each cycle and maximum residual force applied to the sternum midline for each cycle ($F_{COMP,RES}$). Deep breathing is simulated by a sinusoidal signal (Figure 6b), which is applied for a finite number of cycles. Sternum openings at the four locations (M, MS1, MS2 and X) are taken for each cycle at the upper limit of F_{TRAC} (A), while the $F_{COMP,RES}$ applied is taken at the lower limit (B).

To our knowledge, no theoretical model has been developed to evaluate the chest wall force experienced during deep breathing. But in our opinion, deep breathing does not generate forces as significant as those experienced during coughing. Therefore, the separation force applied to the sternum should not provoke a sternum opening. The sternum opening force ($F_{TRAC,O}$ = 1200 N) being already known from the static service mode, it was decided to limit the highest deep breathing simulation force to 75% of $F_{TRAC,O}$ i.e to 800 N. Even though this value is not an exact representation of what is experienced *in-vivo*, it allows the closure system be tested in severe conditions of repetitive loading. Also, the lower limit of deep breathing testing is set to 15 N instead of 0 N in order to avoid having any compressive forces being applied to the sternum midline and causing a false read for the pressure sensors. One cycle is applied every 2 seconds (0.5 Hz), for 350 cycles. As for the number of cycles, the longest test done in the literature had 150 cycles [18]. The current test was designed to further push the repetitive load testing of closure systems by at least twofold.

Example of Deep Breathing Testing

Maximum sternum opening for the 1st and 350th cycle of deep breathing simulation is presented in Table 1 for each control location (M, MS1, MS2 and X). The evolution of the relative residual compression force at the sternum midline ($F_{COMP,RES}$) as a function of the number of cycling is given in Figure 9a (n=3). It can be observed that during cycling, sternum opening measured remains relatively stable (Table 1), while mean value of the residual compression force at the sternum midline continuously decreases (only 42±16% of the $F_{COMP,I}$ is reapplied at the 350th cycle with the 95% CI). The reason for this decay seems to be a local depression at the interface between the Sawbone and each closure wire. These gradually accentuated depressions do not influence sternum opening measurements because of their small values, but given large Young modulus of steel, result in an important loss of compression at the sternum midline.

Figure 9a shows response of each pressure sensor as a function of the number of cycles and Figure 9b represents the evolution of the total (summarized) sternum midline compression force as a function of the number of cycles (100% value corresponds to an initial compression force measured on each specimen prior to deep breathing testing).

COUGHING FIT TESTING MODE

The coughing mode resembles the deep breathing mode, with the difference being the speed at which the load is applied. The maximum traction force is 1200 N, which represents an intrathoratic pressure of 32 kPa (240 mm Hg) according to Casha's mathematical model [19].

Pressure builds up for 200 ms, followed by two expiratory phases, the first one lasting approximately 30 to 50 ms, followed by the second phase, for 200 to 500 ms [21]. The worst case scenario was chosen, and a triangular approximation of the coughing pattern was made (Figure 6c). During this testing, pressure builds up for 200 ms, and the expiratory phase lasts for 230 ms. The residual force at the sternum midline is recorded before and after each coughing fit. This pattern is applied until failure occurs. Given dynamic effects brought up by this testing mode, the use of the videoextensometre in real-time measurement was impossible.

Example of Coughing Fits Testing

Figure 10a shows results for No. 5 Ethicon wires, with the 7S configuration (n=5). 53 ± 8% of the initial compression force is reapplied following the 100th cycle, a percentage similar to what is observed with deep breathing (56 ± 14%). In Figure 10, the evolution of the individual measurements for each pressure sensor as a function of the number of cycles (Figure 10a) is compared to the one of the summarized compression force on the sternum midline (Figure 10b) and shows degradation of the biomechanical stability of the sternal closure similar to that observed during deep breathing testing (Figure 9).

CONCLUSION

A custom test bench was developed for comparative testing of sternal closure devices over a single setup which allows the installation of the closure device and subsequent testing under lateral in-plane distraction forces. The bench is capable of generating a range of testing modes, which comprise static (characterization of the closure device) and dynamic (simulation of deep breathing and coughing fits) testing without additional manipulations of the closed sternum. This method permits the acquisition of the compression force applied to the sternum midline and the measurement of its evolution throughout the different testing stages. In the framework of the present study, an artificial sternum model made of polyurethane is used. If in-depth comparative testing has to be completed, the testing bench can easily be adapted to the testing of biological models. For each testing mode, experimental data with the commonly used seven-wire sternum closure system configuration are provided and statistically treated (see Table 2). The gradual decrease in sternum midline compressive forces is explained by the observed local depression at the wire-sternum interface.

Acknowledgements

This work was performed as part of a research program supported by the Natural Sciences and Engineering Research Council of Canada (NSERC) and Valeo Management L.P.

REFERENCES

1 **Julian, O.** The median sternotomy incision in cardiac surgery with extracorporeal circulation. *Surgery*, **42**, 1957, 753.

2 **Losanoff, J.E., Jones, J.W. and Richman, B.W.** Primary closure of median sternotomy: techniques and principles. *Cardiovascular Surgery*, **10**(2), 2002, 102-110.

3 **Losanoff, J.E., Richman, B.W. and Jones, J.W.** Disruption and infection of median sternotomy: a comprehensive review. *European Journal of Cardio-thoracic Surgery*, **21**(5), 2002, 831-839.

4 **Cohen, D.J. and Griffin, L.V.** A biomechanical comparison of three sternotomy closure techniques. *The Annals of Thoracic Surgery*, **73**(2), 2002, 563-568.

5 **Dasika, U.K., Trumble, D.R. and Magovern, J.A.** Lower sternal reinforcement improves the stability of sternal closure. *The Annals of Thoracic Surgery*, **75**(5), 2003, 1618-1621.

6 **McGregor, W.E., Payne, M., Trumble, D.R., Fakas, K.M. and Magovern, J.A.** Improvement of Sternal Closure Stability With Reinforced Steel Wires. *The Annals of Thoracic Surgery*, **76**(5), 2003, 1631-1634.

7 **Ozaki, W., Buchman, S.R., Iannettoni, M.D. and Frankenburg, E.P.** Biomechanical study of sternal closure using rigid fixation techniques in human cadaver. *The Annals of Thoracic Surgery*, **65**(6), 1998, 1660-1665.

8 **Pai, S., Gunja, N.J., Dupak, E.L., McMahon, N.L., Roth, T.P., Lalikos, J.F., Dunn, R.M., Francalancia, N., Pins, G.D. and Billiar, K.L.** In Vitro Comparison of Wire and Plate Fixation for Midline Sternotomies. *The Annals of Thoracic Surgery*, **80**(3), 2005, 962-968.

9 **Baril, Y., Brailovski, V., Terriault, P. and Cartier, R.** Feasibility study of a new sternal closure device using tubular braided superelastic Nitinol structures. In International, A., ed. *Materials & Processes for Medical Devices*Boston, 2005).

10 **Losanoff, J.E., Collier, A.D., Wagner-Mann, C.C., Richman, B.W., Huff, H., Hsieh, F.-h., Diaz-Arias, A. and Jones, J.W.** Biomechanical comparison of median sternotomy closures. *The Annals of Thoracic Surgery*, **77**(1), 2004, 203-209.

11 **Losanoff, J.E., Foerst, J.R., Huff, H., Richman, B.W., Collier, A.D., Hsieh, F.-H., Lee, S. and Jones, J.W.** Biomechanical porcine model of median sternotomy closure. *Journal of Surgical Research*, **107**(1), 2002, 108-112.

12 **Pai, S., Gunja, N., Dupak, E., McMahon, N., Coburn, J., Lalikos, J., Dunn, R., Francalancia, N., Pins, G. and Billiar, K.** A Mechanical Study of Rigid Plate Configurations for Sternal Fixation. *Annals of Biomedical Engineering*, **35**(5), 2007, 808-816.

13 Trumble, D.R., McGregor, W.E. and Magovern, J.A. Validation of a bone analog model for studies of sternal closure. *The Annals of Thoracic Surgery*, **74**(3), 2002, 739-744.

14 Baleani, M., Peroni, C., Cristofolini, L., Traina, F., Silbermann, M., Sawaed, S. and Viceconti, M. Multiaxial miniaturized load cell for measuring forces acting through a sternotomy. *Experimental Techniques*, **30**(4), 2006, 23-28.

15 McGregor, W.E., Trumble, D.R. and Magovern, J.A. Mechanical analysis of midline sternotomy wound closure. *The Journal of Thoracic and Cardiovascular Surgery*, **117**(6), 1999, 1144-1145.

16 Losanoff, J.E., Basson, M.D., Gruber, S.A., Huff, H. and Hsieh, F.-h. Single Wire Versus Double Wire Loops for Median Sternotomy Closure: Experimental Biomechanical Study Using a Human Cadaveric Model. *The Annals of Thoracic Surgery*, **84**(4), 2007, 1288-1293.

17 Sargent, L.A., Seyfer, A.E., Hollinger, J., Hinson, R.M. and Graeber, G.M. The healing sternum: A comparison of osseous healing with wire versus rigid fixation. *Annals of Thoracic Surgery*, **52**(3), 1991, 490-494.

18 Casha, A.R., Gauci, M., Yang, L., Saleh, M., Kay, P.H. and Cooper, G.J. Fatigue testing median sternotomy closures. *European Journal of Cardio-thoracic Surgery*, **19**(3), 2001, 249-253.

19 Casha, A.R., Yang, L., Kay, P.H., Saleh, M. and Cooper, G.J. A biomechanical study of median sternotomy closure techniques. *European Journal of Cardio-thoracic Surgery*, **15**(3), 1999, 365-369.

20 Mow, V.C. and Huiskes, R., eds. *Basic orthopaedic biomechanics & mechano-biology*. Philadelphia, 2005).

21 McCool, F.D. Global Physiology and Pathophysiology of Cough: ACCP Evidence-Based Clinical Pratice Guidelines. *CHEST The Cardiopulmonary and Critical Care Journal*, **129**(1), 2006, 48-53.

TABLES

Table 1

Maximum sternum opening for the first and last cycles

	Sternum Opening (mm)			
Cycle	M	MS1	MS2	X
1	0.03 ± 0.04	-0.04 ± 0.05	0.16 ± 0.05	0.05 ± 0.04
350	0.00 ± 0.07	-0.02 ± 0.08	0.16 ± 0.05	0.07 ± 0.04

Data comprise means ± SD (n=3)

Table 2

Summary of the testing results for each loading mode

Testing Mode	Nb samples	Output variables	Unity	Mean	Standard deviation
Installation	16	$F_{COMP, I}$	N	411.4	70.2
Static Service	5	$F_{COMP, I}$	N	462	51
		$F_{TRAC,O}$	N	1221	73
		$F_{COMP,RES}$	N	187	41
		δ_{PERM} at MS2	mm	0.13	0.08
Deep Breathing	3	$F_{COMP, I}$	N	391	18
		$F_{COMP,RES}$ at 350^{th}cycle	%	42	16
Coughing Fit	5	$F_{COMP,I}$	N	405	59
		$F_{COMP,RES}$ at 100^{th} cycle	%	53	8

Figure

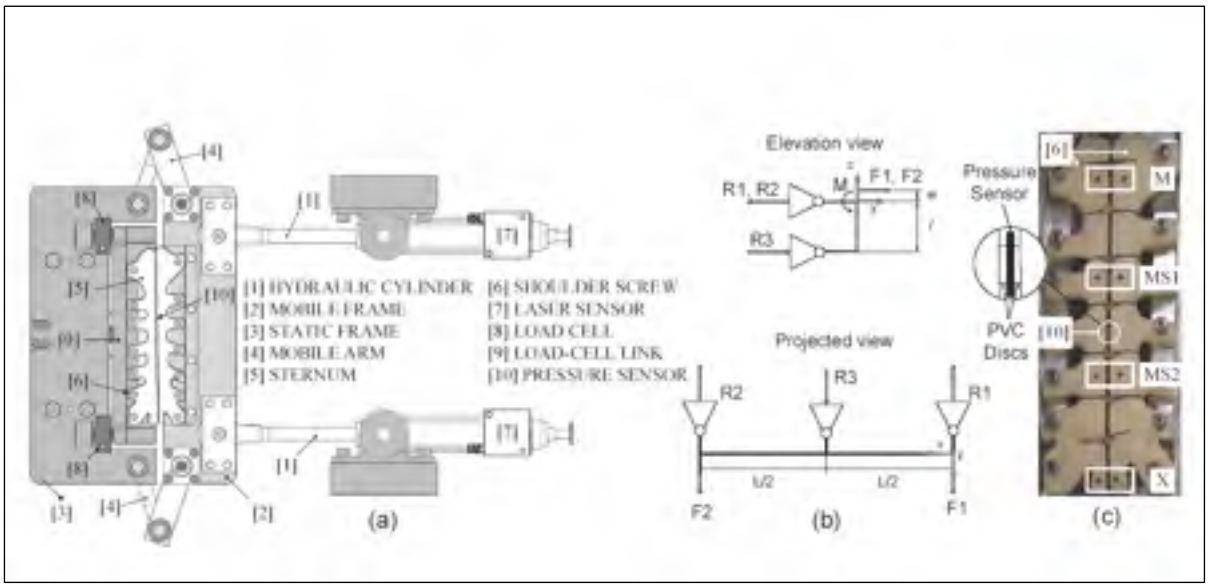

Fig. 1: Schematic of the test bench (a) and closed sternum with the location markers and pressure sensors b)

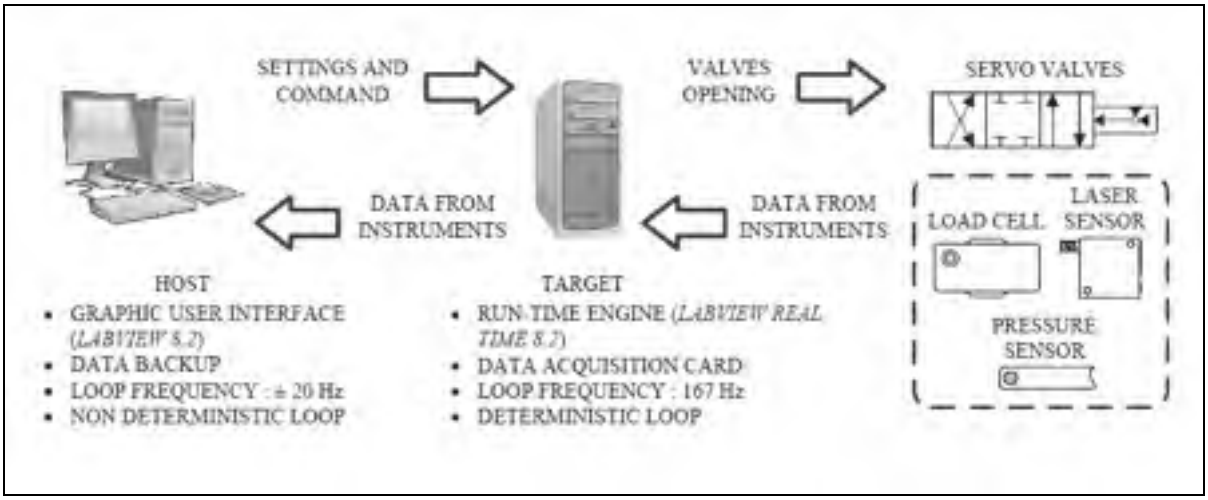

Fig. 2: Software architecture of the test bench

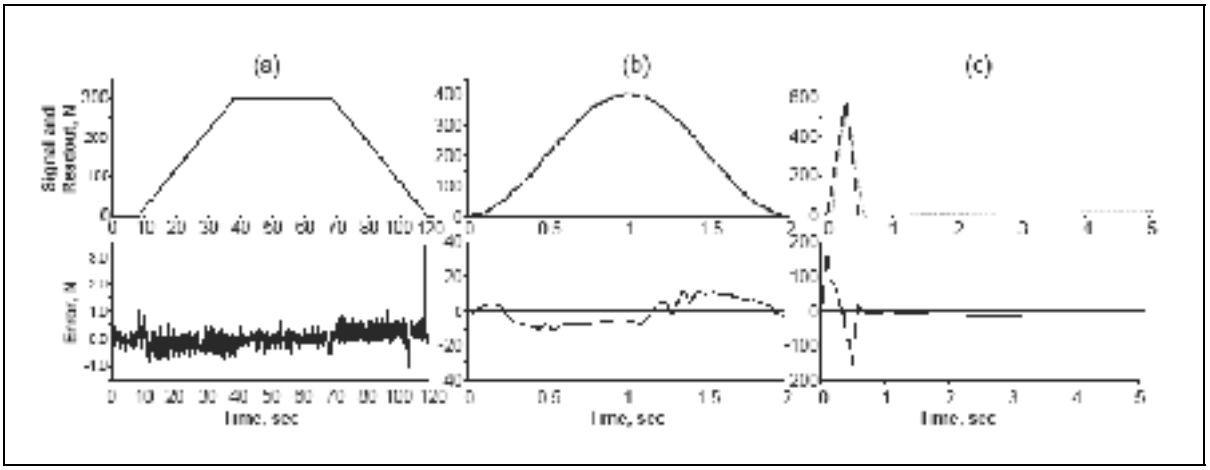

Fig. 3: Typical loading curves in terms of command, response and error for static (a), deep breathing (b) and coughing fit (c) testing modes

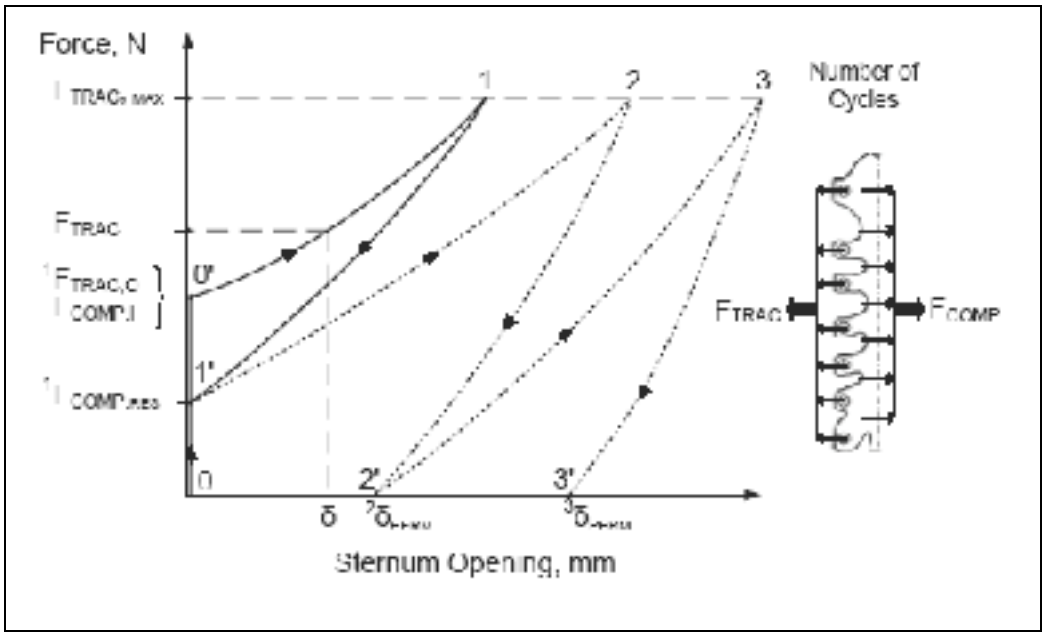

Fig. 4: Performance characteristics measured

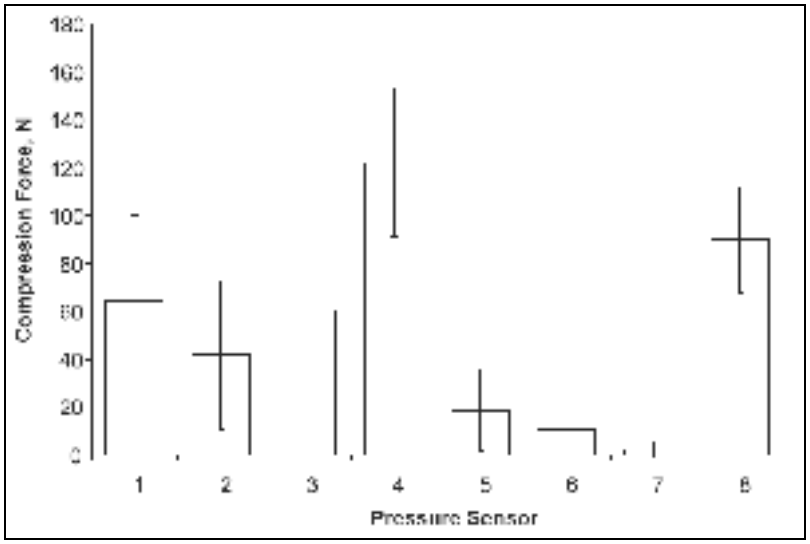

Fig. 5: Compression force at the sternum midline during installation of the No. 5 stainless steel wires with 7S configuration. Data are mean values ± SD (n=16)

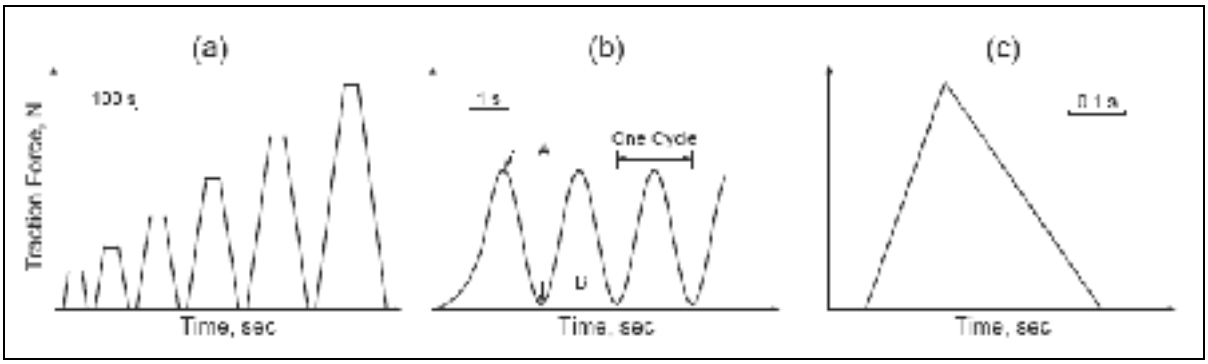

Fig. 6: Force pattern used during static (a), deep breathing (b) and coughing fit (c) testing modes

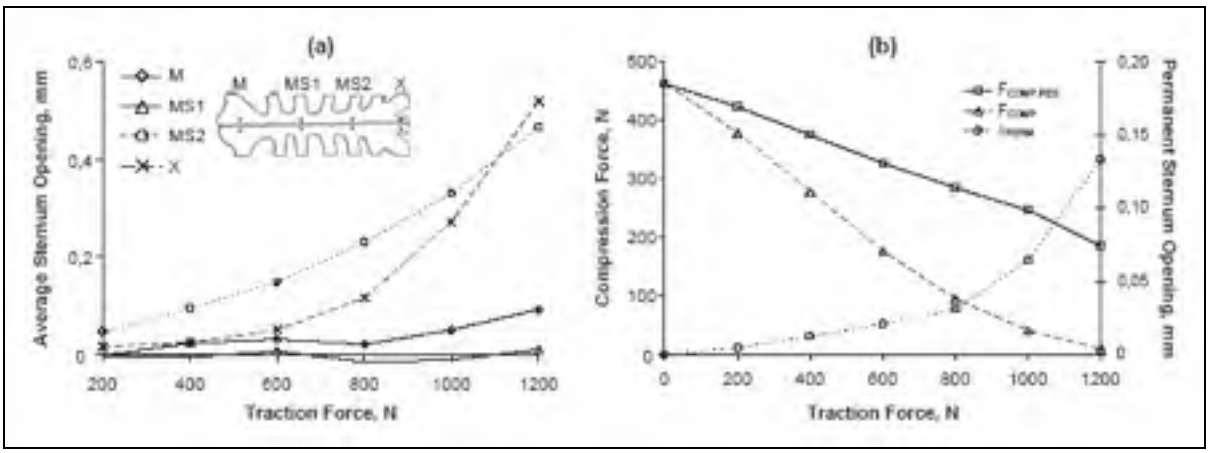

Fig. 7: Mean sternum opening as a function of the traction force (a) and compression, residual compression force and permanent displacement following the application and release of a traction force for the first cycle (b). Standard deviations (SD) are omitted to avoid crowding (n=5)

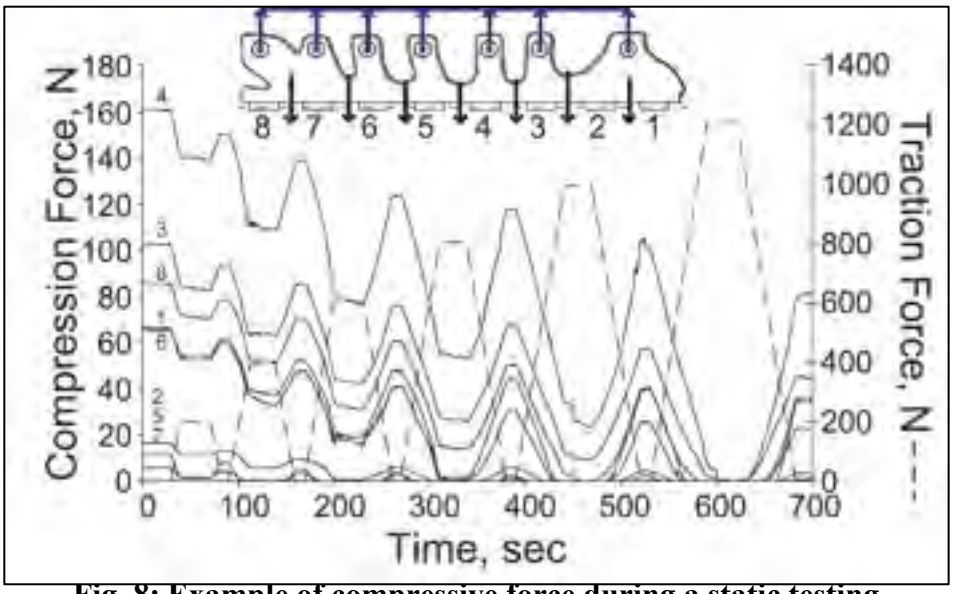

Fig. 8: Example of compressive force during a static testing

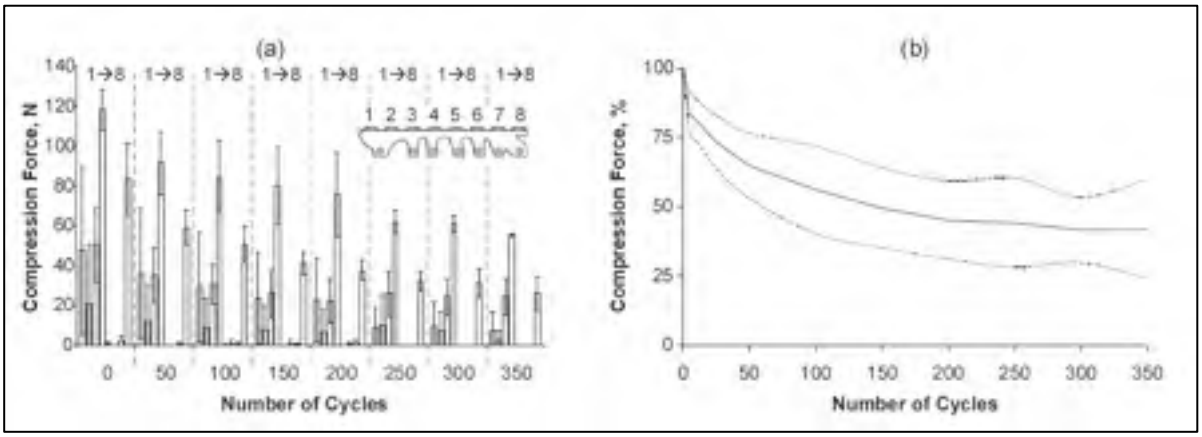

Fig 9: Relative residual compression force as a function of the number of cycles for deep breathing: (a) individual pressure sensor measurements, (b) summarized compression force. Data are mean values with the 95% CI (n=3).

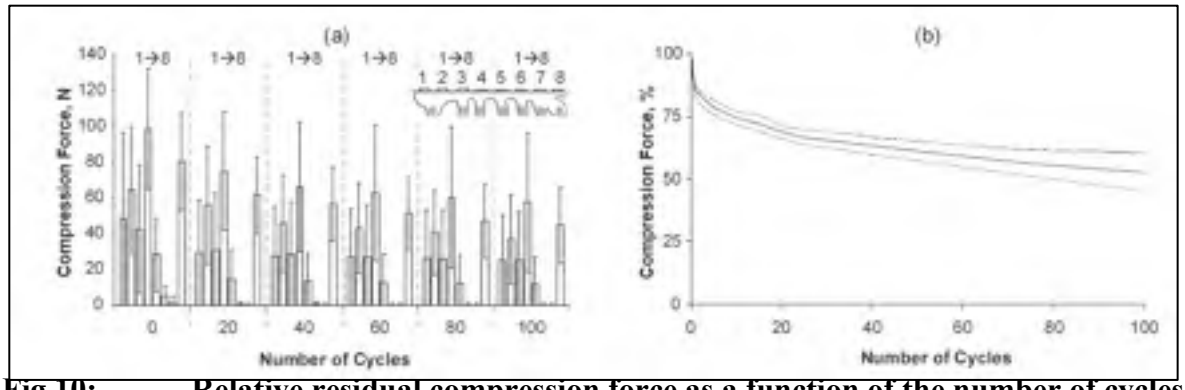

Fig 10: Relative residual compression force as a function of the number of cycles for coughing fits: (a) individual pressure sensor measurements, (b) summarized compression force. Data are mean values with the 95% CI (n=5).

ANNEXE II

BINDING COMPONENT

Cette annexe présente le brevet « Binding component » PCT/CA2005/001859 qui a été parachevé le 6 décembre 2005. Le brevet est présenté ici comme il apparait en date du 19 février 2009 sur le site de l'organisation mondiale de la propriété intellectuelle « http://www.wipo.int ».

(19) World Intellectual Property Organization
International Bureau

(43) International Publication Date
15 June 2006 (15.06.2006)

PCT

(10) International Publication Number
WO 2006/060911 A1

(51) International Patent Classification:

(21) International Application Number:

(22) International Filing Date:

(25) Filing Language: English

(26) Publication Language: English

(30) Priority Data:

(71) Applicants ... INSTITUT DE CARDIOLOGIE DE MONTREAL ...

(72) Inventors; and
(75) Inventors/Applicants (for US only):

(74) Agent:

(81) Designated States

(84) Designated States

Published:
— with international search report

(54) Title: BINDING COMPONENT

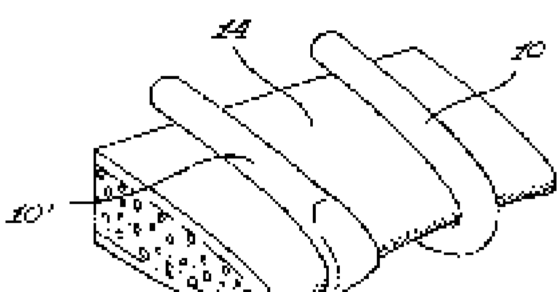

(57) Abstract:

WO 2006/060911 A1

WO 2004/019811 PCT/CA2003/001289

BINDING COMPONENT

FIELD OF THE INVENTION

The present invention relates to the general field of binding components and is particularly concerned with a binding component suitable for binding together a pair of biological tissues.

BACKGROUND OF THE INVENTION

There exists a plurality of situations wherein it is desirable to bind together components having specific properties. For example, there are various circumstances in which separated tissue of a patient needs to be brought together so it can heal. Such tissue may include bone, muscle, fascia or the like that has been divided to gain access for example to the thoracic cavity, the mediastinum, the abdomen or the like.

Typically, most surgical procedures involving the heart or lungs are performed through a pectoral sternal incision, widely referred to as median sternotomy. After an incision is made through the skin, the sternum is cut longitudinally using specialized power saws. The cut extends the entire length of the sternum, from the sternal notch at the neck to the xyphoid. This midline cut allows the two halves of the sternum and the anterior portion of the ribcage to be spread several inches apart, giving the surgeon access to the thoracic cavity. During surgery, the two halves of the sternum are typically held apart by mechanical retractors.

Once the surgeon has finished the procedure regarding the chest cavity, the sternum needs to be closed or reapproximated. For proper healing to occur, the split sternum portions are preferably engaged in face-to-face relationship and compressed together while the sternum heals. The key to the healing process of the sternum is the proper stabilization and contact of the two severed sides together.

Heretofore, there have been many techniques used to bring the separate sides of the sternum together and maintain them in contact so the healing process can occur. In the vast majority of cases, surgeons use stainless steel wire closure devices. These closure devices are composed of a thin stainless steel wire with a diameter typically of about 0.5 to 1.0 mm coupled to a curved needle. The composite device is formed by inserting one end of the stainless steel wire into a cavity in the non-sharpened end of the curved needle which is then crimped tightly to secure the wire to the needle.

The needle is used to pass the wire through the sternum or around the sternal halves between the ribs that connect to the sternal halves. After all the wire segments have been properly positioned, a crimp positioned on each wire are sequentially picked up by the surgeon and the wires are twisted around each other.

The ends are then trimmed and the twisted junctures are twisted again to create an extra-strong closure that will ensure that the sternal bones are pressed tightly against each other to minimize bleeding and ensure proper fusing of the sternal halves into an intact sternum. Normally, the wire loops are left in place permanently. Unless problems arise which require a second surgical operation to remove the wires, they remain in place for the remainder of the patient's life, even after the sternal halves have fused together again.

Despite their widespread use, the stainless steel wires suffer from numerous drawbacks that can cause problems both to the surgeon and to the patient during the operation and to the patient after closure is completed. For example, the relatively stiff and unyielding characteristic of a stainless steel wire renders it unwieldy and sometimes difficult to manage on the operative field. Furthermore, after each wire is in place, the segment that sits below the sternal halves may press down on body tissues such as a coronary artery by-pass graft or the heart itself while the other wires are being placed. Injury to these soft tissues can hence occur from these stiff wire segments during the normal course of sternal closure.

Also, during either preparation or application, the free end of a sternal wire can stab a surgeon, scrub nurse, or assistant. The substantial problem is compounded by the fact that the wire is typically cut using a wire cutter with relatively blunt blades, which generates a chiseled point tip. It is typically quite sharp. To reduce the risks of stab wounds to the surgeons and their assistants, clamps are now typically used to secure the free ends of any wire in a patient's chest. However, such clamps are also plagued with various drawbacks including cluttering of the operating field and being tedious and time consuming to work with and around.

Furthermore, the stainless steel sternal wires can disrupt the entire image generated in a computerized axial tomography or magnetic resonance imaging scan of the chest for the remainder of the patient's life.

Still furthermore, tightening by twisting wires together with a pair of pliers is an inexact method. The surgeon has to develop a sensitive field for how much torque needs to be applied to properly tighten the wire without breaking it. Consequently, some suture wires break during installation. A wire break requires the surgeon to unravel finished sutures and then start the process all over again.

Sternal wires occasionally also break after the surgery. Such breakage can be secondary to the thinning and deformation of the steel strand by the excessive force or stresses that are sometimes applied to the loop during routine closure. For fear of breaking a wire, a surgeon may tend to undertorque the suture, resulting in less than optimal closure pressure on the sternal knife. This, in turn, can lead to dehiscence problems.

A particularly major problem associated with steel wire sutures is that post operative stress on the closure loops may cause the thin wires to cut into and through the bone of the sternum. Indeed, since wires inherently define a relatively small contact surface anatomical structures may experience excessive localized pressure resulting in

damage. For example, bone may fracture or exceriation necrosis, cartilage may tear, etc.

Typically most of the tension resulting from the twisting procedure on the wire is applied at the anterior surface of the sternum. Routine postoperative care of cardiothoracic patients requires aggressive pulmonary rehabilitation including early ambulation. The coughing, deep breathing and movement required to attain these goals imposes substantial stresses on the sternal closure. These substantial stresses may, in turn, cause the wire loops to cut the bone in an inward direction at the posterior side of the sternum. Elderly patients or patients who have thin or osteoporotic bones are particularly susceptible to this complication.

The result is further loosening of the sternal closure which can lead to painful instability of the two sternal halves with respiratory compromise and ultimately sternal dehiscence. Instability of the sternal closure can also result in internal bleeding. This, in turn, can increase the risks of infection and/or result in macerative damage to the cartilage and associated muscle tissue with a consequent increase in post operative discomfort and in the time required for healing. Also, if a second operation for sternal rewiring is required, it is made even more difficult by the fact that the sternal halves are often sliced into pieces by the stainless steel wires.

The problem of sternal dehiscence after closure using suture loops is known, and, various solutions have been proposed. Among these are reinforcement of the sternum by implantation of longitudinally extending wires or weaving reinforcement wires around the ribs adjacent to the sternum and then applying sutures paresternally to join the sternal halves. However, these proposed solutions tend to result in increased damage to blood vessels or other soft tissue, and also may substantially increase the time required for closing the chest. Also, if infection occurs necessitating removal of the sutures, it can be very difficult to remove the reinforcing wires.

In an effort to circumvent some of the disadvantages associated with steel wires and, more particularly, to reduce the risk of having the closure structures cut into and through

the bone of the sternum. Substantially flat bands have been proposed. For example, U.S. Patent No. 4,750,515 issued to Sutherland and Vasconcelos in 1988 describes a flat band made of metal and coated with plastic which slides through a fastener device which was referred to in the patent as a "buckle". The band contains protruding serrations which interact in a ratcheting manner with an angled tang in the buckle. This allows the band to be pulled tight while the tang slides across the raised serrations. Subsequently, if tension exerted attempts to expand or open the loop, the angled tang presses against the shoulder of a serration thereby preventing the band from moving in the opposite direction.

A somewhat similar structure is disclosed in U.S. Patent No. 4,813,416 issued to Pollak and Blasnik in 1989. This patent discloses a flat stainless steel band with notches rather than serrations. The notches interact with bumps in a buckle device, to hold the band securely after the band has been pulled tight.

U.S. Patent No. 5,356,412 issued October 18, 1994 to Golds and Muth discloses a strap assembly to be looped about split sections of human tissue including a flexible elongated member and a buckle member. The buckle member includes a frame member and a clamp member rotatably mounted within the frame member for movement from a non-strap securing position to a strap securing position. The clamp member rotates to the strap securing position in response to tensional forces exerted on the strap during tensioning thereof about the tissue portions.

These band like devices provide an increased contact surface with the sternum as compared to the steel wires and hence, theoretically reduce the risk of cutting into and through the bone of the sternum. However, they nevertheless suffer from various limitations which limit their utility.

For example, being substantially flat and made of relatively stiff and unyielding material, they are typically unable to fittingly contact the geometry of the sternum. Also, their geometry is such that they cannot penetrate easily through the bone and, hence, can

only be positioned anteriorly between the ribs. Being relatively large, they typically displace the pectoral structures such as muscles.

Furthermore, because of their flat configuration, their bending moment of inertia is polarized in a predetermined direction. Consequently, they are considered unorganomical. Typically, they are even more unwieldy and difficult to manage on the operative field than steel wires.

Still furthermore, the substantially flat shape of these bands results in relatively sharp side edges. Such sharp side edges can slice into the surrounding tissues or bones like a blade when they are pulled through behind the needle. This, in turn, may cause internal haemorrhaging and associated problems. The sharp side edges, if unprotected, also have considerable potential to slide into the fingers of the operating surgeon or assistants. Furthermore, they are capable of irritating and/or to the soft tissues below the sternum during closure.

Another type of closure system attempting to circumvent problems associated with steel wires and disclosed in the prior art uses clamps. Examples of such closure systems are disclosed, for example, in U.S. Patent 4,201,216 to Crossett et al and in U.S. Patent 6,217,582 issued April 17, 2001 to L. Scott Levin.

The sternal clamping device disclosed in the latter patent includes a pair of opposed generally J-shaped clamp members which are laterally adjustable relative to one another and can be rigidly joined via a set of machine screws. The threaded coupling of these set screws rigidly unites the clamp members one to another without laterally shifting or creeping over time.

This type of system is relatively rigid and reliable. However, the components thereof are relatively large and may cause serious pain or other ailments to the patient. Its use is hence typically reserved to patients having an increased risk of sternal rupture or with concomitant risk factors for infection.

In an effort to circumvent the problem of cutting into and through bone of the sternum associated with conventional steel wires, attempts have also been made to offer radially compressible sutures offering an increased contact surface area as evidenced by U.S. Patent No. 5,423,821 issued June 13, 1995 to Manuel K. Pasque, the entire contents of which are incorporated expressly herein by reference.

According to the Pasque patent, a strand of thin flexible suture material is used which is compressible in its radial dimension but remains strong and relatively inelastic in its longitudinal dimension. The compressibility in the radial direction results either from the hollow tubular shape or the compressible nature of the materials used. The longitudinal strength may be maintained by nylon fibers or other materials for reinforcement.

The soft suture material helps cushion, distribute and minimize the stresses and damage inflicted on the sternum or ribs post-operatively. Furthermore, when not compressed, the strand has a diameter slightly larger than the diameter of the needle. Hence, after insertion, the expandable suture material provides gentle pressure against the surrounding tissue to minimize bleeding in the needle track.

A common problem with all of the hereinabove mentioned bone binding structures is that they can only be used towards fixation of the sternal halves, i.e. for immobilizing the sternal halves in close proximity to each other. However, for osteogenesis and solidification of the sternal halves to occur, compression of the sternal halves at the break boundary must be maintained during the healing process.

Fixation is a static process whereas compression is a dynamic one. Compression is dynamic because it must be maintained during dimensional redefinition occurring at the break boundary during healing. With the hereinabove mentioned prior art structures compression across the break boundary typically decreases substantially during the healing process.

Indeed, the width of the sternum tends to decrease due to the nature of the healing process. The above-mentioned structures cannot respond to this dimensional change and, consequently, cannot maintain compression across the fusing boundaries of the divided sternum during the healing process. Thus, applied pressure decreases with time.

As stated above, not only do the large initial compression forces generated with the hereinabove mentioned devices diminish in the initial phase of bone healing, but such large forces, in themselves, are detrimental relative to the concentrated forces experienced proximal to the wires. Although the hereinabove mentioned structures provide some stability, they are deficient as a means to establish a known initial force and they never reconcile the need for continuous compressive force. Furthermore, physiological activities such as coughing contribute to the degeneration not only of the sternum but also potentially of the devices themselves.

The need for providing a binding structure capable of inducing a compression at the break boundary of the divided sternum has been recognized and addressed in U.S. Patent No. 5,766,218 issued June 16, 1998 to Richard J. Arnott. The disclosed binding device includes a strap adapted to form a loop about injured tissue and a tension member attached to the strap. The tension member is adapted to maintain a predetermined stress level in the loop which compresses the edges of the tissue together to foster healing. The tension member is preferably a shape memory effect alloy, such as Nitinol, a nickel-titanium alloy. The binding device also includes a one-way locking mechanism which locks the strap in the loop.

Also disclosed is a method of binding together injured tissue under a compressive force to promote healing. The method comprises the steps of drawing together in close proximity opposing edges of injured tissue by tightening a strap which forms loop about the injured tissue and tightening the strap so that a tension member within the strap exerts a substantially constant tension within the strap to maintain the tissue in close proximity.

The use of so-called shape memory materials such as shape memory alloys in the medical field has been disclosed in the prior art. These alloys have different phase structures, hence, different mechanical properties at different temperatures. Information about shape memory alloys may be found, for example, on the web site www.nitinol.com, by Nitinol Devices & Components, copyright 1998.

In brief, FIGS. 9A and 9B, together, schematically illustrate a typical temperature and stress hysteresis, typical elastic stresses, σ_y, in phase transitions, and typical stress strain curves for a shape-memory alloy in the austenitic and martensitic phases. At low temperature, the alloy is martensitic and is soft and plastic, having a low σ_y. At a high temperature, the alloy is austenitic and tough, having a high σ_y.

When a martensitic alloy is heated to a temperature A_s, the austenitic phase begins to form. Above a temperature A_f the alloy is fully austenitic. Likewise, as an austenitic alloy is cooled to a temperature M_s, the martensitic phase begins to form. Below a temperature M_f the alloy is fully martensitic.

The temperature-dependent phase structure gives rise to shape memory. At the fully austenitic phase, under proper heat treatment and working conditions, an SMA element can be given a physical shape and "pre-programmed" to memorize that shape and resume it whenever in the austenitic phase. The "memorized" SMA element may then be cooled to a martensitic phase and plastically deformed. In the martensitic phase. But when heated back to the austenitic phase it will resume its "memorized" shape. The transformation temperature range between the phases is noted as TTR.

The reason for the shape memory is found in the phase structure of the alloy. Most metals deform by atomic slip. Dislocations and atomic planes slide over one another and assume a new crystal position. In the new position, the crystal has no memory of its order prior to the deformation. With increased deformation, there is generally a work-

hardening effect, in which the increased tangle of dislocations makes additional deformation more difficult.

This is the case even when the increased deformation is in the direction of restoring the crystal to its original shape. However, for shape memory alloys, both transitions between the austenitic and martensitic phases and deformation in the martensitic phase change lattice angles in the crystal, uniformly for the whole crystal. The original austenitic lattice structure is "remembered" and can be restored.

FIG. 6C schematically illustrates typical phase structures of a shape memory alloy, as functions of temperature and deformation, as follows:

- in the austenitic phase, the crystal has a cubic structure, and the atoms in the lattice are arranged generally at right angles to each other;
- when the austenitic crystal is cooled to a martensitic phase, a twinned lattice structure is formed;
- when the twinned martensitic crystal is deformed by an amount no greater than 8, the twinned structure "stretches" so that the atoms in the lattice are arranged generally at oblique angles to each other, wherein the oblique angles are determined by the amount of deformation; and
- when the deformed martensitic crystal is heated, the crystal resumes its cubic structure, wherein, again, the atoms in the lattice are arranged generally at right angles to each other.

Another property that can be imparted to SMA elements, under proper heat treatment and working conditions, is so-called superelasticity, or Stress-Induced Martensite (SIM). With this property, a fully austenitic SMA element, at a temperature above A_f, will become martensitic and plastic under high stress and deform under the stress. When the stress is removed, the SMA element will return to the austenitic phase and to its memorized shape in the austenitic phase.

Superelasticity is also referred to as rubber-band like property, because the SMA element behaves like a rubber band or a spring, deforming under stress and resuming its original shape when the stress is removed. However, this property is present only above the temperature A_f and only when it is specifically incorporated in an SMA element by proper heat treatment and working conditions.

FIG. 8(a) schematically illustrates a typical cyclic transformation of a superelastic alloy at a constant temperature above the temperature A_f. The transformation between the austenitic phase and a stress-induced martensitic phase is brought about by stress and is eliminated when the stress is removed.

Bending devices disclosed in the prior art using shape memory alloys typically suffer from numerous drawbacks. For example, the structure disclosed in U.S. Patent 5,765,216 is relatively complex to manufacture and, hence, potentially less reliable and more expensive. Furthermore, the use of a strap is associated with the hereinabove mentioned disadvantages inherent to its geometry.

Other medical binding devices using shape-memory alloys typically take the form of staples or clamps for bone fixation. They are easily inserted in a martensitic phase, then deformed to an open straight-edge state and they resume a closed, clamped state in the body, thus forming a closure on the fracture. However again, they suffer from disadvantages inherently associated with their geometries.

Shape memory materials have also been used, inter alia, in the production of stents. As is well known, a stent is a generally tubular mesh-like device which is useful in the treatment of stenosis, strictures or aneurysms in body conduits defining lumens such as blood vessels. Shape memory material stents are designed so as to be expanded in the austenitic phase and compressed or partially expanded in the martensitic state. The shape memory alloy is typically chosen such that stent will be in the austenitic state at body temperature.

The role of the stent being to support, repair or otherwise enhance the performance of a body lumen, stents are specifically designed to provide a relatively high resistance to radial collapse. Hence, they actually teach away from the principles of the present invention as will be hereinafter disclosed.

Accordingly, against this background, there exists a need for an improved binding structure.

SUMMARY OF THE INVENTION.

It is a general object of the present invention to provide such an improved binding structure. In accordance with the present invention, there is hence provided a binding component for binding together a pair of biological tissues, the binding component comprising an elongated body defining a body longitudinal axis; the body being made, at least in part, of a shape memory material; the body being configured and sized so as to be both substantially flexible and substantially compressible in a direction substantially perpendicular to the longitudinal axis.

Advantageously, the shape memory material demonstrates superelastic properties when subjected to environmental temperatures within the range of expected body temperatures.

Preferably, the body has a substantially uniform moment of inertia of bending in all directions. Typically, the body has a substantially hollow tubular configuration and is made of braided filaments of a shape memory material.

In accordance with the present invention, there is also provided a method for binding biological tissues together, the method including the steps of selecting a suitable binding component comprising an elongated body defining a body longitudinal axis, the body being made, at least in part, of a shape memory material; the body being configured and sized so as to be both substantially flexible and substantially

compressible in a direction substantially perpendicular to the longitudinal axis, positioning the binding component in a binding configuration wherein the binding component places the biological tissues in an opposite contacting relationship relative to each other, and inducing a pre-strain into at least part of the binding component. Preferably, the pre-strain corresponds to an applied stress having a value of between [illegible] and [illegible].

In accordance with the present invention, there is further provided a method for manufacturing a binding component, the method comprising the steps of braiding filaments of shape-memory material into an elongated body defining a body longitudinal axis, the body being configured and sized so as to be both substantially flexible and substantially compressible in a direction substantially perpendicular to the longitudinal axis.

Conveniently, the method further comprises the step of treating the body so that the shape memory material demonstrates superelastic properties when subjected to temperatures substantially in the range of expected human body temperatures.

In accordance with the present invention, there is yet also provided a binding component for binding together a pair of biological tissues, the binding component comprising: an elongated body defining a body longitudinal axis; the body being made at least in part of a shape memory material, the body being provided with at least one therapeutic or prophylactic surgically useful substance.

The processed binding structure is specifically designed so to synergistically combine the advantages associated with shape memory materials with advantages associated with its geometry.

More specifically, advantages of the present invention include that the processed binding structure advantageously applies a substantially consistent compressive force across tissue boundary while being able to accommodate some expansion.

The proposed binding structure protectively controls the maximum force that has to be tolerated during contact therewith experiences. The proposed structure stretches at a known or programmable level and is then capable of returning to its unstretched lengths while generating a substantially constant force. The ability of the proposed structure to allow a relatively unlimited expansive force moderates local forces in the tissue around the binding structure, decreasing the likelihood of damaging or tearing the tissue.

Hence, the proposed binding structure is adapted to maintain cohesion between opposed tissue surfaces during the duration of osteogenesis even in situations wherein it is subjected to various stresses linked to post-operative events such coughing or the like.

The proposed system is also adapted to reduce the risks of a fracture of the sternum by shearing immediately at a large external stress. In the event wherein sternal deterioration occurs, the proposed system is adapted to maintain a predetermined compressive load on the sternum in order to assume its cohesion.

Furthermore, the proposed binding structure is adapted to provide an increased contact surface when effectively providing a compressive force. Still furthermore, while providing an increased contact surface the proposed binding structure is still deprived of relatively sharp edges that could potentially cause haemorrhaging or the like.

In short, the proposed binding structure is adapted to reduce the risks of the latter tearing through the sternal bone by both increasing the contact surface therewith and accommodating some degree of expansion. Furthermore, the proposed structure is adapted to maintain a cohesive force at the interface of the two sternal halves despite the physiological remodeling during fusion thereof and even in situations wherein some degree of tearing as occurred in the bone.

Still, furthermore, the proposed binding structure is designed so as to be ergonomically pliable, having a relatively low bending moment inertia, the latter being also substantially constant in all directions. This, in turn, facilitates ergonomical handling of the binding structure during the surgery and allows the binding structure to more fittingly contact the sternum.

Yet still furthermore, the proposed binding structure is designed to show little if any tendency to kink or shear. Also, the proposed structure is adapted to reduce the risks of injury to the surgeon or assistants thereof. Furthermore, the proposed structure is adapted to reduce the risks of compressing or otherwise damaging biological structures adjacent the sternum during installation thereof.

Also, the proposed binding structure is designed so as to be easily severed or otherwise rendered ineffective or removed in situations wherein, for example, the sternum needs to be re-opened. The proposed binding structure, for example, is adapted to be easily cut using a conventional surgical tool such as a surgical scissor or the like without requiring excessive force or manual dexterity.

Furthermore, the proposed binding structure is adapted to reduce the risks of creating imaging artefacts or otherwise interfering with medical imaging once in place.

Also, the proposed binding structure is designed so as to be manufacturable using conventional forms of manufacturing so as to provide a device that will be economically feasible.

In another broad aspect, the invention provides a method for binding biological tissues together, the biological tissues having a yield limit beyond which the biological tissues are irreversibly deformed. The method comprises:

- selecting a suitable binding component comprising an elongated body defining a body longitudinal axis, the body being made, at least in part, of a shape memory material;

- positioning the binding component in a binding configuration wherein the binding component places said biological tissues in an opposite contacting relationship relative to each other

- wherein the binding component is at least in part prestrained with a prestrain causing the generation of a force within an interval of from about 5% percent to about 10% percent of the yield limit after said positioning of said binding component

In yet another broad aspect, the invention provides a method for manufacturing a binding component.

In yet another broad aspect, the invention provides a binding component

In some embodiments of the invention, the binding component has a binding component ultimate tensile strength within an interval of from about 200 N to about 300 N

The composition, configuration and dimensions of the body may be selected such that an inflection point between an upper plateau of a force-displacement relationship of the binding component and a linear force-displacement relationship representing an elastic deformation of a stress-induced martensite phase in the binding component is substantially coincident with a force and a displacement representative of the prestrain in the body component and a difference in force between a lower plateau of the force-displacement relationship of said binding component and the upper plateau of the force-displacement relationship of said binding component is minimal.

BRIEF DESCRIPTION OF THE DRAWINGS

An embodiment of the present invention will now be disclosed, by way of example, in reference to the following drawings in which

Figure 1, in an elevational view, illustrates a pair of sternum halves being bound together using binding components in accordance with the present invention;

Figure 2, in a partial perspective view with sections taken out, illustrates a pair of binding components partially wrapped around a section of a sternum, one of the binding components is radially uncompressable while the other binding component is in a radially compressed configuration;

Figure 3, in an elevational view, illustrates a binding component in accordance with an embodiment of the present invention the binding component being shown in a substantially rectilinear configuration and in an uncompressed state;

Figure 4, in a top view, illustrates the binding component shown in Fig. 3

Figure 5, in a top view, illustrates the binding component shown in Figs. 3 and 4 in a radially compressed configuration;

Figure 6A and 6B schematically illustrate a typical temperature hysteresis and typical elastic stress-strain hysteresis for a typical shape memory material, in accordance with the prior art

Figure 6C schematically illustrates typical phase structures of a shape memory alloy, as functions of temperature and deformation, in accordance with the prior art;

Figure 6D schematically illustrates a typical cyclic transformation of a typical shape memory alloy, between an austenitic phase and a stress-induced martensitic phase, in accordance with the prior art;

Figure 7 schematically illustrates the principles of safe springback (segments A-B-C) and dynamic interference (segments C-D-E-F-G) of Shape Memory Alloys (SMAs) in a binding device in accordance with an embodiment of the present invention,

Figure 8 schematically illustrates a simplified model a binding component in accordance with the invention I – complete sternum; II – half of the sternum and of the closure system; the force created by an abnormal absorption is transferred to the sternum through the ribs; III – cross-section of the sternum; IV – series of springs replacing the sternum and closure system;

Figure 9A, in a X Y graph, illustrates the stress-strain curve modelling a SMA material for a Ti-50 at % Ni wire with a diameter of 0.71 mm;

Figure 9B, in a X Y graph, illustrates the stress-strain curve modelling a BISO material law parameters for steel modelling a N°5 Ethicon suture wire (Somerville, N.J., USA) having a diameter of 0.79 mm;

Figure 10, in a X-Y graph, illustrates the residual force and sternum opening as a function of an external force for a 0.24 g/cm3 modeled sternum loaded then on the opening curves indicate that the sternum is no longer closed once the disruption is over (h = 0);

Figure 11, in a schematic view, illustrates a testing bench used to test binding components in the form of sternum closing systems;

Figure 12, in a X-Y graph, illustrates the force-displacement diagrams of some components of the testing bench of Figure 11;

Figure 13, in bar graphs, illustrates the relative residual force Rf=Ff/Fi provided by two binding devices in the form of experimental closure systems as a function of thread type (metallation mode (peri-sternal versus transsternal) (panel a); as a function of a loading mode (single impulse versus repetitive loading) (panel b); and foam used to test the closure systems (panel c); and

Figure 14 is a schematic view, illustrates a selection technique for SMA suture force displacement characteristics in accordance with an embodiment of the present invention

DETAILED DESCRIPTION:

Referring to Fig 1, there are shown binding components in accordance with an embodiment of the present invention, the binding components being generally indicated by the reference numeral 10. The binding components 10 are typically used for binding together a pair of biological tissues. In the embodiment shown throughout the Figures, the binding components 10 are shown being used for their preferred application, namely for binding together a pair of sternal halves 12 and 14 of a patient's sternum following a median sternotomy. It should however, be understood that the binding components 10 could be used in other contexts and/or for binding together other types of biological tissues without departing from the scope of the present invention.

In the embodiment shown in Fig. 1, six binding components 10 are positioned at spaced intervals along the sternum. Typically, in the upper portion of the closure, where the manubrium portion of the sternal bone is relatively wide, the binding components 10 are inserted through the bone. Below the manubrium, the binding components 10 are usually passed through parasternal tissue between the ribs and typically do not penetrate the sternal bone except when the sternum is exceptionally wide. It should however, be understood that any suitable number of binding components 10 could be used and that the latter could be used in any suitable combination of parasternal and/or trans-sternal approach without departing from the scope of the present invention.

Also, in Fig. 1, the loops formed by the binding components 10 are shown attached by clips C. It should be understood that the clips C are shown only by way of illustrative example and that other types of loop attachment means could be used without departing from the scope of the present invention.

Furthermore, it is contemplated within the scope of the present invention to provide clips or other suitable binding component attachment means in combination with a gauge or sensing means for gauging or sensing the axial tension in the binding component. The gauge or sensing means is preferably provided with an indicating means for providing the surgeon with an indication of the axial tension in the binding component 10. The indicator could take the form of a substantially continuous read-out of the actual tension in the binding component 10 or, alternatively, could take the form of a warning signal indicating that the tension in the binding component has reached a predetermined threshold. Also, the indicator can be provided in any sensoral modality including a visual signal, an audio signal, a tactile signal or a combination thereof.

In an alternative embodiment of the invention, the clip or other suitable binding component attachment means includes a means for limiting the axial tension in the binding component 10.

As illustrated more specifically in Fig. 2, each binding component 10 has an elongated body 16 defining a body longitudinal axis 18. The body 16 is made, at least in part, of a shape memory material. In a preferred embodiment of the invention, the body 16 is exclusively made out of shape memory material. However, in alternative embodiments of the invention (not shown) the body 16 could be a composite construction using both a shape memory material and one or more other type of material to combine the advantageous characteristics of shape memory materials with that of the other materials.

The body 16 is configured and sized so as to be both substantially flexible and substantially compressible in a compressing direction substantially perpendicular to the longitudinal axis 18. When a body 16 having a substantially circular outer surface is used the compressing direction is inwardly radial. A radial compressive force is schematically indicated by arrow 20 in Fig. 5.

Preferably the body 16 is configured so as to define a substantially uniform moment of inertia of bending in all directions. In an alternative embodiment of the invention (not shown), the body 16 could be configured to define at least one major moment of inertia and at least one minor moment of inertia so as to create at least one preferred bending direction.

When used in the context of a tying aid, in particular, of suturing or binding together sternal halves, the body 16 preferably has a substantially uniform moment of inertia of bending in all directions so as to facilitate ergonomical manipulation during the various steps leading to sternal closure. In the context of use as sutures and in particular, sutures for sternal halves, the body 16 is preferably provided with a relatively low moment of inertia of bending. This relatively low moment of inertia of bending is adapted to facilitate manipulation of the binding component 10 and to increase the fit between the binding component 10 and body parts when in contact with each other.

In order to provide a relatively low moment of inertia of bending that is relatively uniform in all directions, the body 16 preferably has a substantially hollow tubular configuration. As shown in Fig. 4, the body 16 preferably has a substantially annular cross-sectional configuration when radially uncompressed.

Fig. 2 illustrates, on the right-hand side thereof, a segment of an uncompressed binding component partially wrapped around a sternum half 14. The segment on the right hand side is schematically representative of an axially tensioned steel wire or of a non-axially tensioned binding component 10. The left-hand side of Fig. 2 illustrates a binding component 10' tensioned around the sternal half 14. As expected, the axial tension in the binding component 10' creates a radial compression adjacent the point of contact with the sternal half 14. As illustrated, the body 16 responds to the compressive pressure generated by the contact with the sternal half 14 by substantially flattening relative to its uncompressed configuration.

The propensity of the body 16 to substantially flatten upon application thereof of a radial compressive force inherently increases the size of the contact area between the body 15 and corresponding contacting portions of the sternal bone. This, in turn, inherently reduces the strain exerted locally on the sternum for a given axial load in the body 16. In other words, the radial compressibility of the body 16 helps cushion, distribute and reduce the stresses that are inflicted on the sternal bones by the binding component 10.

As illustrated more specifically in Fig. 5, in a preferred embodiment of the invention, the body 16 has a substantially ovaloid cross-section when in a radially compressed configuration. The ovaloid configuration defines an oval long axis 22 and an oval short axis 24. The ratio between the oval long and short axes 22, 24 is typically approximately between 1 and 3 when substantially tightly secured around a sternum, such as shown in Fig. 2. It should however be understood that the ratio between the long and short axes 22, 24 could have other values without departing from the scope of the present invention.

It should, however, be understood that the body 16 could assume other cross-sectional configurations when in a radially compressed configuration without departing from the scope of the present invention. However, the body 16 is preferably configured and sized so as to prevent the formation of thin or squared edges or thin-diameter cross-sections when in a radially compressed configuration so as to reduce the risks of injuring the bone or adjacent tissue surfaces.

The inherent so-called "shape memory" and "superelasticity" associated with shape memory materials are adapted to combine synergistically with the geometrical characteristics of the body 16 to evenly distribute stresses on the bone and minimize the risks of creating potentially sharp edges. Indeed, despite various potential axial loading patterns, the use of shape memory materials ensures that the advantages associated with the preferred body configuration will be retained as the shape memory materials ensure the integrity of the configuration and its compressible characteristics.

More specifically, the body 16 is designed so as to demonstrate superelastic properties when subjected to temperatures substantially in the range of expected human body temperatures. Hence, when the body 16 is laterally compressed against a sternal section, it has a tendency to resiliently bias its configuration towards its initial uncompressed configuration. This, in turn, prevents the formation of relatively sharp edges and substantially reduces the risks of kinking or other deterioration effects.

The reference letter R is used in Fig 5 to designate the radius of curvature of the binding component 16 adjacent the longitudinal ends of the oval long axis Y2 when the binding component 16 is radially compressed by a radial compressive force 20 of a magnitude within the range used for binding together sternal halves. Typically, although by no means exclusively, the radial compressibility and the superelastic properties of the binding component 16 are balanced so that the radius of curvature R varies between (Dext-Dint)/4 and (Dext-Dint)/2 wherein Dext et Dint are respectively a body outer diameter of the body 16 and a body inner diameter of the body 16 when the binding component is radially compressed by a radial compression force 20 of a magnitude within the range used for binding together sternal halves.

Referring back to Fig. 4, there is shown that the body 16 defines a lumen 26 extending longitudinally therethrough. The body 16 also defines a body inner surface 28 in contact with the lumen 26 and a radially opposed body outer surface 30. Typically, the body 16 defines a body thickness 32 extending radially between the body inner and outer surfaces 28, 30. The body thickness 32 typically has a value of approximately between 0.1 and 0.3 mm. It should however be understood that the body thickness 32 could have a different value without departing from the scope of the present invention.

For this range of body thickness, the radius of curvature R varies between about 0.05 mm and about 0.6mm when the binding component is radially compressed by a radial compressive force 20 of a magnitude within the range used for binding together sternal halves.

In alternative embodiments of the invention (not shown), the lumen 18 could be filled with a different type of material or with the same material at various densities. In other words, the body 16 could define a full cross-section and be composed of a central core surrounded by a compressible peripheral sleeve.

The overall size of the body 16 can vary from between 2 mm and 5 mm. It should however be understood that the overall size of the body 16 could vary outside that range without departing from the scope of the present invention.

Preferably, the body 16 is made of braided filaments 34 of a shape memory material. Preferably, the shape memory material is a shape memory alloy. Preferably, the shape memory alloy is the biocompatible nickel and titanium alloy commercially referred to under the acronym NITINOL (for Nickel Titanium Naval Ordnance Laboratory). NITINOL belongs to a family of intermetallic materials that contain a nearly equal mixture of nickel (55 wt. %) and titanium. Titanium-nickle shape-memory alloys are biocompatible and resistant to corrosion, therefore, they are suitable for medical applications.

Alternatively the shape memory material may be selected from another suitable biocompatible shape memory alloy, a suitable biocompatible shape memory polymer or a combination thereof.

Typically, the overall denier or weight of the filaments 34 has a value of approximately 5000. It should however be understood that the overall denier could have another value without departing from the scope of the present invention. Typically, each filament 34 has a substantially disc-shaped cross-sectional configuration. Alternatively, at least some of the filaments 34 could have another cross-sectional configuration.

When the filaments 34 have a substantially disc shaped configuration, they individually define a filament external diameter represented by the letter "d" in Fig. 3. Typically, the

filament external diameter has a value substantially in the range of between 50 and 200 micrometers and preferably of about 100 micrometers. It should however be understood that the filament external diameter could have another suitable value without departing from the scope of the present invention. Also, alternatively, the body 16 could be made up of filaments having different diameters without departing from the scope of the present invention.

Preferably, the body 16 is made of a braided structure including between 16 and 72 filaments 34. More specifically, the body 16 is preferably made up of a braided structure including approximately 24 braided filaments 34. It should however be understood that the braided structure could include any suitable number of filaments without departing from the scope of the present invention.

The thread of the filaments 34, as herein used throughout the text, refers to the distance projected on the longitudinal axis 18 by a given filament 34 as the latter completes a full turn around the longitudinal axis 18. A full thread is schematically illustrated and indicated by the letter "T" in Fig. 3. Preferably, the thread of the braided filaments 34 varies between 5 mm and 30 mm. More specifically, the thread of the braided filaments is preferably approximately 12.7 mm. It should however be understood that the thread of the braided filaments 34 could have another value without departing from the scope of the present invention.

In one embodiment of the invention, the filaments 34 are braided on conventional braider-carriers which travel around the perimeter of a braider deck to result in a tubular body 16 with the filaments 34 crossing over each other on the surface of the body 16 in a so-called criss-cross pattern. It should, however, be understood that other filament patterns such as a spirals pattern or the like could be used without departing from the scope of the present invention.

It is within the scope of the invention to impregnate the body 16 with or otherwise apply thereto one or more medical surgically useful substances, for example, a substance

which accelerates or beneficially modifies the healing process when the suture is applied to a wound or surgical site. The therapeutic agent can be chosen for its osteogenic promoting capability, its capability for promoting wound repair and/or tissue growth, its anti-microbial properties or for any other suitable indication. Anti-microbial agents such as broad-spectrum antibiotics which are solely released into the tissue can be applied in this manner to aid in combatting clinical and sub-clinical infections in a surgical or trauma wound site.

To promote wounds repair and/or tissue growth, one of more biologically active materials known to achieve either or both of these objectives can be applied to the body 16. In the specific context of promoting the fusion of two sternal halves, the body 16 could be designed to release in or around the sternum an osteogenic factor and/or an angiogenic factor. For example, the body 16 could diffuse or otherwise distribute factors such as HGF, VEGF, BMP, PDGF, aHGF, bHGF, TGF alpha, TGF beta, other cytokines or genes.

Furthermore, the body 16 could be designed to release the osteogenic factor and/or angiogenic factor in a controlled manner such as a slow release or according to a predetermined modulated release pattern.

Application of the compositions to the body 16 can be carried out in any number of ways. For example, the body 16 can be submerged in a composition until at least a wound healing enhancing amount of the composition is retained thereby. Alternatively, these healing compositions and solutions can be applied by spraying, brushing, wiping or the like on the surface of the body 16 such that the latter will receive and retain at least an effective amount of the composition. Yet, another procedure which can be used to apply the composition involves kneading the body 16 in a package containing an effective amount of the composition such that intimate contact between the body 16 and the composition will be achieved.

In accordance with the present invention, there is also provided a method for binding biological tissues together. The method includes

selecting a suitable binding component comprising an elongated body defining a body longitudinal axis, the body being made, at least in part, of a shape memory material; the body being configured and sized so as to be both substantially flexible and substantially compressible in a direction substantially perpendicular to the longitudinal axis

- positioning the binding component in a binding configuration wherein the biological tissues are in an opposite contacting relationship relative to each other, and
- inducing a prestrain into at least part of the binding component

Preferably, the prestrain is such that the corresponding applied stress has a value of between σ_{AM} and σ_{FM}. By inducing a precharge or prestrain of a magnitude between σ_{AM} and σ_{FM} appreciable deformation reserve is provided which, in turn, contributes to maintaining a relatively important residual force at the interface between the two sternum halves. In the event of a surcharge, the greater elasticity of the martensite limits opening of the sternum junction. In the event of sternum deterioration, the transformation plateau offers a reserve preserving the strain in the component 10 (up to 6% with a NiTi alloy).

Hence, as expected with the use of shape memory materials, the split sternum experiences continuous, substantially constant, pressure as the components 10 attempts to contract in a shorter length along the hysteresis stress-strain curve associated with such materials. Also, as expected with such materials, not only do the components 10 advantageously apply a substantially constant compressive force across tissue boundary but they are also able to accommodate some expansion.

The components 10 protectively control the maximum force imparted thereby on tissue in intimate contact therewith. The components 10 stretch at a known or programmable force level and are then capable of returning to their pre-stretched length while generating a constant force. The ability of the components to allow a limited expansion

force moderates local forces in the tissue around the binding device, decreasing the likelihood of damaging or tearing the tissue.

The use of Nitinol not only provides interesting mechanical properties but also substantially reduces the risks of creating artefacts or other types of interference during medical imaging. Indeed, Nitinol has a much lesser potential to disrupt the images generated in a computerized axial tomography or magnetic resonance imaging scan of the chest of the patient than, for example, conventional stainless steel sternal wires. The potential to disrupt medical imaging could be even further reduced, for example in situations wherein the body is made with a shape memory polymer or a composite mixture of shape memory alloy and a shape memory polymer.

Validation of the invention was performed in three steps. In accordance with the first step, a unidimensional finite element model was conceived. The model simulated the closure of a sternum by analogy with that of a bolted joint. The model demonstrated that a sternum closure system using shape memory materials provided a residual force greater or equal to that of a standard number 5 steel wire. Accordingly, following a surcharge, the force at the interface between the two sternum halves is for the most part recuperated when a sternum closing system with shape memory materials is used. Furthermore, the rigidity of the system following opening of the sternum and the external force which causes opening of the sternum are both comparable to that of a steel cable.

According to a second step, an empirical model was generated in order to predict the behaviour of braided NiTi alloys using braiding parameters such as the number of filaments and the thread or longitudinal advancement per turn of the braided structure. The interior diameter of the hollow tubular braided structure was defined at 3 mm. The model allows for determination of specific parameters that will be optimized for a given sternum. Although the model incorporates a margin of error substantially in the range of 30%, it nevertheless allows for some degree of parameterization.

In accordance with a third step, laboratory tests were performed using a sternum simulator in order to compare the proposed NiTi structure with a standard stainless steel cable. These tests have demonstrated that the proposed NiTi closure system retains a residual charge greater than that of steel cables, regardless of the type of positioning (peri-sternal or trans-sternal), the density of polyurethane used or the type of loading (incremental or fatigue). Details of the validation procedure along with additional details concerning the proposed binding component or closure system are provided hereinbelow.

Example 1

As seen from Figure 7, the superelastic behaviour of the shape memory alloy (SMA) allows a non-zero zero force to be applied to the sternum even though the width of the sternum tends to decrease as a result of the nature of the healing process. This decrease in the width of the sternum is represented by portions A-B-C of the stress-strain relationship illustrated in Figure 7. In addition, SMA benefit from the dynamic interlaminas phenomenon [9], and manifest significant hardening under external impulses (for example coughing), as seen in the C-D portion of the stress-strain curve illustrated in Figure 7, thus providing a quasi-constant pressure onto the sternum once a predetermined load has been reached, as seen from the D-E portion of the curve of Figure 7. This quasi constant pressure is defined by the height of the upper plateau of the superelastic loop. Once the disruption is over, the force applied by the closure system to the sternum returns to its initial level on the lower plateau, as illustrated in the E-F-C portion of the stress-strain curve.

Most researchers use the rigidity of a closure system as an optimization parameter, the greater the rigidity, the better the closure system. However, the rigidity of the closure system does not necessarily reflect its capacity to maintain the compression of the sternal halves either during post-operative events (for example coughing, deep breathing, sudden movement, etc.) or after the disruption is over.

In fact, it has been determined in several studies (10;11) that the sternum opens before the application of the maximum force that can be supported by the closure system, irrespective of the type of system used. A reason for this resides in the fact that the as the closure system of a given geometry becomes stiffer, a larger part of substantial stresses brought on by post-operative events such as coughing, is transferred to the sternum and can result in its local depression and therefore in the sternum opening under applied forces. Once the disruption is over, any permanent depression will result in a loss of compression forces at the interface between the two halves of the sternum, and consequently, in a decrease in the stability of the bond. It should be mentioned that the capacity of closure systems to reapply compression on the sternum after removing the load is not evaluated in all the aforementioned studies.

In view of the above, the following experiments have been performed. Given that compression, unlike a static fixation, is a dynamic process since it must be maintained during all dimensional redefinitions occurring in the sternum halves to be bonded, two comparison parameters for closure devices have been investigated: (1) the minimum force needed to open the bond (opening force to), and (2) the compressive force reapplied by the closure system once the external disruption is over (residual force fr). In the context of those assessments, closure systems using braided superelastic cables and those using conventional steel wires have been compared with the help of two complementary studies, the first being numerical and the other being experimental. A goal of the first study, which does not take into account the geometric differences between the two systems, is to evaluate the capacity of a superelastic material to accommodate a large proportion of the force exerted by the closure system on the sternum as a result of an external disruption. The second study includes the comparative experimental testing of two closure systems under two different modes of loading: single impulse (initiating coughing or sudden movement of the patient) or repeated (deep breathing).

Numerical Study

Finite elements analysis has been used to evaluate whether SMA allow the maintenance of residual forces greater than conventional materials. The influence of the geometry of the closure system has not been assessed in this portion of the study and the thoracic system (cage and sternum closure suture) has been considerably simplified. The following assumptions have been made:

1) The effect of the external disruption of the sternum is modeled by the simple forces applied at the contact points of the ribs [4].

2) Since the sternum is sufficiently long, all the wires of the closure system support an equal fraction of the force applied to the sternum [4].

3) No bone is considered to be formed between the two halves of the sternum (osteogenese has not begun).

Description of the model

Given its symmetric nature (force and geometry), only one half of the closure system is represented in the model, as seen in Figure 8. The components of the closure and sternum system have been simulated by a series of springs: the closure system has been represented by a spring in tension, while the sternum has been represented by two springs in compression.

The replacement of the sternum by two springs in compression representing the core and the surface layer of the sternum models the interaction between the two halves of the sternum as well as that of the sternum with the closure system. The core spring offers resistance in compression – and not in tension – thus reflecting the absence of a bond between the two halves of the sternum. This spring represents the volume of the sternum that does not undergo any permanent deformation, but stores a part of the energy resulting from the installation of the closure system in compression. The surface layer spring accepts plastic deformations, and thus simulates the deterioration of the sternum under the action of the closure system. The external force Fe is applied at the interface between the two springs representing the sternum.

Finite elements and corresponding material laws

The finite elements model (FEM) has been built with the help of ANSYS 8.0 software by using three types of elements [12]. The SOLID185 finite element has been used to model both superelastic and steel closure systems to represent the superelastic behaviour of the braided tube. The SMA material law has been applied while the BISO material law has been used to simulate the bilinear elastoplastic behaviour of the steel wire. A TS finite element with the BISO material law was representing the surface of the sternum with elastoplastic behaviour while a LINK10 finite element with a Linear Elastic material law, which provides resistance in compression, but not in tension, has simulated the sternum core.

The SMA material law (Table 1) parameters have been obtained from tensile testing up to 8% of strain of a Ti-50.8at.% Ni wire with a diameter of 0.71 mm. The corresponding stress-strain curve is illustrated in Figure 9A.

The BISO material law parameters for steel (Table 2) has been determined from the tensile testing of a N°5 Ethicon suture wire (Somerville, NJ, USA) with a diameter of 0.79 mm. The corresponding stress-strain curve is illustrated in Figure 9B.

The bone depression of the sternum under the contraction of the closing system has been modeled using data obtained with polyurethane sternum simulators (SawBones, Vashon, WA, USA). Two densities of the sternum simulators representes two limit cases defined by Hall et al. [13]: a polyurethane with a 0.24 g/cm^3 density representing a 'weak' sternum while a polyurethane with a 0.48 g/cm^3 density representes a "strong" sternum.

The material law parameters for the BISO sternum surface layer, shown in Table 3, were obtained from the indentation testing of a 0.8 mm thick steel plate into a polyurethane block that was 12.5 mm thick and 10 mm wide. The rigidity of the sternum core was set to 20 times that of the surface layer in order to avoid any significant

modification of the overall sternum rigidity resulting from the surface layer depression. The half width of the sternum was fixed at 25 mm, and the thickness of the surface layer was set at 5 mm. It was assumed that the latter completely absorbs the closure system penetration.

Calculation algorithm

A non-limiting objective pursued with the numerical model was to compare the opening forces and residual forces as provided by SMA and steel sternum sutures. It was assumed that the rigidity of the SMA closure system could be varied by modifying its relative stiffness between 0.05 and 0.35, while the relative stiffness of the steel wire remained constant and equal to 1 (the rigidity of the SMA sternal closure system is in fact adjustable through the modification of its geometry and number of filaments [14]).

The initial force applied during the installation of the system was set at Fi=30 N for a 0.24 g/cm^3 sternum and at Fi=350 N, for a 0.48 g/cm3 sternum since these values were close to the resistance limits for the penetration of the sternum simulators. The force resulting from external disruption varied between Fe=0 and 150 N for the low-density polyurethane and between Fe=0 and 600 N for the high-density polyurethane.

The algorithm of the numerical study could be summarized as follows (see Table 4, for numerical values):

(1) Density is selected for the sternum simulator;

(2) Material is chosen for the closure suture. If it is SMA, its relative stiffness is given an initial 0.05 value, and if it is steel, its relative stiffness is set at 1;

(3) Installation force (Fi) is applied to the closure system;

(4) External disruption is simulated by applying an initial external force Fe; if this force causes the opening of the sternum, the opening force No is recorded;

(5) External force is removed and residual force Fr is recorded;

(6) If Fe > 0, the external force is incremented and steps (4)–(5) are repeated until Fe=0 or maximum external force is allowed.

(7) The cross sectional area of the SMA suture is incremented and steps (3)–(7) are repeated.

Table 4 summarizes the Finite Element Model procedure that were investigated.

Results of the numerical study

The results of the numerical study for the 0.24 g/cm^3 sternum are summarized in Table 5. As an example, Figure 10 illustrates that an SMA suture with an equivalent diameter of 0.22 mm maintained a non-zero residual force at the sternum interface ($f_r \geq 0$) after an external force F_e, which is 80% greater than that supported by a Ø0.76 mm steel wire (45 N as opposed to 80 N). However, this was at the expense of a larger sternum opening: after an identical external force of 80 N, the SMA suture allowed a sternum opening of 1.1 mm, while the steel suture allowed an opening of 0.8 mm. Also, the minimum sternum opening force, f_o, is approximately 70 N for all sternum closure devices, which is comparable to the experimentally obtained data [4].

For the 0.49 g/cm^3 sternum model, SMA sutures allowed a residual force to be maintained for external forces F_e greater than 600 N, which was more than twice the force of a severe coughing fit [10]. In comparison, the residual force provided by steel sutures became zero after an external force of 420 N.

Experimental Study

To consider the geometry of the SMA sternum closure system, a series of experimental tests were undertaken.

Description of the testing bench

Figure 11 shows the outline of the testing bench used. Two identical closure systems (7) were installed simultaneously on polyurethane blocks (2) simulating the sternum.

The installation force was applied with the help of two adjustable sliding clamps (3). Two LC703-100 load cells (5) (Omega Stamford, CT, USA) installed on each extremity of the testing frame (1) allowed the force at the sternum interface to be measured. An Instron ELF 5200 series testing machine (4) was used to apply external force. LabView 8.0 (National Instruments Corp., Austin, TX, USA) data acquisition systems registered the real time displacement of the testing machine's piston as well as the forces measured by the load cells.

Components used

A comparison was made between two closure devices: (1) Ø0.75 mm N° 5 Ethicon steel wire and (2) mm S/A braided 12.5 mm pitch tube made of 24 Ø0.1 mm filaments of Ni-Ti-Cr alloy.

The 25x10x80 mm polyurethane blocks with a density of 0.24 and 0.48 g/cm^3 were used to simulate sternum bones. One of the sides of the samples used for a parasternal installation (Figure 11, right) was rounded to simulate the edge of the sternum, and those used for the transsternal installation (Figure 11, left) featured 2.4 mm diameter holes pierced 10 mm from the symmetric plane in order to allow the threading of the closure device.

The force-displacement diagrams of the sternum simulators (incremental cyclic testing) and of the two types of sternum sutures (tensile testing) are shown in Figure 12.

Experimental procedure

Testing modalities

The experiment was planned to allow two closure systems to be compared under different exploitation conditions: severe coughing (single impulse loading) or deep breathing (cyclical loading), in the case of parasternal or transsternal installations, and for two sternum densities (0.24 and 0.48 g/cm^3) – as seen in Table 6.

The following two-step procedure was performed.

1. Application of the installation (initial) force Fi

The initial force Fi applied to the median sternum closure was a function of the density of the polyurethane sternum simulator. The higher the density, the higher the initial force that can be applied. The initial force for the 0.24 g/cm^3 sternum was set at the same level as for the numerical study: 60 N (see Table 4). For the 0.48 g/cm^3 sternum, it was set at 220 N.

2. Application of the external force Fe

The Single Impulse loading mode simulated coughing or sudden movement and consisted in a series of loading-unloading cycles with incrementally increased amplitude. Each cycle took 10 seconds, and a 15-second dwell time at zero force was respected prior to each subsequent cycle. At each cycle, the force was increased by 25 N up to a maximum value allowed, which was 125 N for the 0.24 g/cm^3 sternum and 445 N for the 0.48 g/cm^3 sternum (the latter value was limited by the capabilities of the testing machine). The measurement of the residual force fr was performed prior to each force increment.

Cyclic loading simulated deep breathing and consisted in 500 cycles of a sinusoidal force varied with a 0.5 Hz frequency between 0 and 60 N (0.24 g/cm^3 sternum) and 0 and 200 N (0.48 g/cm^3 sternum). The measurement of the residual force was completed after the 500th cycle at zero load.

Results

The StatGraphics software (StatPoint Inc., Herndon, VA) was used to analyse the results obtained [15]. The outcome variable was the relative residual force R=fr/Fi. Figure 15 demonstrates that the use of the SMA suture compared to steel suture allowed an average gain of 30% in the relative residual force value as compared to using a steel suture. The results for the other statistically significant ($p \leq 0.05$) input variables show

that the peristernal installation guarantees higher residual forces than the transsternal installation, and that a large single impulse force causes more damage than light repetitive forces. The effect of the sternum model density variation was not significant.

Discussion

The experimental study shows the combined effect of the superelastic behaviour and of the tubular geometry of the SMA to be taken into account. In the context of this study, a unique 24-filament SMA braided tube with an inside diameter of 3 mm was tested with sternum simulators having two limit densities.

For the 0.24 g/cm^3 sternum, the 24-filament SMA suture was a bit too rigid. It is therefore likely that the increased contact area between the sternum and closure system was mostly responsible for the 30% gain in residual force when compared to a steel suture. For the 0.48 g/cm^3 sternum, the 24-filament SMA suture was a bit too compliant. Nevertheless, the advantage of using a superelastic suture led to a similar 30% gain in residual force as compared to a steel suture. In fact, the 24-filament SMA suture would have demonstrated maximum efficiency for an intermediate density 0.32 g/cm^3.

To reduce the risk of sternum breakage, a median sternotomy closure using a superelastic tubular braid was proposed. The numerical model allowed the net benefit of a binding component in the form of an SMA suture to be demonstrated against the performance of a N°5 Ethicon steel suture. It was experimentally proven that the SMA suture preserved compression at the sternum interface when an external distraction occurs, at forces 30 to 60 % greater than those endured by the N° 5 Ethicon suture regardless of the installation technique used (peristernal or transsternal), the type of external force applied (single impulse or repetitive) and the sternum density.

The above suggests a method for selecting a force-displacement characteristic of a binding component and for manufacturing and using the same. This method is

illustrated with the help Figure 14, which shows an example of a suitable stress-strain curve usable for determining parameters of the binding component. The person skilled in the art will easily appreciate that while the present document illustrates by way of example a method for manufacturing and using a binding component for closing a sternum, similar methods are usable to manufacture devices that bind together any other suitable biologic tissues

The method includes selecting a predetermined force-displacement relationship for the structures to bind. For example, this force-displacement relationship is a force-displacement corresponding to a "cut-through" test. This force-displacement relationship may be selected from known force-displacement relationships. For example, if the biological tissues to bind are bones, the force-displacement relationship may be obtained experimentally by a cut-through testing of a bone simulator (for example solid polyurethane biomechanical test blocks) by an indenter taking the form of a wire or of a thin-plate shape. In other examples, the force-displacement curves may be modelled from the density, dimensions and types of bones to bind. The density of the bones may be estimated for a given patient through a CT bone scan or any other suitable imaging modality. In another example, a predetermined bone density is assumed

It should be noted that it is not necessary to measure a bone density to manufacture a binding component in accordance with the claimed invention. Indeed, various binding components corresponding to various predetermined bone densities may be manufactured. Then, when the binding component is installed, a specific binding component is selected for a specific patient according to a selection criterion. An example of a selection criterion includes selecting a binding component that has been manufactured assuming that a bone density of the bones to bind is about equal to a bone density measured in the patient

For a sternum, the bone density is such that the sternum is typically modelled using a solid rigid polyurethane foam having a density of from about 0.24 g/cm³ to about

0.43g/cm^3. The lower end of this range corresponds generally to the sternum of patients suffering from osteoporosis. In some embodiments of the invention, the bone density of the patient is not known. In those cases, the assumption of a low bone density, for example corresponding to a foam having a density of 0.24 g/cm^3, may be advantageous to reduce risks of bone fracture.

The curve identified as (1) sternum in Figure 14 illustrates an example of a model of a cut-through displacement-force relationship for a sternum. This model assumes a bilinear relationship wherein the sternum deforms linearly for small displacements. Then, after the yield limit of the sternum has been reached, the sternum deforms irreversibly and linearly with displacement with a lower resistance to deformation.

As mentioned hereinabove, the force exerted on the binding component by the biological tissues to bind typically diminishes after installation of the binding component. Therefore, to preserve compression between biological structures to bind, it is desirable to exert a relatively large force on the biological tissues when installing the binding component. To that effect, the binding component is constrained at a level corresponding to a predetermined prestrain force. For example, the predetermined prestrain force is from about 80 to about 95% of the yield limit of a sternum. In a specific example of implementation, the predetermined prestrain force is about 90% of the yield limit of the sternum.

To improve the capability of the suture to support post-operative events, such as the patient coughing, with reduced risks of failure, the minimum suture resistance, or in other words the ultimate tensile strength, is achieved at a predetermined level. For example, in the case of a sternum, this predetermined level is set to between about 200N and about 300N, and more specifically to about 250 N, as determined for a severe coughing fit [10].

Parameters of the binding device that maximize the residual force remaining after the post-operative event is finished are determined. For example, the following variables

may be varied: number of filaments, pitch, inside diameter, pitch or helix angle and materials included in the binding device, among others. More details regarding these parameters are found in reference [14]. This maximization is performed, for example, through an iterative modelling process. Methods for optimizing material properties and structures are well-known in the art and will therefore not be described in further details herein.

In some embodiments of the invention, the maximization of the residual force f_r is performed assuming that the displacement force relationship is similar to the relationship illustrated by the parallelogram-shaped hysteresis curve identified as "(4) SMA braid" in Figure 14. As shown from this Figure, this relationship includes upper and lower substantially linear plateaus substantially parallel to each other that are connected through straight line segments at both ends thereof. In a specific example of implementation, the residual force f_r is maximized by selecting the material composition, dimensions, configuration of the binding component or of its body so that the difference in force between the lower plateau of the force-displacement relationship of the binding component and the upper plateau of the force-displacement relationship of the binding component is minimal.

The maximization of f_r may be performed while satisfying the following criterion: the knee point, or inflection point, between the upper plateau of the SMA curve and the elastic slope of a stress-induced martensite phase should be substantially coincident with the point representing the pretension in the binding device during installation.

All the constraints described hereinabove have, when simultaneously satisfied, a synergetic effect and provide binding components that have unexpected characteristics. However, in some embodiments of the invention, only some of these constraints are satisfied in specific binding components.

A specific example of a binding component that has been found to be suitable to bind two halves of a sternum includes 24 filaments of a Ni-Ti-Cr alloy wire having a diameter

of 0.075 mm. The wires are braided with a pitch of about 12.5 mm to produce a substantially tubular structure having a diameter of about 3 mm. While parameters describing this binding component have been found using the above-described method, the reader skilled in the art will readily appreciate that this method should not be used to limit the scope of the claimed invention in apparatus claims.

The above described example also suggests that a difference in force between the lower plateau of the force-displacement relationship of a binding component in accordance with the invention and the upper plateau of the force-displacement relationship of the binding component of from about 10 percent to about 30 percent of the force to which the prestrain corresponds is achievable.

From the results relating to the 0.24 g/cm^3 foam, which models a typical osteoporotic sternum, a suitable value of a prestrain to which the body of the binding component may be prestrained is a prestrain corresponding to that generated by a force having a magnitude of from about 55-65 N, or of about 60 N. The use of this prestrain is advantageous in binding components for binding osteoporotic sternums as it helps in minimizing the risks of fractures of the sternum by the binding component.

Although the present invention has been described hereinabove by way of preferred embodiments thereof, it can be modified without departing from the spirit, scope and nature of the subject invention, as defined in the appended claims.

Table 1: SMA (ANSYS) material law used to model a superelastic binding component

Param	Unit	Value
Ex	MPa	32000
[illegible]	mA/s	0.007
σMs	MPa	535
σMf	MPa	385
σAs	MPa	200
σAf	MPa	150

Table 2: BISO (ANSYS) material law used to model a N°5 Ethicon steel binding component

Param.	Unit	Value
Ex	MPa	50000
Etan	MPa	425
σy	MPa	1300

Table 3: BISO material law for the surface layer and Linear Elastic material law (ANSYS), for a modelled sternum core.

Mat law		Surface layer BISO		Core Linear Elastic	
Param.	Unit	0.24*	0.49*	0.24*	0.49*
Ex	MPa	735	5200	14 720	104 000
E_{tan}	MPa	140	1050		
σ_y	MPa	67	400		

*Polyurethane density (g/cm3)

Table 4: Sequence of FEM procedures followed in numerical modelling of a binding component in accordance with an embodiment of the present invention.

Materials		F (N)	Suture relative stiffness: increment	externs force F_a range: increment (N)
Suture	Sternum density (g/cm^3)			
Steel	0.24	50	1	[0-150]; 5
	0.45	250		[0-600]; 20
SMA	0.24	50	[0.05 0.35], 0.05	[0 150]; 5
	0.45	250	0.5-1.3]; 0.1	[0-600]; 20

Table 5: Results of a numerical model modelling the interaction of a binding device with a foam model of a sternum having a density of 0.24 g/cm³.

Wire type	Sutures relative stiffness	Equivalent diameter (mm)	External force F_A corresponding to A–B (N)
SMA	0.05	0.16	100 (wire break)
	0.10	0.22	145
	0.15	0.27	135
	0.20	0.32	95
Steel (n°5)	1.00	0.78	90

Table 6 Experimental testing modalities for a closure system.

Variable	Modalities	
Closure system	Steel suture	SMA suture
Polyurethane density	0.24 g/cm³	0.46 g/cm³
Threading	Transsternal	Peristernal
Loading	Single impulse	Cyclic

References

[1] Heart disease and stroke statistics - 2005 Update. (2005). Dallas: American Heart Association.

[2] Milton, H. (1987). Mediastinal surgery. Lancet, 1, 872-875.

[3] Rosinski, E., Daugherty, H. K., & Cook, J. W. (1977). The prevention and treatment of sternum separation following open-heart surgery. The Journal of Thoracic and Cardiovascular Surgery, 73(2), 267-269.

[4] Gesha, A. R., Gauci, M., Yang, J., Saleh, M., Kay, P. H., & Cooper, G. J. (2001). Fatigue testing median sternotomy closures. European Journal of Cardio-thoracic Surgery, 19(3), 249-253.

[5] Soroff, H. S., Hartman, A. R., Pak, F., Sosvary, D. H., & Pollack, G. B. (1966). Improved sternal closure using steel bands. Early experience with three-year follow-up. Annals of Thoracic Surgery, 6(4), 1172-1176.

[6] Comtesse, J. M., Carne, J. M., Soula, P., Tricom, J. L., & Cerino, A. (1990). Formation des sternotomies a l'aide des agrafes de Cotre. Annales De Chirurgie, 44(2), 178-183.

[7] Sargent, L. A., Seyfer, A. E., Hollinger, L., Hinson, R. M., & Graeber, G. M. (1991). The healing sternum: a comparison of osseous healing with wire versus rigid fixation. The Annals of Thoracic Surgery, 52(2), 480-484.

[8] Losanoff, J. E., Richman, B. W., & Jones, J. W. (2002). Disruption and infection of median sternotomy: a comprehensive review. European Journal of Cardio-Thoracic Surgery, 21(5), 931-939.

[9] Duerig, T., Pelton, A., & Stockel, D. (1997, March). Superelastic Nitinol for Medical Devices. Medical Plastics and Biomaterial Magazine MPV archive.

[10] Gesha, A. R., Yang, J., Kay, P. H., Saleh, M., & Cooper, G. J. (1999). A biomechanical study of median sternotomy closure techniques. European Journal of Cardio-Thoracic Surgery, 15(3), 365-369.

[11] McGregor, W. E., Trumble, D. R., & Magovern, J. A. (1998). Mechanical analysis of midline sternotomy wound closure. The Journal of Thoracic and Cardiovascular Surgery, 117(6), 1144-1151.

[12] ANSYS. (2003). ANSYS (Version 8.0) [Finite elements]. Canonsburg, Pa. US.

[13] Hale, J. F., Anderson, D. D., & Johnson, G. A. (1999, October 21-23). A polyurethane foam model for characterizing suture pull-through properties in bone. Paper presented at the 25rd Annual Meeting of the American Society of Biomechanics, University of Pittsburgh.

[14] Kent, Y. (2004). Design and Modelisation of a Sternum Closure System (in French). Master Thesis, École de technologie supérieure, Montreal.

[15] Montgomery, D. C. (1998). Design and analysis of experiments (4th edition ed.). New York.

We claim:

1. A binding component for binding together a pair of biological tissues, said binding component comprising:

an elongated body defining a body longitudinal axis;

said body being made, at least in part, of a shape memory material;

said body being configured and sized so as to be both substantially flexible and substantially compressible in a direction substantially perpendicular to said longitudinal axis.

2. A binding component as recited in claim 1 wherein said body has a substantially uniform moment of inertia of bending in all directions.

3. A binding component as recited in claim 2 wherein said body has a substantially disc-shaped cross-sectional configuration when radially uncompressed.

4. A binding component as recited in claim 2 wherein said body has a substantially hollow tubular configuration.

5. A binding component as recited in claim 4 wherein said body has a substantially annular cross-sectional configuration when radially uncompressed.

6. A binding component as recited in claim 5 wherein said body is radially compressible towards a compressed configuration wherein said body has a substantially ovaloid cross section.

7. A binding component as recited in claim 6 wherein said ovaloid configuration defines an oval long axis and an oval short axis, the ratio between said oval long and short axes being approximately between 1 and 3 when said binding component is at least partially bent around a section of a sternum.

8. A binding component as recited in claim 5 wherein said body defines a lumen extending longitudinally therethrough, said body defining a body inner diameter in contact with said lumen and a body outer diameter, said body defining a body thickness between said body inner and outer diameters, said body thickness having a value of approximately between 0.1 and 0.3 mm.

9. A binding component as recited in claim 5 wherein said body defines a lumen extending longitudinally therethrough, said body defining a body inner diameter in contact with said lumen and a body outer diameter, the ratio of said body outer diameter to said body inner diameter having a value of approximately between 1.1 and 1.3.

10. A binding component as recited in claim 5 wherein said body is made of braided filaments of a shape memory material, said shape memory material demonstrating superelastic properties when subjected to temperatures substantially in the range of expected human body temperatures.

11. A binding component as recited in claim 10 wherein said shape memory material is selected from the group consisting of nitinol, other biocompatible shape memory alloys and shape memory polymers.

12. A binding component as recited in claim 10 wherein said body is made up of between 16 and 72 braided filaments.

13. A binding component as recited in claim 12 wherein said body is made up of approximately 24 braided filaments.

14. A binding component as recited in claim 12 wherein the thread of said braided filaments varies between 10 mm and 30 mm.

15. A binding component as recited in claim 14 wherein the thread of said braided filaments is approximately 12.7 mm.

15. A binding component as recited in claim 10 wherein said body is made up of approximately 24 braided filaments, each of said braided filaments has a denier of approximately 5000, and the thread of said braided filaments is approximately 12.7 mm

17. A binding component as recited in claim 10 wherein said filaments cross over each other on the surface of said body in a criss-cross pattern.

16. A method for binding biological tissues together, the biological tissues having a yield limit beyond which the biological tissues are irreversibly deformed, said method including the steps of

- selecting a suitable binding component comprising an elongated body defining a body longitudinal axis; said body being made, at least in part, of a shape memory material; said body being configured and sized so as to be both substantially flexible and substantially incompressible in a direction at least generally perpendicular to said longitudinal axis;
- positioning said binding component in a binding configuration wherein said binding component biases said biological tissues in an opposite contacting relationship relative to each other; and
- inducing a prestrain into at least part of said binding component.

19. A method as recited in claim 18 wherein said prestrain corresponds to that generated by a stress having a magnitude between σ_{ys} and σ_{ult}.

20. A method as recited in claim 19, wherein:

- said binding component is at least in part prestrained with a prestrain causing the generation of a force within an interval of from about 80 percent to about 95 percent of the yield limit after said positioning of said binding component;
- the biological tissues are bones and the binding component has a binding component ultimate tensile strength, said binding component ultimate tensile strength being within the interval of from about 200 N to about 300 N

- said body has a composition, a configuration and dimensions such that an inflection point between an upper plateau of a force-displacement relationship of said binding component and a linear force-displacement relationship representing an elastic deformation of a stress-induced martensite phase in said binding component is substantially coincident with a force and a displacement representative of the prestrain in the binding component; and

- said body has a composition, a configuration and dimensions such that a difference in force between an upper plateau of the force displacement relationship of said binding component and the upper plateau is minimal.

21. A method for manufacturing a binding component, said method comprising:

- braiding filaments of shape-memory material into an elongated body defining a body longitudinal axis;

said body being configured and sized so as to be both substantially flexible and substantially incompressible in a direction substantially perpendicular to said longitudinal axis.

22. A method as recited in claim 21 further comprising the step of treating said body so that said shape memory material demonstrates superelastic properties when subjected to temperatures substantially in the range of expected human body temperatures.

23. A method as recited in claim 21 further comprising the step of:

Subjecting said body to a thermal treatment at a temperature between 200 °C and 700 °C for a period of between 30 minutes and 20 hours.

24. A method as recited in claim 21 further comprising the step of applying to said body at least one therapeutic or prophylactic surgically useful substance.

25. A binding component for binding together a pair of biological tissues, said binding component comprising:

- an elongated body defining a body longitudinal axis

said body being made at least in part of a shape memory material,

- said body being provided with at least one therapeutic or prophylactic surgically useful substance.

26. A binding component as recited in claim 25 wherein said substance is selected from the group including substances providing osteogenic capabilities, substances promoting wound repair and/or tissue growth, and substances having antibiotic properties.

27. A binding component as recited in claim 25 wherein said body is designed to release to or around the stenrum an osteogenic factor and/or an angiogenic factor.

28. A binding component as recited in claim 25 wherein said body allows selective distribution of substances taken from the group including IGF, VEGF, BMP, PDGF, aFGF, bFGF, TGF alpha and TGF beta.

29. A binding component as recited in claim 28, wherein said body is designed to release the osteogenic factor and/or angiogenic factor in a controlled manner.

30. A method for binding biological tissues together, the biological tissues having a yield limit beyond which the biological tissues are irreversibly deformed, said method comprising:

- selecting a suitable binding component comprising an elongated body defining a body longitudinal axis, said body being made at least in part of a shape memory material;

- positioning said binding component in a binding configuration wherein said binding component biases said biological tissues in an opposite contacting relationship relative to each other;

- wherein said binding component is at least in part prestrained with a prestrain causing the generation of a force within an interval of from about 60 percent to about 95 percent of the yield limit after said positioning of said binding component.

31. A method as defined in claim 32 wherein said prestrain causes the generation of a force of about 90 percent of the yield limit after said positioning of said binding component.

32. A method as defined in claim 30, wherein the biological tissues are bones and the binding component has a binding component ultimate tensile strength, said binding component ultimate tensile strength being within the interval of from about 200 N to about 300 N.

33. A method as defined in claim 32 wherein said binding component ultimate tensile strength is about 250 N.

34. A method as defined in claim 30 wherein said prestrain corresponds to that generated by a stress having a magnitude between σ_{op} and σ_M.

35. A method as defined in claim 34, wherein said body has a composition, a configuration and dimensions such that an inflection point between an upper plateau of a force-displacement relationship of said binding component and a linear force-displacement relationship representing an elastic deformation of a stress-induced martensite phase in said binding component is substantially coincident with a force and a displacement representative of the prestrain in the binding component.

36. A method as defined in claim 35, wherein said body has a composition, a configuration and dimensions such that a difference in force between a lower plateau of the force-displacement relationship of said binding component and the upper plateau is minimal.

37. A method as defined in claim 30, wherein:

- the biological tissues are bones and the binding component has a binding component ultimate tensile strength, said binding component ultimate tensile strength being within the interval of from about 200 N to about 300 N;

- said plateau corresponds to that generated by a stress having a magnitude between σ_{ys} and σ_{uts};

said body has a composition, a configuration and dimensions such that an inflection point between an upper plateau of a force displacement relationship of said binding component and a linear force-displacement relationship representing an elastic deformation of a stress induced martensite phase in said binding component is substantially coincident with a force and a displacement representative of the prestrain in the binding component; and

- said body has a composition, a configuration and dimensions such that a difference in force between a lower plateau of the force displacement relationship of said binding component and the upper plateau is minimal.

38. A method as defined in claim 37, wherein said body is configured and sized so as to be both substantially flexible and substantially compressible in a direction substantially perpendicular to said longitudinal axis.

39. A method as defined in claim 38, further comprising measuring the density of the bones and determining the yield limit of the bones using at least in part the measured density of the bones.

40. A method for manufacturing a binding component for binding bones, said method comprising:

- providing filaments of shape-memory material into an elongated body defining a body longitudinal axis;

- said body being configured and sized so as to be both substantially flexible and substantially compressible in a direction substantially perpendicular to said longitudinal axis;

- setting the composition, dimensions and configuration of said body by modeling the bones as a linear elastic material having a yield limit beyond which the bones are irreversibly deformed and modeling the shape-memory material as having a stress strain relationship including an hysteresis and ensuring that:

said binding component has a binding component ultimate tensile strength within the interval of from about 200 N to about 300 N;

- said body is at least in part prestrained with a prestrain corresponds to that generated by a stress having a magnitude between σ_{yc} and σ_{yt}, said prestrain corresponding to that generated by a force having a magnitude within an interval of from about 80 percent to about 85 percent of the yield limit;
- an inflection point between an upper plateau of a force-displacement relationship of said binding component and a linear force-displacement relationship representing an elastic deformation of a stress induced martensite phase in said binding component is substantially coincident with a force and a displacement representative of the prestrain in the binding component; and
- a difference in force between a lower plateau of the force-displacement relationship of said binding component and the upper plateau is minimized.

41. A binding component for binding together a pair of bones, said binding component comprising:

- an elongated body defining a body longitudinal axis

said body having a substantially hollow tubular configuration defining a tube outer diameter

- said body being made of braided filaments of a shape memory material, said shape memory material demonstrating superelastic properties when subjected to temperatures substantially in the range of expected human body temperatures;
- said binding component having a binding component ultimate tensile strength, said binding component ultimate tensile strength being within the interval of from about 200 N to about 300 N,

said body being at least in part prestrained with a prestrain corresponding to that generated by a stress having a magnitude between σ_{yc} and σ_{yt},

- said body having a composition, a configuration and dimensions such that an inflection point between an upper plateau of a force-displacement relationship of said binding component and a linear force-displacement relationship representing an elastic deformation of a stress induced martensite phase in said binding component is substantially coincident with a force and a displacement representative of the prestrain in the body component; and

- said body having a composition, a configuration and dimensions such that a difference in force between a lower plateau of the force-displacement relationship of said binding component and the upper plateau of the force displacement relationship of said binding component is minimal.

42. A binding component as recited in claim 41, wherein a difference in force between the lower plateau of the force-displacement relationship of said binding component and the upper plateau of the force-displacement relationship of said binding component is equal to from about 10 percent to about 20 percent of the force to which the prestrain corresponds.

43. A binding component as recited in claim 41, wherein said body is at least in part prestrained with a prestrain corresponding to that generated by a force having a magnitude of from about 55 N to about 65 N.

44. A binding component as recited in claim 43, wherein said body is at least in part prestrained with a prestrain corresponding to that generated by a force having a magnitude of about 60 N.

45. A binding component as recited in claim 41, wherein said body is made up of approximately 24 braided filaments having a diameter of about 0.075 mm, the thread of said braided filaments being of about 12.5 mm, said tube outer diameter being of about 5 mm.

40. A binding component as recited in claim 41 wherein said shape memory material is selected from the group consisting of Nitinol, other biocompatible shape memory alloys and shape memory polymers.

5

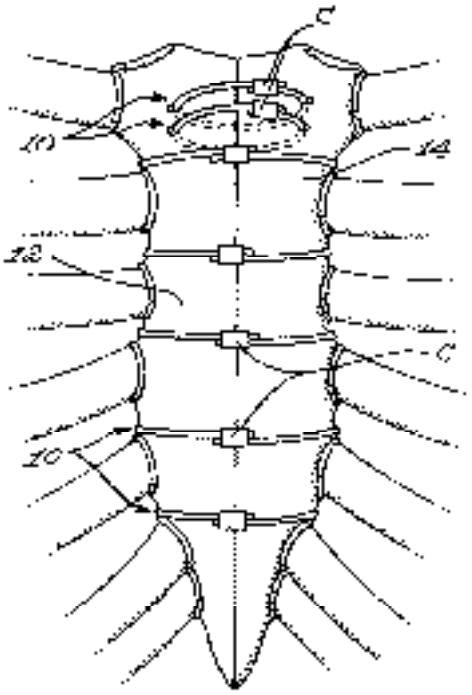

FIG 1

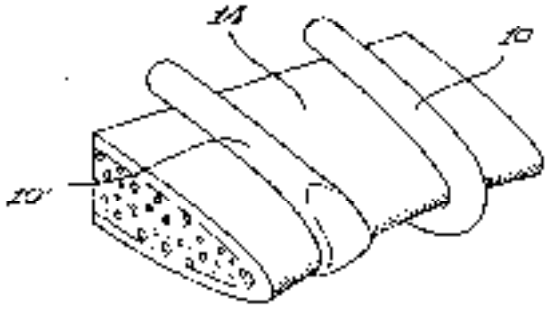

FIG 2

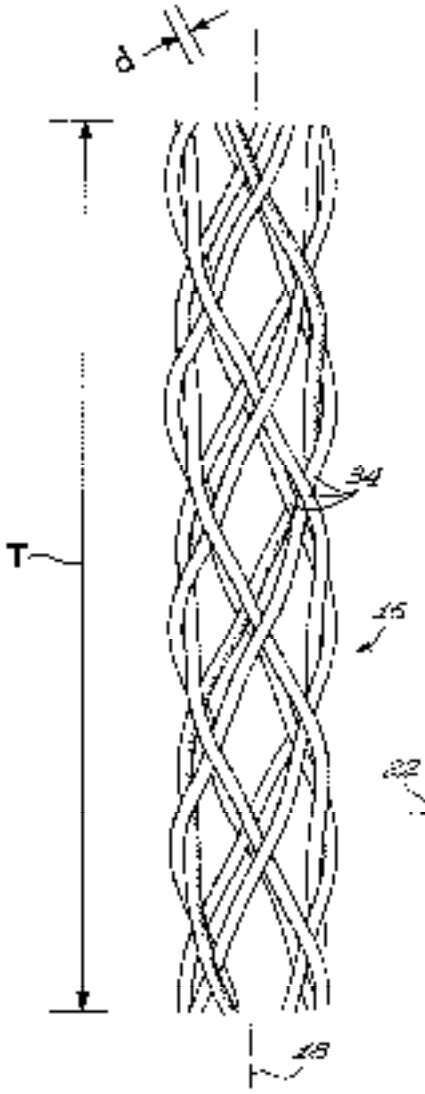

FIG 3

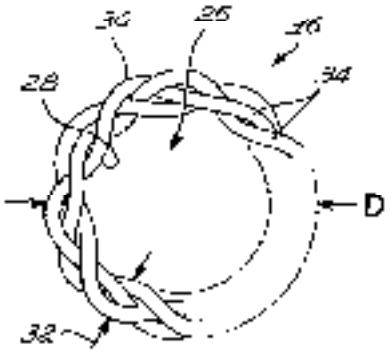

FIG 4

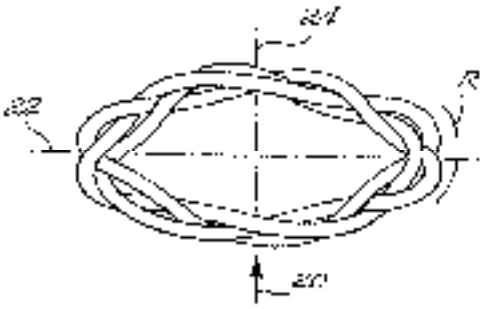

FIG 5

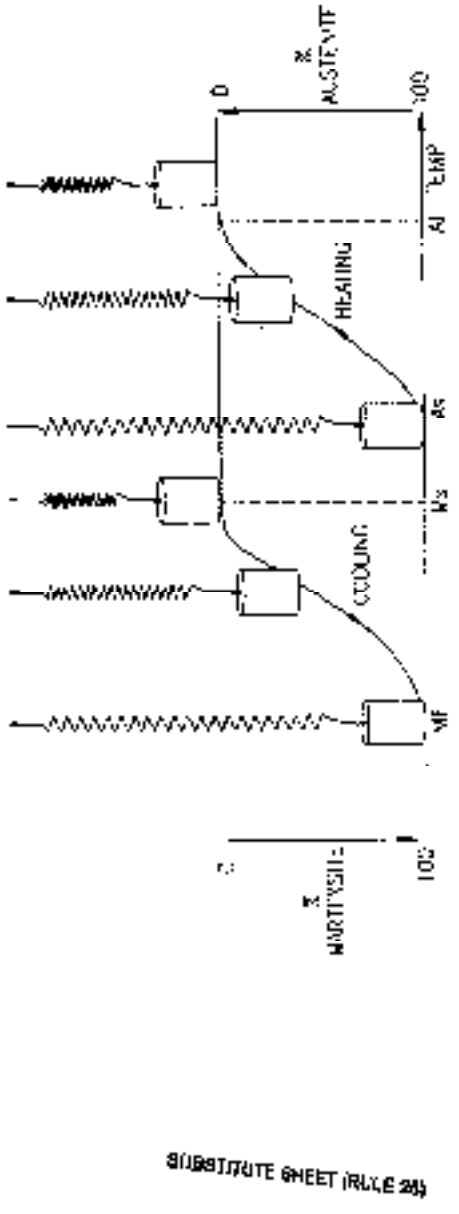

FIG 6A
(PRIOR ART)

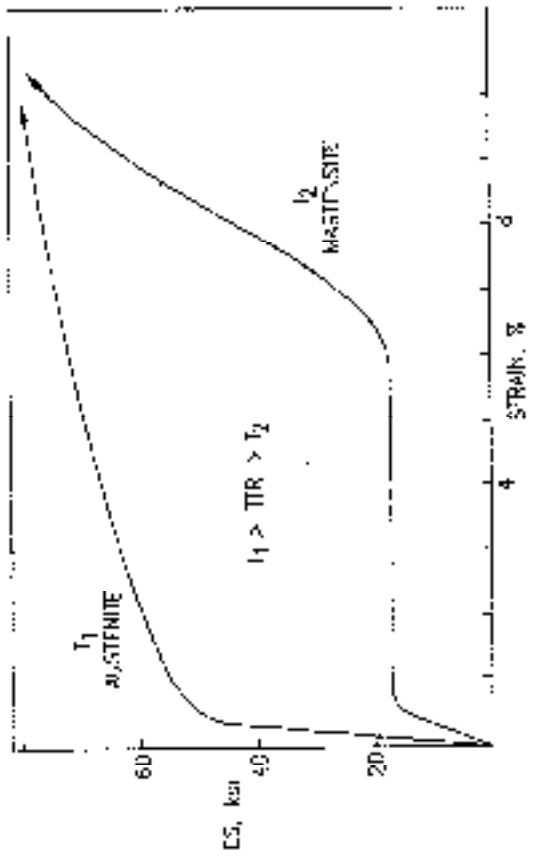

FIG 6B
(PRIOR ART)

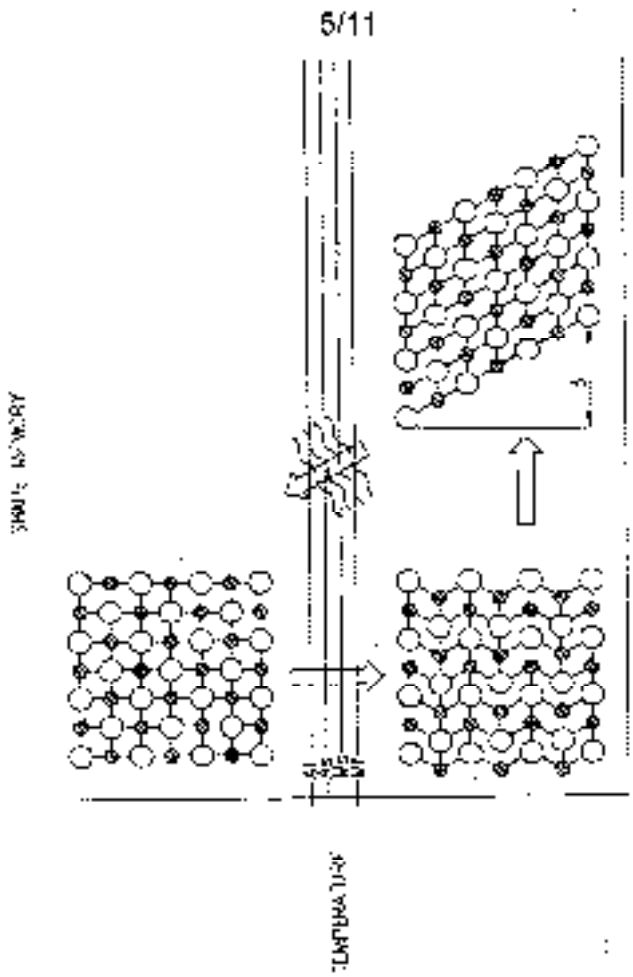

FIG 6C
(PRIOR ART)

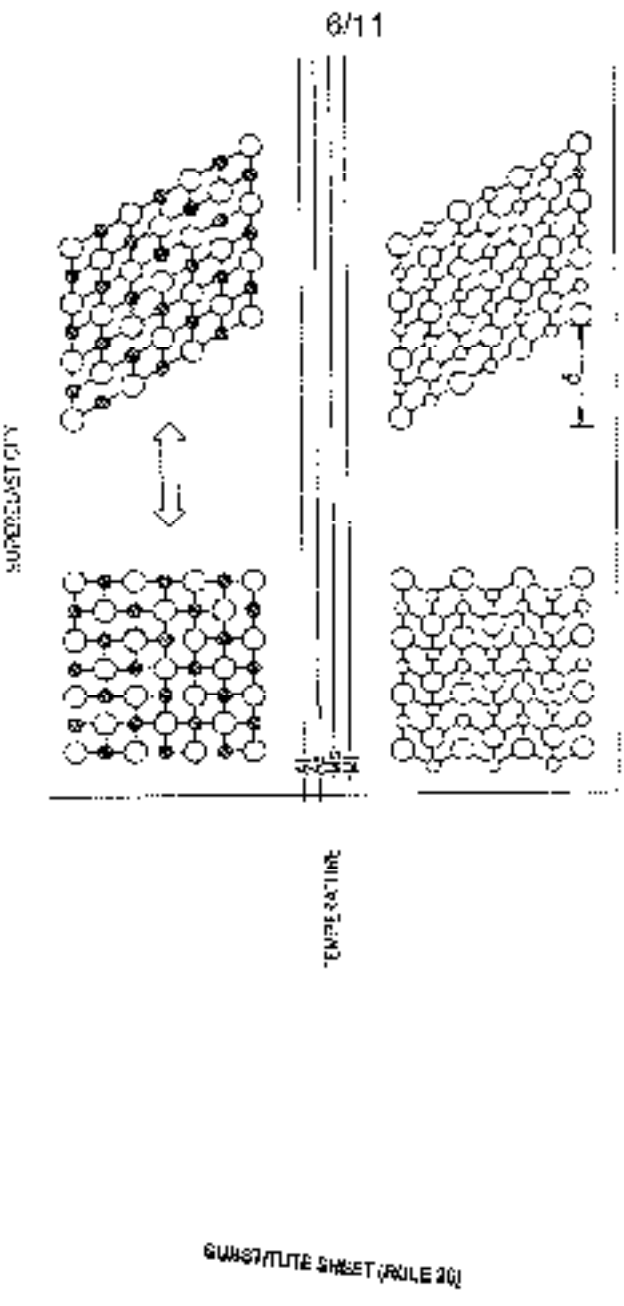

FIG 6D
(PRIOR ART)

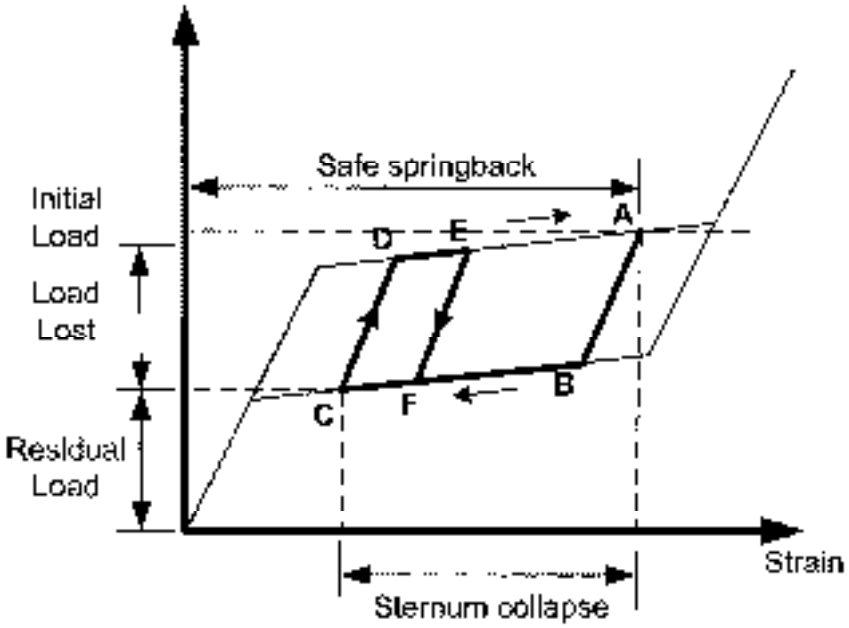
Safe springback
Initial Load
Load Lost
Residual Load
A
B
C
D
E
F
Strain
Sternum collapse

FIG 7

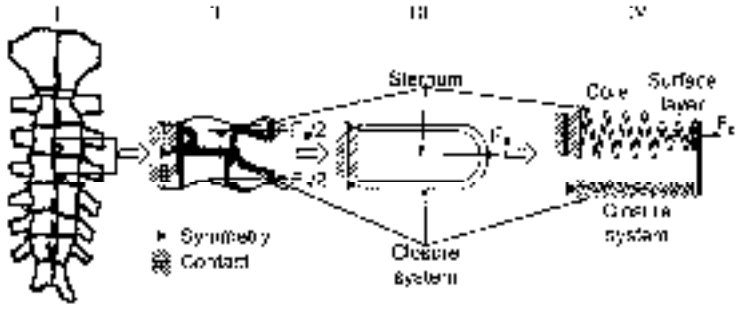

FIG 8

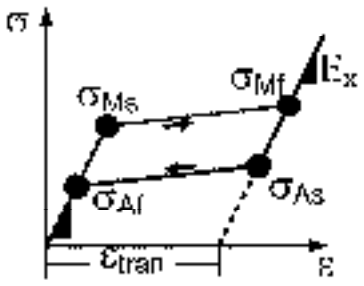

FIG 9A

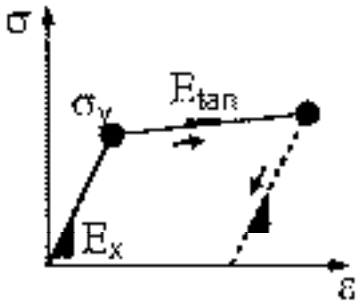

FIG 9B

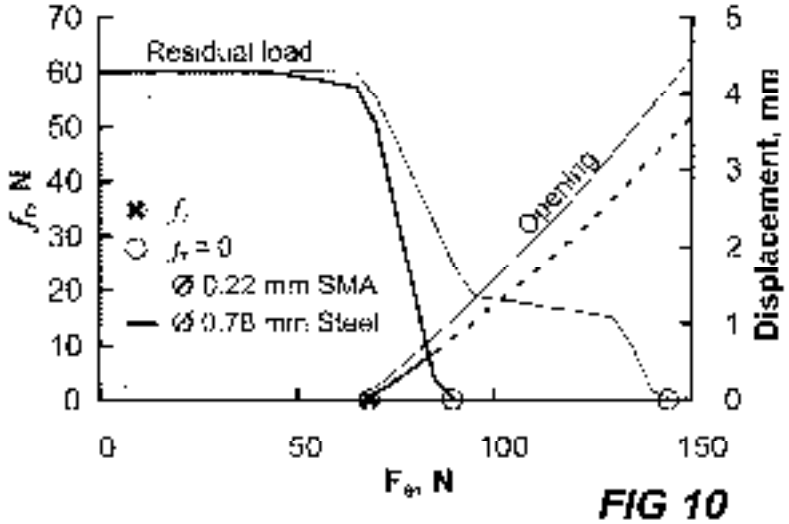
Residual load
Opening
Ø 0.22 mm SMA
Ø 0.78 mm Steel
Displacement, mm
$F_{\theta n}$ N

FIG 10

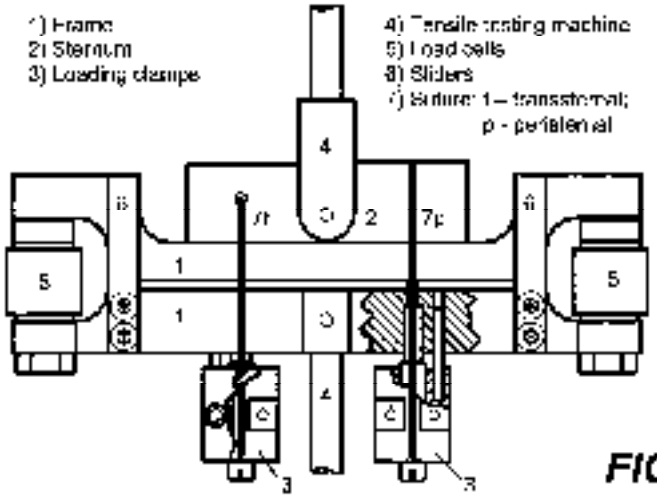
2) Sternum
3) Loading clamps
4) Tensile testing machine
5) Load cells
6) Sliders
1
2
3
4
5
6

FIG 11

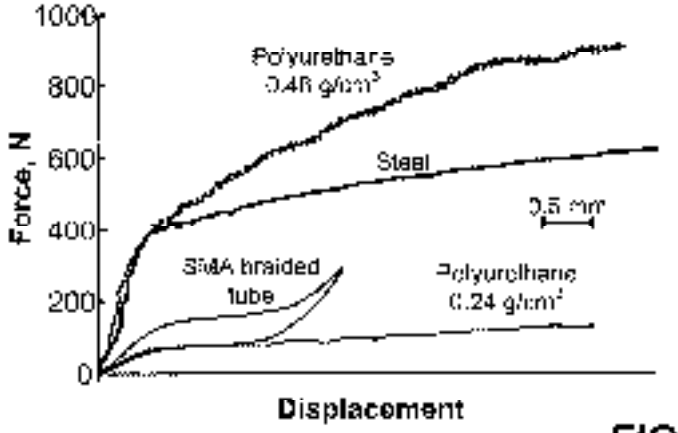
1000
800
600
400
200
0
Force, N
Polyurethane
Steel
SMA braided
tube
Polyurethane
Displacement

FIG 12

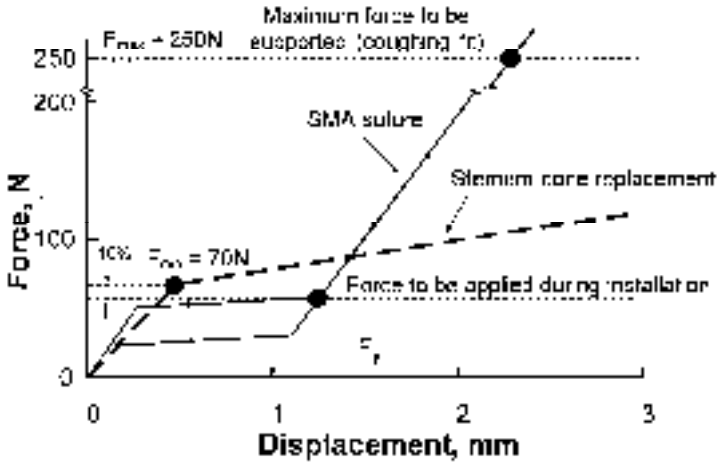
Maximum force to be
250
200
SMA suture
Stenum core replacement
100
Force to be applied dur ng installat on
0
Force, N
0
1
2
3
Displacement, mm

FIG 14

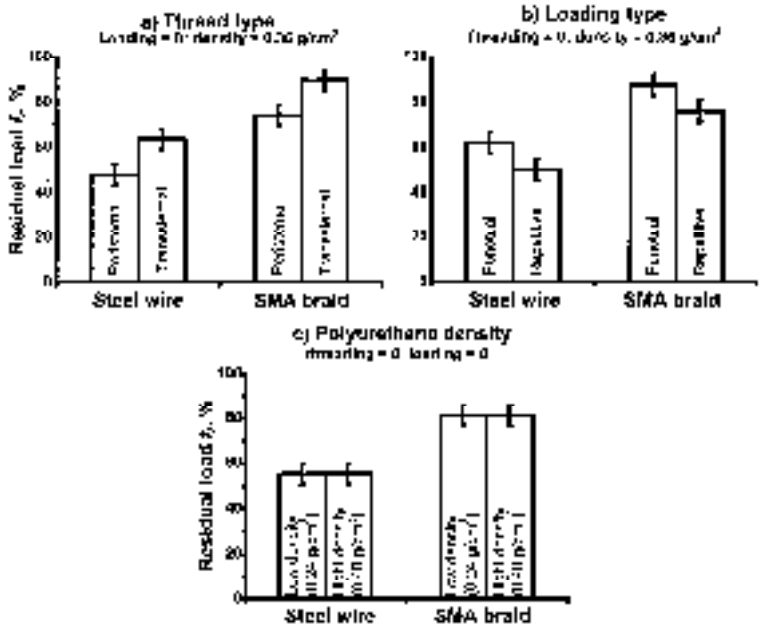
b) Loading type
Steel wire
SMA braid
Fluid
Powder
c) Polyurethane density
Steel wire
SMA braid

FIG 13

ANNEXE III

CLOSURE DEVICE

Cette annexe présente le brevet « Closure Device » PCT/CA2007/002361 qui a été complété le 24 décembre 2007. Le brevet est présenté ici comme il apparait en date du 19 février 2009 sur le site de l'organisation mondiale de la propriété intellectuelle « http://www.wipo.int ».

(12) INTERNATIONAL APPLICATION PUBLISHED UNDER THE PATENT COOPERATION TREATY (PCT)

(19) World Intellectual Property Organization
International Bureau

(43) International Publication Date
3 July 2008 (03.07.2008)

PCT

(10) International Publication Number
WO 2008/077254 A1

(51) International Patent Classification: [illegible]

(21) International Application Number: PCT/[illegible]

(22) International Filing Date: [illegible]

(25) Filing Language: English

(26) Publication Language: English

(30) Priority Data: [illegible]

(71) Applicants (for all designated States except US): [illegible] ... INSTITUT DE CARDIOLOGIE DE MONTREAL [CA/CA]; [illegible]

(72) Inventors; and

(75) Inventors/Applicants (for US only): [illegible] ... CARTIER, Raymond [CA/CA]; [illegible]

(74) Agent: [illegible]

(81) Designated States (unless otherwise indicated, for every kind of national protection available): AE, AG, AL, AM, AT, AU, AZ, BA, BB, BG, BH, BR, BW, BY, BZ, CA, CH, [illegible]

(84) Designated States (unless otherwise indicated, for every kind of regional protection available): ARIPO [illegible]; Eurasian (AM, AZ, BY, KG, KZ, MD, RU, TJ, TM), European [illegible]; OAPI [illegible]

Published:
— with international search report

(54) Title: [illegible]

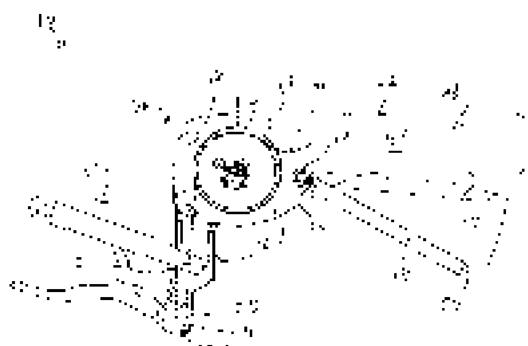

(57) Abstract: [illegible]

WO 2008/077254 A1

Closure apparatus

FIELD OF THE INVENTION

The present invention relates in the general field of closure apparatuses and is particularly concerned with an apparatus suitable for binding together two biological tissue portions with a binding component.

BACKGROUND OF THE INVENTION

There is a need in many medical interventions to bind together two biological tissue portions so that they can be attached to each other temporarily until they bind together through biological healing processes. For example, when performing thoracic surgery, there is a need to re-attach together two sternum halves until the fracture healing process binds them together.

Because of the relatively large forces that must be exerted in many instances onto a binding component that attaches to each other the two biological tissue portions, a specialized apparatus is often used to apply the required force. However, many currently used apparatuses require that the surgeon use both hands to apply the proper force to the binding component. Therefore, the surgeon is unable to use the other hand to guide the apparatus or perform other tasks while the prior art apparatuses are used. In addition, it often happens that the binding component is fixed to the sternum or any other two biological tissue portions using a crimp component that must be crimped to the binding component. In many cases, there is no single apparatus that allows to both apply the proper tension onto the binding component and to crimp the crimped component to the binding component.

Accordingly, against this background, there exists a need for an improved closure apparatus.

SUMMARY OF THE INVENTION.

In a first broad aspect, the invention provides an apparatus for binding together two biological tissue portions with a binding component. The binding component has a substantially elongated configuration and defines substantially opposed binding component first and second end sections and a binding component middle section extending therebetween. The binding component is securable around the two biological tissue portions with a crimp component. The apparatus is useable by an intended user having first and second hands. The apparatus includes a body defining a body handle for receiving one of the first and second hands; at least one drum rotatably mounted to the body, the at least one drum including a binding component attachment for attaching the binding component first end section thereto; a drum actuating lever mounted to the body, the drum actuating lever being movable between a drum actuating lever first position and a drum actuating lever second position, the drum actuating lever being operatively coupled to the at least one drum for rotating the at least one drum in a predetermined direction when the drum actuating lever is moved from the drum actuating lever first position to the drum actuating lever second position; and a crimping assembly operatively coupled to the body for holding the crimp component and selectively crimping the crimp component to the binding component middle section. The body handle, the drum actuating lever and the crimping assembly are configured, sized and positioned in a manner such that the intended user is able to tighten the binding component around the at least one drum by moving the drum actuating lever between the drum actuating lever first and second positions using the first hand; and the intended user is able to operate the crimping assembly to selectively crimp the crimp component to the binding component middle section using the second hand.

Advantageously, the intended user is able to tighten the binding component around the at least one drum using a single hand, which frees the other hand to perform other tasks and operations. In addition to allowing the intended user to use the second hand to crimp the crimp component to the binding component at a suitable moment during the

operation of the proposed apparatus, the intended user may also use the other hand to guide the position of the crimping assembly so as to suitably position the crimp component relatively to the two biological tissue portions and relatively to the binding component to optimize the position of the crimp component. In addition, the second hand may also be used for any other purposes such as, for example, guiding adjacent pieces of biological tissues away from the binding component when tightening the binding component, removing blood from the site at which the crimp component is positioned and any other suitable operation that helps the intended user in performing the binding of the two biological tissue portions to each other rapidly, ergonomically and safely. Therefore, the other hand is usable to enhance the safety of the procedure performed using the proposed apparatus.

In some embodiments of the invention, a clutch is provided for limiting a torque that the drum may exert onto the binding component. In turn, this ensures that excessive pressure is not exerted onto the two biological tissue portions, which facilitates healing. In some embodiments of the invention, the binding component used with the proposed apparatus includes a shape memory alloy and the clutch is therefore, in these embodiments, advantageous in allowing the intended user to tighten the binding component with a force that remains below a damage threshold at which the force exerted onto the binding component would permanently damage the binding component.

The proposed apparatus is manufacturable using known components and methods at relatively low costs. Furthermore, the proposed apparatus is manufacturable using materials that are relatively easily sterilizable. Yet furthermore, the proposed apparatus is usable using a relatively small number of quick and ergonomic steps.

BRIEF DESCRIPTION OF THE DRAWINGS

An embodiment of the present invention will now be disclosed, by way of example, in reference to the following drawings in which:

Figure 1 is a side elevation view, illustrates and apparatus for binding together two biological tissue portions (not shown in Fig. 1), the apparatus being usable with a binding component shown in phantom lines,

Figure 2, is a top elevation view with portions removed, illustrates the apparatus shown in Fig. 1;

Figure 3, is a side partial cross-sectional view, illustrates the apparatus shown in Figs. 1 and 2;

Figure 4, is a front elevation view with portions removed, illustrates the apparatus shown in Figs. 1 to 3, the apparatus being shown binding together two biological tissue portions using a binding component

Figure 5, is a side elevation view, illustrates a drum of the apparatus shown in Figs. 1 to 4, the drum being shown with a binding component attachment thereof in an attachment closed configuration

Figure 6, is a side elevation view, illustrates the drum shown in Fig. 5, the drum being shown with the binding component attachment thereof in an attachment opened configuration;

Figure 7, is a side elevation view with portions removed, illustrates a crimping assembly of the apparatus shown in Figs. 1 to 4, the crimping assembly including a pair of jaws, the jaws being shown in an opened configuration;

Figure 8, is a side elevation view with portions removed, illustrates the crimping assembly shown in Fig. 7, the crimping assembly being shown with the jaws thereof in a closed configuration;

Figure 9, in a side elevation view, illustrates a binding component and a crimp component usable with the apparatus shown in Figs. 1 to 8,

Figure 10, in a side cross-sectional view, illustrates the crimp component shown in Fig. 9

Figure 11, in a side cross-sectional view, illustrates an alternative crimp component usable with the apparatus shown in Figs. 1 to 8 and with the binding component shown in Fig. 9,

Figure 12, in a schematic view, illustrates successive steps in the attachment of two biological tissue portions using the binding and crimp components shown in Figs. 9 and 10,

Figure 13, in a schematic view, illustrates a driving assembly for driving the drums of an apparatus according to an alternative embodiment of the invention

Figure 14, in a partial side cross-sectional view with portions removed, illustrates the apparatus shown in Figs. 1 to 8, the apparatus including two jaws, the two jaws being shown in a jaw opened configuration; and

Figure 15, in a partial side cross-sectional view with portions removed, illustrates the apparatus shown in Figs. 1 to 8, the apparatus including two jaws, the two jaws being shown in a jaw closed configuration

DETAILED DESCRIPTION

Referring to Fig. 1, there is shown an apparatus 10. Referring to Fig. 1, the apparatus 10 is usable for binding together two biological tissue portions 12 and 14 with a binding component 16 (shown in phantom lines). The binding component 16 has a substantially elongated configuration and defines substantially opposed binding components, first and

second end sections 18 and 20 and a binding component middle section 22 extending therebetween. As seen in Fig. 12, the binding component 16 is securable around the two biological tissue portions 12 and 14 with a crimp component 24. The apparatus 10 is usable by an intended user having two hands (not shown in the drawings).

Returning to Fig. 1, the apparatus 10 includes a body 26 defining a body handle 28 for receiving the first hand. The apparatus 10 also includes at least one drum 30 and, typically, a pair of substantially opposed drums 30 (only one of which is shown in Fig. 1) rotatably mounted to the body 26. Each of the drums 30 includes a binding component attachment 32 for attaching the binding component 16 thereto. More specifically, each of the binding component attachments 32 is usable for attaching a respective one of the binding component first and second end sections 18 and 20 thereto (only one of which being shown in Fig. 1).

The apparatus 10 also includes a drum actuating lever 34 mounted to the body 26. The drum actuating lever 34 is movable between a drum actuating lever first position, shown in full lines in Fig. 1, and a drum actuating lever second position, shown in phantom lines in Fig. 1. The drum actuating lever 34 is operatively coupled to the drums 30 for rotating the drums 30 in a predetermined direction when the drum actuating lever 34 is moved from the drum actuating lever first position to the drum actuating lever second position.

The apparatus 10 also includes a crimping assembly 36 operatively coupled to the body 26 for holding the crimp component 24 and selectively crimping the crimp component 24 to the binding component 16 in the binding component middle section 22.

The body handle 28, the drum actuating lever 34 and the crimping assembly 36 are configured, sized and positioned in a manner such that the intended user is able to tighten the binding component 16 around the at least one drum 30 by moving the drum actuating lever 34 between the drum actuating lever first and second positions using a

first hand and to operate the crimping assembly 26 to selectively crimp the crimp component 24 to the binding component middle section 22 using the second hand.

In addition to the body handle 28, the body 26 defines a body central section 38 from which the body handle 28 extends and a crimping assembly spacing segment 40 extending from the body central section 38. Typically, the crimping assembly spacing segment 40 is angled relatively to the body handle 28. For example, it has been found that having a crimping assembly spacing segment 40 that extends substantially perpendicularly to the body handle 28 provides good ergonomics to the apparatus 10 as it facilitates positioning of the crimp component 24 relatively to the two biological tissue portions 12 and 14 while facilitating handling of the apparatus 10 and crimping of the crimp component 24 to the binding component 16.

The body handle 28 has a substantially elongated configuration and defines a handle first surface 42 and a substantially opposed handle second surface 44. Handle lateral surfaces 45 and 46 (only one of which is shown in Fig. 1) extend between the handle first and second surfaces 42 and 44. The handle second surface 44 is substantially closer to the crimping assembly 30 than the handle first surface 42.

Typically, the body central section 38 defines a central section cavity 50, shown in Fig. 3, for receiving components that couple the drum actuating lever 34 to the drums 32, as described in further details hereinbelow.

The crimping assembly spacing segment 40 is also substantially elongated and typically defines a pin 52 extending substantially adjacent to the crimping assembly 26. The pin 52 is described in further details hereinbelow.

As shown for example in Fig. 1, the drum actuating lever 34 is operatively coupled to the drum 30 so as to be movable from the drum actuating lever second position to the drum actuating lever first position with the drums 30 remaining substantially fixed relatively to the body. Typically, the drum actuating lever 34 is substantially freely

movable from the drum actuating lever second position to the drum actuating lever first position with the drums 30 remaining fixed relatively to the body 26. An example of a manner in which this result is achievable is described in further details hereinbelow.

The drum actuating lever 34 is pivotally attached to the body 26 substantially adjacent the handle second surface 44. Typically, the drum actuating lever 34 is pivotally attached to the body 26 so as to pivot substantially perpendicularly to the handle second surface 44 when moving between the drum actuating lever first and second positions.

For example, the drum actuating lever 34 defines a drum actuating lever proximal end 54 and a substantially opposed drum actuating lever distal end 56. The drum actuating lever 34 is pivotally attached to the body 26 substantially adjacent the drum actuating lever distal end 56. The drum actuating lever proximal end 54 is typically closer to the handle second surface 44 when the drum actuating lever is in the drum actuating lever second position than when the drum actuating lever 34 is in the drum actuating lever first position. Typically, the drum actuating lever 34 is pivotally attached to the body 26 so as to extend substantially parallel to the body handle 28 when the drum actuating lever is in one of the drum actuating lever first and second positions, and typically in the drum actuating lever second position. This specific configuration enhances the range of motion through which the drum actuating lever 34 may be operated to tighten the binding component 16 using a single hand and facilitates operation and application of a force by the intended user with a single hand so as to optimize force transfer between the hand and the binding component 16.

A drum actuating lever mounting axle 58 extends from the drum actuating lever 34 substantially perpendicularly in a direction leading from the drum actuating lever proximal end 54 and to the drum actuating lever distal end 56 and extends substantially adjacent the drum actuating lever distal end 56. The drum actuating lever 34 pivots between the actuating lever first and second positions by rotating about the drum actuating lever mounting axle 58. As seen in Fig. 2, the drum actuating lever mounting

axle 58 extends into the central section cavity 50 and is mechanically coupled to a toothed gear 60 for rotating the toothed gear 60 in a predetermined direction. Also, the drum actuating lever mounting axle 58 is mechanically coupled to a roller clutch 62 that allows rotation of the toothed gear 60 in a single direction, for example, when the drum actuating lever 34 is moved from the drum actuating lever first position to the drum actuating lever second position. To that effect, the roller clutch 52 is fixedly mounted in the body 32.

In some embodiments of the invention, the roller clutch 62 allows the drum actuating lever 34 to move substantially freely from the drum actuating lever second position to the drum actuating lever first position. When the apparatus 10 is used with the handle second surface 44 facing generally downward, this movement of the drum actuating lever 34 is performed under the action of gravity, which facilitates the operation of the drum actuating lever 34 with a single hand.

Referring to Fig. 3, a power transmission mechanism 64 is mounted inside the central section cavity 50 and operatively coupled to the drums 30 (not shown in Fig. 3) and to the toothed gear 60 for transmitting forces exerted by the intended user onto the drum actuating lever 34 to the drums 30. The power transmission mechanism 64 functions as a torque multiplier to multiply the torque exerted by the intended user onto the drum actuating lever 34 and only allows rotation of the drums 30 in a predetermined direction so that when tension is first applied to the binding component 16, moving the drum actuating lever 34 from the drum actuating lever second position to the drum actuating lever first position does not result in tension inside the binding component 16 to be reduced.

More specifically, this is achieved by having a power transmission mechanism 64 that includes a toothed gear 66 engaging the toothed gear 60 that is coupled to the drum actuating lever 34 for transmitting a rotational motion of the toothed gear 60 to the toothed gear 66. In addition, the power transmission mechanism 64 includes a power transmitting axle 68 for transmitting a rotational motion of the toothed gear 66 to the

drums 30. The power transmitting axle 68 is rotatably mounted inside the central section cavity 50 and protrudes laterally therefrom. Each of the drums 30 is mechanically connected to the power transmitting axle 68 for joint rotation therewith.

A torque limiting clutch 70 and another roller clutch 72 are operatively coupled to the toothed gear 66 and to the power transmitting axle 68 for preventing the power transmitting axle 68 from rotating when a maximal torque has been applied thereto and for only allowing movement of the power transmitting axle 68 in a single direction corresponding to the predetermined direction in which the drums 30 are allowed to rotate. The roller clutches 62 and 72 are configured such that the toothed gears 60 and 66 can rotate in opposite directions.

Roller clutches 62 and 72 and the torque limiting clutch 70 are components that are well known in the art and the specific arrangement used in the apparatus 10 is therefore not described in further details. In addition, in alternative embodiments of the invention, any other suitable components performing similar functions are used instead of the roller clutches 62 and 72 and the torque limiting clutch 70.

Referring to Figs. 5 and 6, each of the drums 30 includes a drum body 74. The drum body 74 is attached to the power transmitting axle 68 (not shown in Figs. 5 and 6) for joint rotation therewith. The binding component attachment 32 is mounted to the drum body 74. A specific example of implementation of the binding component attachment 32 is described in further details hereinbelow.

In this specific example, the binding component attachment 32 includes an attachment first member 76 and an attachment second member 78. The attachment first and second members 76 and 78 are operatively coupled to the drum body 74 in a manner such that the binding component attachment 32 is configurable between an attachment opened configuration, shown in Fig. 6, and an attachment closed configuration, shown in Fig. 5. In the attachment opened configuration, the attachment first and second members 76 and 78 are substantially spaced apart from each other for allowing

insertion of the binding component 10 therebetween. In the attachment closed configuration, the attachment first and second members 76 and 78 are substantially adjacent to each other for receiving the binding component therebetween and frictionally engaging the binding component 10. In some embodiments of the invention, the binding component includes a biasing element operatively coupled to the attachment first and second members 76 and 78 for biasing the attachment first and second members 76 and 78 towards the attachment closed configuration.

In a specific example of implementation, the attachment first member 76 is substantially annular and substantially eccentrically pivotally attached to the drum body 74 through a first member pivot 80. The attachment first member 76 defines a first member peripheral surface 82 and two substantially opposed first member lateral surfaces 84 and 86, only one of which is shown in Figs. 5 and 6. Also, the attachment first member 76 defines a first member aperture 88 extending between the first member lateral surfaces 84 and 86 in a substantially spaced apart location relatively to the first member pivot 80. Typically, the attachment first member 76 pivots relatively to the drum body 74 about the first member pivot 80 in a plane substantially parallel to a plane in which the drum 30 rotates relatively to the body 26.

The attachment second member 78 is fixed relatively to the drum body 74. Typically, the attachment second member 78 extends integrally from the drum body 74 and is configured and located so that the first member peripheral surface 82 is partially substantially in register therewith.

A pin 90 extends from the drum body 74 through the first member aperture 88. Typically, the pin 90 is co-axial with the power transmitting axle 58. A biasing element in the form of a coil spring 92 biases the attachment first and second members 76 and 78 towards the attachment closed configuration. The coil spring 92 defines a coil spring first end 94 and a coil spring second end 96. The coil spring first and second ends 94 and 96 are secured to the attachment first member 76 with the coil spring 92 wrapping at least partially around the pin 90. The coil spring first and second ends 94 and 96 are

located further away from the attachment second member 78 than the pin 90. In this configuration the coil spring 92 therefore wraps around the pin 90 in a substantially U-shaped configuration. However, in alternative embodiments of the invention the attachment first and second members 76 and 78 are biased towards the attachment closed configuration in any other suitable manner.

In some embodiments of the invention, the attachment first member 76 defines a first member flange 98 extending substantially radially outwardly therefrom substantially adjacent the first member lateral surface 84. The first member flange 98 guides the binding component 18 as it is rolled around the drum 30. The first member flange 98 extends along an arc segment and is located substantially opposed to the attachment second member 78. Typically, the first member flange 98 is absent from locations adjacent the attachment second member 78 to facilitate insertion of the binding component 18 between the attachment first and second members 76 and 78.

Referring to Figs. 14 and 15, there is shown in greater details the crimping assembly 36. The crimping assembly 36 includes a pair of jaws 100 and 102. The jaws 100 and 102 are movable between a jaw opened configuration, shown in 14, and a jaw closed configuration, shown in Fig. 15. The jaws 100 and 102 are substantially spaced apart from each other by a larger distance in the jaw opened configuration than in the jaw closed configuration. Referring to Fig. 14, the jaws 100 and 102 define a crimp component holding recess 104 for holding the crimp component 24 when the jaws 100 and 102 are in the jaw opened configuration. The jaws 100 and 102 crimp the crimp component 24 when moved from the jaw opened configuration to the jaw closed configuration. The crimping assembly also includes a crimp actuator 106 operatively coupled to the body 26 and to the jaws 100 and 102 for selectively moving the jaws 100 and 102 between the jaw opened and closed configurations.

Typically, the jaws 100 and 102 include a fixed a jaw, for example the jaw 100, and a mobile jaw, for example the jaw 102. Referring to Fig. 7, the fixed jaw 100 defines a fixed jaw proximal end 108 and a substantially opposed fixed jaw distal end 110. The

fixed jaw 100 is fixedly attached to the body 26 and, more specifically, to the crimping assembly spacing segment 40 substantially adjacent the fixed jaw distal end 110.

The mobile jaw 102 defines a mobile jaw proximal end 112 and a substantially opposed mobile jaw distal end 114. The mobile jaw 102 is pivotally attached to the fixed jaw 100 with the fixed jaw and mobile jaw distal ends 110 and 114 substantially adjacent to each other. For example, this is performed by having a fixed jaw 100 that defines a pin 116 extending generally parallel to the power transmitting axis 69 (not shown in Figs. 7 and 8) and a mobile jaw 102 that defines a pin receiving aperture 118, the pin 116 being inserted through the pin receiving aperture 118.

In some embodiments of the invention, the mobile jaw 102 defines a biasing component attachment aperture 120 at a location intermediate the mobile jaw proximal and distal ends 112 and 114, the biasing component attachment aperture 120 being useable for attaching a biasing component 122 to the mobile jaw 102 as described in further details hereinbelow.

Having a fixed jaw 100 and a mobile jaw 102, as opposed to having two mobile jaws contributes to the ease of use of the apparatus 10 and facilitates positioning of the crimp component 24 relatively to the two portions of biological tissues 12 and 14 that need to be bound to each other. Also, this configuration facilitates the maintenance of the position of the crimp component 24 when the crimp component 24 is crimped to the binding component 16. However, in alternative embodiments of the invention, both of the jaws 100 and 102 are mobile relatively to the body 26.

A specific configuration of the crimp actuator 106 is described hereinbelow. In this specific configuration, the crimp actuator 106 includes a crimp handle 124 mechanically coupled to the body 26 and a crimp actuating lever 126 located substantially adjacent to the crimp handle 124. The crimp actuating lever 126 is movable between a crimp actuating lever first position and a crimp actuating lever second position. The crimp actuating lever 126 is operatively coupled to the jaws 100 and 102 in a manner such

that the jaw 100 and 102 are in the jaw opened configuration when the crimp actuating lever 126 is in the crimp actuating lever first position shown in Fig. 14 and the jaws 100 and 102 are in the jaw closed configuration when the crimp actuating lever 126 is in the crimp actuating lever second position, shown in Fig. 15. Also, in some embodiments of the invention the biasing component 122 takes the form of a coil spring extending between the mobile jaw 102 and the pin 52 for biasing the mobile jaw 102 towards the jaw opened configuration. The biasing component 122 is therefore attached at one end thereof to the biasing component attachment aperture 120 and attached at the other end thereof to the pin 52.

When the crimping assembly 36 is in use, the intended user, (not shown in the drawings), exerts an input force onto the crimping assembly 36 to crimp the crimp component 24 to the binding component 15. In some embodiments of the invention, the manner in which the input force is transmitted to the jaws 100 and 102 is adjustable by having the crimp actuator 106 that is configurable between a crimp actuator low leverage configuration, seen in Fig. 7, and a crimp actuator high leverage configuration seen in Fig. 8.

The crimp actuator 106 is operatively coupled to the pair of jaws 100 and 102 in a manner such that a larger force is exerted by the crimp actuator onto the jaws 100 and 102 when moving the jaws 100 and 102 from the jaw opened configuration to the jaw closed configuration with the input force when the crimp actuator 106 is in the crimp actuator high leverage configuration than when the crimp actuator 106 is in the crimp actuator low leverage configuration.

The functional characteristics of the crimping assembly 36 described hereinabove are achieved, for example, using the following configuration of the crimping assembly 36. The crimp handle 124 defines a crimp handle proximal end 128 and a crimp handle distal end 130. The crimp handle 124 is attached to the crimping assembly spacing segment 40 substantially adjacent the crimp handle distal end 130 in a substantially spaced apart relationship relatively to the fixed jaw 100.

For example, the crimp handle extends at an angle of from about 20 to about 40 degrees relatively to the body handle 28. It has been found that this configuration enhances the ergonomics of the apparatus 10 as it facilitates operation of the apparatus 10 by the intended user with one hand remaining on the body handle 28 (not shown in Figs. 7 and 8) and the other hand operating the crimping assembly 26. The crimp handle 124 also defines a link receiving recess 132 extending substantially longitudinally therealong for receiving a crimp actuator link 134 which is described in further details hereinbelow.

The crimp handle 124 further defines a handle aperture 136 extending substantially longitudinally between the link receiving recess 132 and the crimp handle proximal end 128. The handle aperture 136 is threaded and receives a bolt 138 that is threadably inserted therein for movement between a bolt first position, seen in Fig. 7, and a bolt second position, seen in Fig. 8. The bolt 138 is used to move the crimp actuator 106 between the crimp actuator low and high leverage configurations.

The crimp actuating lever 126 defines a crimp actuating lever proximal end 140 and a substantially opposed crimp actuating lever distal end 142. The crimp actuating lever 126 is pivotally attached to the mobile jaw 102 with a crimp actuating lever-to-jaw pivot 144. The crimp actuating lever-to-jaw pivot 144 is located substantially adjacent to the crimp actuating lever distal end 142 and to the mobile jaw proximal end 112.

The crimp actuator link 134 extends between the crimp actuating lever 126 and the crimp handle 124. The crimp actuator link 134 is pivotally mounted to both the crimp handle 124 and the crimp actuating lever 126. The crimp actuator link 134 is pivotally mounted to the crimp actuating lever 126 at a location intermediate the crimp actuating lever distal and proximal ends 142 and 140. The crimp actuator link 134 is received inside the link receiving recess 132 and abuts against and is biased towards the bolt 138. Therefore, the crimp actuator link 134 is mounted to the crimp handle 124 so that an end section thereof is selectively movable substantially longitudinally therealong

This movement allows an achievement of the crimp actuator high and low overage configurations when the tip 136 is moved in the handle aperture 135.

Referring to Fig. 9, there is shown a typical configuration of the binding component 16 and the crimp component 24 that are usable with the apparatus 10. As seen in Fig. 9, typically, a needle 148 is attached to the binding component 16 substantially adjacent one of the ends thereof. The needle 148 facilitates the insertion of the binding component 16 through the crimp component 24 and around the two biological tissue portions 12 and 14. In some embodiments of the invention, a stopper 149 is attached to the binding component 16 substantially adjacent the other end thereof.

As seen in Fig. 10, in some embodiments of the invention, the crimp component 24 has a substantially annular cross-sectional configuration. However, in alternative embodiments of the invention, a crimp component 24' shown in Fig. 11 having a substantially oblong tubular configuration is usable. This alternative crimp component 24' is, in some embodiments, more easily positionable between the jaws 100 and 102 and more easily foldable therebetween before crimping.

Fig. 12 illustrates schematically a manner in which the binding component 16 is usable to bind the two biological tissue portions 12 and 14 thereto. First, as seen in panel (i), the binding component 16 is inserted through the crimp component 24 and passed around the two biological tissue portions 12 and 14 to bind. Afterwards, as seen in panel (ii), the binding component 16 is passed back through the crimp component 24 in the same direction in which it was originally passed therethrough to form a loop and a force is exerted on the two end portions of the binding component 16 to pull the two biological tissue portions 12 and 14 towards each other. As seen in panel (iii), when a desired tension has been achieved in the binding component 16, for example, a predetermined tension, a force is exerted onto the crimp component 24 to crimp the crimp component 24 to the binding component 16 and the binding component 16 is cut substantially adjacent the crimp component 24 to remove its free ends.

The method schematically illustrated in Fig. 12 and generally described hereinabove is facilitated by the use of the apparatus 10. In such a use, after the binding component 16 has been passed twice through the crimp component 24, the crimp component 24 is inserted between the two jaw 100 and 102 and the binding component 16 is attached to each of the drums 30 using the binding component attachments 32. This is achieved by opening a gap between the attachment first and second members 76 and 78 by moving the binding component attachment 32 from the attachment closed to the opened configurations and, afterwards, releasing the binding component attachment 32 so that the attachment closed configuration is achieved through the action of the coil spring 92.

Afterwards, the intended user uses a hand to repetitively move the drum actuating lever 34 from the drum actuating lever first position to the drum actuating lever second position and, in between each of these moves, release the drum actuating lever 34 which, under the action of gravity moves back to the drum actuating lever first position. This has for effect to repetitively move the drums 30 in the predetermined direction until a maximal torque is achieved.

Then, the intended user may use the crimping assembly 36 to crimp the crimp component 24 to the binding component 16 by moving the crimp actuating lever 126 towards the crimp actuating lever second position thereby exerting a force pushing the mobile jaw 102 towards the fixed jaw 100. If desired, before this operation is performed, the bolt 138 may be moved in and out of the link receiving recess 132 so that a desired leverage effect is achieved from the crimp actuator link 134 to adjust the force with which the crimp component 24 is crimped to the binding component 16. Afterwards, the crimp actuating lever 126 is released which opens the jaws 100 and 102 and allows removal of the apparatus 10 from the site of operation after the free ends of the binding component 16 have been cut off.

As seen in Fig. 15, in alternative embodiments of the invention, the toothed gear 66 and therefore the drums 30 are rotated by an electric motor 150 connected to a power source 152, for example a battery. To that effect, an output axle 156 is coupled to the

electric motor 150 for being rotated thereby. A toothed gear 158 is attached to the output axle 156 for joint rotation therewith. The toothed gear 156 engages the toothed gear 66 and rotates the toothed gear 66 when rotated. A switch 154 allows to selectively energize the electric motor 150 to rotate the toothed gear 66.

Although the present invention has been described hereinabove by way of preferred embodiments thereof, it can be modified without departing from the spirit, scope and nature of the subject invention, as defined in the appended claims.

We claim:

1. An apparatus for binding together two biological tissue portions with a binding component, said binding component having a substantially elongated configuration and defining substantially opposed binding component first and second end sections and a binding component middle section extending therebetween, said binding component being securable around said two biological tissue portions with a crimp component, said apparatus being usable by an intended user having first and second hands, said apparatus comprising

- a body defining a body handle for receiving said first hand;

at least one drum rotatably mounted to said body, said at least one drum including a binding component attachment for attaching said binding component first end section thereto;

a drum actuating lever mounted to said body, said drum actuating lever being movable between a drum actuating lever first position and a drum actuating lever second position, said drum actuating lever being operatively coupled to said at least one drum for rotating said at least one drum in a predetermined direction when said drum actuating lever is moved from said drum actuating lever first position to said drum actuating lever second position; and

- a crimping assembly operatively coupled to said body for holding said crimp component and selectively crimping said crimp component to said binding component middle section;

- wherein said body handle, said drum actuating lever and said crimping assembly are configured, sized and positioned in a manner such that

  - said intended user is able to tighten said binding component around said at least one drum by moving said drum actuating lever between said drum actuating lever first and second positions using said first hand, and

  - said intended user is able to operate said crimping assembly to selectively crimp said crimp component to said binding component

middle section using said second hand while simultaneously holding said body handle with said first hand.

2. An apparatus as defined in claim 1, wherein said drum actuating lever is operatively coupled to said at least one drum so as to be movable from said drum actuating lever second position to said drum actuating lever first position with said at least one drum remaining substantially fixed relatively to said body.

3. An apparatus as defined in claim 2, wherein said drum actuating lever is substantially freely moveable from said drum actuating lever second position to said drum actuating lever first position with said at least one drum remaining fixed relatively to said body.

4. An apparatus as defined in claim 1, wherein said drum actuating lever is pivotally attached to said body so as to extend substantially parallel to said body handle when said drum actuating lever is in one of said drum actuating lever first and second positions.

5. An apparatus as defined in claim 4, wherein said drum actuating lever is pivotally attached to said body so as to extend substantially parallel to said body handle when said drum actuating lever is in said drum actuating lever second position.

6. An apparatus as defined in claim 1, wherein said body handle defines a human first surface and a substantially opposed handle second surface, said handle second surface being closer to said crimping assembly than said handle first surface, said drum actuating lever being pivotally attached to said body substantially adjacent said handle second surface.

7. An apparatus as defined in claim 6, wherein said drum actuating lever is pivotally attached to said body so as to pivot substantially perpendicularly to said handle

second surface when moving between said drum actuating lever first and second positions.

8. An apparatus as defined in claim 7, wherein said drum actuating lever defines a drum actuating lever proximal end and a substantially opposed drum actuating lever distal end, said drum actuating lever being pivotally attached to said body substantially adjacent said drum actuating lever distal end, said drum actuating lever proximal end being closer to said handle second surface when said drum actuating lever is in said drum actuating lever second position than when said drum actuating lever is in said drum actuating lever first position.

9. An apparatus as defined in claim 1, further comprising a clutch operatively coupled to said at least one drum and to said drum actuating lever for preventing said drum from rotating in said predetermined direction when a torque substantially larger than a maximal torque is exerted on said at least one drum.

10. An apparatus as defined in claim 9, wherein said clutch is a variable torque clutch allowing a selective adjustment of said maximal torque.

11. An apparatus as defined in claim 1, said apparatus comprising a pair of substantially opposed drums each rotatably mounted to said body, each of said drums including a binding component attachment for attaching one of said binding component first and second end sections thereto, each of said drums being operatively coupled to said drum actuating lever in a manner such that both of said drums rotate in said predetermined direction when said drum actuating lever is moved from said drum actuating lever first position to said drum actuating lever second position.

12. An apparatus as defined in claim 1, wherein said crimping assembly includes:

a pair of jaws, said pair of jaws being movable between a jaw opened configuration and a jaw closed configuration, wherein said jaws are

substantially spaced apart from each other by a larger distance in said jaw opened configuration than in said jaw closed configuration, said jaws defining a crimp component holding recess for holding said crimp component when said jaws are in said jaw opened configuration, said jaws crimping said crimp component when moved from said jaw opened configuration to said jaw closed configuration; and

a crimp actuator operatively coupled to said body and to said pair of jaws for selectively moving said pair of jaws between said jaw opened and closed configurations.

13. An apparatus as defined in claim 12, wherein said pair of jaws includes a fixed jaw fixedly attached to said body and a mobile jaw operatively coupled to said fixed jaw in a manner such that said pair of jaws are movable between said jaw opened and closed configurations.

14. An apparatus as defined in claim 12, wherein said crimp actuator includes a crimp handle mechanically coupled to said body and a crimp actuating lever located substantially adjacent to said crimp handle, said crimp actuating lever being moveable between a crimp actuating lever first position and a crimp actuating lever second position, said crimp actuating lever being operatively coupled to said pair of jaws in a manner such that said pair of jaws are in said jaw opened configuration when said crimp actuating lever is in said crimp actuating lever first position and said pair of jaws are in said jaw closed configuration when said crimp actuating lever is in said crimp actuating lever second position.

15. An apparatus as defined in claim 12, wherein said intended user exerts an input force onto said crimping assembly to crimp said crimp component in said bringing component, said crimp actuator being configurable between a crimp actuator low leverage configuration and a crimp actuator high leverage configuration, said crimp actuator being operatively coupled to said pair of jaws in a manner such

that a larger force is exerted by said crimp actuator onto said pair of jaws when moving said pair of jaws from said jaw opened configuration to said jaw closed configuration with said input force when said crimp actuator is in said high leverage configuration than when said crimp actuator is in said low leverage configuration.

16. An apparatus as defined in claim 12 wherein

said pair of jaws includes a fixed jaw and a mobile jaw, said fixed jaw defining a fixed jaw proximal end and a substantially opposed fixed jaw distal end, said fixed jaw being fixedly attached to said body substantially adjacent said fixed jaw distal end, said mobile jaw defining a mobile jaw proximal end and a substantially opposed mobile jaw distal end, said mobile jaw being pivotally attached to said fixed jaw with said fixed jaw and mobile jaw distal ends substantially adjacent to each other,

said crimp actuating lever defines a crimp actuating lever proximal end and a substantially opposed crimp actuating lever distal end, said crimp actuating lever being pivotally attached to said mobile jaw with a crimp actuating lever-to-jaw pivot, said crimp actuating lever to jaw pivot being located substantially adjacent to both said crimp actuating lever distal end and said mobile jaw distal end;

said crimp actuator includes a crimp actuator link extending between said crimp actuating lever and said crimp handle, said crimp actuator link being pivotally mounted to both said crimp handle and said crimp actuating lever, said crimp actuator link being pivotally mounted to said crimp actuating lever at a location intermediate said crimp actuating lever distal and proximal ends.

17. An apparatus as defined in claim 16, wherein said crimp actuator link defines a link end section mounted to said crimp handle so as to be selectively movable substantially longitudinally therealong.

18. An apparatus as defined in claim 12, wherein said crimping assembly includes a biasing component 122 operatively coupled to said pair of jaws for biasing said pair of jaws towards said jaw opened configuration.

19. An apparatus as defined in claim 1, wherein said body defines a crimping assembly spacing segment extending between said at least one drum and said crimping assembly for spacing said crimping assembly and said at least one drum relatively to each other, said crimping assembly spacing segment being angled relatively to said body handle

20. An apparatus as defined in claim 19, wherein said crimping assembly spacing segment is substantially perpendicular to said body handle

21. An apparatus as defined in claim 1, wherein

said at least one drum includes a drum body

said binding component attachment includes an attachment first member and an attachment second member, said attachment first and second members being operatively coupled to said drum body in a manner such that said binding component attachment is configurable between an attachment opened configuration and an attachment closed configuration wherein in said attachment opened configuration, said attachment first and second members are substantially spaced apart from each other for allowing an insertion of said binding component therebetween and in said attachment closed configuration, said attachment first and second members are substantially adjacent to each other for receiving said binding component therebetween and frictionally engaging said binding component

22. An apparatus as defined in claim 21, further comprising a biasing element operatively coupled to said attachment first and second members for biasing said

attachment first and second members towards said attachment closed configuration.

23. An apparatus as defined in claim 22 wherein

- said attachment first member is substantially annular and substantially eccentrically pivotally attached to said drum body at a first member pivot location, said attachment first member defining a first member peripheral surface; and
- said attachment second member is substantially fixed relatively to said drum body, said first member peripheral surface being partially substantially in register with said first member peripheral surface.

24. An apparatus as defined in claim 23, wherein

- said attachment first member defines substantially opposed first member lateral surfaces and a first member aperture extending therebetween substantially spaced apart from said first member pivot location;
- said drum includes a pin extending through said first member aperture;
- said biasing element includes a coil spring defining a coil spring first end and a coil spring second end, said coil spring first and second ends being secured to said attachment first member with said coil spring wrapping at least partially around said pin, said coil spring first and second ends being located further away from said attachment second member than said pin.

25. An apparatus as defined in claim 24, wherein said attachment first member defines a first member flange extending substantially radially outwardly therefrom substantially spaced apart from said drum body.

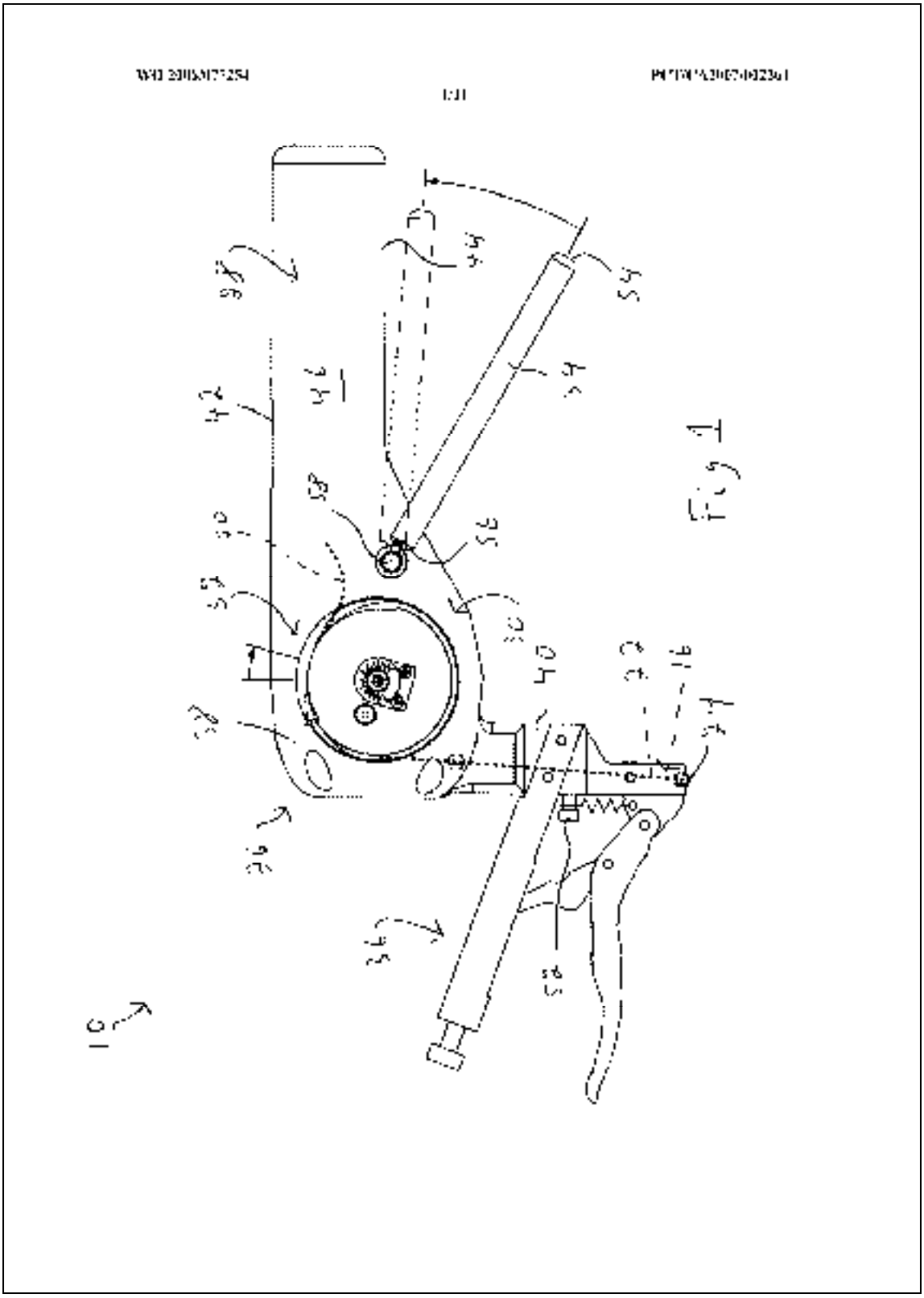
WO 2005/077254
PCT/US2005/003261
1/11
10
12
14
16
18
20
22
24
26
28
30
32
34
36
38
40
42
44
46
48
50
52
54
56
58

Fig. 1

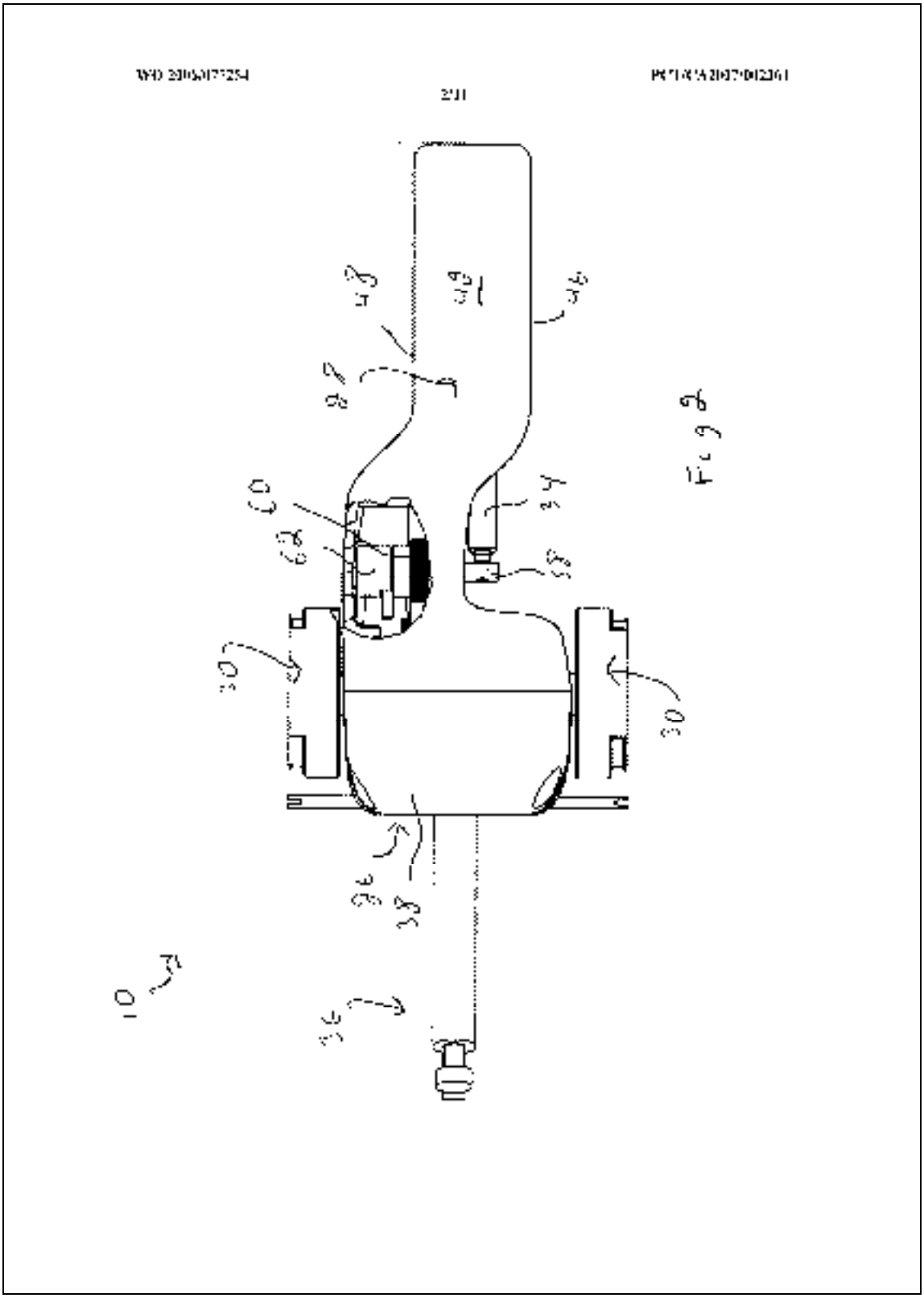
WO 2005077254
211
Fig 9a
10
16
24
28
30
30
60
62
82
84
86
87
88

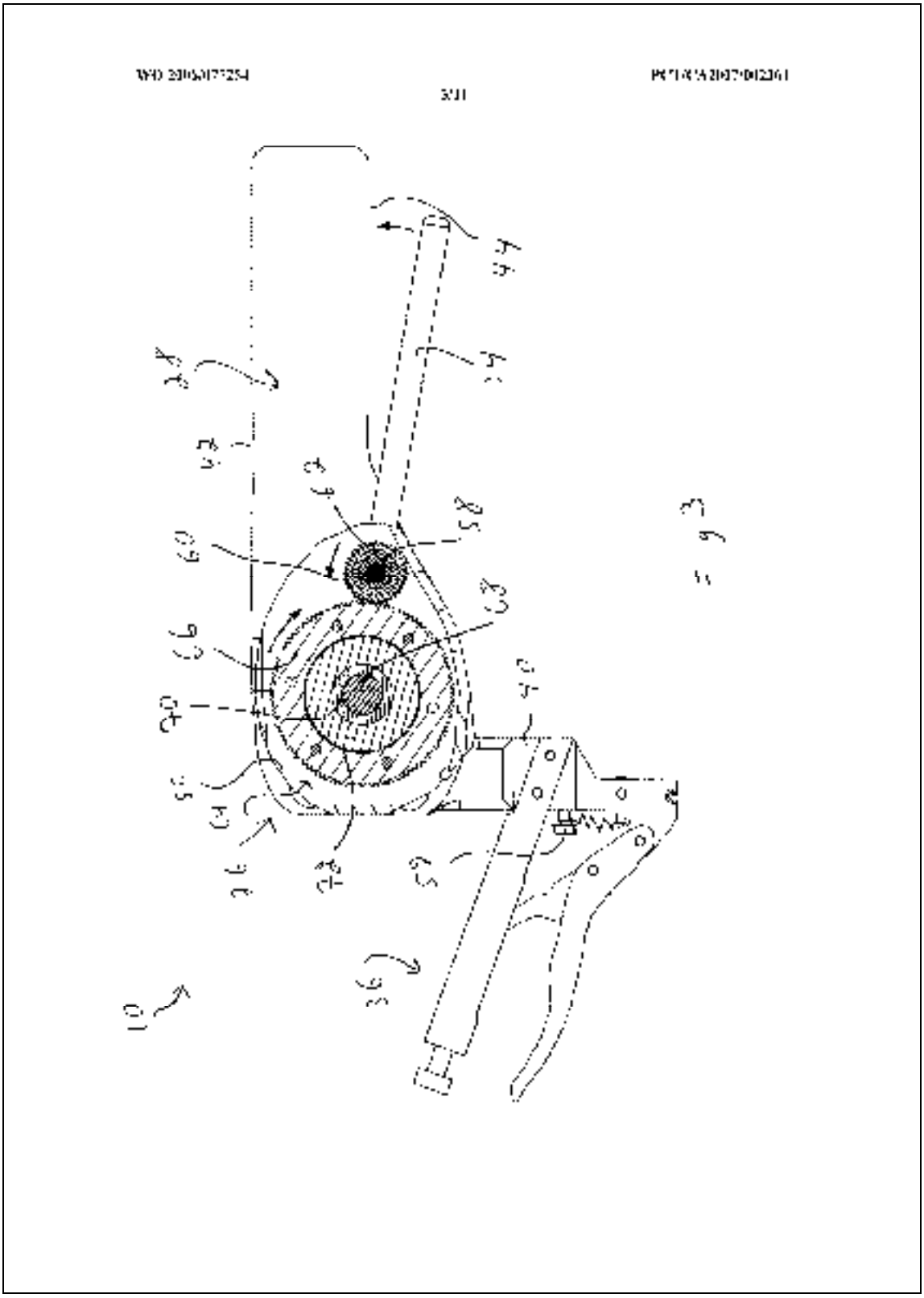
WO 2006077254
PCT/EP2006/050261
3/11
Fig. 3
10
12
14
16
18
20
22
24
26
28
30
32
34
36
38
40
42
44
46
48
50
52
54
56
58
60
62

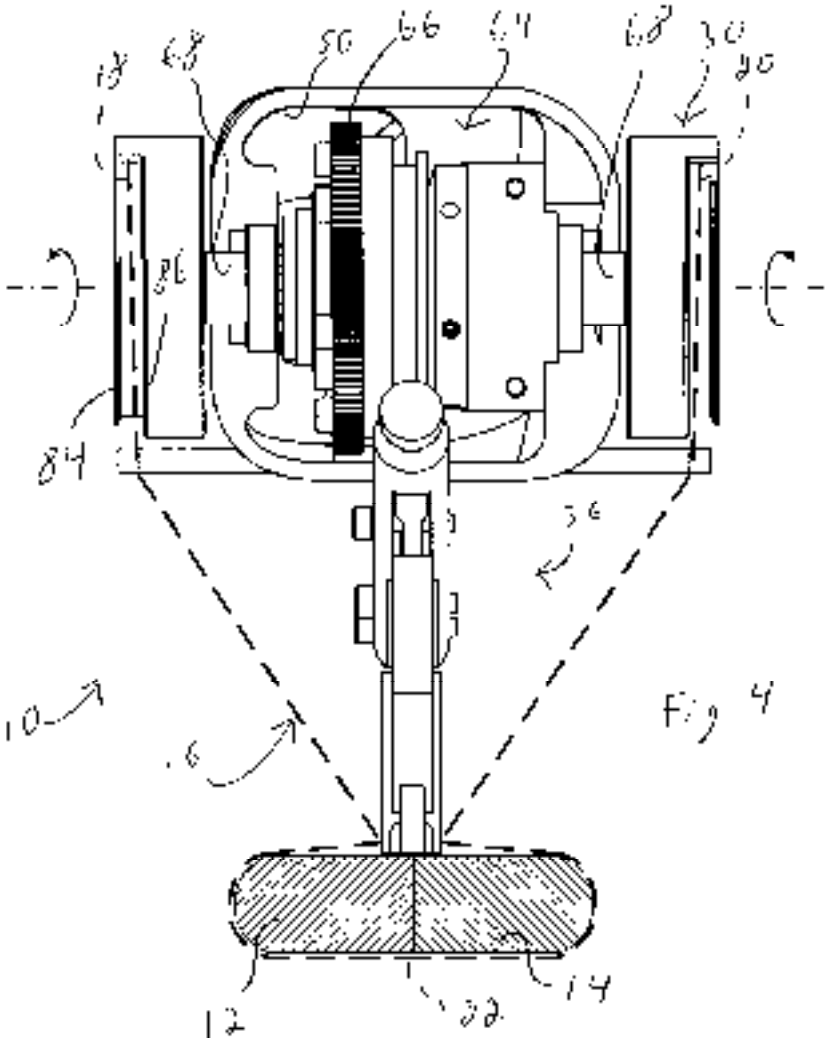
WO 2006077254
PCT/EP2006/050261
4/11
18
68
50
66
64
68
30
20
26
84
36
10
16
12
32
14

Fig 4

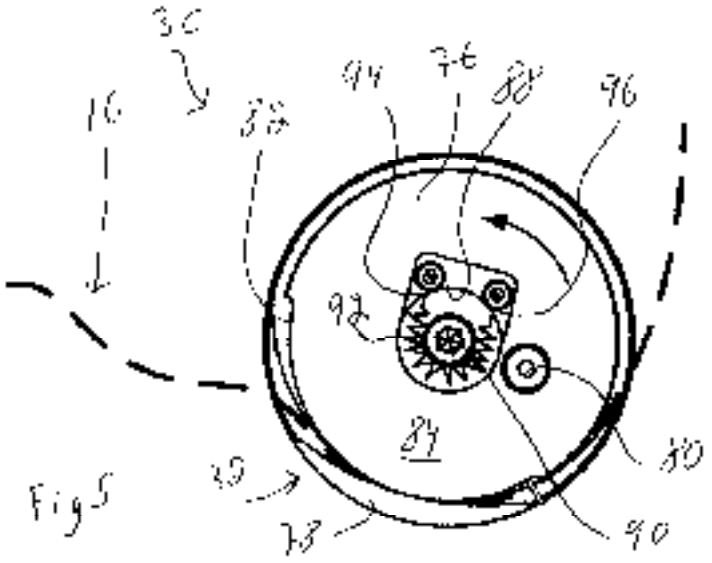
30
16
82
94
76
84
96
92
84
80
90
78

Fig 5

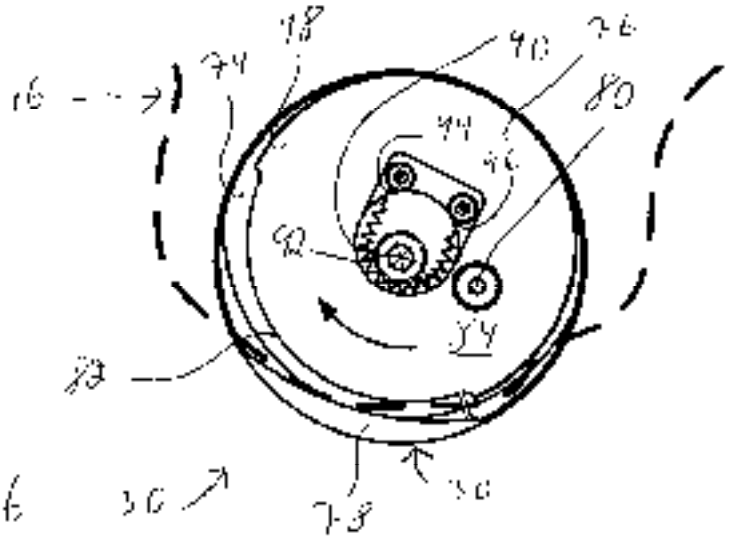
18
16
74
90
76
80
94
96
92
74
78
30
78

Fig 6

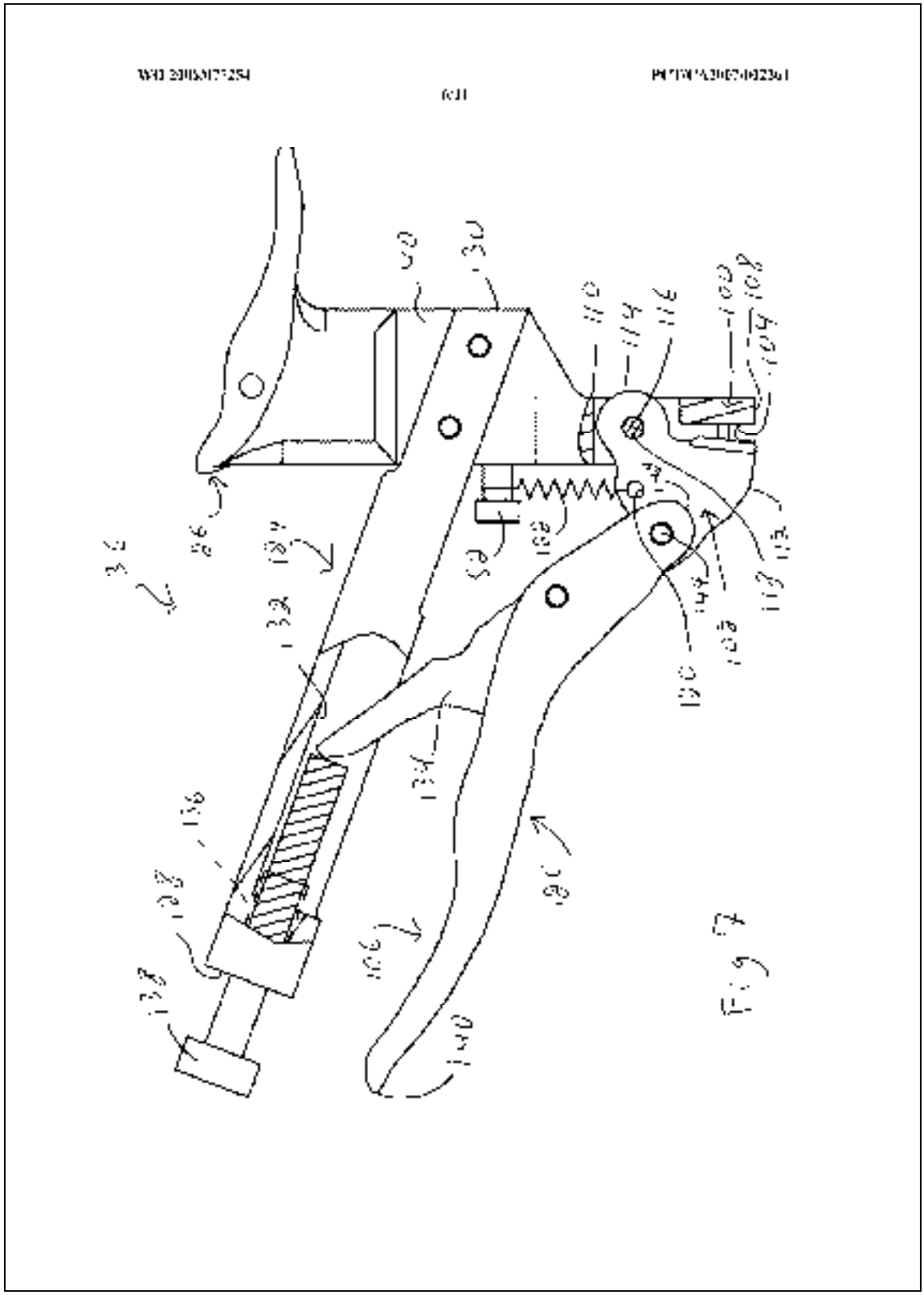
WO 2005/077254
6/11
Fig. 7

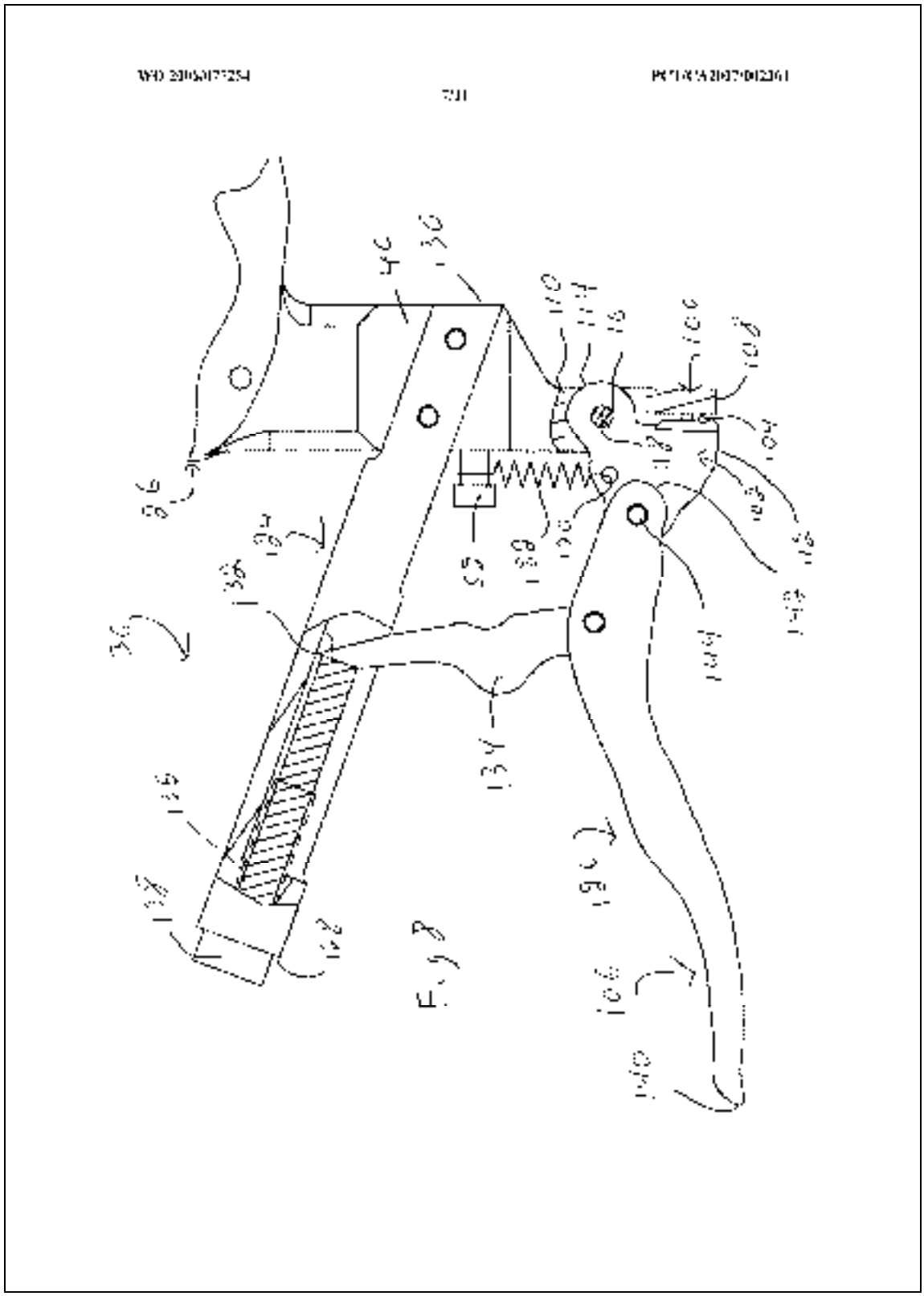

Fig 7

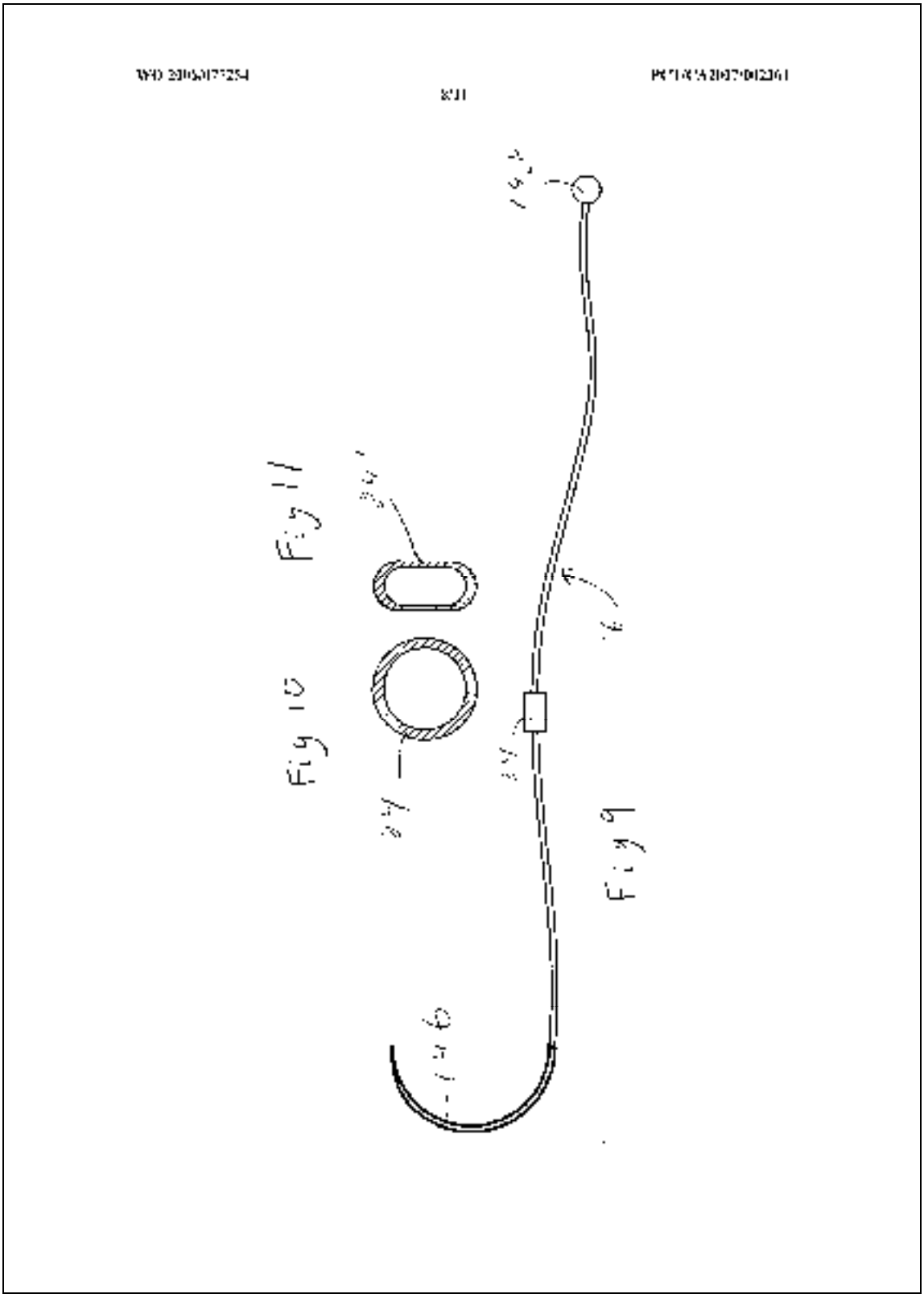
WO 2006077254
8/11
Fig 9
Fig 10
Fig 11

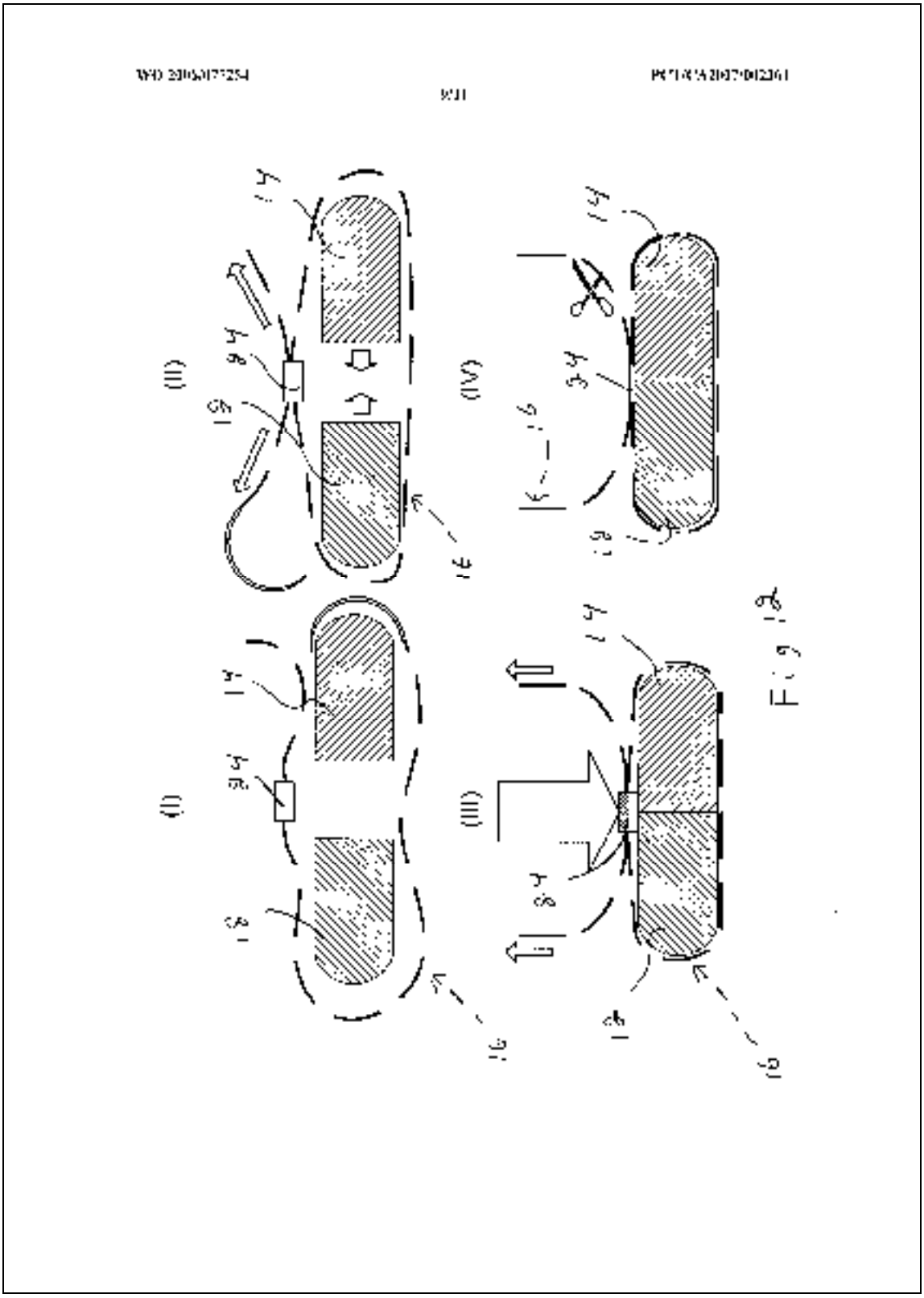

Fig. 9

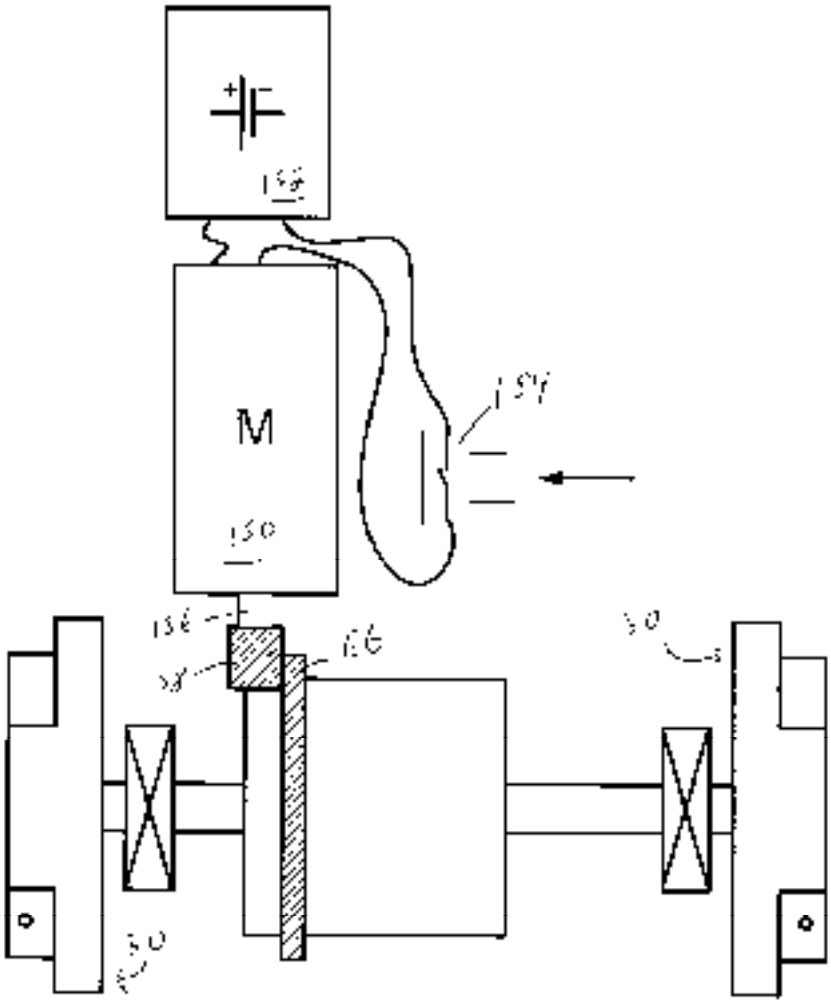

Fig 13

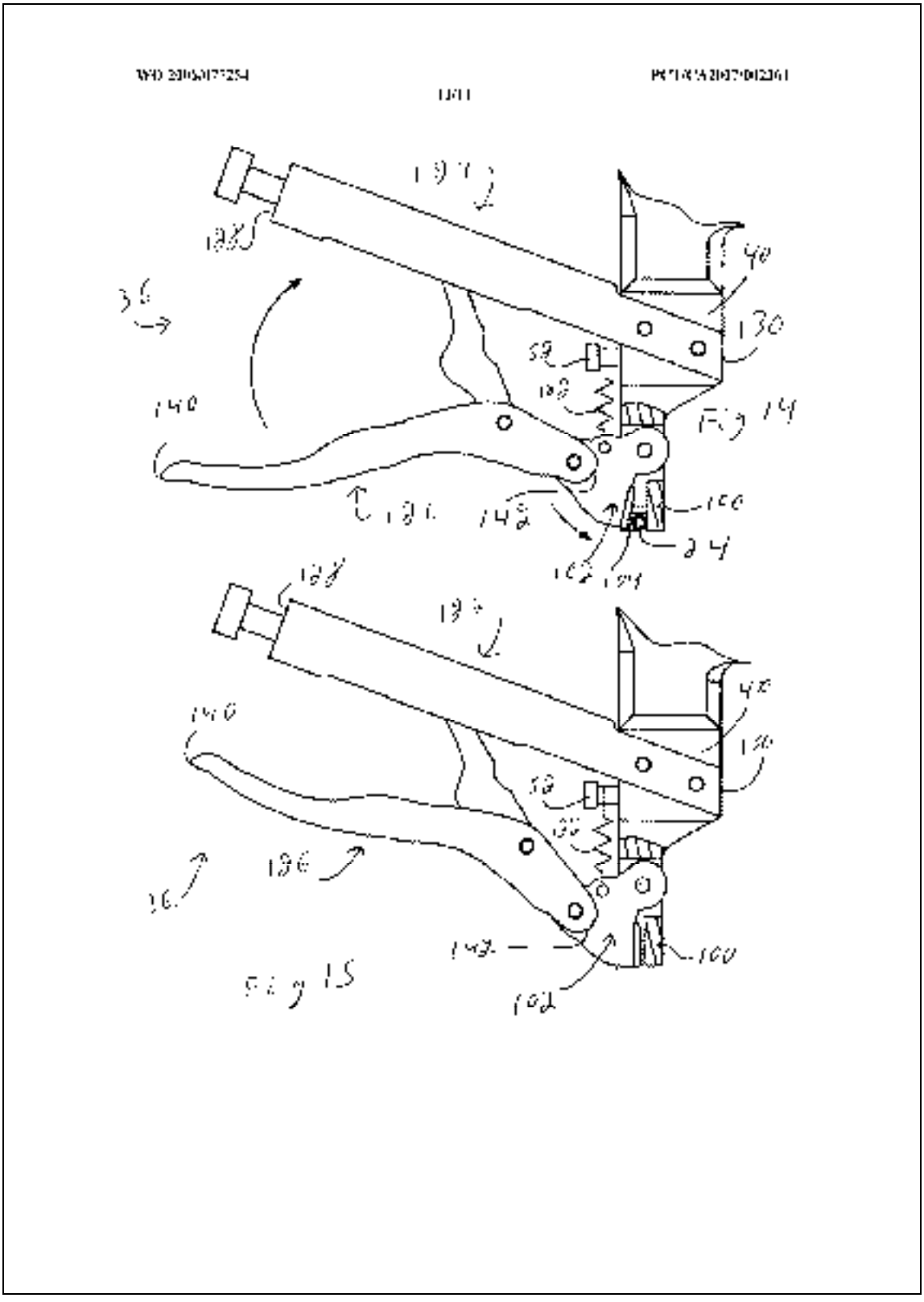
WO 2005077254
PCT/US2005/002261
13/11
Fig 14
Fig 15

ANNEXE IV

MODELING AND TESTING OF A NEW STERNAL CLOSURE DEVICE USING TUBULAR MESH-LIKE SUPERELASTIC NITINOL STRUCTURE

Y. Baril, V. Brailovski, P. Terriault
École de technologie supérieure, Montreal, Quebec, Canada

R. Cartier
Montreal Heart Institute, Montreal, Quebec, Canada

This paper was published as a proceeding of SMST-2006 : International Conference on Shape Memory and Superelastic Technology (mai 2006), Pacific Grove, É.-U. pp. 665-680

ABSTRACT

To reduce a risk of sternal dehiscence of the patients subjected to median sternotomy, a new sternal closure device is developed. This device prevents the cut in and through the sternum bones during aggressive post-surgery physiological activities as coughing, deep breathing and sudden movement. Furthermore, the new device is capable of maintaining a nearly constant pressure between sternum halves during rehabilitation of such patients, thus improving the bone healing conditions. The principal element of such a device consists in a tubular mesh-like structure made of superelastic Nitinol, which tends towards a flat form when it is in contact with the sternum. Finite element modeling and in-vitro laboratory testing of the tubular superelastic device confirm a 30% reduction in contact pressure exerted by this device on the sternum bones, and a 25% increase in compressive pressure between the sternum halves, as compared to the conventional sternal steel wire closure device.

INTRODUCTION

Today, median sternotomy is still one of the most important surgical procedures used to gain access to the thoracic cavity. In 2002, there were 709,000 open-heart surgeries performed in the United States [1]. This surgery begins with the thoracic cavity being opened by cutting the sternum using a specialized power saw, and ends with the sternum being closed in order to stabilize the contact between the two severed sections during osteogenesis. So far, many techniques have been used to bring the separate sides together and to maintain them in contact in order to allow the healing process to proceed (Fig 1).

In the vast majority of cases, surgeons use between 6 to 10 stainless steel wires with a diameter of about 0.7 to 0.9 mm, which they pass through the sternum or around the sternum halves according to a procedure described by Milton [2]. Though this technique provides significant rigidity for the sternum, its major drawback resides in the fact that post-operative stresses on the closure loops may cause the thin wires to cut into and through the bone of the sternum [3, 4].

In an effort to reduce the risk of having the closure structures cut through the bone and to increase the rigidity of the closure, several techniques have been proposed, such as sternal bands [5], staples [6] or rigid plates [7]. These latter systems bring about additional problems such as a risk of haemorrhaging due to their sharp edges [8], pain, and a risk of infection that increases with the size of the foreign object.

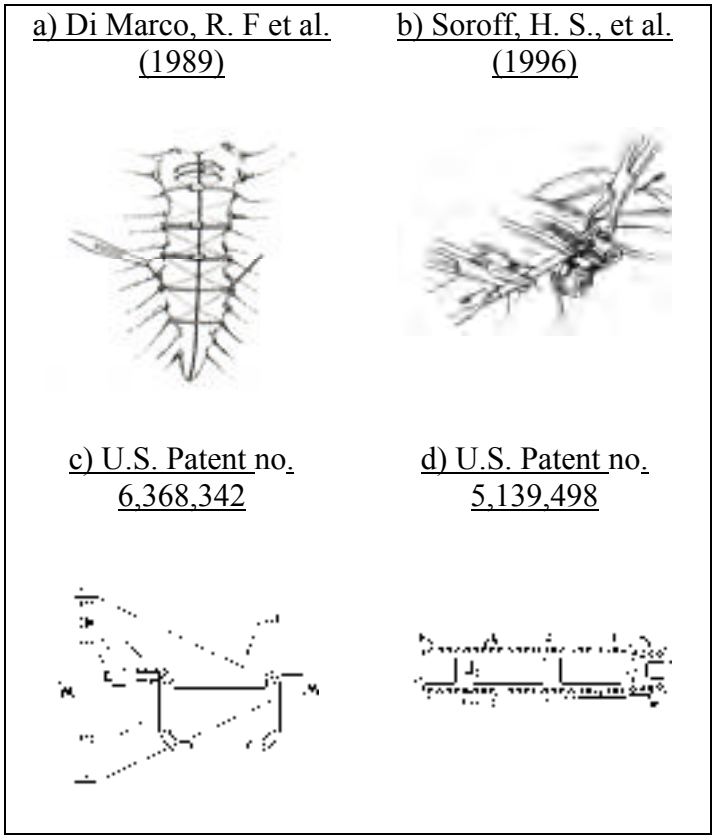

Figure 1 : Modern techniques of sternum closure: a) standard wires; b) metallic band; c) staple; d) rigid plate.

To correct those problems, an original technology[4] combining the advantages of wires and bands is proposed to obtain a closure system that offers ease of manipulation and a stable closure, while decreasing the contact pressure with the sternum and the risk of haemorrhaging. The system developed is a tubular mesh-like device shaped as a braided tube (Fig 2), and made of shape memory alloys (SMA). The proposed structure synergistically combines the advantages associated with tubular geometry with the advantages of the superelastic behaviour of SMA.

[4] Binding component, U.S. Patent Pending US60/633,1523.

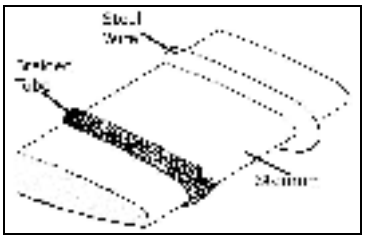

Figure 2 : Braided tube and steel wire surrounding a sternum.

The tubular geometry offers a highly flexible axisymmetric structure, which allows easy installation, which in turn preserves the surrounding tissues and requires the same suturing procedure as steel wires. The tubular form reduces contact stresses through a planar contact with the sternum when it is partially wrapped around the latter. This form resembles the flattened form of a sternal band.

The superelastic behaviour of SMA allows a non-zero force to be applied to the sternum even though the width of the sternum tends to decrease as a result of the nature of the healing process (A-B-C, Fig 3). In addition, SMA benefit from the dynamic interference phenomenon [9], and manifest significant hardening under external impulses (for example coughing) (C-D) thus providing a quasi-constant pressure (D-E) defined by the height of the upper plateau of the superelastic loop. Once the disruption is over, the force applied by the closure system to the sternum returns to its last level on the lower plateau. (E-F-C).

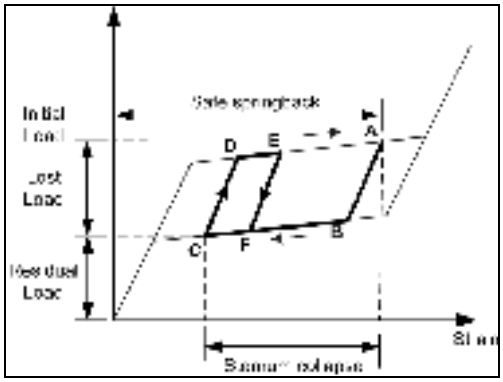

Figure 3: Illustration of the principles of safe springback (A-B-C), dynamic interference (C-D) and quasi-constant pressure (D-E) of SMA.

To take advantage of the SMA suture, a new suture installation device must be designed. The device stretches the suture by applying the calibrated installation force and fixes it in place whit a sleeve.

PERFORMANCE PARAMETERS

Most researchers use the rigidity of the closure system as an optimisation parameter: the greater the rigidity, the better the closure system. However, it is our opinion that the rigidity of the closure system does not reflect its capacity to maintain the compression of the sternal

halves either during post-operative events (for example coughing, deep breathing, sudden movement, etc.), or after the disruption is over.

In fact, it has been determined in several studies [4, 10, 11] that the opening of the sternum occurs well before the application of the maximum force that can be supported by the closure system, irrespective of the type of system used. The reason for this resides in the fact that as the closure system of a given geometry becomes stiffer, a larger part of substantial stresses brought on by post-operative events such as coughing, is transferred to the sternum, and can result in its local depression, and therefore in the sternum opening under applied forces. Once the disruption is over, any permanent depression will result in a loss of compression forces at the interface between the two halves of the sternum, and consequently, in a decrease in the stability of the bond. It should be noted that the mentioned capacity of closure systems to reapply compression on the sternum after removing the load is completely neglected in all the aforementioned studies.

Noting that compression, unlike a static fixation, is a dynamic process since it must be maintained during all dimensional redefinitions occurring in two sternum halves to be bonded, two comparison parameters for closure devices are used in this study: (1) the force needed to open the bond (opening force f_o), and (2) the compressive force reapplied by the closure system once the external disruption is over (residual force f_r).

In the context of this study, closure systems using braided superelastic tubes and those using conventional steel wires are compared with the help of two complementary studies, the first being numerical and the other being experimental. The goal of the first study, which does not take into account the geometric differences between the two sutures, is to evaluate the capacity of a superelastic material to accommodate a large proportion of the force exerted by the closure system on the sternum as a result of an external disruption. The second study consists in the comparative experimental testing of two closure systems under two different modes of loading: single impulse (imitating coughing or sudden movement of the patient) or repeated (deep breathing).

NUMERICAL STUDY

Finite elements analysis is used to evaluate whether superelastic material allows the maintenance of greater residual forces than conventional materials, without consideration for the geometry of the closure system. The thoracic system (cage and sternum closure suture) is considerably simplified for the purpose of this study:

1) The effect of the external disruption of the sternum is reduced to simple forces applied at the contact points of the ribs [11].
2) Since the sternum is sufficiently long, all the sutures of the closure system support an equal fraction of the force applied to the sternum.
3) No bond is considered to be formed between the two halves of the sternum (osteogenesis has not begun).

Description of the model

Given its symmetric nature (force and geometry), only one half of the closure system is represented in the model (Fig 4), whose components are simulated by a series of springs: the closure system is represented by a spring in tension, while the sternum is represented by two springs in compression.

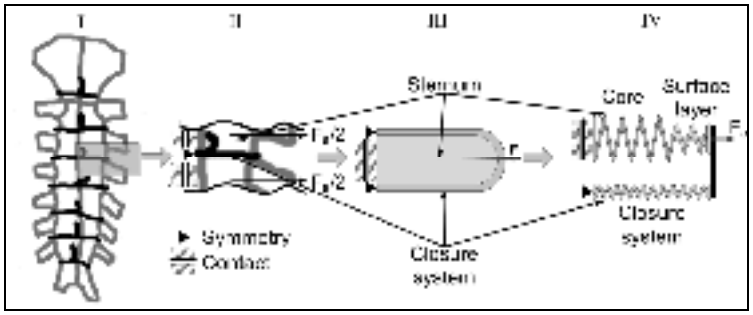

Figure 4: Simplification of the closure device: I - complete sternum (I); II – half of the sternum and of the closure system (the force created by an external load is transferred to the sternum through the ribs; III – cross-section of the sternum; IV – series of springs replacing the sternum and closure system.

The replacement of the sternum by two springs in compression representing the core and the surface layer of the sternum models the interaction between the two halves of the sternum. The core spring offers resistance in compression – and not in tension – thus reflecting the absence of a bond between the two halves of the sternum. This spring represents the volume of the sternum that does not undergo any permanent deformation, but stores a part of the energy resulting from the compression of the closure system during installation. The surface layer spring accepts plastic deformations, and thus simulates the deterioration of the sternum under the action of the closure system. The external force F_e is applied at the interface between the two springs representing the sternum (Fig 4).

Finite elements and corresponding material laws

The finite elements model (FEM) is built with the help of ANSYS 8.0 software by using three types of elements [12]. The *SOLIDE185* finite element is used to model both superelastic and steel closure systems: to represent the superelastic behaviour of the braided tube, the *SMA* material law is applied, while the *BISO* material law is used to simulate the bilinear elastoplastic behaviour of the steel suture. A 1D finite element with the *BISO* material law represents the surface of the sternum with elastoplastic behaviour, while a LINK10 finite element with a *Linear Elastic* material law, which provides resistance in compression, but not in tension, simulates the sternum core.

Note that material constants represent normalized stiffnesses. For example: during the tensile test, an Nº5 *Ethicon* suture wire yields at 425 N under a strain of 0.00470. For a linear element having 1 mm^2 cross-section area, it stiffness is replaced by an equivalent Young

modulus of 90 000 MPa and its yield force, by an equivalent yield stress of 425 MPa (Table 2).

The *SMA* material law parameters (Table 1) are obtained from tensile testing to up to 8% of strain of a Ti-50.8at.% Ni wire with a diameter of 0.71 mm .

Table 6.1:

SMA (ANSYS) material law for superelastic suture

Param.	Unit	Value	Strain-stress curve
E_x	MPa	32000	
ε_{trans}	m/m	0.037	
σ_{Ms}	MPa	335	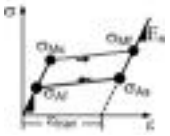
σ_{Mf}	MPa	385	
σ_{As}	MPa	200	
σ_{Af}	MPa	150	

The BISO material law parameters for steel suture (Table 2) are determined from the tensile testing of a Nº5 *Ethicon* suture wire (Somerville, NJ, USA) with a diameter of 0.78 mm.

Table 6.2

BISO (ANSYS) material law for Nº5 Ethicon steel suture

Param.	Unit	Value	Strain-stress curve
E_x	MPa	90000	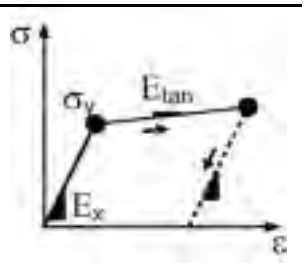
σ_y	MPa	425	
E_{tan}	MPa	1600	

The bone depression of the sternum under the cut-in action of the closing system is modeled using data obtained with polyurethane sternum simulators (*SawBones,* Vashon, WA, USA). For comparative testing of sternum closure devices, solid rigid polyurethane foams are routinely used as an alternative test medium instead of cadavers. Two densities of the sternum simulators used in this study represent two limit cases defined by Hale et al. [13]: a polyurethane with a 0.24 g/cm^3 density represents a "weak" sternum, while a polyurethane with a 0.48 g/cm^3 density represents a "strong" sternum.

The material law parameters for the BISO sternum surface layer (table 6.3) are obtained from the indentation testing of a 0.8 mm thick steel plate into a polyurethane block that is 12.5 mm thick and 10 mm wide. The rigidity of the sternum core is set to 20 times that of the surface layer in order to avoid any significant modification of the overall sternum rigidity resulting from the surface layer depression. The half-width of the sternum is established at 25 mm, and the thickness of the surface layer is set at 5 mm, and it is assumed that the latter completely absorbs the closure system penetration.

Table 6.3

BISO (ANSYS) material law for the surface layer and
Linear Elastic material law (ANSYS), for the sternum core

Mat law		Surface layer		Core	
		BISO		Linear Elastic	
Param.	Unit	0.24*	0.48*	0.24*	0 48*
E_x	MPa	735	5200	14 700	104 000
E_{tan}	MPa	140	1050		
σ_y	MPa	67	400		

*Polyurethane density (g/cm^3)

Calculation algorithm

The numerical model is aimed at comparing the opening (f_o) and residual (f_r) forces provided by SMA and steel sternum sutures.

It is assumed that the rigidity of the SMA closure system can be varied by modifying its relative stiffness between 0.05 and 0.35, for a 0.24 g/cm^3 sternum and between 0.5 and 1.3, for a 0.48 g/cm^3 sternum, while the relative stiffness of the steel suture remains constant and equal to 1 (the rigidity of the SMA braided closure system is in fact adjustable through the modification of its geometry and number of filaments [14]).

The initial force applied during the installation of the system is set at F_i=60 N for a 0.24 g/cm^3 sternum and at F_i=350 N, for a 0.48 g/cm^3 sternum since these values are close to their respective resistance limits for penetration. The force resulting from an external disruption varies between F_e=0 and 150 N for the low-density polyurethane and between F_e=0 and 600 N, for the high-density polyurethane.

The algorithm of the numerical study can be summarized as follows (see Table 4, for numerical values):

(1)Density is selected for the sternum simulator (either 0.24 or 0.48 g/cm^3);
(2)Material is chosen for the closure suture; if it is SMA, its relative stiffness is given an initial value, and if it is steel, its relative stiffness is set at 1;
(3)Installation force (F_i) is applied to the closure system;

(4)External disruption is simulated by applying an initial external force F_e; if this force causes the opening of the sternum, the opening force f_0 is recorded;
(5)External force is removed and residual force f_r is recorded;
(6)If $f_r > 0$, the external force is incremented and steps (4)–(5) are repeated until $f_r=0$ or maximum external force allowed for a given sternum simulator.
(7)The relative stiffness of the SMA suture is incremented and steps (3)–(7) are repeated.

Table 6.4

Sequence of FEM procedure

Materials		F_i (N)	Suture relative stiffness; increment	External force F_e range; increment, (N)
Suture	Sternum density (g/cm^3)			
Steel	0.24	60	1	[0-150]; 5
	0.48	350		[0-600]; 20
SMA	0.24	60	[0.05-0.35]; 0.05	[0-150]; 5
	0.48	350	[0.5-1.3]; 0.1	[0-600]; 20

Results of the Numerical Study

The results of the numerical study for the 0.24 g/cm^3 sternum are summarized in table 6.5. As an example, Fig 5 illustrates that an SMA suture with an equivalent diameter of 0.22 mm maintains a non-zero residual force at the sternum interface ($f_r \geq 0$) after an external force F_e, which is 60% greater than that supported by a ∅0.78 mm steel wire: 145 N towards 90 N. However, this is at the expense of a larger sternum opening: after an identical external force of 90 N, the SMA suture allows a sternum opening of 1.1 mm, while the steel suture allows an opening of 0.8 mm. It is also important to note that the minimum sternum opening force f_o is approximately 70 N for all sternum closure devices, which is comparable to the experimentally obtained data [4].

Table 6.5

Results of the numerical study for the 0.24 g/cm^3 sternum

Wire type	Suture relative stiffness	Equivalent diameter (mm)	External force F_e corresponding to f_r=0 (N)
SMA	0.05	0.16	100 (wire break)
	0.10	0.22	145
	0.15	0.27	135
	0.20	0.32	95
Steel (n°5)	1.00	0.78	90

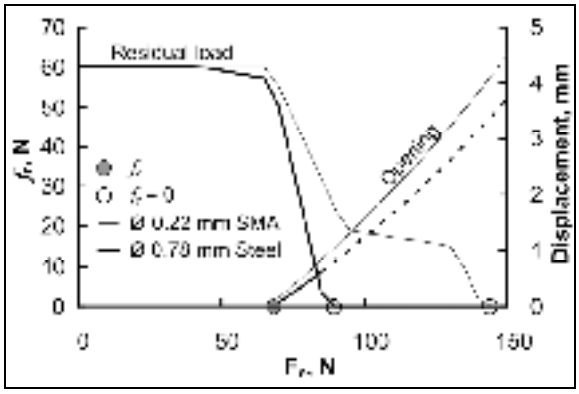

Figure 5: Residual force and sternum opening as functions of the external force for the 0.24 g/cm^3 sternum (dotted lines on the opening curves indicate that the sternum is no longer closed once the disruption is over (f_r = 0)).

For the 0.48 g/cm^3 sternum, SMA sutures allow a residual force to be maintained for external forces F_e greater than 600 N, which is more than twice the force of a severe coughing fit [11]. In comparison, the residual force provided by steel sutures becomes zero after an external force of 400 N.

EXPERIMENTAL STUDY

To consider both the geometry and the superelastic properties of the SMA sternum closure system, a series of experimental tests is undertaken.

Description of the testing bench

Fig 6 shows the outline of the testing bench used. Two identical closure systems (1) are installed simultaneously on the polyurethane blocks (2) simulating the sternum. The installation force is applied with the help of two adjustable loading clamps (3). Two LC703-100 load cells (4) (*Omega*, Stamford, CT, USA) installed on each extremity of the testing frame (5) allow the force at the sternum interface to be measured. An *Enduratec ELF 3200* tensile testing machine (6) is used to apply external force. LabView 6.0 (*National Instruments Corp.*, Austin, TX, USA) data acquisition system registers the real time displacement of the testing machine's piston as well as the forces measured by the load cells.

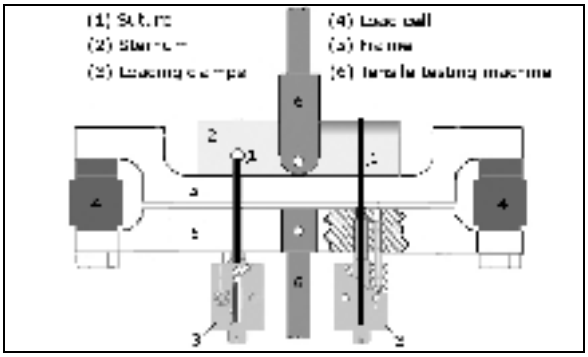

Figure 6: Schematics of the testing bench: closure system passes transsternally (left) and peristernally (right).

Components used

A comparison is made between two closure devices: (1) ∅0.78 mm Nº 5 *Ethicon* steel wire and ∅3 mm SMA braided 12.5 mm pitch tube made of 24 ∅0.1 mm filaments of Ni-Ti-Cr alloy.

The 25x10x90 mm polyurethane blocks with a density of 0.24 and 0.48 g/cm^3 are used to simulate sternum bones. One of the sides of the samples used for a peristernal installation (Fig 6, right) is rounded to simulate the edge of the sternum, and those used for the transsternal installation (Fig 6, left) feature 2.4 mm diameter holes pierced 10 mm from the symmetric plane in order to allow the threading of the suture.

The force-displacement diagrams of the sternum simulators (indentation testing) and of the two types of sternum sutures (tensile testing) are shown in Fig 7. Given that a sternum bone is contoured by a suture loop, the tension force on each side of the suture is supported by the one-half of the sternum. Consequently, the axial force-displacement characteristic of each suture is compared to that of the one-half of the sternum simulator (see Fig 4).

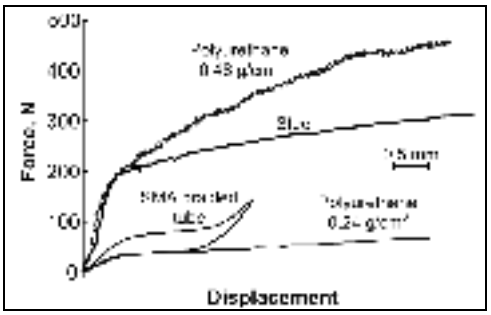

Figure 7: Force-displacement diagrams of the principal components of the testing bench.

Experimental Procedure

T**esting modalities**

The experiment is planned to allow two closure systems to be compared under different exploitation conditions: severe coughing (single impulse loading) or deep breathing (cyclical loading), in the case of peristernal or transsternal installations, and for two sternum densities (0.24 and 0.48 g/cm^3) – see table 6.6.

Table 6.6.

Experimental testing modalities

Variable	Modalities	
Closure system	Steel suture	SMA suture
Polyurethane density	0.24 g/cm^3	0.48 g/cm^3
Threading	Transsternal	Peristernal
Loading	Single impulse	Cyclic

To perform testing, the following two-step procedure is applied:

1. Application of the installation (initial) force Fi

The initial force F_i applied to the median sternum closure is a function of the density of the polyurethane sternum simulator. The higher the density, the higher the initial force that can

be applied. The initial force for the 0.24 g/cm^3 sternum is set at the same level as for the numerical study: 60 N (see table 6.4). For the 0.48 g/cm^3 sternum, it is set at 200 N.

2. Application of the external force Fe

The Single impulse loading mode simulates coughing or sudden movement, and consists in a series of loading-unloading cycles with incrementally increased amplitude. Each cycle takes 10 seconds, and a 15-second dwell time at zero force is respected prior to each subsequent cycle. At each cycle, the force is increased by 25 N, up to a maximum value allowed, which is 125 N for the 0.24 g/cm^3 sternum and 445 N for the 0.48 g/cm^3 sternum (the latter value is limited by the capabilities of the testing machine). The measurement of the residual force f_r is performed prior to each force increment.

The Cyclic loading mode simulates deep breathing and consists in 500 cycles of a sinusoidal force varied with a 0.5 Hz frequency between 0 and 60 N (0.24 g/cm^3 sternum) and 0 and 200 N (0.48 g/cm^3 sternum). The measurement of the residual force is completed after the 500th cycle at zero load.

Results

The *StatGraphics* software (StatPoint Inc., Herndon, VA) is used to analyse the results obtained [15]. The outcome variable is the relative residual force $R=f_r/F_i$. Fig 8 demonstrates that the use of the SMA suture compared to steel suture allows an average gain of 30% in the relative residual force value as compared to using a steel suture. The results for the other statistically significant ($p \leq 0.5$) input variables show that the peristernal installation guarantees higher residual forces than the transsternal installation, and that a large single impulse force causes less damage than light repetitive forces. The effect of the sternum density variation is proven to be not significant.

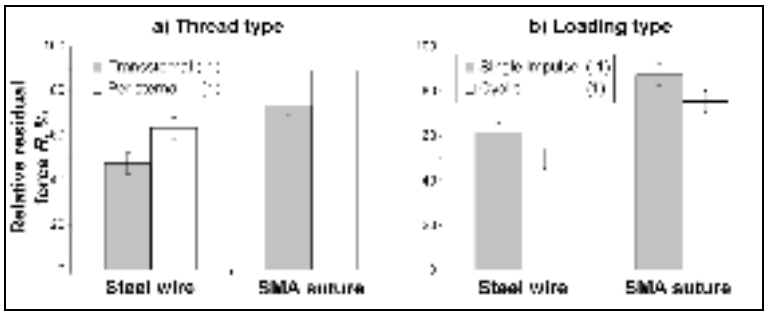

Figure 8: Relative residual force $R=f_r/F_i$ provided by both closure systems: a) influence of the installation mode (peristernal versus transsternal); b) influence of the loading mode (single impulse versus repetitive loading).

DISCUSSION

The experimental study allows the combined effect of the superelastic behaviour and of the tubular geometry of the SMA to be taken into account. In the context of this study, a unique 24-filament SMA braided tube with an inside diameter of 3 mm is tested with sternum simulators having two limit densities (see Fig 7):

1) For the 0.24 g/cm^3 sternum, the 24-filament SMA suture is too rigid. It is mainly the increased contact area between the sternum and closure system which is responsible for the 30% gain in residual force when compared to a steel suture.
2) For the 0.48 g/cm^3 sternum, the 24-filament SMA suture is too compliant. Nevertheless, the advantage of using a superelastic suture leads to a similar 30% gain in residual force as compared to a steel suture.
3) In fact, the 24-filament SMA suture would have demonstrated maximum efficiency for an intermediate density 0.32 g/cm^3 Sawbones sternum simulator (these tests are under preparation).

Principles of the SMA Suture Selection

General remarks

To prevent failure of the sternum suture caused by post-operative disturbances such as coughing, while maximizing the residual compressive force between sternum halves when the disturbance is over, the optimum force-displacement characteristic to be ensured by the SMA suture should comply with following conditions (see Fig 9):

I. The force of suture prestrain during installation up to approximately 6% of elongation should be slightly lower of the yield limit of the sternum bone. (If the suture prestrain force is under this limit, sternum opening will occur at lower external forces; if this prestrain exceeds this limit, sternum bones will be damaged by the suture.)

II. The suture should be capable of sustaining maximum forces generated by post-operation disturbances. (If this condition is not respected, suture failure can result from severe coughing fit, for example.)

Note: The narrower the mechanical hysteresis of the superelastic loop (F_u-F_l), the lower the closure force fluctuations during healing process and the higher the residual compressive

force between sternum halves. Moreover, the condition $F_l>0$ should necessarily be respected to benefit from superelastic behaviour of the suture. The later condition becomes especially important given possible shift downward of the superelastic loop during cyclic loading.

To summarize, the SMA suture should simultaneously comply with three conditions:

$$\begin{cases} F_u \le \text{sternum yield}\,(F_{min}) \\ F_r \ge \text{maximum disturbance}\,(F_{max}) \\ F_l > 0\,(\text{preserving superelasticity}) \end{cases} \quad (1)$$

Based on these criteria, a force-displacement tensile loop of the superelastic tubular braided suture can be traced as shown in Fig 9. To reproduce this behaviour, geometric parameters of the SMA braided structure (number of filaments and pitch of braiding) should be adequately selected for a given SMA filament.

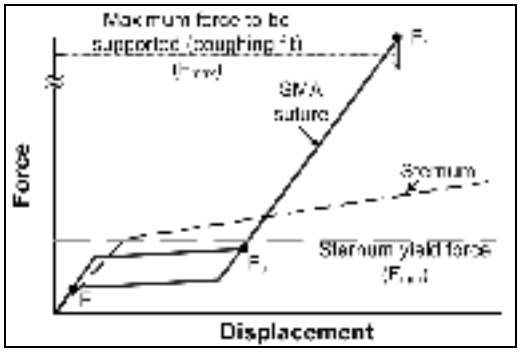

Figure 9: Selection of the SMA suture force-displacement characteristic.

Example

Sternum properties

SMA sutures are mainly beneficial for patients having risks of sternum fragmentation during post-operative disturbances. Since such patients generally have osteoporosis problems leading to a gradual decline of bones resistance, 15-grade 0.24 g/cm^3 polyurethane foam represents an ideal testing material for this example.

SMA filament selection

To manufacture the SMA suture, a 0.1 mm filament of BTR-BB (Ti-50.7at%Ni) alloy with 40% of cold-work supplied by *Memry corp.* (Bethel, CT, USA) is considered.

SMA braided structure manufacturing

To manufacture a superelastic suture, 24 filaments with a 12.7 mm pitch are braided on a 3.2 mm aluminium core using *Wardwell* braiding machine. Without removing the core, the braided structure is then heat treated at 300°C (1h) to obtain stable tubular shape.

Characterization of SMA filament and braided structure

To compare superelastic properties of the 24-filament braided structure with those of a single filament (both heat treated at 300°C, 1h), tensile testing is performed using an *Enduratec* ELF 3200 testing machine. Ten cycles up to 8% of strain with 0.092 mm/s displacement rate are used to stabilize the material behaviour and the eleventh cycle is performed until failure (Fig 10a and 10b).

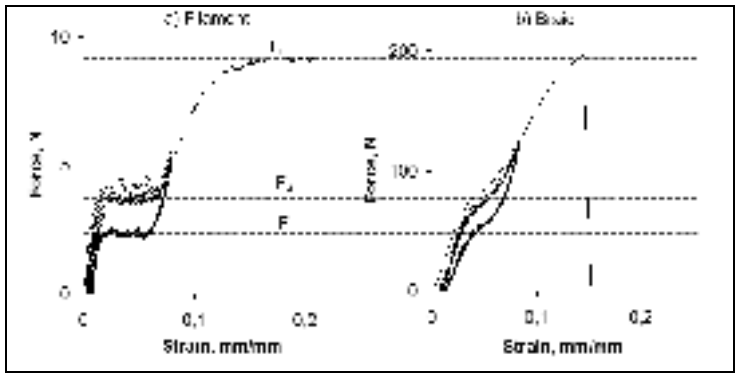

Figure 10: Force-displacement diagrams for a single 0.1 mm filament and 24-filament braided structure (heat treatment: 300°C, 1h)

Table 6.7 compares critical forces (F_r, F_u, F_l) obtained for a single filament and 24-filament braided structure for the 10^{th} superelastic loop and during failure testing. It can be observed that the critical forces for the braided structure are proportional to those measured for a single filament with a factor approximately equal to the number of filaments used.

Table 6.7

Critical forces for a single 0.1 mm filament and 24-filament braided suture after 10-cycles stabilization in tension (average of 4 tests).

Critical forces	Filament	Braid	Ratio Filament/Braid
F_r, N	9.2	195	21.2
F_u, N	3.7	91	24.6
F_l, N	2.2	45	20.5

Selection of number of filaments

While it is assumed that a variety of braids can be offered, and since the braid behaviour is roughly proportional to the number of filaments, it is now possible to find the number of filaments needed to produce a suture that will be adequate for the given 24 g/cm^3 sternum. To perform this selection, a yield force for the sternum is taken as 35 N and the maximum force for post-operative disruption, 125 N. Note that the latter force is evaluated on the basis of 6 sutures per sternum and can be decreased if the number of sutures increases.

In Fig 11, the critical forces F_r and F_u of the braided structure traced as a function of the number of filaments are superposed on the limit forces to be respected by the suture.

Applying now the criteria (1), it can be seen from Fig 11, that to prevent sternum damage by the suture, the number of filaments should not exceed 9. In this case however, the suture resistance to failure is only 75 N, which is significantly lower than the maximum force of post-operative disturbance (125 N) and does not prevent the suture from failure. To comply with the minimum suture resistance condition, 10 sutures per sternum instead 6 should be used to decrease the maximum force applied to the suture down to the sustainable 75 N.

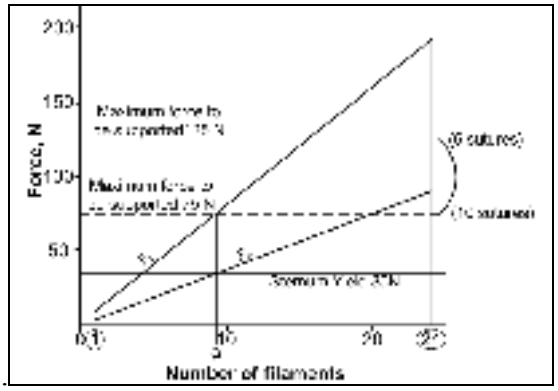

Figure 11: Critical forces of the superelastic braided structure as a function of a number of filaments; the yield force for the 0.24 g/cm^3 sternum and maximum forces from the external disturbances for the case of 6 and 10 sutures per sternum.

Adjustment of the heat treatment conditions

There exists another possibility to modify properties of the filament and therefore of the braded structure. It consists in varying post-braiding thermal treatment conditions. As an example, critical forces obtained after 10-cycles training of the BTR-BB 0.1 mm filament are plotted as a function of heat treatment temperature in Fig 12.

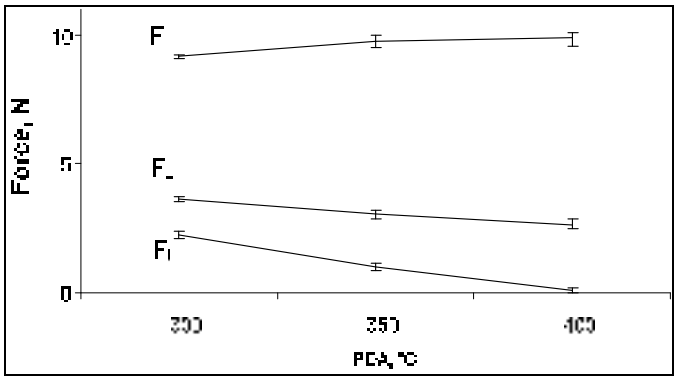

Figure 12: Critical forces for a single 0.1 mm filament as a function of heat treatment temperature (1 h); 4 tests average.

It can be seen that both the upper and the lower plateau forces are significantly modified by shape-setting processing: the higher the heat treatment temperature, the lower the critical forces of the superelastic loop. (The failure resistance of the filament is not significantly affected by thermal treatment.) This phenomenon can be used to increase the number of filaments in the suture from 9 to 13 by performing thermal treatment at 350^{o}C instead of 300^{o}C. This modification will improve the smoothness of the suture surface and increase the contact area between the suture and the sternum. Note that these enhancements will be done at the expense of the higher mechanical hysteresis of the suture and therefore of the higher force variations during sternum healing.

It is also clear that 400°C heat treatment should be avoided because in this case, the low plateau force dangerously approaches to zero, which can lead to a permanent deformation of the suture.

SUTURE INSTALLATION

The suture installation procedure is shown in Fig 13. The treading around or through the sternum (I) and a preliminary closure of the sternum halves (II) are similar to the installation of any suture involving a joint. On step III, the new installation device acts in two ways. Firstly, it applies a calibrated prestrain force (F_i) which is just above the end of the direct transformation plateau. As mentioned, this force maximises the safe springback of the SMA suture. Secondly, it will set the joint. To finish the installation procedure, loose ends are cut near the joint.

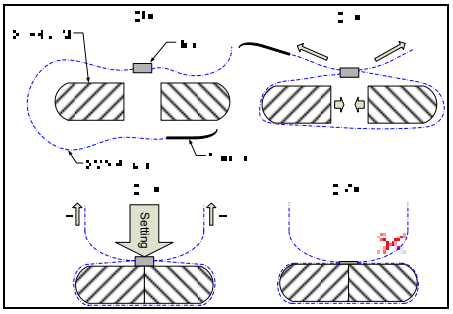

Figure 13: Suture installation procedure: I) suture treading; II) first closure of sternum halves; III) suture prestrain and joint setting; IV) suture cutting.

CONCLUSION

To reduce the risk of sternum breakage, a median sternotomy closure using a superelastic tubular braid is proposed. The numerical model allows the net benefit of the SMA suture to be demonstrated against the performance of a N°5 *Ethicon* steel suture. It is experimentally proven that the SMA suture preserves compression at the sternum interface when an external disruption occurs, at forces 30 to 60% greater than those endured by the N°5 *Ethicon* suture regardless of the installation technique used (peristernal or transsternal), the type of external force applied (single impulse or repetitive), and the sternum density.

For the remainder of the project, the use of 0.1 mm BTR-BB wire of *Memry Corporation* is considered. The dynamic fatigue testing of the SMA braided suture will be performed first in axial tension and then installed on the sternum model. These two steps are essential for the completion of the engineering stage of the project and for the clinical study to be started.

ACKNOWLEDGEMENT

This work has been performed in the framework of the research program supported by the Natural Sciences and Engineering Research Council of Canada (NSERC) and Valeo Management L.P.

BIBLIOGRAPHY

[1] *Heart disease and stroke statistics - 2005 Update*. 2005, American Heart Association: Dallas. p. 50.

[2] Milton, H., "Mediastinal surgery," *Lancet*, Vol. 1 (1987), pp. 872-875.

[3] Robicsek, F., H. K. Daugherty and J. W. Cook, "The prevention and treatment of sternum separation following open-heart surgery," *J. Thorac. Cardiov. Sur.*, Vol. 73, No. 2 (1977), pp. 267-268.

[4] Casha, A. R., et al., "Fatigue testing median sternotomy closures," *Eur J Cardio-Thorac*, Vol. 19, No. 3 (2001), pp. 249-253.

[5] Soroff, H. S., et al., "Improved sternal closure using steel bands : Early experience with three-year follow-up," *Ann. Thorac. Sur.*, Vol. 61, No. 4 (1996), pp. 1172-1176.

[6] Combes, J. M., et al., "Fermeture des sternotomies à l'aide des agrafes de Cotrel," *Ann. Chir.*, Vol. 47, No. 2 (1993), pp. 179-183.

[7] Sargent, L. A., et al., "The healing sternum: a comparison of osseous healing with wire versus rigid fixation," *Ann. Thorac. Sur.*, Vol. 52, No. 3 (1991), pp. 490-494.

[8] Losanoff, J. E., B. W. Richman and J. W. Jones, "Disruption and infection of median sternotomy: a comprehensive review," *Eur J Cardio-Thorac*, Vol. 21, No. 5 (2002), pp. 831-839.

[9] Duerig, T., A. Pelton and D. Stockel, "Superelasitic Nitinol for Medical Devices," *Med. Plast. Buimat. Mag. MPV Arch.* (1997)

[10] McGregor, W. E., D. R. Trumble and J. A. Magovern, "Mechanical analysis of midline sternotomy wound closure," *J. Thorac. Cardiov. Sur.*, Vol. 117, No. 6 (1999), pp. 1144-1145.

[11] Casha, A. R., et al., "A biomechanical study of median sternotomy closure techniques," *Eur J Cardio-Thorac*, Vol. 15, No. 3 (1999), pp. 365-369.

[12] ANSYS, *ANSYS*. 2003: Canonsburg, Pa, US.

[13] Hale, J. E., D. D. Anderson and G. A. Johnson. "A polyurethane foam model for characterizing suture pull-through properties in bone," *Proc 23rd Annual Meeting of the American Society of Biomechanics*, University of Pittsburgh, October 21-23 1999, 2.

[14] Baril, Y., *Design and Modelisation of a Sternum Closure System (in French)*, in *Mecanic*. 2004, École de technologie supérieure: Montreal. p. 180.

[15] Montgomery, D. C., Design and analysis of experiments. 4th edition ed, ed. J.W.a. Sons, (New York, 1996). 418 pages.

LISTE DE RÉFÉRENCES

Abboudi, S. Y. 1996. *Surgical clamping assemblies and methods of use*. 9 p. U.S. Patent 5,849,012.

Abboudi, S. Y. 2001. *Apparatus and methods for clamping split bone sections*. U.S. Patent 6,287,307.

Astudillo, L. 1992. *Device for closing sternum in heart surgery*. U.S. Patent 4,201,215.

Bahia, M. G. A., B. M. Gonzalez et V. T. L. Buono. 2006. « Fatigue behaviour of nickel-titanium superelastic wires and endodontic instruments ». Fatigue & Fracture of Engineering Materials &Structures, vol. 29, p. 518-523.

Bahia, M. G. d. A., R. Fonseca Dias et V. T. L. Buono. 2006. « The influence of high amplitude cyclic straining on the behaviour of superelastic NiTi ». International Journal of Fatigue, vol. 28, n^{o} 9, p. 1087-1091.

Baril, Y. 2004. « Conception et modélisation d'un système de fermeture du sternum ». Mémoire de maîtrise, Montréal, École de technologie supérieure, 180 p.

Baril, Y., V. Brailovski, M. Chartrand, P. Terriault et R. Cartier. 2009. « Median sternotomy: comparative testing of braided superelastic and monofilament stainless steel sternal sutures ». Proceedings of the Institution of Mechanical Engineers, Part H: Journal of Engineering in Medicine, vol. 223, n^{o} 3, p. 363-374.

Baril, Y., V. Brailovski, P. Terriault et R. Cartier. 2008. « Modeling and testing of a new sternal closure device using tubular mesh-like superelastic structure ». Présenté à: SMST-2006, International Conference on Shape Memory and Superelastic Technology (May 2006), qui s'est déroulé à Pacific Grove, Ca, U.S.A., p. 665-680.

Brailovski, V., Y. Baril, P. Terriault et R. Cartier. 2007. *Closure apparatus*. 39 p. PCT/CA2007/002361.

Brailovski, V., R. Cartier, P. Terriault et Y. Baril. 2006. *Binding component*. 72 p. WO/2006/060911.

Brown, R. P. 1998. *Apparatus and method for surgically securing bone parts*. U.S. Patent 5,722,976.

Bruhin, R., U. A. Stock, J.-P. Drücker, T. Azhari, J. Wippermann, J. M. Albes, D. Hintze, S. Eckardt, C. Könke et T. Wahlers. 2005. « Numerical Simulation Techniques to Study the Structural Response of the Human Chest Following Median Sternotomy ». The Annals of Thoracic Surgery, vol. 80, n^{o} 2 (2005/8), p. 623-630.

Casha, A. R., et M. Gauci. 2003. « Mechanical comparison of three sternotomy closure techniques using a polyurethane foam sternal model ». The Annals of Thoracic Surgery, vol. 75, n° 6, p. 2009-2010.

Casha, A. R., M. Gauci, L. Yang, K. P. H. et G. J. Cooper. 2001a. « Reply to Jutley et al. ». European Journal of Cardio-Thoracic Surgery, vol. 20, n° 5, p. 1072-1073.

Casha, A. R., M. Gauci, L. Yang, M. Saleh, P. H. Kay et G. J. Cooper. 2001b. « Fatigue testing median sternotomy closures ». European Journal of Cardio-Thoracic Surgery, vol. 19, n° 3 (15 December 2000), p. 249-253.

Casha, A. R., L. Yang et G. J. Cooper. 1999. « Measurement of chest wall forces on coughing with the use of human cadavers ». Journal of Thoracic and Cardiovascular Surgery, vol. 118, n° 6 (Dec), p. 1157-1158.

Casha, A. R., L. Yang, P. H. Kay, M. Saleh et G. J. Cooper. 1999. « A biomechanical study of median sternotomy closure techniques ». European Journal of Cardio-Thoracic Surgery, vol. 15, n° 3 (Mar), p. 365-369.

Chartrand, M. 2008. « Banc d'essai et méthodologie pour essais comparatifs sur systèmes de fermeture du sternum ». Montreal, École de technologie supérieure, 77 p.

Chartrand, M., V. Brailovski et Y. Baril. 2009. « Test Bench and Methodology for Sternal Closure System Testing ». Experimental Techniques (Accepted january 5th, 2009).

Cheng, W., D. E. Cameron, K. E. Warden, J. D. Fonger et V. L. Gott. 1993. « Biomechanical study of sternal closure techniques ». The Annals of Thoracic Surgery, vol. 55, n° 3 (Mar), p. 737-740.

Cheung, G. S. P., et B. W. Darvell. 2007. « Low-cycle fatigue of NiTi rotary instruments of various cross-sectional shapes ». International Endodontic Journal, vol. 40, n° 8, p. 626-632.

Chinzei, K., R. Kikinis et F. A. Jolesz. « MR compatibility of mechatronic devices: Design criteria ». Présenté à: Medical Image Computing and Computer-Assisted Intervention, Miccai'99, Proceedings, p. 1020-1030.

Chun-Ming, S., S. Yea-Yang, L. Shing-Jong et S. Chun-Che. 2005. « Failure analysis of explanted sternal wires ». Biomaterials, vol. 26, n° 14, p. 2053-9.

Cohen, D. J., et L. V. Griffin. 2002. « A biomechanical comparison of three sternotomy closure techniques ». The Annals of Thoracic Surgery, vol. 73, n° 2 (Oct), p. 563-568.

Crossett, E. S., L. Willard et N. Albuquerque. 1980. *Apparatus and method for surgically securing bone parts*. U.S. Patent 4,201,215.

Dasika, U. K., D. R. Trumble et J. A. Magovern. 2003. « Lower sternal reinforcement improves the stability of sternal closure ». The Annals of Thoracic Surgery, vol. 75, n° 5 (May), p. 1618-1621.

Di Marco, R. F. J., M. W. Lee, S. Bekoe, K. J. Grant, G. F. Woelfel et R. V. Pellegrini. 1989. « Interlocking figure-of-8 closure of the sternum ». The Annals of Thoracic Surgery, vol. 47, n° 6 (Feb 20, 1989), p. 927-929.

Duerig, T., A. Pelton et D. Stockel. 1997. « Superelastic Nitinol for Medical Devices ». Medical Plastics and Biomaterial Magazine MPV archive (March), p. 1-14.

Eggers, G. W. N., T. O. Shindler et C. M. Pomerat. 1949. « The influence of the contact-compression factor on osteogenesis in surgical fractures ». Journal of Bone and Joint Surgery, vol. 31-A, n° 4 (Oct. 1949), p. 693 à 716.

Eiselstein, L. E., R. A. Sire et B. A. James. 2006. « Review of fatigue and fracture behavior in NiTi ». Présenté à: Materials & Processes for Medical Devices Conference III (14-16 November), qui s'est déroulé à Boston, Ma, U.S.A, p. 135-147.

Gabbay, S., D. Randall et S. Hills. 1989. *A Sternum closure device*. U.S. Patent 4,802,477.

Gong, X., A. R. Pelton, T. Duerig et H. A. 2005. « Cyclic properties of superelastic nitinol tubing ». Présenté à: Materials & Processes for Medical Devices Conference (25-27 Aug.), qui s'est déroulé à St. Paul, Mn, USA, p. 26-31.

Gray, H., et W. H. Lewis. 1918. « Anatomy of the Human Body ». In. web. < www.bartleby.com >.

Hale, J. E., D. D. Anderson et G. A. Johnson. « A polyurethane foam model for characterizing suture pull-through properties in bone ». Présenté à: 23rd Annual Meeting of the American Society of Biomechanics (October 21-23), qui s'est déroulé à University of Pittsburgh, p. 2.

Harrison, W. J., et Z. C. Lin. 2001. « The study of nitinol bending fatigue ». Présenté à: SMST-2000, International Conference on Shape Memory and Superelastic Technologies (30 april to 4 may), qui s'est déroulé à Pacific Grove, Ca, U.S.A., p. 391-396.

Inconue. 2002. « Glossary Version6 ». In. Image. < http://www.gmedmedia.com/glossv6/pages/031sternotomy.htm >.

John, L. C. H. 2008. « A mathematical analysis of alternative sternal wound closures - An aid to reducing cardiac surgical mortality ». Bio-Medical Materials and Engineering, vol. 18, n° 1, p. 35-44.

Johnson, G. A., J. F. Antaki, J. A. Magovern, M. R. Frushell, T. D. Will et J. A. Holmes. 2002. *Hard or soft tissue closure*. U.S. Patent 6,485,504.

Jutley, R. S., D. E. T. Shepherd et D. W. L. Hukins. 2003. « Fatigue strength of a wire passing through a cannulated screw: Implications for closure of the sternum following cardiac surgery ». Proceedings of the Institution of Mechanical Engineers Part H: Journal of Engineering in Medicine, vol. 217, n° 3, p. 221-226.

Jutley, R. S., D. E. T. Shepherd, R. R. Jeffrey et D. W. L. Hukins. 2001. « Calculating stress magnitude between sternotomy closures and sternum ». European Journal of Cardio-Thoracic Surgery, vol. 20, n° 5 (25 July 2001), p. 1071.

Kiessling, A.-H., F. Isgro, U. Weisse, A. Moltner, W. Saggau et J. Boldt. 2005. « Advanced Sternal Closure to Prevent Dehiscence in Obese Patients ». The Annals of Thoracic Surgery, vol. 80, n° 4 (2005/10), p. 1537-1539.

Lemer, J. 2002. *Strernum closure device and pincers for mounting staples and approximator brackets*. U.S. Patent 6,368,342.

Losanoff, J. E., M. D. Basson, S. A. Gruber, H. Huff et F. H. Hsieh. 2007. « Single wire versus double wire loops for median sternotomy closure: Experimental biomechanical study using a human cadaveric model ». Annals of Thoracic Surgery, vol. 84, n° 4 (Oct), p. 1288-1293.

Losanoff, J. E., A. D. Collier, C. C. Wagner-Mann, B. W. Richman, H. Huff, F.-h. Hsieh, A. Diaz-Arias et J. W. Jones. 2004. « Biomechanical comparison of median sternotomy closures ». The Annals of Thoracic Surgery, vol. 77, n° 1 (January), p. 203-209.

Losanoff, J. E., J. W. Jones et B. W. Richman. 2002. « Primary closure of median sternotomy: techniques and principles ». Cardiovascular Surgery, vol. 10, n° 2 (Apr), p. 102-110.

Losanoff, J. E., B. W. Richman et J. W. Jones. 2002. « Disruption and infection of median sternotomy: a comprehensive review ». European Journal of Cardio-Thoracic Surgery, vol. 21, n° 5 (May 5), p. 831-839.

Magovern, J. A. 2000. *System, apparatus and method for closing severed bone or tissue of a patient*. U.S. Patent 6,033,429.

McCool, F. D. 2006. « Global Physiology and Pathophysiology of Cough: ACCP Evidence-Based Clinical Practice Guidelines ». Chest, vol. 129, n° 1_suppl (January 1, 2006), p. 48S-53.

McGregor, W. E., M. Payne, D. R. Trumble, K. M. Fakas et J. A. Magovern. 2003. « Improvement of Sternal Closure Stability With Reinforced Steel Wires ». The Annals of Thoracic Surgery, vol. 76, n° 5, p. 1631-1634.

McGregor, W. E., D. R. Trumble et J. A. Magovern. 1999. « Mechanical analysis of midline sternotomy wound closure ». Journal of Thoracic and Cardiovascular Surgery, vol. 117, n° 6 (june), p. 1144-1145.

Miller, I., et A. S. 2003. *Method and apparatus for closing a severed sternum*. U.S. Patent 6,540,769.

Milton, H. 1987. « Mediastinal surgery ». Lancet, vol. 1, p. 872-875.

Morgan, N. B., J. Painter et A. Moffat. 2004. « Mean Strain Effects and microstructural observations during in vitro fatigue testing of NiTi ». Présenté à: SMST-2003, International Conference on Shape Memory and Superelastic Technologies (5-8 May), qui s'est déroulé à Asilomar Conference Center, Pacific Grove, Ca, USA, p. 303-310.

Negri, A., J. Manfredi, A. Terrini, G. Rodella, G. Bisleri, S. El Quarra et C. Muneretto. 2002. « Prospective evaluation of a new sternal closure method with thermoreactive clips ». European Journal of Cardio-Thoracic Surgery, vol. 22, n° 4 (Oct), p. 571-575.

Okutan, H., C. Tenekeci et A. Kutsal. 2005. « The Reinforced Sternal Closure System® is reliable to use in elderly patients ». Journal of Cardiac Surgery, vol. 20, n° 3 (2005///), p. 271-273.

Pai, S., N. Gunja, E. Dupak, N. McMahon, J. Coburn, J. Lalikos, R. Dunn, N. Francalancia, G. Pins et K. Billiar. 2007. « A Mechanical Study of Rigid Plate Configurations for Sternal Fixation ». Annals of Biomedical Engineering, vol. 35, n° 5 (May 18), p. 808-816.

Pai, S., N. J. Gunja, E. L. Dupak, N. L. McMahon, T. P. Roth, J. F. Lalikos, R. M. Dunn, N. Francalancia, G. D. Pins et K. L. Billiar. 2005. « In Vitro Comparison of Wire and Plate Fixation for Midline Sternotomies ». The Annals of Thoracic Surgery, vol. 80, n° 3 (2005/9), p. 962-968.

Pelton, A. R., X.-Y. Gong et T. Duerig. 2003. « Fatigue testing of diamond-shaped specimens ». Materials & Processes for Medical Devices Conference (8-10 Sep.), p. 199-204.

Puc, M. M., C. H. Antinori, D. T. Villanueva, M. Tarnoff et J. A. Heim. 2000. « Ten-year experience with Mersilene-reinforced sternal wound closure ». The Annals of Thoracic Surgery, vol. 70, n° 1 (2000/7), p. 97-99.

Robertson, S. W., A. Mehta, A. R. Pelton et R. O. Ritchie. 2007. « Evolution of crack-tip transformation zones in superelastic Nitinol subjected to in situ fatigue: A fracture mechanics and synchrotron X-ray microdiffraction analysis ». Acta Materialia, vol. 55, n° 18, p. 6198-6207.

Robicsek, F., H. K. Daugherty et J. W. Cook. 1977. « The prevention and treatment of sternum separation following open-heart surgery ». Journal of Thoracic and Cardiovascular Surgery, vol. 73, n° 2 (Fevrier), p. 267-268.

Rosamond, W., K. Flegal, G. Friday, K. Furie, A. Go, K. Greenlund, N. Haase, M. Ho, V. Howard, B. Kissela, S. Kittner, D. Lloyd-Jones, M. McDermott, J. Meigs, C. Moy, G. Nichol, C. J. O'Donnell, V. Roger, J. Rumsfeld, P. Sorlie, J. Steinberger, T. Thom, S. Wasserthiel-Smoller, Y. Hong, C. for the American Heart Association Statistics et S. Stroke Statistics. 2007. « Heart Disease and Stroke Statistics--2007 Update: A Report From the American Heart Association Statistics Committee and Stroke Statistics Subcommittee ». Circulation, vol. 115, n° 5 (February 6), p. e69-171, 10.1161/circulationaha.106.179918.

Rousseau, R. A., K. S. Weadock et E. S. Chatlynne. 2008. *Sternal closure device and method*. Ethicon, Inc. (Somerville, NJ) (inv.). 7,361,179.

Scott, L. L. 2001. *Methods of closing a patient's sternum following median sternotomy*. U.S. Patent 6 007 538.

Shabalovskaya, S., J. Ryhanen et L. H. Yahia. 2001. « Bioperformance of Nitinol: Surface tendencies ». In *Shape Memory Materials and Its Applications*. Vol. 394-3, p. 131-138. Coll. « Materials Science Forum ». <<Go to ISI>://000176290100029>.

Shroyer, A. L. W., L. P. Coombs, E. D. Peterson, M. C. Eiken, E. R. DeLong, A. Chen, J. Ferguson, T. Bruce, F. L. Grover et F. H. Edwards. 2003. « The society of thoracic surgeons: 30-day operative mortality and morbidity risk models ». The Annals of Thoracic Surgery, vol. 75, n° 6 (2003/6), p. 1856-1865.

Songer, M. N., et F. J. Korhonen. 1998. *Cable system for bone securance*. U.S. Patent 5,741,260.

Soroff, H. S., A. R. Hartman, E. Pak, D. H. Sasvary et S. B. Pollak. 1996. « Improved sternal closure using steel bands : Early experience with three-year follow-up ». The Annals of Thoracic Surgery, vol. 61, n° 4 (Avril 1996), p. 1172-1176.

Stahle, E., A. Tammelin, R. Bergstrom, A. Hambreus, S. O. Nystrom et H. E. Hansson. 1997. « Sternal wound complications--incidence, microbiology and risk factors ». European Journal of Cardio-Thoracic Surgery, vol. 11, n° 6 (1997/6), p. 1146-1153.

Stankiewicz, J. M., S. W. Robertson et R. O. Ritchie. 2007. « Fatigue-crack growth properties of thin-walled superelastic austenitic Nitinol tube for endovascular stents ». Journal of Biomedical Materials Research Part A, vol. 81A, n° 3, p. 685-691.

Sutherland, L. A., et E. Vascocellos. 1988. *Apparatus and method for surgically securing bone parts*. U.S. Patent 4,730,615.

Tabanli, R., N. Simha et B. Berg. 2001. « Mean strain effects on the fatigue properties of superelastic NiTi ». Metallurgical and Materials Transactions A, vol. 32, n° 7, p. 1866-1869.

Tobushi, H., T. Nakahara, Y. Shimeno et T. Hashimoto. 2000. « Low-Cycle Fatigue of TiNi Shape Memory Alloy and Formulation of Fatigue Life ». Journal of Engineering Materials and Technology, vol. 122, n° 2, p. 186-191.

Trumble, D. R., W. E. McGregor et J. A. Magovern. 2002. « Validation of a bone analog model for studies of sternal closure ». The Annals of Thoracic Surgery, vol. 74, n° 3 (Sep), p. 739-744.

Young, J. M., et K. J. V. Vliet. 2005. « Predicting "in vivo" failure of pseudoelastic NiTi devices under low cycle, high amplitude fatigue ». Journal of Biomedical Materials Research, vol. 72B, n° 1, p. 17-26.